2016

Sm and Dy Interaction with Dissolved Organic Matter (DOM) in Freshwater Measured by Ion-Selective Electrode and Fluorescence Quenching Analytical Techniques

Alexandra Carvajal
Wilfrid Laurier University, carv4710@mylaurier.ca

Sm and Dy Interactions with Dissolved Organic Matter (DOM) in Freshwater Measured by Ion-Selective Electrode and Fluorescence Quenching Analytical Techniques

by

Alexandra Carvajal

Honours Bachelor of Science, University of Toronto, 2011

THESIS

Submitted to the Department of Chemistry and Biochemistry

Faculty of Science

in partial fulfilment of the requirements for the

Master of Science in Chemistry and Biochemistry

Wilfrid Laurier University

2016

Abstract

With the increased demand for lanthanide metals in various industries, companies are looking into mining of these metals in Northern Canada. The release of these metals into the environment may have adverse effect on aquatic ecosystems; thus, it is important to understand potential toxicological effects of lanthanides on aquatic organisms. One way to predict these effects is by using a Biotic Ligand Model (BLM). Although incorporation of lanthanides into the model will require a substantial amount of future research, initial studies into speciation and toxicity can provide a useful basis for future reference. There are two main objectives to this thesis; (1) development and validation of analytical techniques for measurement of lanthanide speciation, (2) application of these techniques to assess the metal binding to dissolved organic matter (DOM) of variable sources. The techniques that were tested are fluorescence quenching (FQ) and ion-selective electrode (ISE), and the experiments were done with Sm and Dy, as representatives of light and heavy groups of lanthanides, with five DOM sources. Lanthanide binding by DOM was observed by both techniques with generally good agreement between methods, as shown by similar values of free metal concentrations reported by both speciation techniques. These values were within one log unit of each other, and a large portion of them was within 0.3 log units. ISE revealed presence of non-fluorescent ligands that are able to bind Sm; such ligands cannot be measured by FQ, as it relies on the fluorescence of ligands. Although ISE produced a more complete model, there were intrinsic issues associated with cation competition. Due to this limitation, ISE analysis was not possible on the samples containing high concentrations of dissolved salts.

Generally, the binding of lanthanides with DOM could be characterized as medium to strong with values for binding constants (log K) ranging, for both techniques, from 5.08±0.17 to 6.78±0.0170, with binding capacities varying from 0.53±0.00030 μM/mg C to 12.±1.6 μM/mg C, with little differences between Sm and Dy. There is some DOM source dependence between the colour and the source of samples, measured by SAC_{340} and FI_{370}. The darkest and more allochthonous DOM (Luther Marsh DOM source with SAC_{340} and FI_{370} of 38.88 and 1.05, respectively) is able to bind more metal, especially evident in FQ experiments. The sensitivity of speciation models is observed with respect to pH and pK_{sp} values of hydroxide and carbonate solids. The stability of pH measurements is essential for the determination of lanthanide species for the models to be applied in toxicity studies. Additionally, understanding of solid formation and experimentally determined solubility products may provide a more realistic picture of how lanthanides tend to distribute between species in samples.

A generally accepted speciation model used in toxicity tests analysis is Windermere Humic Aqueous Model (WHAM). Both FQ and ISE models were compared to WHAM. The model shows a dramatic overestimation of DOM and metal binding at low concentrations of metal compared to the ISE and FQ models. One of the main disadvantages of the WHAM modeling is that it does not incorporate precipitation for lanthanides; however, solid formation is shown to be an important part of lanthanide speciation. Further research into speciation of these metals is required, before this model can be applied in the BLM calculations.

Acknowledgements

First and foremost, I would like to thank my amazing supervisor Dr. Scott Smith, whose support and guidance has been absolutely essential during the course of my Master's degree. I have learned so much from you, from that first talk in Milton library through all the lectures and meetings to final draft of this thesis. Every meeting I had with you when I felt discouraged, you managed to put me back on track and give me faith in myself, and that is a rare gift. So thank you for everything you have done for me.

I would also like to show my appreciation to everyone who provided me with their help and knowledge. This includes Dr. Jim McGeer for insightful questions and feedback on my research; Dr. Ken Maly for help with all things related to organic chemistry, as well as Dr. Vladimir Kitaev for challenging discussion on chemistry fundamentals. Thank you for supplying your valuable time to be on my committee. Special thank you goes to Katie Psutka, Aaron Howe and Matt Halloran for their assistance in the organic lab and for an occasional friendly banter; as well as Oliver Vukov, Che Lu and Alyssa Verdin for supplying me with their data, which was central to validation of my methods. I would also like to acknowledge two very bright young individuals who lay the basis for my work Maya Ashoka and James Mori.

I have to express a special thank you to Holly Gray for all the morning coffee talks about both personal and academic life. I was lucky enough to find such a good friend in what seems like such a short period of time. You made my days a lot more enjoyable than they would probably be otherwise. I also cannot forget my closest friends Anya, Jenny and Mihaela; usually worlds apart but yet still very close. Sanity didn't come easy, but you managed to steady me and not let me topple over the edge. These few years would also be a lot more stressful if it wasn't for the love and support of my amazing family: Mom, Dad and my "big bro" Roman. I am forever grateful.

Finally, I would like to thank all the research and funding partners that participated in this project: BIOMET Research Group, which includes Kevin Wilkinson (Université de Montréal), Peter Campbell and Claude Fortin (INRS-ETE), as well as Environment Canada, Avalon Rare Metals Inc., NSERC and OGS.

Table of Contents

List of Abbreviations

BA	Benzyl Acetate
BB DOM	Burlington Bay DOM
BLM	Biotic Ligand Model
CCME	Canadian Council of Minister of the Environment
CI	Confidence Interval
DOC	Dissolved Organic Carbon
DOM	Dissolved Organic Matter
DOS	Dioctyl Sebacate
EEM	Excitation Emission Matrix
EPA	US Environmental Protection Agency
FA	Fulvic Acid
FI_{370}	Fluorescence Index
FQ	Fluorescence Quenching
HA	Humic Acid
IET	Ion Exchange Technique
IHSS	International Humic Substances Society
IS	Ionic Strength
ISE	Ion-Selective Electrode
KB DOM	Kouchibouguac DOM
LC_{50}	Lethal Concentrations at 50% Survival
LM DOM	Luther Marsh DOM
Log K	Binding Constant
Lt	Binding Capacity
MC	Monte Carlo Analysis
NaTPB	Sodium Tetraphenylborate
NIST	National Institute of Standards and Technology
NOM	Natural Organic Matter
NPOE	Nitrophenyloctyl Ether
ppm	parts per million
PVC	Polyvinyl Chloride
REE	Rare Earth Elements
RW	Ryan Weber model
SAC_{340}	Specific Absorbance Coefficient
SD	Standard Deviation
SE	Standard Error
SH DOM	Southampton DOM
SIMPLISMA	SIMPLe to use Interactive Self-modeling Mixture Analysis
SW DOM	Suwannee River DOM
THF	Tetrahydrofuran
TIC	Total Inorganic Carbon
WHAM	Windermere Humic Aqueous Model

List of Figures

List of Tables

CHAPTER 1: BACKGROUND INFORMATION

1.1 Lanthanides

Lanthanides are a group of metals that are characterized by their unique chemistry. The lanthanides group includes 15 elements located in row 6 of periodic table, they are: Lanthanum (La), Cerium (Ce), Praseodymium (Pr), Neodymium (Nd), Promethium (Pm), Samarium (Sm), Europium (Eu), Gadolinium (Gd), Terbium (Tb), Dysprosium (Dy), Holmium (Ho), Erbium (Er), Thulium (Tm), Ytterbium (Yb), and Lutetium (Lu). The main characteristic of this group of metals that distinguishes them from transition metals is the presence of occupied *f* orbitals. La is the only metal within this group that does not contain an occupied *f* orbital. The electrons found in these orbitals do not usually participate in the complex formation or bonding of lanthanides as they have lower energy than the valence shell electrons (Karraker 1970). Consequently, lanthanides are similar in their chemical behaviour. The most common oxidation state for all lanthanides is +3 (Moeller, 1970). Due to their unique chemistry, lanthanides were incorporated into many products (Section 1.1.1); this drives the interest in mining of these metals, thus, promoting economic development.

1.1.1 Lanthanides as REEs: Uses and Mining

Lanthanides are also commonly known as "rare earth metals or elements" or REEs. This term is often used within industrial circles; however, in this definition, REEs also include Sc and Y, which are not part of the lanthanide group. For the purpose of this project, only lanthanides are discussed. Although lanthanides are a part of REEs, in

reality they are more abundant in the earth crust (0.3 - 60 ppm by weight, Table 1-1) than the more commonly known metals such as silver and gold (0.08 ppm and 0.0031 ppm, respectively). The term "REE" was coined as a result of earlier metallurgical work. With existing technology of mid-twentieth century it was difficult to isolate any particular lanthanide from a mixture of other metals from the same chemical group; thus, making metal oxide compounds a rare commodity (EPA 2012).

Table 1-1. Crustal abundance of select metals, including lanthanides (**in bold**) (EPA 2012).

Elements (atomic number)	**Crustal Abundance (ppm by weight)**
Nickel (28)	90
Zinc (30)	79
Copper (29)	68
Cerium (58)	**60.0**
Lanthanum (57)	**30.0**
Cobalt (27)	30
Neodymium (60)	**27.0**
Lead (82)	10
Praseodymium (59)	**6.7**
Thorium (90)	6
Samarium (62)	**5.3**
Gadolinium (64)	**4.0**
Dysprosium (66)	**3.8**
Tin (50)	2.2
Erbium (68)	**2.1**
Ytterbium (70)	**2.0**
Europium (63)	**1.3**
Holmium (67)	**0.8**
Terbium (65)	**0.7**
Lutetium (71)	**0.4**
Thulium (69)	**0.3**
Silver (47)	0.08
Gold (79)	0.0031
Promethium (61) [a]	**10^{-18}**

(a) Promethium is radioactive

Since the 1960s, extraction and separation process were improved dramatically. The general process now involves the concentration of the mineral from the ore by flotation, magnetic or gravity methods (EPA 2012, Xie et al. 2014). Individual lanthanides are then separated generally in stages by solvent extraction during hydrometallurgical processing. Organophosphorus compounds are used extensively for this purpose, as they have a preferential selection of lanthanides increasing with the atomic number (Xie et al. 2014). The development of more sophisticated technology made lanthanides more available.

The metals gained use in a number of industries including automotive, medical and electronics manufacturing (ChemInfo 2012). They are often incorporated into the products of these industries as magnets, due to their enhanced performance over other magnetic materials (Trout 1990; RNNR 2014; Xie et al. 2014). Lanthanides are also often divided into two groups, light (La-Gd) and heavy (Tb-Lu), with heavy lanthanides considered more valuable (ChemInfo 2012). A detailed list of their applications can be found in Table 1-2 (EPA 2012, original source U.S. DOE). Currently, the U.S. Department of Energy identifies a number of lanthanides to be in critical or near critical supply risk, which include La, Ce, Nd, Eu, Tb and Dy (EPA 2012). One of the current increases in application of lanthanides is within the clean/green technology sector (EPA 2012), which makes these metals an important commodity for the economic market as well as for the future of sustainable development.

As the demand for these metals increases, mining companies are in search of the viable lanthanide mining sites (EPA 2012). Currently, the main supplies of lanthanides

come from China (ChemInfo 2012; RNNR 2014). In 2009, the export of lanthanides was restricted by the Chinese government, which encouraged companies to explore deposits in other areas of the globe (ChemInfo 2012). Canada became a country of interest as it contains about 50% of all REEs worldwide outside of China (RNNR 2014). There are over 26 sites within Canada that are currently being evaluated for mining of lanthanides, with 3 most notable projects located in Northwest Territories, Northern and Southern Quebec (ChemInfo 2012). These projects are still in their beginning stages, as they face many challenges that have to do with transportation infrastructure due to remote locations, as well as extraction and processing of mixtures of lanthanides (ChemInfo 2012). Nevertheless, the future development of lanthanides mines has a potential positive effect on Canadian economy.

Table 1-2. A list of applications of Lanthanides in various industries.

Element	**Applications**
Lanthanum	Batteries; catalysts for petroleum refining; electric car batteries; high-tech digital cameras; video cameras; laptop batteries; X-ray films; lasers; communication devices.
Cerium	Catalysts; polishing; metal alloys; lens polishes (for glass, television faceplates, mirrors, optical glass, silicon microprocessors, and disk drives).
Praseodymium	Improved magnet corrosion resistance; pigment; searchlights; airport signal lenses; photographic filters; guidance and control systems and electric motors.
Neodymium	High-power magnets for laptops, lasers, fluid-fracking catalysts; guidance and control systems, electric motors, and communication devices.
Promethium	Beta radiation source, fluid-fracking catalysts.
Samarium	High-temperature magnets, reactor control rods; guidance and control systems and electric motors.
Europium	Liquid crystal displays (LCDs), fluorescent lighting, glass additives; targeting and weapon systems and communication devices.
Gadolinium	Magnetic resonance imaging contrast agent, glass additives.
Terbium	Phosphors for lighting and display; guidance and control systems, targeting and weapon systems, and electric motors.
Dysprosium	High-power magnets, lasers; guidance and control systems and electric motors.

Table 1-2 continued

Element	Applications
Holmium	Highest power magnets known.
Erbium	Lasers, glass colorant.
Thulium	High-power magnets.
Ytterbium	Fiber-optic technology, solar panels, alloys (stainless steel), lasers, radiation source for portable X-ray units.
Lutetium	X-ray phosphors.

1.1.2 Lanthanides in the Environment

Lanthanides are naturally present in freshwater at low dissolved concentrations ranging worldwide from 0.0023 μg/L to 0.041 μg/L in rivers (259 samples), 0.0049 μg/L to 0.23 μg/L in lakes (74 samples) and 0.00024 μg/L to 0.0020 μg/L in seawater (178 samples) (Noack et al. 2014). The concentrations exhibit an overall decrease in values with increasing atomic number; however, there is a notable "zig-zag" pattern in the distribution of lanthanides (Figure 1-1). This trend is commonly observed in the periodic table and is defined by Oddo-Harkins rule (Faure and Mensing 2007), which state that elements with even atomic numbers are generally more commonly found in nature than the ones with odd atomic number. As a result of this phenomenon, Ce is the most abundant element in the naturally occurring lanthanides group and Tm the least abundant. This trend can also be observed

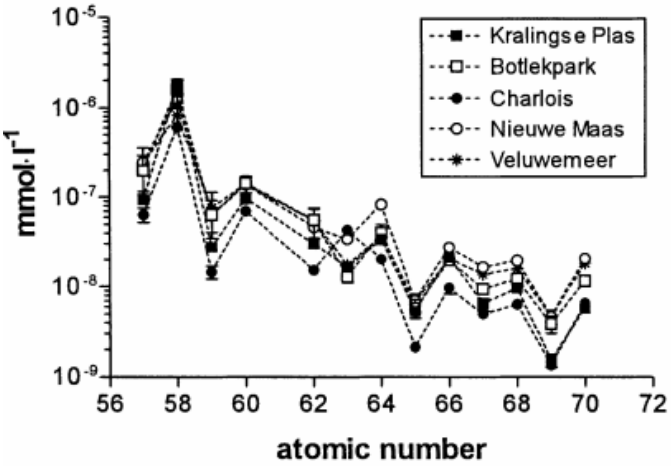

Figure 1-1. Freshwater lanthanide concentrations in mmol/L vs. atomic number. The samples were collected from five streams and rivers in The Netherlands in the catchment of the Rhine and Meuse Rivers (Weltje et al. 2002).

in the crustal concentrations of lanthanides (Table 1-1). Similarly, it can be seen in aqueous dissolved concentrations, measured in five streams and rivers in The Netherlands, as shown in Figure 1-1 (Weltje et al. 2002). The exception to the rule is Pm (atomic number 61), which is rarely found in nature, as it is the only metal in the series that is radioactive and is mostly produced artificially (EPA 2012). In rivers and streams the distribution of lanthanides varies between the water column, sediment pore water and solid sediments. River waters usually contain similar but often slightly lower concentrations than sediment pore water, with values ranging from 0.17 ng/L for Tm and 176.5 ng/L for Ce, while sediment pore water concentrations range from 0.27 ng/L for Tm to 150 ng/L for Ce, as measured in five streams and rivers in the Netherlands (Weltje et al. 2002). This trend is usually attributed to the lower pH value in the pore water. Ce was the only exception to this trend in this study with a slightly lower value in pore water as opposed to river water. The authors (Weltje et al. 2002) explained this by the dissolution of the CeO_2 upon acidification of the sample that contained Ce enriched colloids found in the water stream. Finally, sediment lanthanides concentrations are orders of magnitude greater than water concentrations, ranging from 168.9 µg/L for Tm to 56 mg/L for Ce. Lanthanides were proven to be part of the sediment matrix, as the measurements were similar between two different particle sizes, which, if they were adsorbed from the water column, would show an increase for smaller size particles (Weltje et al. 2002). This relationship might change in waters that are contaminated with lanthanides from industrial processes.

In freshwater lanthanides can be bound to carbonates, phosphates, and hydroxides; however their solubility depends on pH and salinity of water (Elbaz-

Poulichet and Dupuy 1999; Gammons et al. 2005; Sneller et al. 2000). Depending on the type of solid, solubility may increase or decrease between the light and heavy lanthanides (Table 1-3). Carbonate complexes are considered to be one of more dominate aqueous species, especially in neutral and alkaline waters, where they form stable complexes (Johannesson et al. 1995; Wood 1990). Phosphate precipitates also play an important role in the removal of lanthanides from the water column due to their high insolubility (Johannesson et al. 1995). In fact, the strong affinity and binding between lanthanides and phosphate is sometimes utilized for the removal of either one of them from media of interest, such as removal of lanthanide from contaminated waters or even dialysate (fluid from the dialysis process) via silica support functionalized with different forms of phosphonic acid (Yantasee et al. 2009); or the removal of phosphate from wastewater via lanthanides-loaded adsorption gels (Biswas et al. 2007). At lower pH concentrations, however, lanthanides are usually found bound to sulfates or in their free form, depending on the concentration of sulfate in water (Elbaz-Poulichet and Dupuy 1999; Wood 1990). Complexes with chloride and nitrates were found to be negligible even at high concentration of the anions (Wood 1990).

Table 1-3. pK_{sp} values for inorganic solids of lanthanides, values obtained from NIST database (Martell and Smith 2004; Verweij 2013).

Lanthanide (M^{3+})	**Inorganic Ligand (L)**				
	OH^-	**CO_3^{2-}**	**F^-**	**PO_4^{3-}**	**AsO_4^{3-}**
La	22.2	34.4	18.7	25.75	21.4
Ce	23.9	31.1	19.1	26.3	-
Pr	24.4	-	18.9	26.4	22
Nd	26	19.9/33[a]	20.3	26.2	21.9
Sm	25.9	32.5	17.9	26.19	22.7
Eu	26.5	20.2/32.3[a]	21.9	26.96	22.5
Gd	26.9	32.2	16.8	25.6	22.7
Tb	26.3	-	16.7	25.39	23.1

Table 1-3 Continued

Lanthanide	**Inorganic Ligand (L)**				
Dy	25.9	31.5	16.3	25.2	23.8
Ho	26.6	-	15.8	25.1	22.9
Er	26.6	-	18	25.1	22.5
Tm	26.7	-	15.8	25	23.1
Yb	26.6	31.1	15	24.9	22.7
Lu	27	-	15	24.8	22.7
Stoichiometry	ML_3	M_2L_3	ML_3	*ML*	*ML*

(a) First value corresponds to MOHL stoichiometry

Depending on the natural geology of the study site the aqueous concentrations of lanthanides may vary. Table 1-4 provides a summary of the natural occurrence of the metals of interest to this project (Sm and Dy) in various locations around the world. The concentrations of Sm and Dy were found to be elevated in acidic waters in Italy (1,881-7,890 ng/L as opposed to background of 2.5-59 ng/L), which usually occur as a result of the mining activities, a process also known as acid mine drainage (Gimeno et al. 2000, Gammons et al. 2005; Protano and Riccoboni 2002). These mines may not necessarily be related to REE exploitation; some of them extract other metals, for example a Cu-Pb-Zn mine in Italy (Protano and Riccoboni 2002). However, the acid mine drainage forces the release of lanthanides into the stream from the local rock formations, which can be enhanced further during rainstorm events in the vicinity of the mine by tripling the concentrations of the metals (Protano and Riccoboni 2002). As a result, low pH values and extreme weather events can increase dissolved concentrations of lanthanides and that may have an effect on the aquatic life.

Table 1-4. Concentrations of Sm and Dy in nM and ng/L in natural and mining impacted waters. Unless otherwise specified, all of the values reported represent dissolved concentrations (filtered using 0.45 μm filters). Values from Weltje et al. (2002) and Noack et al. (2014) were approximated from figures.

[Sm], nM	[Dy], nM	[Sm], ng/L	[Dy], ng/L	Reference	Number of locations/samples	General locations
Background or natural occurring concentrations						
0.0003-0.04	0.01-0.014	0.05-6.0	2.3-1.6	Weltje et al. 2002	5	Rotterdam, Neatherlands
0.053-0.086	0.047-0.049	8-14	7-8	Mayfield and Fairbrother 2015	136	Washington, USA
0.20, 0.20[a]	0.20, 0.79[a]	30, 30[a]	32, 129[a]	Noack et al. 2014	259,74	Worldwide
0.017-0.36	0.29-0.26	2.5-59	43-43	Protano and Riccoboni 2002	6	Tuscany, Italy
0.6[b]	0.8[b]	90[b]	130[b]	Gimeno et al. 2000	11	Colour lake, NWT, Canada
Mining affected areas concentrations						
0.19-5.19[b]	0.14-5.25	28.9-844	20.6-854	Gammons et al. 2005	9	Montana, USA
14.3-48.6	12.6-42.7	2,150-7,890	1,881-6,937	Protano and Riccoboni 2002	7	Tuscany, Italy
27-242	23-172	4,060-36,390	3,737-27,950	Gimeno et al. 2000	3	Arroyo de Val, Spain
NWT mining site						
82.5	57.7	12,400	9,370	Avalon 2013	tailings effluent	NWT, Canada
0.33	0.30	50	48	Avalon 2013	treated effluent	NWT, Canada

(a) The values represent average concentrations measured in rivers and lakes and are not the range of values
(b) Naturally occurring acidic lake (pH~4), high dissolved concentrations observed (averaged)
(c) The samples were filtered using 0.1 μm filters

1.2 Metal Toxicity and Speciation

Metals can be released into the environment as a result of mining and other industrial activities. While in streams and rivers, metals can potentially cause toxicity to aquatic organisms. For the protection of aquatic life it is important to have a way to measure risk, which in turn relies on the most accurate data available on metal behaviour in water, which is governed by other components such as other chemicals present in water. The following section will go into details of the model that is often used to measure risk, dissolved organic matter that can control the speciation of metals, as well as discuss some of the toxicity values that are known for lanthanides.

1.2.1 Biotic Ligand Model

In order to effectively establish water quality guidelines or perform environmental risk assessments, a prediction of toxicological effects of the metals is often required. This can be accomplished by the development of a framework that will be able to predict toxicity. An example of such a framework is the Biotic Ligand Model (BLM, Figure 1-2). It is a quantitative model that considers the bioavailability and bioreactivity of the metal in order to predict the potential adverse effects on the organism (Di Toro et al. 2001; Paquin et al. 2002; Santore et al. 2001; Slaveykova and Wilkinson 2005). It is a chemical equilibrium-based model with one of the components representing a site of action of toxicity, which is called the biotic ligand. According to the model the toxic response associated with a metal is proportional to the interaction of the metal with the biotic ligand, especially the free metal ion, as it is assumed to be the most bioavailable form. Thus metal toxicity can be correlated with the concentration of free metal ion in water.

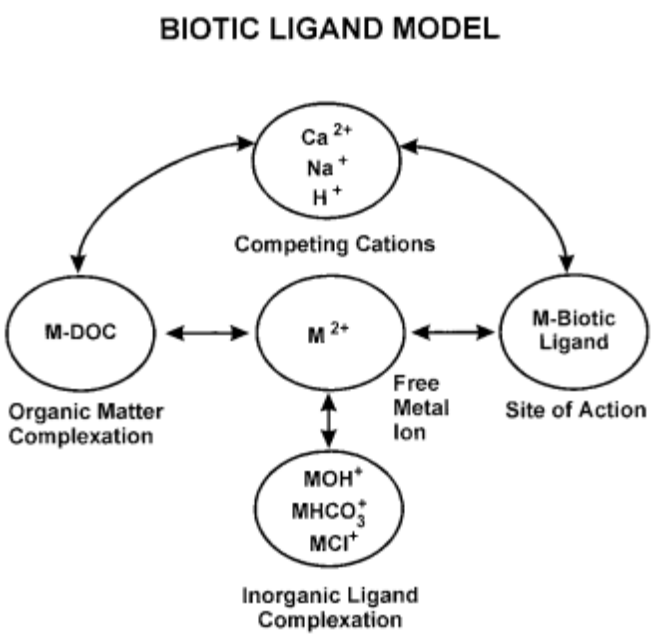

Figure 1-2. Schematic representation of the Biotic Ligand Model (Di Toro et al. 2001).

This concentration in turn depends on the interactions of metal with other components of the aquatic environments, such as organic and inorganic ions and molecules, as well as competition with other cations. The presence of dissolved organic matter (DOM) and inorganic anions (e.g. chloride, sulfides, hydroxides, carbonates, etc.) alters the distribution of metals by forming metal-ligand complexes governed by equilibrium binding constants (Figure 1-2). Additionally, competing cations may block the site of action, where free metal ion binds to the biotic ligand. Some of the advantages of BLM is that it allows for the prediction of toxicity at varying water quality conditions and relate it back to the total dissolved concentrations of metal in water; in addition, the toxicity of smaller inorganic complexes (e.g. metal-hydroxides) can be incorporated into the model, thus producing a more realistic prediction (Paquin et al. 2002).

1.2.2 Dissolved Organic Matter

Dissolved organic matter (DOM) is a macromolecule that can vary in size from a few hundred to 100,000 daltons and is usually composed of an aggregation of smaller organic molecules (Leenheer and Croue 2003). An example of humic acid, which makes up a portion of DOM, can be seen in Figure 1-3. As seen in the figure DOM has a

number of aromatic and aliphatic areas, which allows DOM to absorb and emit light (Leenheer and Croue 2003; Fellman et al. 2010). The main sources of the fluorescent region of DOM are compounds such as lignin, tannins and polyphenols (Fellman et al. 2010). Due to a presence of a number of functional groups, such as carboxyl, phenol and amino groups (Leenheer and Croue 2003; Tipping et al. 2011), DOM can bind metals and decrease their toxicity by making the metal less bioavailable. The streams that contain a high concentration of DOM will show more protection against metals toxicity than streams with lower concentrations. It is important to note that structure and ability of DOM to bind metals is pH dependent, due to a presence of acidic groups (carboxylic acids) that can be found in protonated and deprotonated form based on pH. This may alter the actual structure of DOM by either extending or recoiling of the macromolecule (Hudson et al. 2007), thus, changing the accessibility of binding sites.

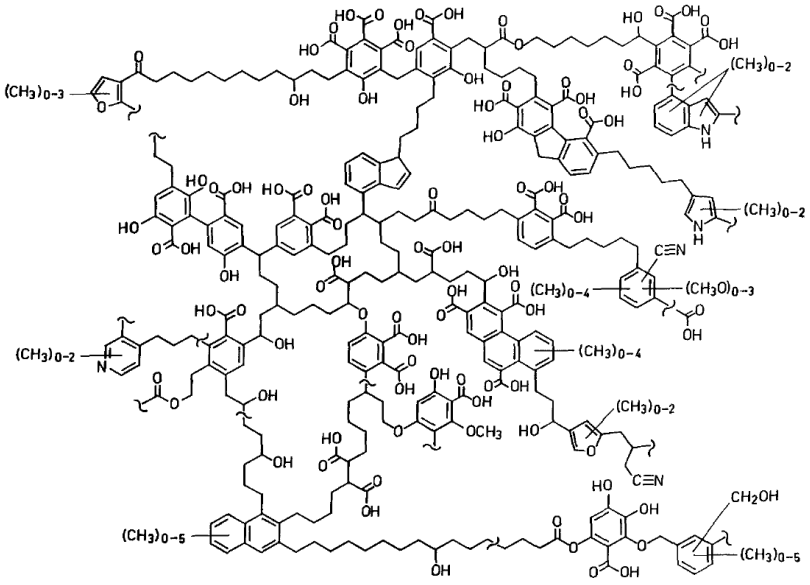

Figure 1-3. Schematic representation of a humic acid chemical structure (Schulten and Schnitzer 1993).

There are two broad classes of DOM that can be present in water, they are autochthonous and allochthonous DOM. Autochthonous DOM is produced within the lake or a stream via algal or microbial photodegradation, while allochthonous DOM is deposited into water from land-based sources (Leenheer and Croue 2003; Wood et al. 2011). The source of organic matter will determine its general chemical composition. One way to assess sources differences is to determine the amount of humic, fulvic and proteinaceous components, which can all be a part of DOM (Leenheer and Croue 2003; Hudson et al. 2007). Excitation Emission Matrices (EEMs) can be used to do that, and they are further discussed in Section 1.4.1.1.

Another way to characterize DOM is by measuring the aromaticity of the molecule using absorbance and fluorescence data. In DOM (Figure 1-3) functional metal binding groups were shown to be associated with aromatic regions (Al-Reasi et al. 2013). One way to do these comparisons is to calculate specific absorbance coefficient (SAC_{340}), which defines how dark the DOM is per mg of C, and fluorescence index (FI_{370}), which can be used to predict the source of the DOM (Al-Reasi et al. 2011; Curtis and Schindler 1997; McKnight et al. 2001). These parameters can be calculated using these equations:

$$SAC_{340} = \frac{2.303\ x\ A/l}{[DOC]/1000} \qquad \text{Equation 1-1}$$

A – absorbance at excitation wavelength of 340 nm
l – pathlength (1 cm cuvette)
[DOC] – dissolved organic carbon concentration measured in mg/L, DOC is often used as a measure of DOM

$$FI_{370} = \frac{F\ at\ 450}{F\ at\ 500}$$ Equation 1-2

F – fluorescence intensity at emission wavelength of 450 nm and 500 nm measured at the excitation wavelength of 370 nm

It was reported previous that darker DOM (higher SAC_{340}, Wood et al. 2011), containing more of the humic-like components (low FI_{370}, McKnight et al. 2001), have a greater affinity to some metals (Cu, Ag and Pb), thus it is more protective against metal toxicity (Al-Reasi et al. 2011; Wood et al. 2011). These easily measurable properties of DOM can be used in the assessment of protective qualities of any particular DOM sample.

1.2.3 Lanthanides Speciation with DOM and Toxicity

Lanthanides are considered to be data poor metals, as there is limited information available on their speciation and toxicity (Gonzalez et al. 2014). A study done by Borgmann et al. (2005) examined toxicity of 63 metals, including lanthanides, to *Hyalella azteca*. The results showed that generally lanthanides were not as toxic as Cd, Ag, Cr or Pb (with one exception being Tm). Lethal concentration at which 50% of the population has died (LC_{50}), however, revealed that there is a significant difference in values calculated using nominal vs. measured concentrations of the metal, especially evident in case of Tm. Tm LC_{50} value decreased dramatically from 721 μg/L using nominal concentrations to a very low value of 0.01 μg/L using measured concentrations compared to other lanthanides which decreased from 120-559 μg/L to 18-191 μg/L. Observed higher toxicity using measured concentrations imply that metal was lost during the experiment most likely by forming insoluble complexes (Borgmann et al., 2005;

Gonzalez et al. 2014). Therefore, lanthanide speciation is an important factor to consider when evaluating metal toxicity.

The BLM predictions rely strongly on accurate speciation models. Especially, with current research (Zhao and Wilkinson 2015) showing that the lanthanide bioavailability may not be defined using the BLM concept of the model where the free metal ion is the most bioavailable form of the metal. It was shown that the formation of the ternary metal complex, where the metal is bound to organic ligands (citric, malic, and nitrilotriacetic acid) on one side and the biological receptor site on the other, increased biouptake of the metal into freshwater algae (Zhao and Wilkinson 2015). The increased biouptake may not directly translate into the increase in toxicity, but it might have an adverse effect. Thus, understanding the interactions of these metals with the organic ligands is essential for prediction of bioavailability.

Lanthanides are known to have a high affinity to the oxygen-containing inorganic ligands, as opposed to insoluble sulfides, which are more common with the transition metals (e.g. Cu, Zn) (Sneller et al. 2000). Similarly, when it comes to complex formation with the organic molecules in aqueous environment, lanthanides tend to interact with oxygen containing groups such as carboxylic groups and phenolic groups (Karraker 1970). There is some evidence from the geochemical modeling of difference between ‘light” and “heavy” lanthanides preferential binding, where lanthanides from the “light” group tend to bind more to carboxylic groups, while “heavy” lanthanides bind to phenolic groups (Marsac et al. 2011). This implies that it is possible for them to form strong complexes with humic and fulvic acids, which contain both types of groups. The binding

of lanthanides to humic and fulvic acids is expected to be similar to other trivalent metals such as Al and Fe. Both of these metals have been shown to compete with lanthanides for the binding site on humic acids at various pH conditions (Marsac et al. 2012; Marsac et al. 2013).

The majority of research into lanthanide and organic matter speciation has been done using Eu and fulvic acids (Tipping et al. 2011). The reason for these select studies is that Eu is often used as an analogue for actinides, especially americium, which is identified as a radiological hazard (Lead et al. 1998). It was reported that Eu has a strong binding with fulvic acid (Dong et al. 2002; Lead et al. 1998). The measured stability constants at times differed by orders of magnitude with log K values ranging from 3.5-5.95 for fulvic acids and 7.38-7.9 for humic acids at pH values of 3.5-6 (Shin et al. 1996). Humic acids were also reported to have slightly higher affinity for lanthanides (Tb, Gd and Yb) than fulvic acids by Dong et al. (2002), with values for conditional stability constants ranging from 9.9-11.0 for fulvic acids and 10.3-11.6 for humic acids at alkaline pH (8.98-9.09). Another study reported conditional constants at pH 6.0 and IS of 0.045 M with fulvic acids for La, Ce, Sm and Gd ranging from 4.21 to 4.53, measured by ion exchange technique (Gu et al. 2001). At slightly different conditions, fulvic acid and Ce binding constants were 5.39 (pH 7), 6.03 (pH 6) and 5.83 (pH 5) in IS of 0.01 M, measured by fluorescence quenching (El-Akl et al. 2015). The difference in the binding of lanthanides between two sources of DOM was assessed as well, and it was reported that forest soil humic acids tend to have higher binding constants for one of the ligands identified (6.26-6.82, pH 6.3) than lake sediment humic acids (5.1-5.57, An-Chao et al. 1998), while the second ligand was similar between the two types (log K: 4.4-4.7). The

difference in stability constant values may arise from the variety of techniques used, such as equilibrium dialysis, ultrafiltration coupled with ICP-MS and ion exchange technique.

The results of lanthanide and DOM binding are often compared to Model VII, VI or V, which are a part of a Windermere Humic Aqueous Model (WHAM, Tipping 1994), frequently used in risk assessment (CCME 2011). The model incorporates only a small number of datasets for lanthanides, usually no more than one (Tipping et al. 2011). Most of the experimental information is available for Eu, some of it is also available for Tb, Dy and Sm, however, for the rest of lanthanides binding parameters were first estimated for Model V (Tang and Johannesson 2003), and later a single calibration dataset was added for each lanthanide in Models VI and VII (Sonke 2006; Sonke and Salters 2006; Tipping et al. 2011). Nevertheless, it was found that the model can effectively predict the metal binding to DOM (Lead et al. 1998; Pourret et al. 2007; Shin et al. 1996). The model separates the organic matter into fulvic and humic components that contain different groups of binding sites, which are separated into two types, weak and strong binding sites (Tipping et al. 2011). The necessity of separation into two types of sites is evident from the experimental data (An-Chao et al. 1988; Shin et al. 1996). The preference of the site was observed to be dependent on the concentration of the metal and pH values. Low metal concentration is more likely to form 1:1 complexes with strong binding sites on fulvic acids; however, 1:2 complex can form at higher metal concentration (Shin et al. 1996). Similarly, acidic conditions favour 1:1 complex formation, while alkaline conditions can support both ratios (Dong et al. 2002). The difference between the light and heavy REEs is observed when it comes to speciation, with light REEs more likely to form humic acid complexes, while heavy REEs readily form both carbonate and humic

acid complexes (Pourret et al. 2007). Due to high natural concentrations of carbonate in water it may participate in lanthanide speciation, as discussed previously (Section 1.1.2). However, it was found that at most naturally occurring pH values DOM complexes are more dominant (Pourret et al. 2007). A study into geochemistry of lanthanides in groundwater (Janssen and Verweij 2003), also showed an importance of the DOM complexation, as it turned out to be one of the dominant factors controlling speciation of lanthanides together with sulfates (depending on concentration) and pH. This was also supported by the Model V results showing DOM-lanthanide complex formation at pH values 3-10 (Sonke 2006). All of these facts make WHAM an attractive choice for obtaining speciation information of lanthanides in natural environments.

Although, there has been some evidence of Model V, VI and VII validation with experimental results, the variety of the binding constants produced from different methods makes it difficult to fully understand DOM and lanthanide speciation. The lack of solid formation prediction in the model also has an impact on accurate free ion estimations when it comes to lanthanides as precipitates play an important role in metal distribution of these elements (Johannesson et al. 1995). Additionally, the heterogeneity of natural DOM can create more variability from the commercially available humic and fulvic substances often used in these studies. Finally, the model relies on a very limited dataset for lanthanide binding to organic ligands (Tipping et al. 2011). More experimental information is needed to produce more reliable and accurate model predictions.

1.3 Measuring Metal Speciation

Measuring the concentrations of various forms of metal found in the environment also known as metal speciation is an important part of risk assessment, since metal toxicity is related to the type of metal species found in water as discussed earlier (Section 1.2.1). It is important to use reliable and accurate analytical techniques for this purpose. There are a number of such techniques that are commonly practiced, such as chromatography, dialysis, ultrafiltration, Donnan membrane technique, all coupled with a detection method (e.g. ICP-MS), and voltammetry (Hamilton-Taylor et al. 2011; Saar and Weber 1982). These methods can generally be divided into two categories, separation and non-separation techniques (Saar and Weber 1982), which focus on sample processing prior to detection. Many of techniques (e.g. voltammetry) measure labile form of the metal, which means that it can be easily interchanged between species, including free metal and inorganic species. Therefore, values measured by these techniques do not represent actual free metal ion concentrations, which is often required for modeling.

Ultrafiltration and gel permeation chromatography are all examples of separation techniques, which rely on size exclusion. There is no relationship established between toxicity and molecular size of a metal species, however it is accepted that the majority of the larger metal complexes are relatively non-toxic (Florence et al. 1992). There are two main concerns associated with this type of technique: adsorption of the metal onto the membrane or filter material, as well as shifting equilibrium during the experiment, which would result in the over or under estimation based on the equilibrium constants (Saar and Weber 1982). Additionally, the size exclusion experiment cannot effectively separate the

truly dissolved and the adsorbed metals on colloidal particles and smaller organic molecules (Saar and Weber 1982), which can result in less accurate binding parameters estimations.

Donnan membrane and equilibrium dialysis techniques rely on both the size exclusion as well as the charge of the particles. These techniques often take a long time, as they require equilibrium to be established prior to final measurement. Similarly with other size exclusion techniques equilibrium based technique may suffer from adsorption of metal onto membrane (Saar and Weber 1982). Additionally, other charged species may enter the membrane solution and thus cause the overestimation of free metal ion. In this case an appropriate equilibrium modeling is required (Hamilton-Taylor et al. 2011). Thus, the results produced by these analytical techniques may not be representative of the actual metal speciation of the samples.

Anodic stripping voltammetry is another determination technique, which involves concentration of the metal of interest onto an electrode by electroreduction. The metal is oxidized back into the solution by reversing the potential at the electrode, the magnitude of current flow from oxidation can be used to calculate metal concentration in solution (Harris 2003). Main advantages of voltammetry technique are high sensitivities and no sample preparation, however it measures labile fraction of the metal, which is not representative of the free metal species; additionally, it is subjected to adsorption problems as well as equilibrium shift discussed previously (Florence et al. 1992; Saar and Weber 1982).

Other techniques used to measure metal speciation include fluorescence quenching (FQ), ion-selective electrodes (ISE) and ion exchange technique (IET). IET as an analytical technique has been used to determine metal speciation with DOM for metals such as Ni^{+}, Cd^{2+}, Zn^{2+} and Ag^{+} (Worms and Wilkinson 2008; Fortin and Campbell 1998; Chen et al. 2012). This technique is based on chemical equilibrium of metal ion with the weakly binding cation exchange resin (Chen et al. 2012). IET is usually time-consuming and it has not been yet optimized for lanthanide speciation measurements. The most recent research has shown that it tends to dramatically underestimate inorganic lanthanide concentrations (Leguay et al. 2015, accepted). FQ and ISE are two techniques that were chosen and are discussed in the consequent Section 1.4. The main advantages of these methods are that they are not time consuming, and they focus on ion interactions in equilibrium, thus, minimize adsorption and shifting equilibrium issues (Saar and Weber 1982).

1.4 Analytical methods

For the purpose of this study, techniques that use free ion equilibrium measurements were selected. The first technique, fluorescence quenching (FQ), looks at the effect of metal interactions with DOM on the fluorescence of DOM and translates it into binding parameters that can be used to calculate free ion concentrations. The second technique, ion-selective electrode (ISE), measure free ion directly in the sample.

1.4.1 Fluorescence Quenching

Natural DOM is fluorescent due to a presence of many aromatic components with electron-donating functional groups (Chen et al. 2003). In the presence of paramagnetic metal ions (containing unpaired electrons) the quenching of the fluorescence of fulvic and humic components of the DOM can be observed (Ryan and Weber 1982). Diamagnetic metals tend to form new fluorescent species and thus cause either the enhancement or suppression of fluorescence depending on the excitation wavelength chosen for observation (Smith and Kramer 1998). The experiments involve titration of the DOM sample with the metal at fixed pH value. The relationship between the decrease in the intensity of fluorescence and concentration of the metal added can be used to calculate the binding constant and binding capacity. This can be done assuming the following relationships, which are a part of Ryan-Weber model (RW model):

$$F = k_L[L] + k_{ML}[ML] \qquad \text{Equation 1-3}$$

F - total fluorescence intensity
k - proportionality constant of ligand (L) or metal ligand fluorescence
[L] - free ligand concentration
[ML] - metal-ligand complex concentration
Assuming $k_L > k_{ML}$, which signifies the presence of quenching. Additionally, $k_{ML} \neq 0$, which shows that some of the fluorescence comes from the residual fluorescence of the metal-ligand complex

Mass balance equations:

$$L_T = [L] + [ML] \qquad \text{Equation 1-4}$$

L_T - total ligand concentrations, binding capacity

$$M_T = [M] + [ML] \quad \text{Equation 1-5}$$

M_T - total metal concentration
[M] - free metal concentration

$$K = \frac{[M][L]}{[ML]} \quad \text{Equation 1-6}$$

K - conditional binding constant (equilibrium constant, as it depends on pH and ionic strength)

The total metal concentration (M_T) is defined by the experimental design of the titration, while total fluorescence intensity (F) is measured during the experiment. Taking the relationships described by Equations 1-1 to 1-4 into account, it is possible to use non-linear regression analysis to determine both binding constant (K) and binding capacity (L_T), by varying free metal ([M]), free ligand ([L]), metal-ligand complex concentrations ([ML]), as well as fluorescence proportionality constants (k_L and k_{ML}). The resulting K value is conditional to the pH value as well as ion concentrations of the water matrix. By incorporating the inorganic complexation model, the resulting binding constants can be used to indirectly calculate free metal ion (Tait et al. 2015). A collection of the inorganic species formation constants can be found in the NIST database (Martell and Smith 2004; Verweij 2013). Combining organic and inorganic speciation, thus, provides a speciation model, which can be used to predict free metal concentration, which can be used in the toxicity prediction model discussed in Section 1.2.1.

There are a number of assumptions associated with FQ, (1) the fluorophore forms the complex with the metal, not another non-fluorescent part of the molecule; (2) the quenching occurs via a static interactions (chemical complexation) and not collisional or

dynamic (physical interactions) (Ryan and Weber 1982). In the case of the first assumption, fluorophores that do not bind the metal will not show any changes in the intensity, however, if there are other parts of the molecule that bind metal but do not fluoresce will not be detected by FQ technique, and thus result in the underestimation of the binding strength. There are no ways to directly measure this binding unless FQ is combined with other techniques, such as ISE. Analysis similar to this was performed on copper (Cu) and DOM by Cabaniss and Shuman (1986). The study found that at low Cu concentrations the two techniques predicted similar values for bound Cu concentrations; however, there was a discrepancy at higher Cu concentrations. The authors proposed a possibility of the inappropriate assumptions for FQ associated with higher Cu concentrations and DOM interactions. The model was later improved by Smith and Kramer (2000) by incorporating a multiple site assumption. Five different DOM components were identified and included in the modeling. Nevertheless, by combining two techniques it was possible to validate the results of both techniques for a certain range of Cu concentrations, and, in this case, there were no non-fluorescent ligands detected.

The second assumption used in FQ is that the reduction in fluorescence intensity is a result of the direct chemical binding of metal to DOM. However, FQ can also occur as a result of physical collisions of the quencher with the fluorophore in the excited state, which would results in a loss of energy via heat (Lakowicz 2010; van de Weert and Stella 2011). A diagram of this process can be seen on Figure 1-4, where the fluorophore is shown to absorb energy, which promotes the electrons to a more energetic state (F*). From this state in the absence of a quencher the return of the electron to the ground state

would result in the release of a photon, however, in the presence of a quencher the energy can be absorbed by either the collision with the excited fluorophore in case of dynamic quenching or the formation of excited fluorophore-quencher complex, which would result in the non-fluorescent molecule in case of the static quenching. It is important to note that the absence of fluorescence of the complex is assumed by Stern-Volmer theory of fluorescence (Lakowicz 2010); however, it is not by RW model that is used for this study.

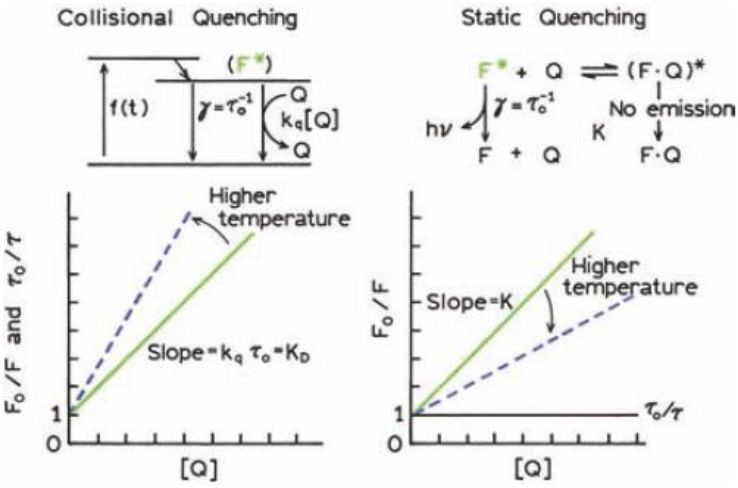

Figure 1-4. Comparison of static and dynamic quenching mechanism and its dependence on temperature, where F - fluorescence intensity, K - rate constant and Q - quencher (Lakowicz, 2010).

It is impossible to determine the mechanism of quenching looking at the FQ results. The most effective way of distinguishing between the static and dynamic quenching is to observe the lifetimes of fluorescence (Lakowicz and Weber 1973), however, it requires specialized equipment. There are two other ways of determining the mechanism; they are absorbance readings and temperature dependence. A decrease of absorbance values at an excitation wavelength used in fluorescence measurements during

titration can signify static interactions as the formation of complex alters the structure of the fluorophore (Lakowicz 2010). Alternately, obtaining the fluorescence readings at higher temperatures may reveal a decrease or an increase in the slope of the Stern-Volmer plot (initial F divided by observed F versus concentration of a quencher), which would signify static or dynamic quenching, respectively (Figure 1-4, Lakowicz 2010). This occurs due to an increase of collisions at higher temperatures and a decrease of the complex stability. These techniques are often used in biochemistry field, when studying proteins interactions in biochemical systems. Theoretically, similar approaches can be applied to DOM and metal studies. However, the main difference between DOM and proteins is the heterogeneity of DOM, which has a possibility of multiple site of action as well as multiple fluorophores. It is possible that the molecular structure of DOM is too complex, and these techniques may not be appropriate for the determination of the quenching mechanism (Appendix A1).

1.4.1.1 Emission-Excitation Matrices (EEMs) and SIMPLISMA

DOM can contain a number of fluorophores due to heterogeneous nature of the molecule. One way to capture the diversity of fluorescent species is to create an excitation-emission matrix (EEM) of the DOM, which can be viewed as a contour plot with major fluorescent peaks identified. Humic-like and fulvic-like components of DOM fluoresce at longer wavelength than proteinaceous components (Baker 2001). Generally, humic-like components can be found in the Ex/Em range of 250-390 nm/450-500 nm, while fulvic-like component emit light at lower wavelength of 400-450 nm, but they have similar excitation wavelengths (Chen et al. 2003; Leenheer and Croue 2003; Stedmon and Markager 2005; Stedmon et al. 2003; Wu et al. 2011). Protein-like peaks are often

divided into tyrosine and tryptophan-like, which have Ex/Em ranges of 225-274 nm/300 nm and 225-270 nm/340 nm, respectively (Chen et al. 2003; Leenheer and Croue 2003; Stedmon and Markager 2005; Stedmon et al. 2003; Wu et al. 2011). Thus, the EEMs can be used as a qualitative technique to characterize DOM, based on the intensity and position of the major fluorophore peaks (Baker 2001; Cory and McKnight 2005).

Metals can interact with more than one component within the DOM, thus, it is important to capture these interactions during a titration. One way to do so effectively is to run a variable angle synchronous scan, which takes a slice through EEM representative of the best selection of components (Galapate et al. 1998). The spectra obtained from this type of scan can be resolved into single components using a data analysis technique described by Windig and Guilment (1991), also known as simple-to-use interactive self-modeling mixture analysis (SIMPLISMA). SIMPLISMA uses the concept of pure variable which defines an area of the spectrum where the intensity is derived from only one component in the system. Multiple spectra with variable concentrations are required for this analysis, an example being a FQ spectrum, where the concentration of components changes upon addition of metal. The definition of first pure variable is determined using the following equation:

$$p_{i,j} = \frac{\sigma_i}{(\mu_i + \alpha)}$$ Equation 1-7

σ – standard deviation
μ – mean of intensity at each variable (wavelength) calculated using all spectra
α – correction factor, for mean that is close to zero

After the pure variables have been identified pure spectra and concentrations of each component are determined. These components can then be analyzed independently using a RW model discussed previously. Such an approach has been used previously (Smith and Kramer 2000) for multisite binding of fulvic acids with copper.

1.4.3 Ion-Selective Electrode

Another technique that can be used to measure free metal ion directly in water is an ion-selective electrode (ISE). The name suggests that these electrodes are able to selectively detect an ion of interest. There are three main types of electrodes that have been in use, a glass electrode, solid state electrode and liquid-ion exchanger membrane electrode (Fisher 1974). Both glass electrode and solid state electrodes (crystalline sensing membrane made of compounds other solids than glass, such as inorganic salts) rely on the interaction of the ion with the immobilized membrane, whereas liquid ion exchange membranes have a level of mobility associated with the ionophore more appropriate for the multivalent metals (Fisher 1974). In this project a liquid membrane electrode was used. In the liquid ion exchanger membrane the ionophore is imbedded into a PVC matrix, which can be inserted into a commercially available electrode body. Electrodes prepared using this type of membrane have been developed and applied since the 1960s (Bakker et al. 1997; Craggs et al. 1974; Ross 1967). An ideal ISE responds to the presence of only one type of metal ion in water (Harris 2003). A schematic representation of the ISE is shown in Figure 1-5. The ligand (L) is imbedded within the PVC membrane and it is able to bind ion (C^+). For charge neutrality as well as for improved cation transfer across the membrane, a negatively charged but hydrophobic ion (R^-) is added to the PVC matrix (Bakker et al. 1997; Harris 2003). Both inner filling

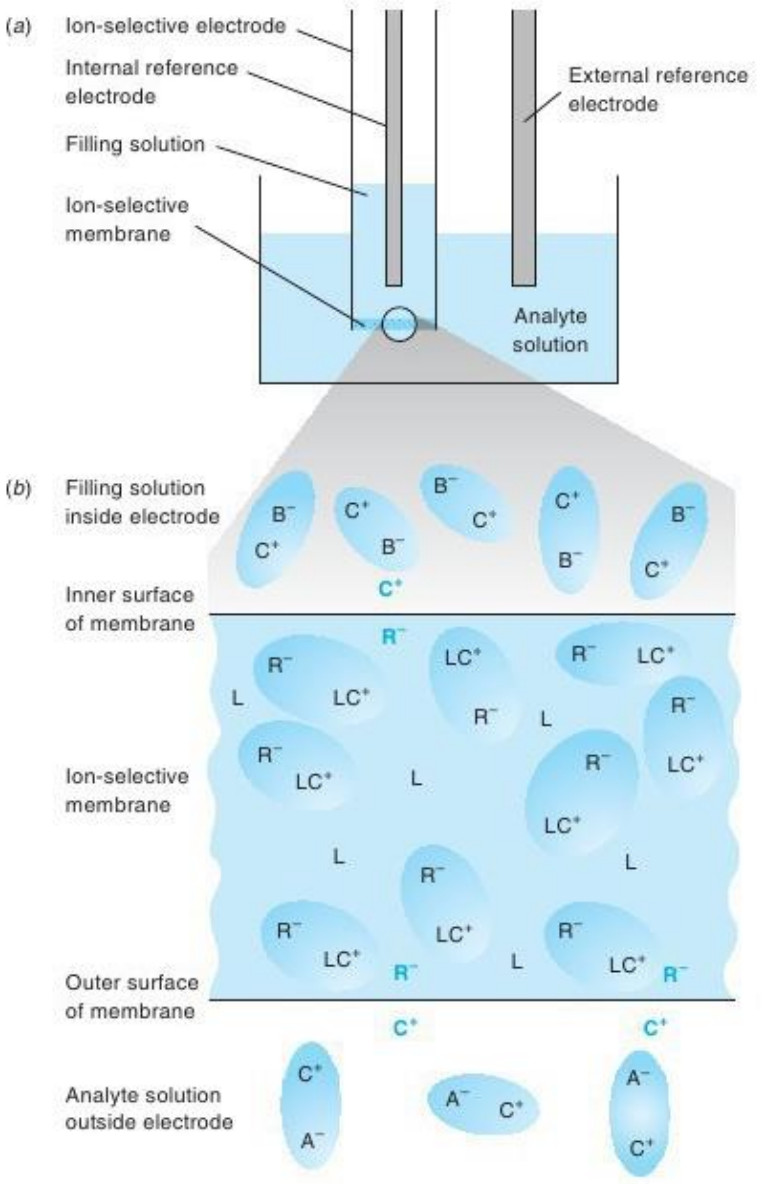

Figure 1-5. Schematic representation of the ISE, adapted from Harris (2003). (a) ISE in the solution containing analyte of interest (C^+) together with the external reference electrode. (b) Closer look at the PVC membrane containing sensing ligand (L), lipophilic ion (R^-) and saturated with analyte. Bolded blue ions represent excess charge. The electric potential difference across the membrane depends on the activity of analyte in the solution.

solution and analyte solutions contain the ion of interest, which creates a difference in electric potential across the membrane that can be measured using two reference electrodes (usually Ag/AgCl based), one placed inside the ISE (internal reference) and one immersed in the sample solution (external reference) (Harris 2003). Free metal concentration, thus, can be calculated using the Nernst equation (Gilbert et al. 2014; Harris 2003; Umezawa et al. 1995):

$$E = E° - \frac{RT}{nF}\ln(\frac{1}{(\alpha i + K'\alpha X)}) \qquad \text{Equation 1-8}$$

E and E° - electric potential, measured and reference, respectively
R – gas constant (8.314 J/mol K)
F – Faraday constant ($9.65*10^4$ C/mol)
T – temperature (assume room temperature of 298K)
α – activity of ion of interest (i) or competitive ion (X)
K' – selectivity coefficient, which is proportional to ratio of α_i and α_X
n – number of electrons exchanged

The term containing a selectivity coefficient (K') is introduced into the equation, since the electrode is likely to respond to more than one ion. The term calculates the ratio of response to the ion *X* over the response for ion *i*. For the purpose of measuring free metal ion in the solution during titration the selectivity of the ion is not vital, as the change in the response of the electrode will only be attributed to the increasing concentrations of one type of metal ion. Therefore, this term maybe removed from the equation. After substituting the constants and converting ln to log Nernst equation becomes:

$$E = E° - \frac{0.0592}{n} log\left(\frac{1}{\alpha i}\right) \qquad \text{Equation 1-9}$$

To make it more specific to Sm, which is measured in this study, *n* variable can be substituted with 3, as Sm has an oxidation state of 3+; and log ($1/\alpha_{Sm3+}$) can be represented by pSm. The final equation can be written as:

$$E = E° - 0.0197pSm$$ Equation 1-10

During an experiment a calibration curve can be created by plotting the measured electric potential (E) against – log(Sm) to obtain a linear equation that can used to calculate Sm ion activity. The conversion between ion activity and concentration ((Sm) = ɣ[Sm]) can be accomplished by calculating an activity coefficient (ɣ) using extended Debye-Huckel equation, which is as follows (already adjusted for measurement of Sm ion):

$$\log \gamma = \frac{-0.51\ x\ (+3)^2\ x\ \sqrt{IS}}{1 + \left(\frac{900\ pm\ x\ \sqrt{IS}}{305}\right)}$$ Equation 1- 11

IS – ionic strength, see Equation 1-12
(+3) – the charge of Sm ion
900 pm – ionic size of Sm ion (Harris 2003)

$$IS = \frac{1}{2}\sum_{i=1}^{n} c_i z_i^2$$ Equation 1- 12

n – number of ions
c – molar concentration
z – ion charge

There are four main components to creating an ISE membrane: polymer, plasticizer, lipophilic salt and ion-selective ligand (Figure 1-5). PVC is commonly used as a polymer in the creation of ISEs. It is composed of the repeating units of vinyl chloride monomer with the chemical formula of (CH2–CHCl). PVC is naturally a very

rigid molecule due to strong polar chloride and hydrogen interactions (Stark et al. 2001), and for the purpose of membrane construction it is vital to introduce an additive that will make the membrane more flexible (Harris 2003; Stark et al. 2001). Such additives are known as plasticizers and by weight they are the major constituent of the membrane (Armstrong and Horvai 1990). It was shown that the plasticizer/PVC percentages of 60%/30% within the membrane produce the optimal results (Armstrong and Horvai 1990; Bakker et al. 1997; Oesch and Simon 1980). In fact leaching of the plasticizer from the membrane over time is the main contributor to the decreased lifetime of the electrode (Stark et al. 2001). The polarity of the plasticizer is also very important to the response of the ISE; it is usually represented by dielectric constant with higher value signifying a more polar substance. Electrode membranes prepared with plasticizers that have high dielectric constants (such as o-NPOE with the values in the range of 21-23.9) are more selective and have lower detection limits than the membrane prepared with plasticizers with low dielectric constants (such as DOS with the values in the range of 3.9-4.2) (Zahran et al. 2010; Zahran et al. 2014; Bakker et al. 1997; Armstrong and Horvai 1990). High polarity of the plasticizer tends to stabilize the charge within membrane (Bakker et al. 1997). As mentioned previously, the positive charge from the analyte can also be neutralized by the addition of lipophilic anion; lipophilicity, in this case, is an outmost importance as the anion should not leave the membrane mixture (Harris 2003). Finally, the ligand for the ISE is usually an organic molecule that can selectively bind the analyte of interest; however, the binding should be reversible (Bakker et al. 1997; Harris 2003). The proper selection of membrane ingredients and their amounts is vital for the

construction of a working ISE. Optimal membrane composition is determined experimentally.

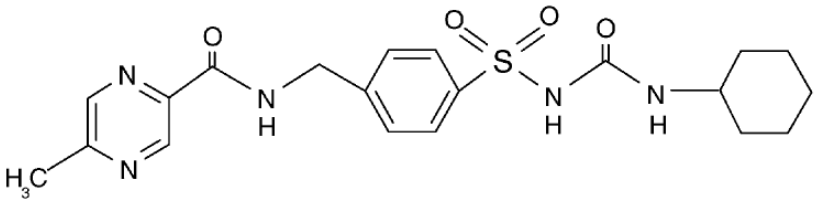

Figure 1-6. Chemical structure of glipizide.

There are no commercially available lanthanide-selective electrodes on the market; however, it is possible to find 'recipes' for construction of ISE in literature. A Sm-selective electrode design was proposed by Ganjali et al. (2003) using glipizide as a ligand (Figure 1-6). The authors provide calibration curve, which shows a linear response of electric potential for Sm concentrations ranging from 10^{-6} M to 10^{-1} M. The slope value of 19.8 was observed, which is close to the Nernstian slope of 19.7 (Ganjali et al. 2003). Additionally, the electrode performed well within the wide range of naturally occurring neutral pH values (2-11). The interference from other ions was considered to be negligible with the selectivity coefficients values below 10^{-3} for all major cations and other lanthanide ions. The electrode was reported to have a lifetime of 4 weeks. Based on these characteristics the electrode was selected for this study.

1.5 Project Objectives

There were two main objectives to this thesis. They include method validation, which involves development of analytical techniques through comparison of their ability to measure lanthanide speciation, and the application of these techniques in the

measurement of DOM and lanthanide interactions. The two techniques selected were fluorescence quenching and ion-selective electrode. The objectives are further discussed in more detail.

1. Method validation through comparison

Two analytical techniques were considered for lanthanide speciation measurements: fluorescence quenching (FQ) and ion-selective electrode (ISE). ***Hypothesis:*** *Both techniques will measure and give estimates of the free lanthanide ion in freshwater environment.* The results from the experiments will be discussed in Chapter 2 and 3 of this thesis. The selected techniques are assumed to measure free metal ion, as they rely on equilibrium ion interactions and do not measure the labile metal portion, as do techniques that use size exclusions and/or charge separation, such as ultrafiltration and Donnan membrane technique (Saar and Weber 1982). ISE was the most promising of the techniques as it directly measures free metal ion, whereas FQ does so indirectly and require modeling and calculations. Another advantage of ISE over FQ is that it is able to capture a wider range of potential ligands, whereas FQ is only able to measure binding to the fluorescent ligands. The techniques were evaluated by comparing free metal concentrations predicted or measured by both techniques. Since ISE was only developed for Sm, the comparisons between FQ and ISE will be discussed with respect to Sm in Chapter 3. Preliminary results and method development performed during the course of the thesis will be covered in Appendix A, since they do not directly fall under this objective.

2. Method application

The second portion of the project relies on the application of both techniques to measure Sm and Dy speciation. Both analytical techniques were used to measure free Sm ion in samples from five DOM sources. And only FQ was used to measure Dy ion in the same samples. ***Hypotheses:*** (1) *DOM will bind lanthanide ions, thus lowering free metal ion in water;* (2) *DOM will provide protective qualities against toxicity as a result of the lower free metal ion;* (3) *There will be a difference in the binding parameters for various DOM sources.* There is limited data available on the speciation of lanthanide with DOM; however, there is some evidence of binding discussed in Section 1.2.3. Five different sources of DOM were chosen to assess if the quality of DOM has an effect on the metal binding. The results of this comparison are discussed in Chapters 2 and 3. The binding parameters calculations were performed on both techniques, which were used to create two speciation models. These models were then used to analyze LC_{50} values provided by a toxicology group; and they were also compared to WHAM predictions. These comparisons and analysis are discussed in Chapter 4.

1.6 References

Al-Reasi, H.A., Wood, C.M., Smith, D.S. 2011. Physicochemical and spectroscopic properties of natural organic matter (NOM) from various sources and implications for ameliorative effects on metal toxicity to aquatic biota. Aquatic Toxicology 103: 179-190.

Al-Reasi, H.A., Wood, C.M., Smith, D.S. 2013. Characterization of freshwater natural dissolved organic matter (DOM): Mechanistic explanations for protective effects against metal toxicity and direct effects on organisms. Environment international 59: 201-207.

An-Chao, G., Shen, Z., Høiland, H. 1998. Complex behaviour of trivalent rare earth elements by humic acids. Journal of Environmental Sciences 10: 302-308.

Armstrong, R.D., Horvai, G. 1990. Review Article: properties of PVC based membrane used in ion-selective electrodes. Electrochimica Acta 35: 1-7.

Avalon Rare Metals Inc. (Avalon). 2013. Nechalacho rare earth element project effluent quality criteria report. Prepared by TetraTech. Accessed: http://www.mvlwb.ca/Boards/mv/Registry/2010/MV2010L2-0005/MV2010D0017%20-%20MV2010L2-0005%20-%20Avalon%20-%20Attachment%20J_Effluent%20Quality%20Criteria.pdf on January 15, 2016.

Baker, A. 2001. Fluorescence excitation-emission matrix characterization of some sewage-impacted rivers. Environmental Science and Technology 35: 948-953.

Bakker, E., Buhlmann, P., Pretsch, E. 1997. Carrier-based ion-selective electrodes and bulk optodes. 1. General characteristics. Chemical Reviews 97: 3083-3132.

Biswas, B.K., Inoue, K., Ghimire, K.N., Ohta, S., Harada, H., Ohto, K., Kawakita, H. 2007. The adsorption of phosphate from an aquatic environment using metal-loaded orange waste. Journal of Colloid and Interface Science 312: 214-223.

Borgmann, U., Couillard, Y., Doyle, P., Dixon, D.G. 2005. Toxicity of sixty-three metals and metalloids to *Hyalella azteca* at two levels of water hardness. Environmental Toxicology and Chemistry 24: 641-652.

Cabaniss, S.E., Shuman, M.S. 1986. Combined ion selective electrode and fluorescence quenching detection for copper-dissolved organic matter titrations. Analytical Chemistry 58: 398-401.

CCME (Canadian Council of Ministers of the Environment). 2011. Canadian Water Quality Guidelines for the Protection of Aquatic Life. CCME, Winnipeg.

ChemInfo Services Inc. 2012. Review of the rare earth elements and lithium mining sectors. Final Report. Prepared for Environment Canada. Accessed http://www.miningwatch.ca/sites/www.miningwatch.ca/files/review_of_the_rare_earth_elements_and_lithium_mining_sectors.pdf January 15, 2016.

Chen, J., LeBoeuf, E.J., Dai, S., Gu, B. 2003. Fluorescence spectroscopic studies of natural organic matter fractions. Chemosphere 50: 639-647.

Chen, W., Westerhoff, P., Leenheer, J.A., Booksh, K. 2003. Fluorescence excitation-emission matrix regional integration to quantify spectra for dissolved organic matter. Environmental Science and Technology 37: 5107-5710.

Chen, Z., Campbell, P.G.C., Fortin, C. 2012. Silver binding by humic acid as determined by equilibrium ion-exchange and dialysis. The Journal of Physical Chemistry 116: 6532-6539.

Cory, R.M., McKnight, D.M. 2005. Fluorescence spectroscopy reveals ubiquitous presence of oxidized and reduced quinones in dissolved organic matter. Environmental Science and Technology 39: 8142-8149.

Craggs, A., Moody, G.J., Thomas, J.D.R. 1974. PVC matrix membrane ion-selective electrodes. Journal of Chemical Education 51: 541-544.

Curtis, P.J., Schindler, D.W. 1997. Hydrologic control of dissolved organic matter in low-order Precambrian Shield lakes. Biogeochemistry 36: 125-138.

Di Toro, D.M., Allen, H.E., Bergman, H.L., Meyer, J.S., Paquin, P.R., Santore, R.C. 2001. Biotic Ligand Model of the acute toxicity of metals. 1. Technical basis. Environmental toxicology and Chemistry 20: 2383-2396.

Dong, W., Li, W., Tao, Z. 2002. Use of the ion exchange method for the determination of stability constants of trivalent metal complexes with humic and fulvic acids II. Tb^{3+}, Yb^{3+} and Gd^{3+} complexes in weakly alkaline conditions. Applied Radiation and Isotopes 56: 967-974.

El-Akl, P., Smith, S., Wilkinson, K.J. 2015. Linking the chemical speciation of cerium, to its bioavailability in water for freshwater alga. Environmental Toxicology and Chemistry 34: 1711-1719.

Elbaz-Poulichet, F., Dupuy, C. 1999. Behaviour of rare earth elements at the freshwater-seawater interface of two acid mine rivers: the Tinto and Odiel (Andalucia, Spain). Applied Geochemistry 14: 1063-1072.

EPA (United States Environmental Protection Agency). 2012. Rare Earth Elements: A Review of Production, Processing, Recycling, and Associated Environmental Issues.

Office of Research and Development. EPA/600/R-12/575. Revised December 2012. Accessed http://www.miningwatch.ca/files/epa_ree_report_dec_2012.pdf on January 15, 2016.

Faure, G., Mensing, T.M. 2007. Chapter 4: Life and Death of Stars, Introduction to Planetary Science: The Geological Perspective. Netherlands: Springer p. 42.

Fellman, J.B., Hood, E., Spencer, R.G. 2010. Fluorescence spectroscopy opens new windows into dissolved organic matter dynamics in freshwater ecosystems: A review. Limnology and Oceanography 55: 2452-2462.

Fischer, R.B. 1974. Ion-selective electrodes. Journal of Chemical Education 51: 387-390.

Florence, T.M., Morrison, G.M., Stauber, J.L. 1992. Determination of trace element speciation and the role of speciation in aquatic toxicity. The Science of the Total Environment 125: 1-13.

Fortin, C., Campbell, P.G.C. 1998. An Ion-Exchange Technique for Free-Metal Ion Measurements (Cd^{2+} Zn^{2+}): Applications to Complex Aqueous Media. International Journal of Environmental Analytical Chemistry 72: 173-194.

Galapate, R.P., Baes, A.U., Ito, K., Mukai, T., Shoto, E., Okada, M. 1998. Detection of domestic waste in Kupose river using synchronous fluorescence spectroscopy. Water Resources 32: 2232-2239.

Gammons, C.H., Wood, S.A., Nimick, D.A. 2005. Diel behavior of rare earth elements in a mountain stream with acidic to neutral pH. Geochimica et Cosmochimica Acta 69: 3747-3758.

Ganjali, M.R., Pourjavid, M.R., Rezapour, M., Haghgoo, S. Novel samarium(III) selective membrane sensor based on glipizid. Sensors and Actuators B 89: 21-26.

Gilbert, T.R., Kirss, R.V., Foster, N. 2014. Chemistry: an Atoms-focused approach. New York: W.W. Norton&Company pp. 109, 777.

Gimeno Serrano, M.J., Auque Sanz, L.F., Nordstrom, D.K. 2000. REE speciation in low-temperature acidic waters and the competitive effects of aluminum. Chemical Geology 165: 167-180.

Gonzalez, V., Vignati, D.A.L., Leyval, C., Giamberini, L. 2014. Environmental fate and ecotoxicity of lanthanides: Are they a uniform group beyond chemistry? Environment International 71: 148-157.

Gu, Z., Wang, X., Gu, X., Cheng,J., Wang, L., Dai, L., Cao, M. 2001. Determination of stability constants for rare earth elements and fulvic acids extracted from different soils. Talanta 53: 1163-1170.

Hamilton-Taylor, J., Ahmed, I.A.M., Davison, W., Zhang, H. 2011. How well can we predict and measure metal speciation. Environmental Chemistry 8: 461-465.

Harris, D.C. (ed). 2003. Quantitative Chemical Analysis (6th ed). USA (NY): W.H. Freeman and Company pp. 320-337, 393.

Hudson, N., Baker, A., Reynolds, D. 2007. Fluorescence analysis of dissolved organic matter in natural, waste and polluted waters – a review. River Research and Application 23: 631-649.

Janssen, R.P.T., Verweij, W. 2003. Geochemistry of some rare earth elements in groundwater, Vierlingsbeek, The Netherlands. Water Research 37: 1320-1350.

Johannesson, K.H., Lyons, W.B., Stetzenbach, K.J., Byrne, R.H. 1995. The Solubility control of rare earth elements in natural terrestrial waters and the significance of PO_4^{3-} and CO_3^{2-} in limiting dissolved rare earth concentrations: a review of recent information. Aquatic Geochemistry 1: 157-173.

Karraker, D.G. 1970. Coordination of trivalent lanthanide ions. Journal of Chemical Education 47: 424-430.

Lakowicz, J.R. 2010. Principles of Fluorescence Spectroscopy (3rd ed). USA (NY): Springer p. 277-318.

Lakowicz, J.R., Weber, G. 1973. Quenching of fluorescence by oxygen. A probe for structural fluctuations in macromolecules. Biochemistry 12: 4161-4170.

Lead, J.R., Hamilton-Taylor, J., Peters, A., Reiner, S., Tipping, E. 1998. Europium binding by fulvic acids. Analytica Chimica Acta 369: 171-180.

Leenheer, J.A., Croue, J-P. 2003. Characterizing dissolved aquatic organic matter. Environmental Science and Technology 37: 19A-26A.

Leguay, S., Campbell, P., Fortin, C. 2015 (Accepted). Determination of the free ion concentration of rare earth elements by an ion-exchange technique: implementation, evaluation and limits. Environmental Chemistry. Accessed http://www.publish.csiro.au/view/journals/dsp_journals_pip_abstract_scholar1.cfm?nid=188&pip=EN15136 on January 15, 2016.

Marsac, R., Davranche, M., Gruau, G., Dia, A., Le Coz-Bouhnik, M. 2012. Aluminium competitive effect on rare earth elements binding to humic acid. Geochmica et Cosmochimica Acta 89: 1-9.

Marsac, R., Davranche, M., Gruau, G., Dia, A., Pedrot, M., Le Coz-Bouhnik, M., Braint., N. 2013. Effects of Fe competition on REE binding to humic acid: Origin of REE pattern variability in organic waters. Chemical Geology 342: 119-127.

Marsac, R., Davranche, M., Gruau, G., Le Coz-Bouhnik, M., Dia, A. 2011. An improved description of the interactions between rare earth elements and humic acids by modeling: PHREEQC-Model VI coupling. Geochmica et Cosmochimica Acta 75: 5625-5637.

Martell, A.E., Smith, R.M. 2004. NIST Standard Reference Database 46 Version 8.0, Gaithersburg, USA.

Mayfield, D.B., Fairbrother, A. 2015. Examination of rare earth element concentration patterns in freshwater fish tissues. Chemosphere 120: 68-74.

McKnight, D.M., Boyer, E.W., Westerhoff, P.K., Doran, P.T., Kulbe, T., Andersen, D.T. 2001. Spectrofluorometric characterization of dissolved organic matter for indication of precursor organic material and aromaticity. Limnology and Oceanography 46: 38-48.

Noack, C.W., Dzombak, D.A., Kramalidis, A.K. 2014. Rare earth element distribution and trends in natural waters with focus on groundwater. Environmental Science and Technology 48: 4317-4326.

Oesch, U., Simon, W. 1980. Lifetime of neutral carrier based ion-selective liquid-membrane electrodes. Analytical Chemistry 52: 692-700.

Paquin, P.R., Gorsuch, J.W., Apte, S., Batley, G. E., Bowles, K.C., Cambell, P.G.C., Delos, C.G., Di Toro, D.M., Dwyer, R.L., Galvez, F., Gensemer, R.W., Goss, G.G., Hogstrand, C., Janssen, C.R., McGeer, J.C., Naddy, R.B., Playle, R.C., Santore, R.C., Scheider, U., Stubblefield, W.A., Wood, C.M., Wu, K.B. 2002. The biotic ligand model: a historic overview. Comparative Biochemistry and Physiology, Part C 133, 3-35.

Pourret, O., Davranche, M., Gruau, G., Dia, A. 2007. Competition between humic acid and carbonates for rare-earth elements complexation. Journal of Colloid and Interface Science 305: 25-31.

Protano, G., Riccobono, F. 2002. High contents of rare earth elements (REEs) in stream waters of a Cu–Pb–Zn mining area. Environmental Pollution 117: 499-514.

Ross, J.W. 1967. Calcium-selective electrode with liquid ion exchanger. Science 156: 1378-1379.

Ryan, D.K, Weber, J.H. 1982. Fluorescence quenching titration for determination of complexing capacities and stability constants of fulvic acid. Analytical Chemistry 54: 986-990.

Saar, R.A., Weber, J.H. 1982. Fulvic acid: modifier of metal-ion chemistry. Environmental Science and Technology 16: 510A-517A.

Santore, R.C., Di Toro, D.M., Paquin, P.R., Allen, H.E., Meyer, J.S. 2001. Biotic ligand model of the acute toxicity of metals. 2. Application to acute copper toxicity in freshwater fish and daphnia. Environmental Toxicology and Chemistry 20: 2397-2402.

Schilten, H.R., Schnitzer, M. 1993. A state of the art structural concept for humic substances. Naturwissenschaften 80: 29-30.

Shin., H.S., Lee, B.H., Yang, H.B., Yun, S.S., Moon, H. 1996. Bimodal normal distribution model for binding of trivalent europium by soil fulvic acid. Journal of Radioanalytical and Nuclear Chemistry 209: 123-133.

Slaveykova, V.I., Wilkinson, K.J. 2005. Predicting the bioavailability of metals and metal complexes: critical review of the biotic ligand model. Environmental Chemistry 2: 9-24.

Smith, D.S, Kramer, J.R., Jenne, E.A. (ed). 1998. Adsorption of Metals by Geomedia: Variable, Mechanisms, and Model Applications. USA (California): Academic Press (Chapter 21): p. 448.

Smith, D.S., Kramer, J.R. 2000. Multisite metal binding to fulvic acid determined using multiresponse fluorescence. Analytica Chimica Acta 416: 211-220.

Sneller, F.E.C, Kalf, D.F., Weltje, L., Van Wezel, A.P. 2000. Maximum permissible concentrations and negligible concentrations for rare earth elements (REEs). National Institute of Public Health and The Environment, Report #601501011. Accessed https://www.researchgate.net/publication/27452531_Maximum_Permissible_Concentrations_and_Negligible_Concentrations_for_Rare_Earth_Elements_REEs on January 15, 2016.

Sonke, J.E. 2006. Lanthanide-humic substances complexation. II. Calibration of humic ion-binding model V. Environmental Science and Technology 40: 7481-7487.

Sonke, J.E., Salters, V.J.M. 2006. Lanthanide–humic substances complexation. I. Experimental evidence for a lanthanide contraction effect. Geochimica et Cosmochimica Acta 70: 1495-1506.

Standing Committee on Natural Resources (RNNR). 2014. The rare earth elements industry in Canada - summary of evidence. 41st Parliament, 2nd session. Accessed http://www.miningwatch.ca/sites/www.miningwatch.ca/files/rareearthelements-summary-e.pdf on January 15, 2016.

Stark, T.D., Choi, H., Diebel, P.W. 2005. influence of plasticizer molecular weight on plasticizer retention on PVC geomembranes. Geosynthetics international 12: 1-12.

Stedmon, C.A., Markager, S. 2005. Resolving the variability in dissolved organic matter fluorescence in a temperate estuary and its catchment using PARAFAC analysis. Limnology and Oceanography 50: 686-697.

Stedmon, C.A., Markager, S., Bro, R. 2003. Tracing dissolved organic matter in aquatic environments using a new approach to fluorescence spectroscopy. Marine Chemistry 82: 239-254.

Tait, T.N., Rabson, L.M., Diamond, R.L., Cooper, C.A., McGeer, J.C., Smith, D.S. 2015. Determination of cupric ion concentrations in marine waters: an improved procedure and comparison with other speciation methods. Environmental Chemistry 13: 140-148.

Tang, J., Johannesson, K.H. 2003. Speciation of rare earth elements in natural terrestrial waters: Assessing the role of dissolved organic matter from the modeling approach. Geochimica et Cosmochimica Acta 67: 2321-2339.

Tipping, E. 1994. WHAM - a chemical equilibrium model and computer code for waters, sediments, and soils incorporating a discrete site/electrostatic model of ion-binding by humic substances. Computers and Geosciences 20: 973-1023.

Tipping, E., Lofts, S., Sonke, J. E. 2011. Humic ion-binding model VII: a revised parameterisation of cation-binding by humic substances. Environmental Chemistry 8: 225-235.

Trout, S.R. 1990. Permanent magnets based on the lanthanides. Proceedings of the international symposium on magnets. NY USA pp. 79-90. Accessed http://spontaneousmaterials.com/Papers/Koreapaper.pdf on January 15, 2016.

Umezawa, Y., Umezawa, K., Sato, H. 1995. Selectivity coefficients for ion-selective electrodes: recommended methods for reporting KA, Bpot values. International Union of Pure and Applied Chemistry (IUPAC) 67: 507-618.

van de Weert, M., Stella, L. 2011. Fluorescence quenching and ligand binding: A critical discussion of a popular methodology. Journal of Molecular Structure 998: 144-150.

Verweij, W. 2013. Equilibria and constants in CHEAQS: selection criteria, sources and assumptions. Model Version 10 (February 2013). Accessed http://home.tiscali.nl/cheaqs/ on March 10, 2013.

Weltje, L., Heidenreich, H., Zhu, W., Wolterbeek, H.Th., Korhammer, S., de Goeij, J.J.M., Markert, B. 2002. Lanthanide concentrations in freshwater plants and molluscs, related to those in surface water, pore water and sediment. A case study on the Netherlands. The Science of the Total Environment 286: 191-214.

Windig, W., Guilment, J. 1991. Interactive self-modeling mixture analysis. Analytical Chemistry 63: 1425-1432.

Wood, C.M., Al-Reasi, H.A., Smith, D.S. 2011. The two faces of DOC. Aquatic Toxicology 105S: 3-8.

Wood, S.A. 1990. The aqueous geochemistry of the rare-earth elements and yttrium. 1. Review of available low-temperature data for inorganic complexes and the inorganic REE speciation of natural waters. Chemical Geology 82: 159-186.

Worms, I. A.M., Wilkinson, K.J. 2008. Determination of Ni^{2+} using an equilibrium ion exchange technique: Important chemical factors and applicability to environmental samples. Analytica Chimica Acta 616: 95–102

Wu, J., Zhang, H., He, P-J., Shao, L-M. 2011. Insight into the heavy metal binding potential of dissolved organic matter in MSW leachate using EEM quenching combined with PARAFAC analysis. Water Research 45: 1711-1719.

Xie, F., Zhnag, T.A., Dreisinger, D., Doyle, F. 2014. A critical review on solvent extraction of rare earth from aqueous solutions. Minerals Engineering 56: 10-28.

Yantasee, W., Fryxell, G.E., Addleman, R.S., Wiacek, R.J., Koonsiripaiboon, V., Pattamakomsan, K., Sukwarotwat, V., Xu, J., Raymond, K.N. 2009. Selective removal of lanthanides from natural waters, acidic streams and dialysate. Journal of Hazardous Materials 168: 1233-1238.

Zahran, E.M., Hua, Y., Li, Y., Flood, A.H., Bachas, L.G. 2010. Triazolophanes: a new class of halide-selective ionophores for potentiometric sensors. Analytical Chemistry 82: 368-375.

Zahran, E.M., New, A., Gvalas, V., Bachas, L.G. 2014. Polymeric plasticizer extends the lifetime of PVC-membrane ion-selective electrodes. Analyst 139: 757-763.

Zhao, C-M., Wilkinson, K.J. 2015. Biotic ligand model does not predict the bioavailability of rare earth elements in the presence of organic ligands. Environmental Science and Technology 49: 2207-2214.

CHAPTER 2: DETERMINATION OF SAMARIUM AND DYSPROSIUM SPECIATION USING FLUORESCENCE QUENCHING TECHNIQUE

ABSTRACT

In recent years there has been an increased interest in mining of lanthanide metals in Northern Canada. In order to protect northern aquatic ecosystems from the potential threat posed by the release of these metals, it is important to understand their toxicological effects on the aquatic organisms. For this purpose the biotic ligand model (BLM) is often used. According to the model metal toxicity is proportional to the concentrations of free metal in water, which is controlled by inorganic ligands as well as dissolved organic matter (DOM). The focus of this chapter is to measure Sm and Dy speciation with DOM using fluorescence quenching (FQ) as an analytical technique. Five DOM sources were selected to be titrated separately with Sm and Dy at concentrations ranging from 0 μM to 100 μM. SIMPLISMA was used to resolve the resulting spectra, and the Ryan-Weber model was applied to these quenching curves to calculate binding constants and capacity. Sm and Dy show very similar behaviour, with small range of binding constants (log K: 6.48-6.78) for all samples. In contrast, binding capacity shows source dependence with darkest, more allochthonous DOM having the highest binding capacity (2.72-2.86 μmol/mg C), while lighter autochthonous DOM had the lowest capacity (0.53-0.63 μmol/mg C). The measured parameters of DOM such as specific absorption coefficient (SAC_{340}) and fluorescence index (FI_{370}) show significant (p values of 0.0065-0.034, 95% confidence) but weak correlation with the binding capacity (R^2 values of 0.45-0.62). These predictors of DOM quality, however, may be useful for general assessment of DOM-metal binding. The presence of inorganic ligands, especially carbonate, are proven to play a central role in lanthanide speciation, with the majority of the metal bound in a 1:1 complex with carbonate during the titrations. In natural waters, this would depend on anion and dissolved carbon concentrations; thus, DOM has variable importance as a ligand. FQ must be verified with another technique, before these results can be incorporated into BLM for accurate toxicity prediction.

2.1 Introduction

Recently, there has been an increased interest into research associated with lanthanides in the environment. This group consists of 15 metals (La-Lu), which are incorporated into many products in automotive, medical and electronics manufacturing industries (ChemInfo 2012). Currently, a number of lanthanides are identified to be in critical or near critical supply risk (EPA 2012). It is especially important for the future of sustainable development as lanthanides are required for the production of clean/green technology (EPA 2012). As the demand for these metals increases, so does the interest in their mining and extraction. Canada has large deposits of lanthanides, which are currently considered for mining (ChemInfo 2012). The future development of these projects will have an impact on both Canadian economy and the local environment.

There is a potential for increase of lanthanide concentrations in rivers and lakes, due to leaching from stockpiles and landfills. In order to protect aquatic life, adequate risk assessment is required. The model that is often used for this purpose is called the Biotic Ligand Model (BLM). It assumes that the interaction of the metal at the biotic ligand is proportional to the observed toxicity (Di Toro et al. 2001; Paquin et al. 2002; Santore et al. 2001; Slaveykova and Wilkinson 2005). Special significance lies in the concentration of free metal as it assumed to be the most bioavailable form. Thus, accurate metal speciation model is essential for BLM prediction. Currently, there is little data available for both speciation and toxicity of lanthanides (RNNR 2014); however, it is well known that other constituents in water, such as organic and inorganic ligands, will have an impact on free metal concentration.

The relationship between inorganic ligands and lanthanides (carbonates, phosphates, sulfates, etc.) has been well studies previously (Elbaz-Poulichet and Dupuy 1999; Gammons et al. 2005; Johannesson et al. 1995; Wood 1990). The main complex that controls lanthanides speciation in water is carbonate, especially in neutral and alkaline conditions (Johannesson et al. 1995; Wood 1990). Phosphate precipitates also play an important role by removing lanthanides from the water column due to their low solubility (Johannesson et al. 1995). At lower pH values, however, lanthanides may be bound to sulfates or found in their free form, depending on the concentration of sulfate in water (Elbaz-Poulichet and Dupuy 1999; Wood 1990). The binding stability constants for these species can be found in NIST database (Martell and Smith 2004; Verweij 2013). The main factor that is less well known is the interaction of lanthanides with the organic ligands such as DOM.

DOM has a potential to bind metals due a presence of various binding sites such as on the macromolecule (Tipping et al. 2011). It can be classified into two broad classes, autochthonous (algal or microbial photodegradation) and allochthonous (terrestrially derived) DOM (Leenheer and Croue 2003; Wood et al. 2011). DOM derived from these sources will have different composition and, thus, properties, which can be represented by measuring DOM absorbance and fluorescence. Often excitation-emission matrices (EEMs) are used to determine the presence of different constituents such as humic, fulvic or protein-like components (Chen et al. 2003; Stedmon and Markager 2005; Stedmon et al. 2003; Wu et al. 2011). Calculations of specific index coefficient (SAC_{340}, measure of aromaticity) and fluorescence index (FI_{370}, source predictor) (Al-Reasi et al. 2011; Curtis and Schindler 1997; McKnight et al. 2001), discussed in Section 1.2.2, can provide a way

to categorize different DOM samples. These parameters have previously been shown to correlate with toxicity (Al-Reasi et al. 2011; McKnight et al. 2001; Wood et al. 2011), where higher SAC_{340} and lower FI_{370} are indicative of greater affinity of DOM to some metals (Cu, Ag and Pb). This type of DOM is more protective against metal toxicity. DOM is predicted to bind lanthanide, due to a presence of carboxylic and phenolic groups, to which they have high affinity (Karraker 1970; Sneller et al. 2000; Tipping et al. 2011). There has been some research done into the relationship between lanthanides and DOM (An-Chao et al. 1998; Dong et al. 2002; El-Akl et al. 2015; Gu et al. 2001; Lead et al. 1998; Shin et al. 1996); however, it produces a variable range of stability constants (log K: 3.5-11.6) most likely due to differences in experimental conditions and analytical techniques used.

The accurate measurement of DOM-lanthanide binding parameters can be used to predict free metal concentration in water vital for the BLM prediction of toxicity. Additionally, a metal-DOM complex itself was shown to have some effect on the toxicity (Zhao and Wilkinson 2015). In order to measure this speciation, it is important to select an analytical technique that looks at the equilibrium of the metal and the ligand without influencing it (Saar and Weber 1982). The technique that will be discussed in this chapter is fluorescence quenching (FQ). It relies on the fact that DOM is naturally fluorescent. During a titration with the metal, the decrease of the DOM fluorescence can be recorded and the binding parameters can be calculated using a relationship defined by Ryan and Weber (1982), see Section 1.4.1. Since DOM is a heterogeneous molecule, lanthanides can interact with multiple components. A spectral resolution technique, SIMPLISMA, was utilized (Windig and Guilment 1991) in order to obtain the quenching information

for multiple components that may be present. Incorporation of the inorganic model together with the DOM binding created a more complete speciation model, which can provide support for the use of the model in BLM. Finally, conclusions were drawn about the ability of measured characteristic of DOM to predict the general binding strength and capacity.

2.2 Materials and Methods

The following sections describe sample preparation and experimental procedure of fluorescence quenching, which includes instrumental set up and data analysis.

2.2.1 Chemicals

All chemicals were purchased with the highest purity possible. They were stored according to the recommendations of the manufacturer. The list of chemicals can be found in Table 2-1.

Table 2-1. List of chemicals and their suppliers used in the fluorescence quenching experiments.

Chemical Name	**Supplier**
Dysprosium (III) chloride hexahydrate (>99.9%)	Sigma-Aldrich Corp. (St. Louis, MO, USA)
Samarium (III) sufate octahydrate	Sigma-Aldrich Corp. (St. Louis, MO, USA)
Hydrochloric acid (~30%) (GR ACS)	EMD Chemicals (Gibstown, NJ, USA)
Sodium hydroxide standard (5.0N)	Sigma-Aldrich Corp. (St. Louis, MO, USA)
Sodium bicarbonate (GR ACS)	EMD Chemicals (Gibstown, NJ, USA)
Sodium sulfate decahydrate (Ultra >99%)	Fluka Analytical, Sigma-Aldrich Corp. (St. Louis, MO, USA)

2.2.2 Sample Description and Preparation

Five DOM sources were used for the experiment (Table 2-2). Dissolved organic carbon (DOC) was measured in all DOM concentrates using Shimadzu TOC-$L_{CPH/CPN}$ Analyzer (Shimadzu Corp., Kyoto, Japan). The samples were prepared by filtering the concentrate that have been stirring for 20 minutes (to ensure homogeneity) using 0.45 µm filters. The samples were acidified with a drop of a concentrated HCl before analysis. All DOM titration samples were prepared no more than 3 days prior to the experiments. Filtered (0.45 µm) DOM concentrates were diluted to DOC concentration of 10 ppm using IS (ionic strength) solution representative of freshwater environment (0.011 M prepared with $NaHCO_3$ and Na_2SO_4 with molarity of 0.001 M and 0.0033 M, respectively). $NaHCO_3$ served as a pH buffer. The samples were adjusted to pH of 7.30±0.05 at the beginning of each experiment using 0.1 M HCl and 0.1 M NaOH, and this pH value was maintained throughout the experiment. DOM samples were titrated using standard additions of either Sm or Dy from their respective stock solutions (5000 µM); with the range of metal concentrations of 0 µM to 100 µM. The experiments were done in triplicates. Experimental condition and DOM selection was influenced by the conditions used in toxicological studies performed on *Hyalella azteca*, so that the comparisons can be made, discussed later in Chapter 4.

Table 2-2. DOM sources geographic location, measurements of DOC, SAC_{340} and FI_{370}.

DOM Source Name	**Name**	**Location**	**Coordinates**	**DOC (ppm)[a]**	**SAC_{340}[b]**	**FI_{370}[b]**
Suwannee River[c]	SW DOM	GA	29°17'N 83°9'W	260	29.56	1.04
Southampton	SH DOM	PEI	46°21'N 62°35'W	334	28.5	1.11
Kouchibouguac	KB DOM	NB	46°48'N 64°55'W	394	35.34	1.09

Table 2-2. Continued

DOM Source Name	Name	Location	Coordinates	DOC (ppm)[a]	SAC_{340}[b]	FI_{370}[b]
Luther Marsh	LM DOM	ON	43°54'N 80°26'W	794	38.88	1.05
Burlington Bay	BB DOM	ON	43°48'N 79°50'W	81	7.12	1.51

(a) DOC of samples concentrates was measured after filtering it with 0.45 µm filters
(b) SAC_{340} and FI_{370} were calculated using absorption and fluorescence data as written in Equation 1-1 and 1-2, respectively (Section 1.2.2).
(c) Suwannee River Reference Aquatic NOM was purchased from International Humic Substance Society (IHSS). The powder (300 mg) was diluted in ultrapure water (MilliQ, 18.2Ω) (500 mL) and DOC was measured from that sample. BB DOM was collected by S. Smith in 2014 and LM DOM was collected by J. McGeer in 2014. More information on KB DOM and SH DOM can be found in Cooper (2013) and Nasir (2014).

2.2.3 Fluorescence Measurements

Fluorescence measurements were performed using Varian Cary Eclipse Fluorescence Spectrophotometer (Agilent Technologies, Santa Clara, CA, USA), using flow-through 1 cm quartz cuvette (Starna Cells Inc., Atascadero, CA, USA). The sample was pumped using a peristaltic pump (GILSON, Minipuls 2, France) and flexible PTFE tubing (Tygon®, 2.79 mm I.D.) at all times during the experiment. The tubing and the cuvette were rinsed with MilliQ followed by acidified MilliQ water, prepared by the addition of 0.1 M HCl until measured pH was around 2.00, and with the final rinse of MilliQ water. A MilliQ blank was run before the tubing and the cuvette were emptied and filled with the sample. Between each metal addition and reading the sample was left to stir for about 20 minutes, to ensure equilibrium is reached. The single fluorescence reading at Ex/Em of 340 nm/450 nm was monitored to ensure the equilibrium indeed is reached in 20 minutes. Variable angle synchronous scan was used to make fluorescence reading. The line for the scan was selected visually from the EEM plots. The criterion for line selection included the least complex line that is able to capture the majority of

potential fluorophores or components. The same line was picked for SW, LM, KB and SH DOMs, while BB DOM was scanned using different line, as it was the most spectrally different sample (Table 2-2). The lines can be found in Figure B1. A simple code (Appendix C1) was used for synchronous scan using a built-in spectroscopy language, the Applications Development Language (ADL). High photomultiplier tube setting and medium scan speed settings were set within the regular instrument set up window. All scan readings were done in triplicate.

2.2.4 Data Processing and Analysis

The average of 3 readings as well as the running average using 5 points was used to create the fluorescence spectra (Figure B2, Figure B3 and Figure B7). The resolution of spectral components was accomplished using SIMPLISMA, described in Section 1.4.1.1. The MATLAB^{TM} code for the analysis (Appendix C2) is publically available on MathWorks website (Matlab Central, Artyushkova 2007). There are two parameters that can be changed in the code by the user; they are offset and a number of components. Offset value or correction factor is used for the spectra when mean intensity is approaching zero. When that happens, according to Equation 1-7, the first purity calculation will approach infinity and give false identification of the components; this can be prevented by incorporating an offset value. In this study offset value was set to zero, as there were no regions of such low intensity selected for SIMPLISMA analysis. The number of components was determined based on the shape of the resolved spectra. If one of the component's spectra resembled noise and not an actual spectrum the number was

decreased by one. SIMPLISMA-resolved data of the quenching components was used as an input for the RW model.

Binding constants and capacities were calculated using the RW model (Section 1.4.1). A 1:1 binding ([ML] = [M] + [L]) was used for the modeling. Binding parameters were determined using nonlinear regression analysis with least squares method optimization. Initial guesses were determined heuristically. Monte Carlo (MC) simulations were used to estimate the 95% confidence intervals (95% CI) for the modeled parameters. During these MC simulations a third of the data points were replaced with the model fit and 2% variance to the data points was added to produce a new data set to model. This process was repeated 100 times for each of the samples, thus producing a data set containing 100 points, which was used for statistical calculations. For the purpose of error estimation, 95% CI was calculated using standard deviation (SD) instead of standard error (SE) to stay within the conservative estimate of the data spread, as there was very little noise associated with the data.

The model was incorporated into an inorganic speciation model for a complete speciation picture. The concentrations of inorganic CO_3^{2-} and SO_4^{2-} in matrix were calculated from IS solution preparation (0.001 M and 0.0033 M, respectively). The contribution of CO_3^{2-} and Cl^- from DOM concentrates were also measured using total inorganic carbon (TIC) function on the Shimadzu TOC-$L_{CPH/CPN}$ Analyzer (Shimadzu Corp., Kyoto, Japan) and Cl-selective combination electrode (Mantech, Guelph, ON) and are reported in Table 2-3. The log K values for inorganic species were obtained from NIST database (Martell and Smith 2004; Verweij 2013). The hydroxide solid constants

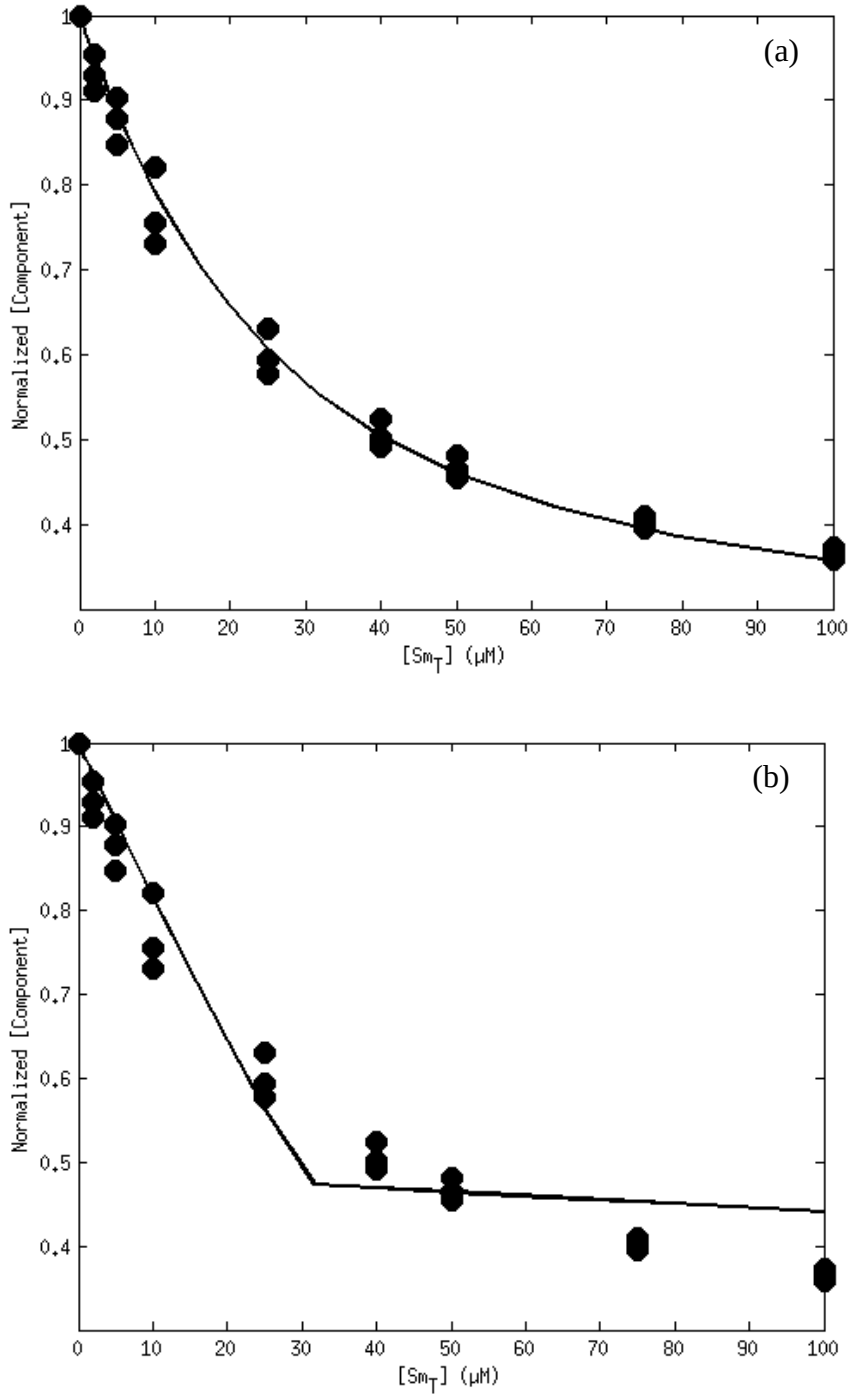

Figure 2-1. Normalized component concentrations for SW DOM titrated with Sm, (a) excluding and (b) including carbonate precipitation. Circles represent measured values and the line shows RW model fit. $Sm_2(CO_3)_3$ solid is predicted to be observed, however it is not seen in the data.

have a large error associated with them (e.g. $Sm(OH)_3$ pK_{sp} = 25.9±9.00). The variation in the values is attributed to the differences in experimental conditions, i.e. IS, temperature and recording time (kinetics) of solid formation (Diakonov et al. 1998). Due to high sensitivity of the model to this value, a selection of a constant was done based on the result of the ISE model (Chapter 3). The selected pK_{sp} value for Sm was 25.5 (Spahiu and Bruno 1995), which was the optimal value that was able to describe the precipitate formation in all ISE samples. The formation of carbonate solid complexes was removed based on the experimental results. Trends in residuals were observed; the model predicted a flat associated with precipitate formation (Figure 2-1b) but it was not observed in the data (data shows no evident flat line). Upon removal of carbonate solid, the RW model was able to fit the data (Figure 2-1a) with no observed trends in residuals. The lack of carbonate formation is likely attributed to slow kinetics of solid formation. It is known that the nucleation of the solid is the slowest step in the precipitate formation of salts; this also translates into slower crystal growth of smaller particles (Johnson and O'Rourke 1954). It is possible that the experiments were not long enough for the precipitation to occur. All MATLAB™ codes for the analysis can be found in Appendix C3.

Table 2-3. Chloride and carbonate measurements in DOM titrations samples. Chloride was not measured in KB DOM sample.

DOM Source	**Cl^- (mM)**	**CO_3^{2-} (mM)**
SW DOM	0.041	0.0023
SH DOM	0.56	0.0018
KB DOM	-	0.0018
LM DOM	0.089	0.0014
BB DOM	5.5	0.25

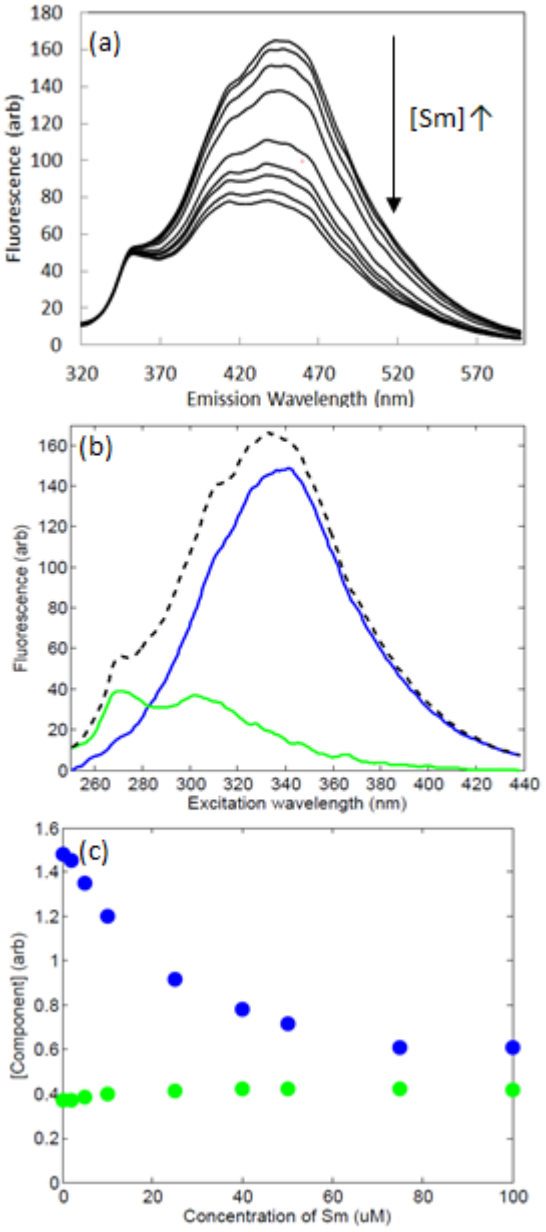

Figure 2-2. (a) A quenching of fluorescence intensity during titration of SH DOM with Sm. The values that at plotted are an average of all trials. Ex: 250-440 nm. (b) SIMPLISMA-resolved spectra and (c) components' concentrations. There were two components identified (blue and green), with the dominant blue exhibiting quenching. The dashed line represents the data of the DOM fluorescence alone.

2.3 Results and Discussion

All of the samples showed quenching with addition of either one of two lanthanides. A representative titration spectrum (Sm with SH DOM) can be seen in Figure 2-2a. The full list of all figures can be found in Appendix B (Figure B2, Figure B3, Figure B7). All spectra had a presence of more than one component as predicted and selected by the synchronous scan lines (Figure B1). That is why they were resolved using SIMPLISMA.

2.3.1 SIMPLISMA Resolved Spectra

SIMPLISMA resolved spectra (Figure 2-2b) identify 2 main components in each of the 4 more allochtonous samples (LM, SH, SW and KB, all had FI_{370} values below 1.4 (McKnight et al. 2001)). The BB DOM sample (FI_{370}=1.51, indicative of more autochtonous DOM), although contained multiple changing peaks, was not able to be resolved by SIMPLISMA. Upon further inspection only one of the peaks

was changing consistently throughout the titration over all the trials (Ex/Em 300-340 nm/400-430 nm); thus, it was treated as one component. Between the two components identified by SIMPLISMA, one of them with a peak found at the longer excitation wavelength (around 340-350 nm with emission at 420-470 nm) was the dominant one having its contribution to the fluorescence spectra calculated by SIMPLISMA as being five times greater than those of the other component. This component is most likely representative of the humic and/or fulvic-like region (Ex: 320-380 nm) of the EEMs (Chen et al. 2003; Stedmon and Markager 2005; Stedmon et al. 2003; Wu et al. 2011). The change in these concentrations at each point in the titration revealed (Figure 2-2c) that the dominant component is also the one that exhibits quenching, whereas the minor component remains the same in its concentration. The minor component is likely representative of the proteinaceous material, which often absorb at lower wavelength (~280 nm). The quenching of this component is not observed, as lanthanides have stronger affinity towards oxygen-containing groups (e.g. carboxylic group found in humic/fulvic acids) than nitrogen-containing groups (e.g. amino group of the proteins) (Sneller et al. 2000; Karraker 1970).

2.3.2 Binding Constants, Binding Capacity and Speciation

The RW modeling was performed on the dominant component quenching curve. A complete list of RW model fits can be seen in Appendix B (Figure B10 to Figure B13) and an example for SW DOM with Sm on Figure 2-1a. All samples with the exception of BB DOM had generally similar quenching curves. The approximate amount of fluorescence intensity quenching observed in KB, SH, and SW DOM was 60%; it was 80% for LM DOM and only 20% for BB DOM. The calculated binding constants and

capacities are shown in Table 2-4 and in Figure 2-3. The binding constants values (log K) are similar across all samples ranging from 6.48 to 6.78, and they are representative of strong binding. The values are similar to the binding between one of the ligands identified in forest soil humic acid and La, Ce, Ho and Yb (log K: 6.26-6.82; An-Chao et al. 1998). Although it is not representative of the aqueous DOM, some of the more allochthonous DOM might have similar composition to the forest soil humic acid (HA). The values are also in between the ones reported for fulvic (FA) and HA interactions with Eu and Ce, separately (FA: 3.5-5.95 (Eu), 5.39 (Ce) and HA: 7.38-7.9 (Eu); Shin et al. 1996; El-Akl et al. 2015). Natural DOM contains a mixture of both FA and HA; and since both are fluorescent in the same region in the EEM, they most likely were not separated by SIMPLISMA and were present in the data as one component. Therefore, it is possible the log K values characterize a mixture of both of these binding entities. Finally, there were no significant differences between Sm and Dy.

Table 2-4. The binding parameters for all samples were calculated using RW model with the input of the quenching data from SIMPLISMA resolved spectra. Statistical parameters were calculated from MC simulations of the model fit, which included inorganic complexation. 95% CI was calculated using SD, not SE.

Sample	**Binding Constant**		**Binding Capacity**	
	Log K	**95% CI**	**Lt (µmol/mg C)**	**95% CI**
Samarium				
SW DOM	6.66	0.036	1.34	0.12
SH DOM	6.62	0.035	1.45	0.082
KB DOM	6.60	0.023	1.20	0.035
LM DOM	6.78	0.017	2.72	0.20
BB DOM	6.48	0.003	0.53	0.0003
Dysprosium				
SW DOM	6.59	0.022	1.39	0.035
SH DOM	6.66	0.043	1.86	0.18
KB DOM	6.60	0.042	1.25	0.068
LM DOM	6.70	0.028	2.86	0.15
BB DOM	6.58	0.002	0.63	0.0004

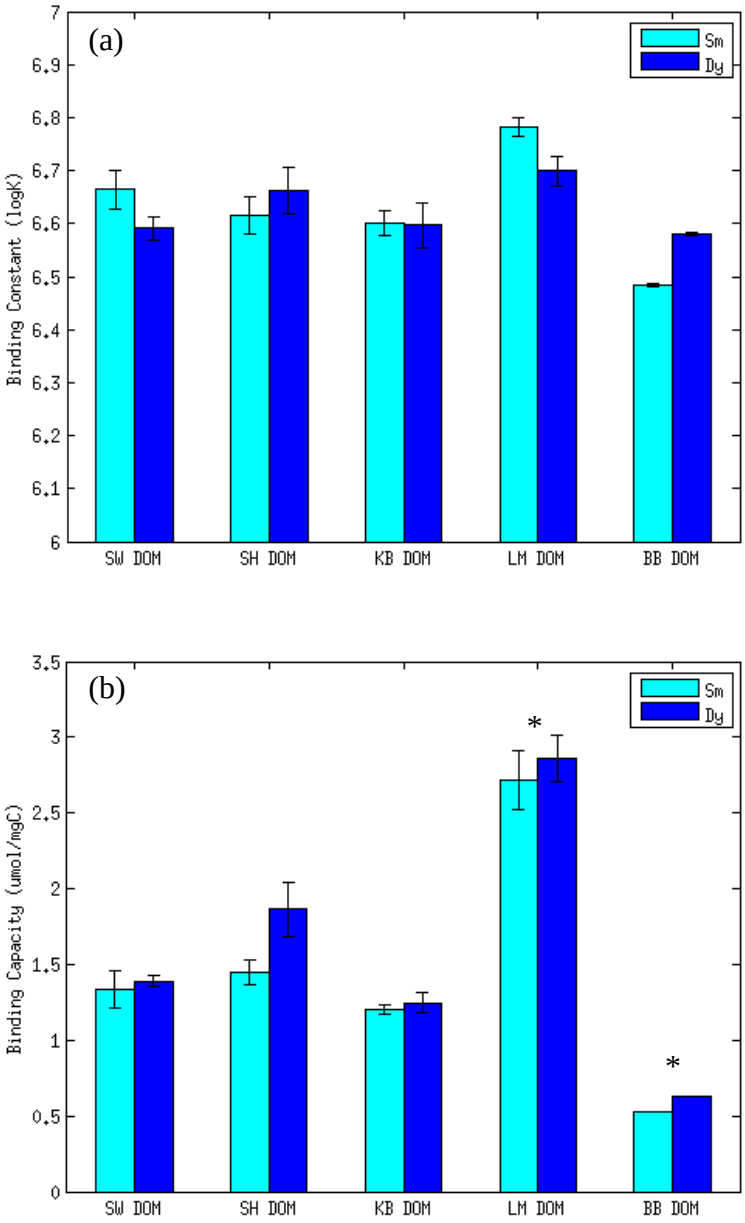

Figure 2-3. Comparison of (a) binding constants (log K) and (b) capacity (µmol/mg C) for Sm and Dy with five DOM samples. The error bars represent 95% CI using SD. There is no difference between binding constants of the samples; however, LM DOM had the highest binding capacity and BB DOM the lowest (* - shows significance, based on the differences between 95% CI overlap). Small 95% CI was observed for BB DOM due to model limitation to capture low amounts of quenching.

Although there were no differences in the binding constants between samples, binding capacity (Lt) show significant source dependence. Amongst all the samples LM DOM has the highest binding capacity (2.72-2.86 μmol/mg C), while BB DOM has the lowest (0.53-0.63 μmol/mg C), the other 3 samples range between 1.20-1.86 μmol/mg C. It is important to note that BB DOM is the most unique of the DOM samples (Table 2-2). It showed the least amount of quenching upon metal addition, and as a result the MC analysis had difficulties in creating a more diverse dataset, which is apparent in the low 95% CI. There are still no distinguishable differences between Dy and Sm. This lack of variability between both constants and capacity for the two lanthanides can be attributed to the uniformity in the chemistry of this group of metals that is associated with the presence of *f* orbitals (Karraker 1970).

Higher binding capacity has a dramatic effect on the lanthanides modeled species distribution during the titration. Table 2-5 shows percentages of the metal species that were observed during the titration, only initial and final values are shown; a visual representation of this change can be seen in Appendix B (Figure B17 to Figure B19 and Figure B23 to Figure B25). Additionally, Figure 2-4 shows an example of the species concentrations during the titration for SH DOM with Sm (all plots are shown in Figure B14 to Figure B16 and Figure B20 to Figure B22). Due to high amounts of CO_3^{2-} and SO_4^{2-} in the sample matrix from the IS solution, a large fraction of the metals is bound to these anions. On average between both lanthanides and overall titration about 60% and 13% are bound to CO_3^{2-} and SO_4^{2-}, respectively, including 1:1 and 1:2 complexes. Additionally, on average about 26% of metal is found as part of the DOM-lanthanide complex; whereas, free metal is present at less than 1%. Differences between samples,

however, are evident. LM DOM, which has the highest binding capacity, is able to bind more of the metal (59% and 68% of Sm and Dy, respectively, at the start of the titration) than BB DOM (14% and 15% of Sm and Dy, respectively) with lower binding capacity. During the course of the titration the lanthanide-DOM complex becomes less dominant in the metal distribution, as the concentrations starts to approach the binding capacity (Figure 2-4). All of the other complexes continue to bind lanthanides. This can be observed in the overall decrease in the percentage of metal bound to DOM from the start to the end of the titration in comparison to increase in percentages of other complexes. Upon addition of the lanthanide, free metal ion increase in the percentage, however, it is still the least abundant species found at about 1% out of the most dominant lanthanide species.

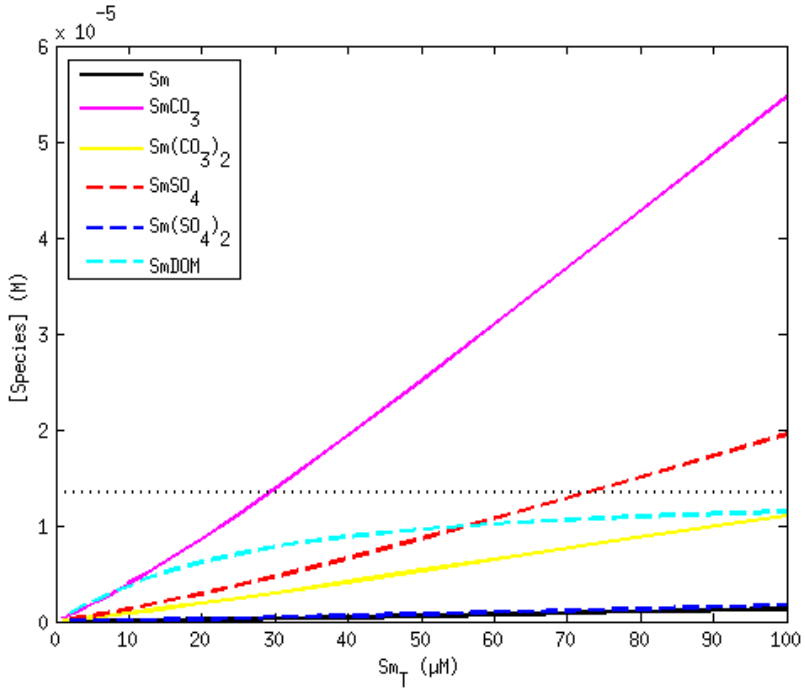

Figure 2-4. Sm species concentrations observed in the FQ titration of SH DOM plotted against total Sm. The black dotted line represents the binding capacity of the DOM. Charges were omitted for clarity.

Table 2-5. Distribution of Sm and Dy during FQ titrations, presented as percentage of the metal (M) species out of the total metal added. Sum of the percentages is close to 100%, which shows that these were the main species found in solution.

Species	SW DOM		SH DOM		KB DOM		LM DOM		BB DOM	
	Start	**End**	**Start**	**End**	**Start**	**End**	**Start**	**End**	**Start**	**End**
Samarium										
$M(CO_3)^+$	35	55	35	54	38	56	20	47	54	61
M-DOM	44	11	44	12	38	10	68	24	14	4
$M(CO_3)_2^-$	8	11	8	11	8	11	4	10	15	16
$M(SO_4)^+$	11	20	12	19	13	20	7	17	14	17
$M(SO_4)_2^-$	1.0	1.7	1.0	1.7	1.1	1.7	0.6	1.5	1.2	1.5
M^{3+}	0.7	1.3	0.8	1.3	0.8	1.3	0.4	1.1	0.9	1.1
SUM[a]	***99.8***	***99.7***	***99.8***	***99.7***	***99.8***	***99.7***	***99.9***	***99.7***	***99.8***	***99.7***
Dysprosium										
$M(CO_3)^+$	39	54	32	51	40	54	25	46	49	56
M-DOM	35	11	46	15	33	10	59	23	15	5
$M(CO_3)_2^-$	16	20	13	19	17	20	10	18	26	27
$M(SO_4)^+$	9	13	7	13	9	14	6	11	9	11
$M(SO_4)_2^-$	0.5	0.7	0.4	0.7	0.5	0.7	0.3	0.6	0.4	0.5
M^{3+}	0.7	1.0	0.6	1.0	0.7	1.0	0.4	0.9	0.6	0.8
SUM[a]	***99.9***	***99.9***	***100.0***	***99.9***	***99.9***	***99.9***	***100.0***	***99.9***	***99.9***	***99.9***

(a) Sum was calculated using non-rounded values

2.3.3 Correlation between DOM Characteristics and Binding Parameters

It is evident from the binding capacity comparisons that the source of DOM has an influence on how it binds metal (BB DOM with Lt of 0.53-0.63 µmol/mg C binds 14-15% of metal vs. LM DOM with Lt of 2.72-2.86 µmol/mg C binds 59-68% of metal). For the prediction of metal binding capability or for monitoring purposes, it is important to have a quick and simple way to assess the quality of DOM. It has been reported that characteristics such as SAC_{340} and FI_{370} have correlation with the observed toxicity (Al-Reasi et al. 2011; Wood et al. 2011). The protective effect of darker more allochthonous DOM can be attributed to the increase in metal binding of this type of DOM.

The five sources of DOM used in these experiments had a variation in SAC_{340} and FI_{370} values. Comparisons between these and the binding parameters are presented in Figure 2-8 through to Figure 2-8 and the correlation is summarized in Table 2-6. In case of Sm, both binding constants and capacity show a positive correlation with SAC_{340} values and a negative correlation with FI_{370} values (Figure 2-5 and Figure 2-6), as evident by the sign of the slope (Table 2-6), with p values (0.0019-0.029) indicating significance with 95% confidence. This implies that the DOM with higher SAC_{340} and lower FI_{370} would be able to bind more Sm than the opposite type of DOM, which would mean a more protective sample against toxicity as was shown previously (Al-Reasi et al. 2011; Wood et al. 2011). The correlation between these parameters was moderately strong to weak with R^2 range of 0.47-0.72.

Similar trends are observed for Dy between both SAC_{340} and FI_{370} and Lt values (Figure 2-7 and Figure 2-8), where p values (0.011-0.034) indicate significance with 95% confidence. However, there is no significant correlation with log K values (p values 0.078-0.16). Although, Sm binding parameters and DOM characteristics showed correlation there were no significant differences between the two lanthanides in the comparison of log K values discussed in Section 2.3.2. The strength of binding constants depends on the functional groups, which are usually very similar between different DOM sources. Therefore, it is unlikely that there should be much difference between various types of DOM.

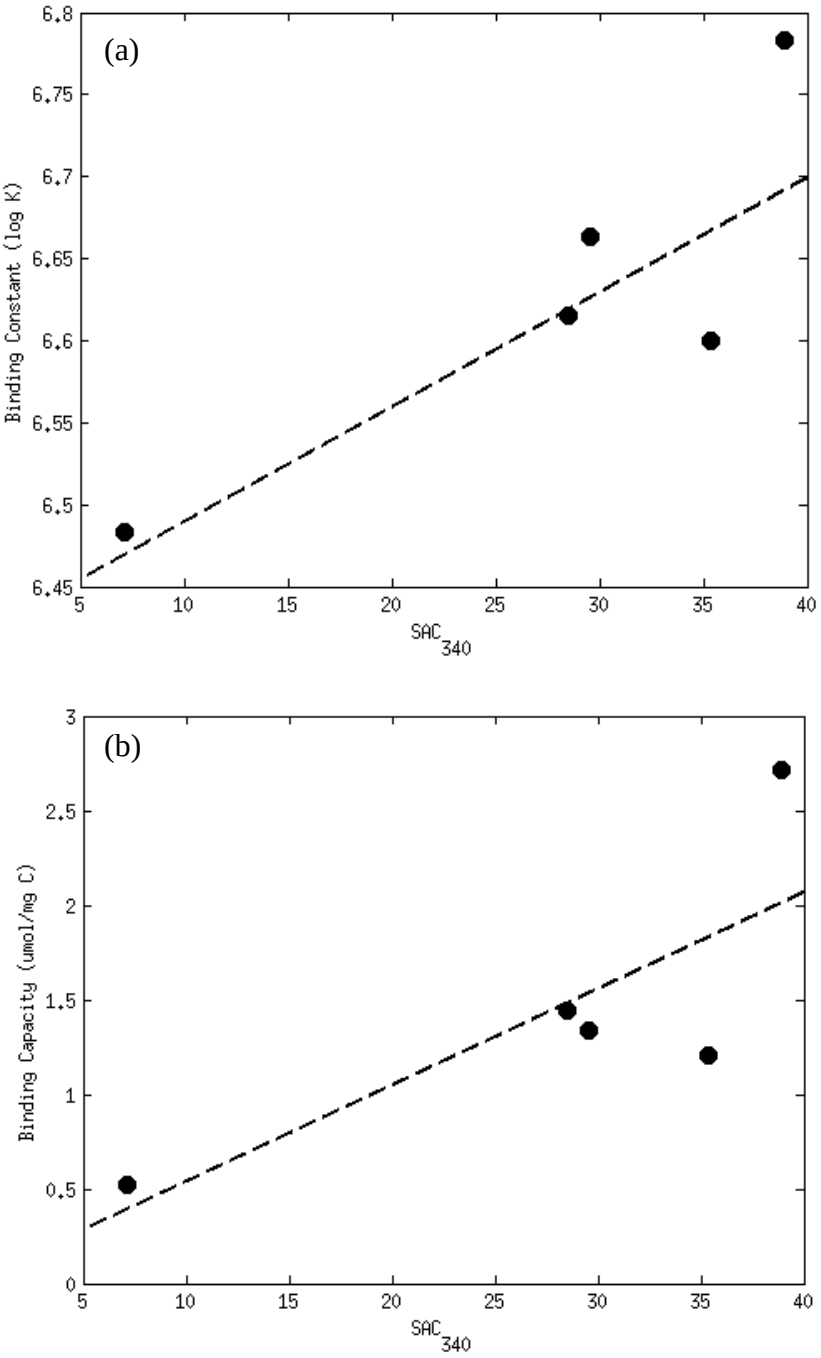

Figure 2-5. Comparisons plots of SAC_{340} with Sm binding constants (a) and capacities (b). The dashed line represents the line of best fit.

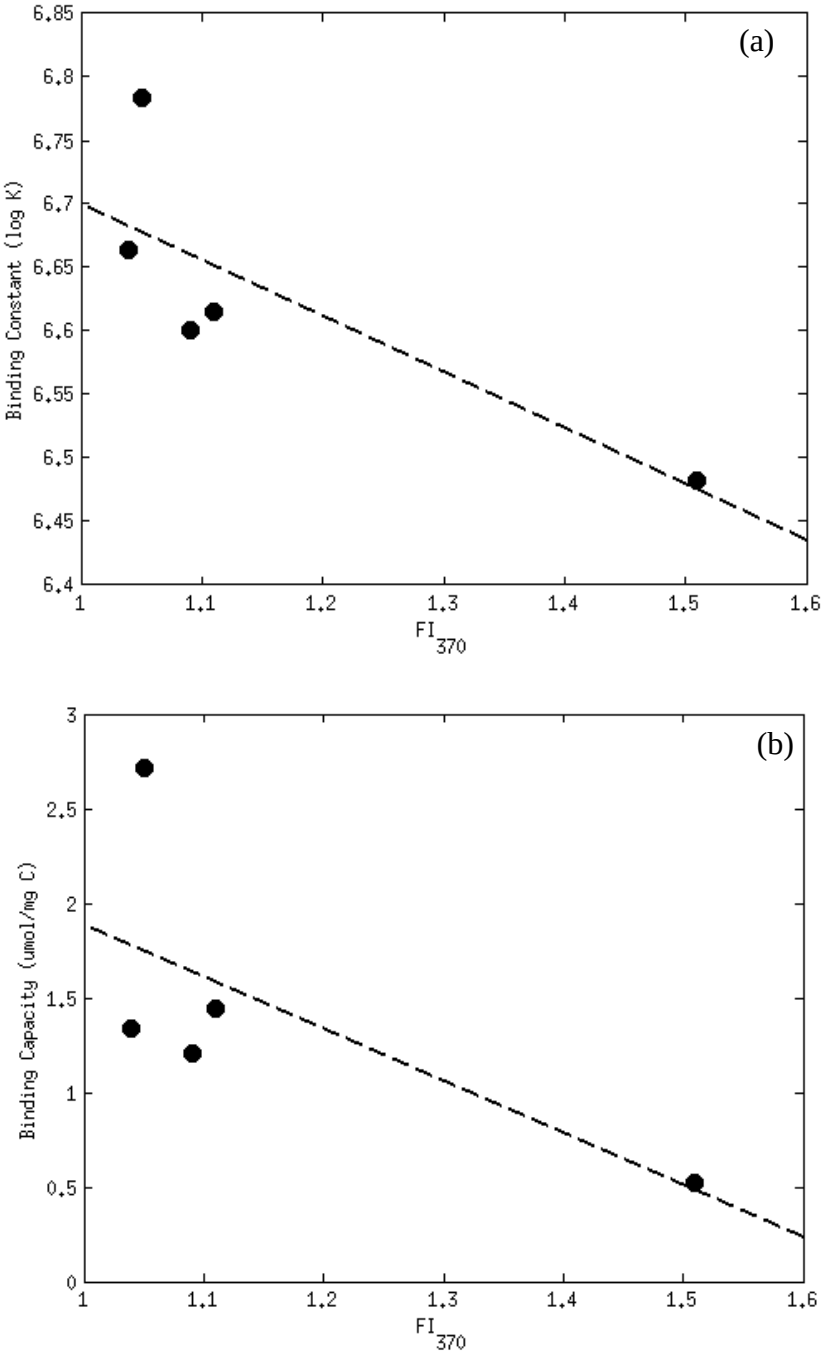

Figure 2-6. Comparisons plots of FI_{370} with Sm binding constants (a) and capacities (b). The dashed line represents the line of best fit.

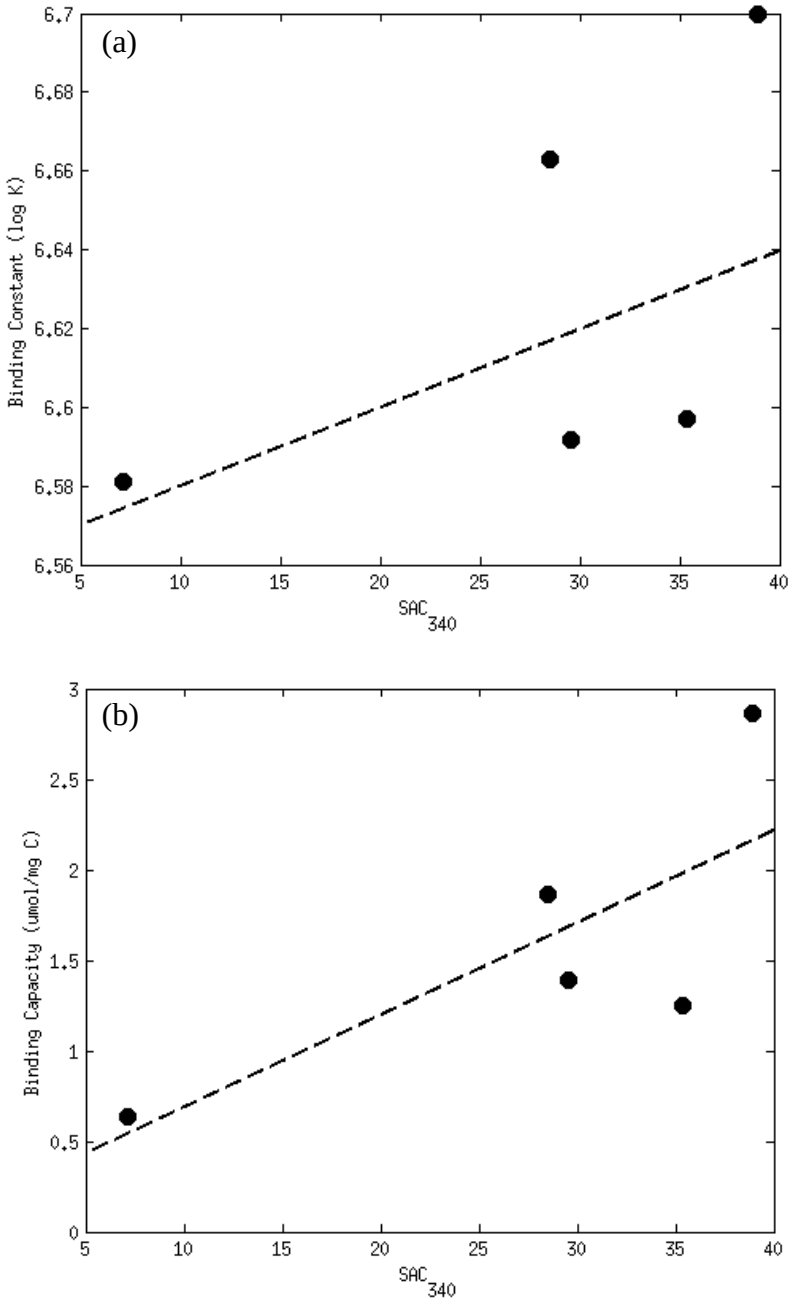

Figure 2-7. Comparisons plots of SAC_{340} with Dy binding constants (a) and capacities (b). The dashed line represents the line of best fit.

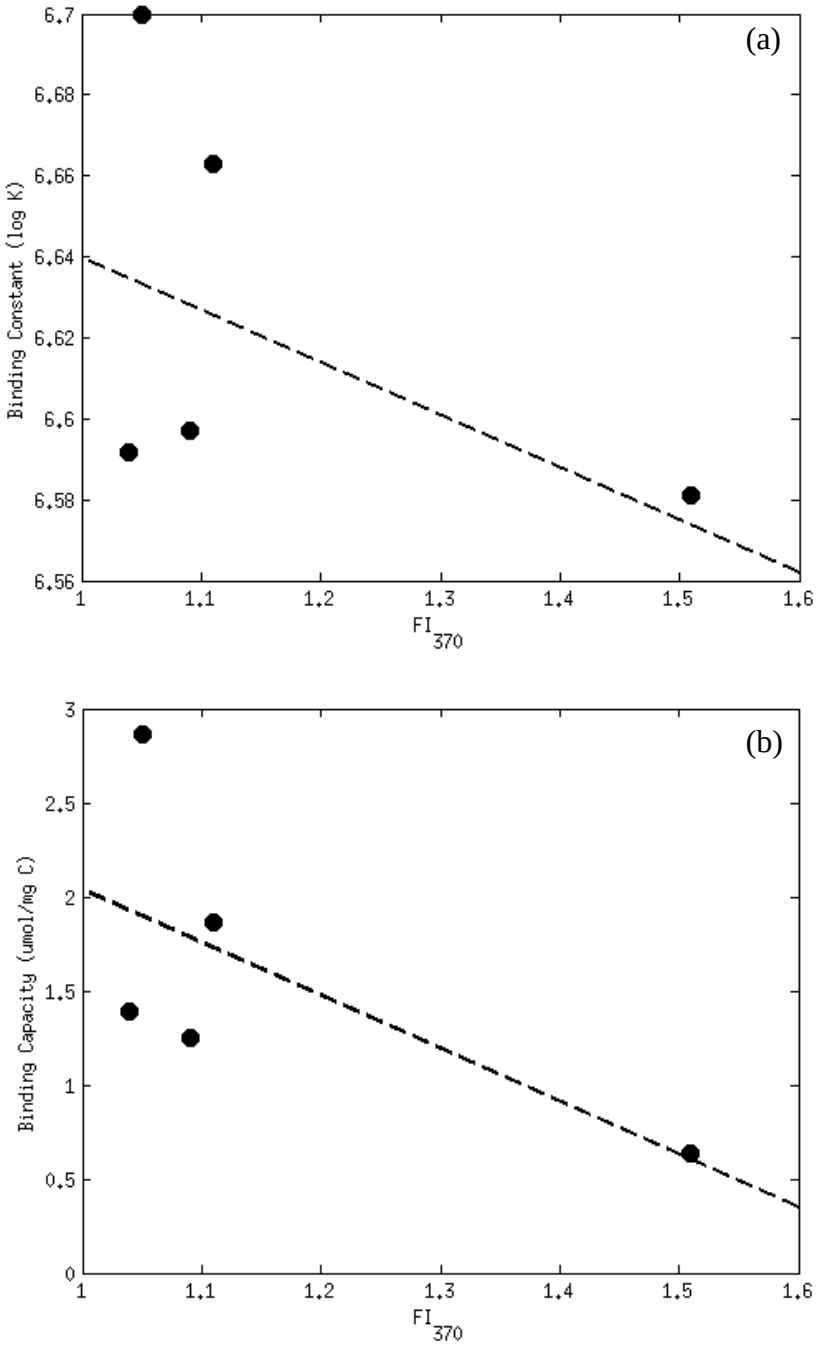

Figure 2-8. Comparisons plots of FI_{370} with Dy binding constants (a) and capacities (b). The dashed line represents the line of best fit.

Table 2-6. Line of best fit parameters for the comparison between SAC_{340} and FI_{370} and binding parameters presented in Figure 2-8 for FQ experiments. (*) shows significance ($p<0.05$).

Comparison	Slope	Intercept	R^2 value	p values
Samarium				
Log K vs SAC_{340}	0.007	6.4	0.72	0.0019*
Log K vs FI_{370}	-0.44	7.1	0.65	0.0046*
Lt vs SAC_{340}	0.051	0.03	0.62	0.0065*
Lt vs FI_{370}	-2.8	4.7	0.47	0.029*
Dysprosium				
Log K vs SAC_{340}	0.002	6.6	0.34	0.078
Log K vs FI_{370}	-0.13	6.8	0.23	0.16
Lt vs SAC_{340}	0.051	0.18	0.57	0.011*
Lt vs FI_{370}	-2.8	4.9	0.45	0.034*

A strongest relationship was observed between binding capacity and SAC_{340} (R^2 = 0.57-0.62) for both lanthanides. The two sources that stood out from the rest with respect to their characteristics and binding parameters were LM DOM and BB DOM. LM DOM has the highest SAC_{340} (38.88) and second lowest FI_{370} (1.05); it also has the highest capacity. In contrast, BB DOM, which has the lowest Lt value, also has the lowest SAC_{340} (7.12) and highest FI_{370} (1.51). It is important to note that both SAC_{340} and Lt values (~0.5-3 µmol/mg C) had a similar, almost an order of magnitude change, between the two DOM sources. Although DOM characteristics did not show a very good correlation with the binding parameters, there is enough supporting evidence that these simple calculations can provide some information about the potential binding capacity of lanthanides with DOM in the aquatic systems.

2.4 Summary and Conclusions

In this study speciation of Sm and Dy with five DOM sources was measured using FQ as an analytical technique. The quenching of the natural DOM fluorescence is observed upon addition of either lanthanide. SIMPLISMA was employed in order to resolve the spectra for the multiple components that were captured using a variable-angle synchronous scan. It identifies a presence of two components in four DOM samples, with the exception of BB DOM, which was not able to be resolved and was treated as one component. The dominant component, most likely belonging to humic/fulvic-like components of the DOM, in SH, KB, LM and SW DOM samples exhibited quenching. RW model was applied to all of these quenching curves in order to calculate the binding constants and capacities.

There are little differences observed between these binding parameters for Sm and Dy, which is expected as lanthanides are characterized by similar chemical behaviour across the group. The binding constants reveal strong binding and vary very little (log K: 6.48-6.78), most likely because lanthanides bind to similar oxygen-containing groups present in all DOM samples. In contrast, the differences are observed in the binding capacity of the DOM samples. With darker more allochthonous LM DOM having the highest Lt value (2.72-2.86 μmol/mg C), while the lightest and more autochthonous BB DOM has the lowest Lt value (0.53-0.63 μmol/mg C). These differences in DOM were measured using SAC_{340} and FI_{370} calculations. Positive correlation of both binding parameters is observed with SAC_{340}, and negative correlation with FI_{370}. The correlations betwenn Lt and SAC_{340} are significant with 95% confidence (p values of 0.0065-0.034)

but not very strong (R^2 ~ 0.5). A larger pool of DOM samples would be able to provide more information.

The metal distribution plots of lanthanide species reveal that in the presence of high concentrations of CO_3^{2-} and SO_4^{2-}, a large portion of the metal (~73%) is found as part of the complexes with these anions. DOM plays an important role at the beginning of the titrations; however, that changes as the binding capacity is reached. In the aquatic systems that would contain less of the anions than found in the matrix solution (0.001 M and 0.0033 M, CO_3^{2-} and SO_4^{2-}, respectively) DOM would play a more dominant role. Nevertheless, DOM presence in the water column could provide protection against lanthanide toxicity to the aquatic life. FQ results need to be verified with the use of another analytical technique (such as ISE) before this model can be used for the measurement of lanthanide speciation with DOM. This comparison will be discussed in the next chapter.

2.5 References

Al-Reasi, H.A., Wood, C.M., Smith, D.S. 2011. Physicochemical and spectroscopic properties of natural organic matter (NOM) from various sources and implications for ameliorative effects on metal toxicity to aquatic biota. Aquatic Toxicology 103: 179-190.

An-Chao, G., Shen, Z., Høiland, H. 1998. Complex behaviour of trivalent rare earth elements by humic acids. Journal of Environmental Sciences 10: 302-308.

Artyushkova, K. 2007. Multivariate analysis and preprocessing of spectral data. Matlab Central File Exchange. Accessed at http://www.mathworks.com/matlabcentral/fileexchange/15391-multivariate-analysis-and-preprocessing-of-spectral-data/content/simplisma.m on November 4, 2015.

ChemInfo Services Inc. 2012. Review of the rare earth elements and lithium mining sectors. Final Report. Prepared for Environment Canada. Accessed http://www.miningwatch.ca/sites/www.miningwatch.ca/files/review_of_the_rare_earth_elements_and_lithium_mining_sectors.pdf January 15, 2016.

Chen, W., Westerhoff, P., Leenheer, J.A., Booksh, K. 2003. Fluorescence excitation-emission matrix regional integration to quantify spectra for dissolved organic matter. Environmental Science and Technology 37: 5107-5710.

Cooper, C.A., Tait, T., Gray,H., Cimprich, G., Santore, R.C., McGeer, J.C., Wood, C.M., Smith, D.S. 2013. Influence of salinity and dissolved organic carbon on acute Cu toxicity to the rotifer *Brachionus plicatilis*. Environmental Science and Technology 48: 1213-1221.

Curtis, P.J., Schindler, D.W. 1997. Hydrologic control of dissolved organic matter in low-order Precambrian Shield lakes. Biogeochemistry 36: 125-138.

Di Toro, D.M., Allen, H.E., Bergman, H.L., Meyer, J.S., Paquin, P.R., Santore, R.C. 2001. Biotic Ligand Model of the acute toxicity of metals. 1. Technical basis. Environmental toxicology and Chemistry 20: 2383-2396.

Diakonov, I.I., Ragnarsdottir, K.V., Tagirov, B.R. 1998. Standard thermodynamic properties and heat capacity equations of rare earth hydroxides: II. Ce III/-, Pr-, Sm-, Eu III/-, Gd-, Tb-, Dy-, Ho-, Er-, Tm-, Yb-, and Y-hydroxides. Comparison of thermochemical and solubility data. Chemical Geology 151: 327-347.

Dong, W., Li, W., Tao, Z. 2002. Use of the ion exchange method for the determination of stability constants of trivalent metal complexes with humic and fulvic acids II. Tb^{3+},

Yb^{3+} and Gd^{3+} complexes in weakly alkaline conditions. Applied Radiation and Isotopes 56: 967-974.

El-Akl, P., Smith, S., Wilkinson, K.J. 2015. Linking the chemical speciation of cerium, to its bioavailability in water for freshwater alga. Environmental Toxicology and Chemistry 34: 1711-1719.

Elbaz-Poulichet, F., Dupuy, C. 1999. Behaviour of rare earth elements at the freshwater-seawater interface of two acid mine rivers: the Tinto and Odiel (Andalucia, Spain). Applied Geochemistry 14: 1063-1072.

EPA (United States Environmental Protection Agency). 2012. Rare Earth Elements: A Review of Production, Processing, Recycling, and Associated Environmental Issues. Office of Research and Development. EPA/600/R-12/575. Revised December 2012. Accessed http://www.miningwatch.ca/files/epa_ree_report_dec_2012.pdf on January 15, 2016.

Gammons, C.H., Wood, S.A., Nimick, D.A. 2005. Diel behavior of rare earth elements in a mountain stream with acidic to neutral pH. Geochimica et Cosmochimica Acta 69: 3747-3758.

Gu, Z., Wang, X., Gu, X., Cheng,J., Wang, L., Dai, L., Cao, M. 2001. Determination of stability constants for rare earth elements and fulvic acids extracted from different soils. Talanta 53: 1163-1170.

Johannesson, K.H., Lyons, W.B., Stetzenbach, K.J., Byrne, R.H. 1995. The Solubility control of rare earth elements in natural terrestrial waters and the significance of PO_4^{3-} and CO_3^{2-} in limiting dissolved rare earth concentrations: a review of recent information. Aquatic Geochemistry 1: 157-173.

Johnson, R.A., O'Rourke, J.D. 1954. The kinetics of precipitate formation: barium sulfate. Journal of American Chemical Society 76: 2124-2126.

Karraker, D.G. 1970. Coordination of trivalent lanthanide ions. Journal of Chemical Education 47: 424-430.

Lead, J.R., Hamilton-Taylor, J., Peters, A., Reiner, S., Tipping, E. 1998. Europium binding by fulvic acids. Analytica Chimica Acta 369: 171-180.

Leenheer, J.A., Croue, J-P. 2003. Characterizing dissolved aquatic organic matter. Environmental Science and Technology 37: 19A-26A.

Martell, A.E., Smith, R.M. 2004. NIST Standard Reference Database 46 Version 8.0, Gaithersburg, USA.

McKnight, D.M., Boyer, E.W., Westerhoff, P.K., Doran, P.T., Kulbe, T., Andersen, D.T. 2001. Spectrofluorometric characterization of dissolved organic matter for indication of precursor organic material and aromaticity. Limnology and Oceanography 46: 38-48.

Nasir, R. 2014. Effects of salinity and dissolved organic matter on Cu toxicity to *Americamysis bahia* in estuarine environments. (Master's Thesis) Thesis and Dissertations. Wilfrid Laurier University.

Paquin, P.R., Gorsuch, J.W., Apte, S., Batley, G. E., Bowles, K.C., Cambell, P.G.C., Delos, C.G., Di Toro, D.M., Dwyer, R.L., Galvez, F., Gensemer, R.W., Goss, G.G., Hogstrand, C., Janssen, C.R., McGeer, J.C., Naddy, R.B., Playle, R.C., Santore, R.C., Scheider, U., Stubblefield, W.A., Wood, C.M., Wu, K.B. 2002. The biotic ligand model: a historic overview. Comparative Biochemistry and Physiology, Part C 133, 3-35.

Ryan, D.K, Weber, J.H. 1982. Fluorescence quenching titration for determination of complexing capacities and stability constants of fulvic acid. Analytical Chemistry 54: 986-990.

Saar, R.A., Weber, J.H. 1982. Fulvic acid: modifier of metal-ion chemistry. Environmental Science and Technology 16: 510A-517A.

Santore, R.C., Di Toro, D.M., Paquin, P.R., Allen, H.E., Meyer, J.S. 2001. Biotic ligand model of the acute toxicity of metals. 2. Application to acute copper toxicity in freshwater fish and daphnia. Environmental Toxicology and Chemistry 20: 2397-2402.

Shin., H.S., Lee, B.H., Yang, H.B., Yun, S.S., Moon, H. 1996. Bimodal normal distribution model for binding of trivalent europium by soil fulvic acid. Journal of Radioanalytical and Nuclear Chemistry 209: 123-133.

Slaveykova, V.I., Wilkinson, K.J. 2005. Predicting the bioavailability of metals and metal complexes: critical review of the biotic ligand model. Environmental Chemistry 2: 9-24.

Sneller, F.E.C, Kalf, D.F., Weltje, L., Van Wezel, A.P. 2000. Maximum permissible concentrations and negligible concentrations for rare earth elements (REEs). National Institute of Public Health and The Environment, Report #601501011. Accessed https://www.researchgate.net/publication/27452531_Maximum_Permissible_Concentrations_and_Negligible_Concentrations_for_Rare_Earth_Elements_REEs on January 15, 2016.

Spahiu, K., Bruno, J. 1995. A selected thermodynamic database for REE to be used in HLNW performance assessment exercises. MBT Technologia Ambiental. Cerdanyola, Spain.

Standing Committee on Natural Resources (RNNR). 2014. The rare earth elements industry in Canada - summary of evidence. 41st Parliament, 2nd session. Accessed http://www.miningwatch.ca/sites/www.miningwatch.ca/files/rareearthelements-summary-e.pdf on January 15, 2016.

Stedmon, C.A., Markager, S. 2005. Resolving the variability in dissolved organic matter fluorescence in a temperate estuary and its catchment using PARAFAC analysis. Limnology and Oceanography 50: 686-697.

Stedmon, C.A., Markager, S., Bro, R. 2003. Tracing dissolved organic matter in aquatic environments using a new approach to fluorescence spectroscopy. Marine Chemistry 82: 239-254.

Tipping, E., Lofts, S., Sonke, J. E. 2011. Humic ion-binding model VII: a revised parameterisation of cation-binding by humic substances. Environmental Chemistry 8: 225-235.

Verweij, W. 2013. Equilibria and constants in CHEAQS: selection criteria, sources and assumptions. Model Version 10 (February 2013). Accessed http://home.tiscali.nl/cheaqs/ on March 10, 2013.

Windig, W., Guilment, J. 1991. Interactive self-modeling mixture analysis. Analytical Chemistry 63: 1425-1432.

Wood, C.M., Al-Reasi, H.A., Smith, D.S. 2011. The two faces of DOC. Aquatic Toxicology 105S: 3-8.

Wood, S.A. 1990. The aqueous geochemistry of the rare-earth elements and yttrium. 1. Review of available low-temperature data for inorganic complexes and the inorganic REE speciation of natural waters. Chemical Geology 82: 159-186.

Wu, J., Zhang, H., He, P-J., Shao, L-M. 2011. Insight into the heavy metal binding potential of dissolved organic matter in MSW leachate using EEM quenching combined with PARAFAC analysis. Water Research 45: 1711-1719.

Zhao, C-M., Wilkinson, K.J. 2015. Biotic ligand model does not predict the bioavailability of rare earth elements in the presence of organic ligands. Environmental Science and Technology 49: 2207-2214.

CHAPTER 3: DETERMINATION AND COMPARISON OF SAMARIUM SPECIATION USING ION-SELECTIVE ELECTRODE TECHNIQUE.

ABSTRACT

It is well established that metal speciation plays an important role in accurate metal toxicity prediction. Both inorganic and organic ligands, such as dissolved organic matter (DOM), will have an effect on metal distribution in water. The purpose of this chapter is to measure Sm speciation with DOM using ion-selective electrode (ISE) as an analytical technique, as well as to compare it to the results obtains from fluorescence quenching (FQ) technique. Five DOM sources were titrated with Sm at concentrations ranging from 0 μM to 100 μM. Only three resulted in useful data, as there was an observed interference from other ions present in the DOM concentrates. These interferences are most likely attributed to the low selectivity of the ligand used in the construction of ISE. The data from the other three sources were modeled to obtain the binding capacity and constants. Moderate to strong binding constants are observed (log K: 5.08-6.29) with binding capacities of 3.7-12 μmol/mg C. Comparisons between ISE and FQ reveal a presence of a non-fluorescent ligand, not measured in the FQ experiments. The ligand potentially has weaker binding than the one found by FQ. ISE, thus, may be a better suited technique for measurements of Sm speciation; however, a more selective ligand must be developed before it can be applied higher ionic strength samples.

3.1 Introduction

The increased demand for lanthanides (EPA 2012) and the resulting development of lanthanide mines in Northern Canada, Northwest Territories and Quebec (ChemInfo 2012) is driving the research into the environmental chemistry and toxicity of these metals. It is accepted that the form of the metal or metal speciation is important to the prediction of metal toxicity (Di Toro et al. 2001; Paquin et al. 2002; Santore et al. 2001; Slaveykova and Wilkinson 2005). When it comes to lanthanides, current research shows that the traditional assumption of free metal ion being the most bioavailable form (the form of metal that can be directly related to toxicity) does not necessarily apply to these metals(Zhao and Wilkinson 2015). It was shown that the formation of the ternary metal complex, where the metal is bound to organic ligands (citric, malic, and nitrilotriacetic acid) on one side and the biological receptor site on the other, increased biouptake of the metal into freshwater algae (Zhao and Wilkinson 2015). The increased biouptake may not directly translate into the increase in toxicity, but it might have an adverse effect. Thus, understanding the interactions of these metals with the organic ligands is essential for prediction of lanthanide toxicity.

Interaction of the metal with dissolved organic matter (DOM) is an important aspect of metal speciation in natural waters. DOM is able to bind metals due to a presence of a number of functional groups, such as carboxyl, phenol and amino groups (Leenheer and Croue 2003; Tipping et al. 2011). It has been demonstrated to be protective against metal toxicity as a result of this binding (Al-Reasi et al. 2011; Al-Reasi

et al. 2013). Together with the inorganic ligands such as carbonate and hydroxide, DOM will govern the distribution of metal species in water.

For accurate toxicity prediction the measurement of metal speciation has to produce accurate results. The research into lanthanide speciation with DOM has been very limited, with most studies looking at Eu interactions with fulvic acids (Tipping et al. 2011), as an analogue for radioactive actinides (Lead et al. 1998). Most of the studies available thus far report strong DOM binding to lanthanides (An-Chao et al. 1998; Dong et al. 2002; El-Akl et al. 2015; Gu et al. 2001; Lead et al. 1998; Shin et al. 1996); however, the range of stability constants is very variable (log K: 3.5-11.6). In previous chapter, fluorescence quenching (FQ) was used and discussed as an analytical technique for lanthanide speciation measurements. Lanthanides show strong binding with DOM with log K values range of 6.48-6.78. One of the assumptions made with the FQ method is that the metal must bind to the fluorescent part of the molecule; thus, FQ will not detect binding to the non-fluorescent entities. In order to validate the results from FQ chapter, another analytical technique is used here, ion-selective electrode (ISE).

The general principal of ISE involves the measurement of the electric potential differences across an ion-selective membrane (Harris 2003). The electric potential is related to the free metal ion activity in the sample as defined by Nernst equation (Equation 1-10). The electrode that was selected for Sm measurements in this study uses a liquid ion exchange membrane, where the ligand is incorporated into a polyvinyl chloride (PVC) matrix, which allows a certain level of mobility of the ligand within it. The other components in the membrane are plasticizer, lipophilic salt and ion-selective ligand. Plasticizer is used to make the membrane more flexible (Harris 2003; Stark et al.

2001) and is the largest membrane portion by weight (Armstrong and Horvai 1990; Bakker et al. 1997; Oesch and Simon 1980). Lipophilic anion is used to keep the contents of the membrane at neutral charge and assist with cation transfer across the membrane. Finally, the ligand for the ISE is usually an organic molecule ionophore that can bind the metal of interest selectively, but reversibly (Bakker et al. 1997; Harris 2003). The best membrane composition is usually determined experimentally. The Sm-selective electrode membrane recipe for this study was found in literature (Ganjali et al. 2003). The paper used commercially available glipizide as the ionophore.

One of the main advantages of ISE over FQ is that ISE is able to directly measure free lanthanide in water, whereas FQ requires modeling to do so. Although free metal ion may not be the only driver of lanthanide toxicity, traditionally it is assumed that free metal ion is the most bioavailable form and is usually the one that can be related to toxicity. Another advantage of the ISE is that it can measure metal binding with all types of moieties, regardless of the DOM fluorescence. In this study Sm speciation was measured and analyzed using ISE. It was then compared to the FQ results, in order to validate the techniques and provide more information into lanthanide speciation.

3.2 Materials and Methods

The following sections describe sample preparation and experimental procedure of ion-selective electrode, which includes instrumental set up and data analysis.

3.2.2 Chemicals

All chemicals were purchased with the highest purity possible. They were stored according to the recommendations of the manufacturer. The list of chemicals can be found in Table 3-1.

Table 3-1. List of chemicals and their suppliers used in the ISE experiments.

Chemical Name	**Supplier**
Samarium (III) sufate octahydrate	Sigma-Aldrich Corp. (St. Louis, MO, USA)
Hydrochloric acid (~30%) (GR ACS)	EMD Chemicals (Gibstown, NJ, USA)
Sodium hydroxide standard (5.0N)	Sigma-Aldrich Corp. (St. Louis, MO, USA)
Ethylenediaminetetraacetic acid tetrasodium salt hydrate, Sigma Ultra	Sigma-Aldrich Corp. (St. Louis, MO, USA)
Glipizide	Sigma-Aldrich Corp. (St. Louis, MO, USA)
Sodium tetraphenylborate (ACS reagent >99.5%)	Sigma-Aldrich Corp. (St. Louis, MO, USA)
Polyvinyl chloride (high molecular weight) K-value ~70	Sigma-Aldrich Corp. (St. Louis, MO, USA)
Benzyl acetate (>99.0%)	Sigma-Aldrich Corp. (St. Louis, MO, USA)
Sodium chloride	Anachemia Canada Co. (Montreal, QC)
Sodium bicarbonate (GR ACS)	EMD Chemicals (Gibstown, NJ, USA)
Sodium sulfate decahydrate (Ultra >99%)	Fluka Analytical, Sigma-Aldrich Corp. (St. Louis, MO, USA)

3.2.2 Membrane Preparation

All of the membrane constituents were mixed in scintillation vials. The amounts of each of the chemical compound are outlined in Table 3-2. The mixture was stirred using a glass rod until all the powders were completely dissolved. The clear mixture was transferred onto a glass disk (~2 cm in diameter), which was tightly fitted to the glass plate with rubber bands. A heavy object was placed on top, separated from the top of the

glass disk by a folded sheet of filter paper for controlled evaporation (Craggs et al. 1974). The mixture was left to dry for approximately 48 hrs, after which the membrane was removed and a 7 mm circular piece was cut out using a metal hole punch. It was incorporated into a commercially available ISE electrode body (Fluka Analytical, Sigma-Aldrich Corp., St. Louis, MO, USA). The inner filling glass tube containing Ag/AgCl internal reference electrode was filled with solution of 0.01 M Sm, 0.01 M EDTA and 0.1 M NaCl. EDTA was added to the inner filling solution as free Sm ion buffer, which lowers Sm ion concentration in the inner filling solution, in order to improve detection limits (Sokalski et al. 1997). The electrode was left to condition for 24 hrs in 0.001 M Sm before performing a calibration. It was also stored in this solution between experiments.

Table 3-2. List of membrane mixture components, including their role and amounts.

Chemical	**Role**	**Amount***
Polyvinyl Chloride (hmw)	Polymer	30 mg
Benzyl Acetate	Plasticizer	50.2 μL
Sodium Tetraphenylborate	Lipophilic anion source	5 mg
Glipizide	Ligand	15 mg
Tetrahydrofuran	Solvent	3-4 mL

* Values were slightly changed from the original paper (Ganjali et al. 2003), based on the electrode performance discussed in Appendix A2.
hmv: high molecular weight (K-value ~70)

3.2.3 Sample Description, Preparation and Measurements

External calibration solution was prepared each day by diluting 25 μL of 0.01 M Sm stock solution in 25 mL of MilliQ water. A three point calibration was performed daily by titrating this solution to the final Sm concentration of 0.00013 M at pH of around 5. Similarly to FQ experiments, five DOM sources were used for the experiments (Table 2-2), however BB DOM and SH DOM were excluded from further analysis, as their

concentrates had high ionic strength (IS). High IS interfered with the ISE response, discussed in Section 3.3.1 and Appendix A2; therefore, IS matrix was not used for DOM sample preparation. DOM concentrates were, thus, diluted with MilliQ water to DOC concentration of 10 ppm. The samples were adjusted to pH of 7.30±0.06 at the beginning of each experiment using 0.1 M HCl and 0.1 M NaOH, and this pH value was maintained throughout the experiment. DOM samples were titrated using standard additions of Sm stock solution (5000 µM) with the range of metal concentrations of 2 µM to 100 µM. The experiments were done in duplicates.

The potentiometric measurements were done using Tanager Scientific System Inc. potentiometer (Model 9501, Ancaster, ON, Canada) with a Ag/AgCl Orion double junction reference electrode (Thermo Electron Corp., Gormley, ON, Canada). The reference electrode inner filling solution was replenished weekly using a solution provided by the manufacturer and the outer filling solution was changed daily with the 0.011 M IS solutions (prepared with $NaHCO_3$ and Na_2SO_4). The DOM samples were acidified after titration was done to the pH of 5, in order to release all of the bound metal. This value was used as an internal calibration described below.

The electrode performance was verified by titrating EDTA with Sm. Concentration of EDTA was calculated from this titration and compared to the expected concentration. A 50 mL EDTA (0.000025 M) sample was prepared from the stock solution of 0.01M. It was titrated with Sm ranging from 5 µM to 100 µM from 5000 µM stock solution. pH was kept around 5.0±0.1, and the experiment was repeated 3 times.

3.2.4 Data Processing and Analysis

Sm ion concentrations were converted into Sm activities using an extended Debye-Huckel relationship (Equation 1-11). IS value was determined from calculated concentrations of SO_4^{2-} (based on the titration values with Sm stock solution volumes (5000 μM), prepared using $Sm_2(SO_4)_3$), measured CO_3^{2-} (TIC function on the Shimadzu TOC-$L_{CPH/CPN}$ Analyzer (Shimadzu Corp., Kyoto, Japan)), Cl^- (Cl-selective combination electrode (Mantech, Guelph, ON)), K^+, Ca^{2+} and Mg^{2+} (Perkin Elmer Optima 8000 ICP-OES (Guelph, ON), summarized in Table 2-3 and Table B1. The calibration curve was created by plotting electrode response (mV) vs. log of Sm activities (Figure 3-1a). The slope from this external calibration replaced Nernstian slope in the relationship defined in Section 1.4.3 by Equation 1-10. E° was calculated using the acidified value from the internal calibration, which represents the final total Sm activity ($E° = E + slope * pSm$). Finally, Sm activities were converted back to Sm concentrations using activity coefficient calculated for each point in the titration.

Binding isotherm curves were used to calculate binding constant and capacity. A one ligand model was selected as it was the simplest model that was able to describe the data. A 1:1 binding was assumed ([ML] = [M] + [L]). Binding parameters were calculated using least squares method optimization together with Monte Carlo (MC) simulations to estimate the 95% confidence intervals (95% CI). The model had inorganic speciation integrated into it using measured concentrations of CO_3^{2-} and Cl^- and calculated SO_4^{2-}. The log K values for inorganic species were obtained from NIST database (Martell and Smith 2004; Verweij 2013), with the exception of the pK_{sp} value of

the hydroxide solid mentioned in Section 2.2.4, which came from Spahiu and Bruno (1995); the selection was made based on the experimental evidence from ISE titrations. All MATLAB^{TM} codes for the analysis can be found in Appendix C4. Additionally, ISE free Sm measurements were plotted together with the FQ predicted free Sm for the ISE experimental conditions, in order to compare the two techniques and determine any consistencies or inconsistencies between methods.

3.3 Results and Discussion

The ideal Nernstian response (slope 19.7 mV) of the Sm-SE was never achieved (slope range 5.9-24.3 mV). Some of the challenges that were encountered during the ISE development stages are discussed in Appendix A2-A4. The three main lessons that were taken away from this stage is that (1) the electrode required daily calibration, as there were a lot variation in the slope; (2) IS had to be kept at a minimum for the best ISE response; and (3) increased ligand concentration in membrane produced larger slope (increase from ~10 mV to ~15 mV). The results of the DOM titration with Sm are discussed in the following sections.

3.3.1 Calibrations and DOM titrations

Overall two electrodes were prepared and used for DOM titrations. Electrode #1 (membrane #22, see Appendix A2 for more details on membrane composition) had an average slope of 11.7±3.70 (SD) and an R^2 value of 0.986±0.024 (SD), while electrode #2 (membrane #23) values were 18.0±4.0 (SD) and 0.988±0.010 (SD), respectively. Electrode #2 showed a much better response both in the magnitude of the slope and the linearity of the calibration line; however, the measured free Sm ions are similar between

both electrodes. An example of a calibration line as well as DOM titration curve can be seen in Figure 3-1. All DOM titrations are summarized in Table 3-3; however, as mentioned previously (Section 3.2.3), BB DOM and SH DOM were omitted from further analysis. Most of the DOM titrations show an increase in mV values upon addition of Sm until they plateau at higher concentrations of Sm. Stable reading closer to the end of the titration, also seen in vertical increase in the binding isotherms (Figure 3-2b), may signify formation of a precipitate. Overall, the three selected DOM sources show binding, as calculated free Sm was below a 1:1 line of the total Sm added during the titration (Figure 3-2a). The data was overall very noisy (Figure 3-2); however, free Sm concentrations are mostly within one log unit for all samples, and they have similar binding isotherm shapes (Figure 3-2b). In order to assure that the electrode was responding to the Sm ion in a reasonable fashion, it was validated by EDTA titration with Sm. The calculated EDTA concentration (24±2.0 μM) determined from the titration is within the standard deviation of the actual EDTA value of the prepared sample (25 μM).

Table 3-3. Summary of all DOM titrations performed by monitoring the titrations with the ISE. All reading are reported in mV.

DOM Source	**LM DOM**		**KB DOM**		**SW DOM**		***SH DOM***		***BB DOM***	
Concentrate IS [a]	0.000059 M		0.000019 M		0.000036 M		*0.00049M*		*0.0058 M*	
pH [b]	7.33	7.34	7.36	7.33	7.34	7.34	*7.35*	*7.35*	*7.33*	*7.32*
Electrode #	1	2	1	2	2	2	*1*	*2*	*2*	*2*
Slope	16.02	23.71	6	23.36	18.3	22.6	*14.89*	*19.28*	*7.9*	*13.78*
Intercept	104.7	144.5	78.3	132	119	136.5	*106.8*	*117.6*	*81.8*	*90.8*
Total log[Sm], M	**Trial 1**	**Trial 2**	**Trial 1**	**Trial 2**	**Trial 1**	**Trial 2**	***Trial 1***	***Trial 2***	***Trial 1***	***Trial 2***
-5.7	-5 [c]	-25.7	31.9	-29.9	-16.3	-32.8 [c]	*24.3*	*9.2*	*34.4*	*42.9*
-5.3	-4.8 [c]	-24.95	32.3	-25.6	-13	-28.7 [c]	*25.8*	*9.1*	*35.8*	*42.8*
-5.0	-2.2 [c]	-21.2	33.6	-22.2	-8.2	-20.2 [c]	*18.5*	*11.1*	*33.1*	*41.2*
-4.6	6.3	-9.05	35.7	-12.3	0.3	-5.7	*21.7*	*12.9*	*31.6*	*38.7*
-4.4	18.1	1.6	36.8	-4.4	2.2	0.1	*23.7*	*16.3*	*33.2*	*39.5*
-4.3	21	5.1	36.7	-3	6.8	0.8	*24.6*	*16.7*	*31.4*	*36.8*
-4.1	23	8.9	37.7	-1.04	7.7	4.9	*25.6*	*17.1*	- [d]	*39.2*
-4.0	23.1	13.1	37.2	0.7	7.2	7.1	*28.3*	*17.9*	*33.5*	*36*
-4.0 [e]	38	39.6	45.5	26.2	32.2	36.5	*39.8*	*36.3*	*34.3*	*40.8*

(a) Concentrate IS calculation includes CO_3^{2-}, Cl^-, K^+, Ca^{2+} and Mg^{2+} concentrations.
(b) Average of pH values recorded at the beginning of each reading. pH values tended to decrease slightly during reading.
(c) Different total [Sm] was used: LM (-5.4, -5.2, -4.9); SW (-5.3, -5.1, -4.9)
(d) The last two additions were combined together.
(e) Acidified reading at pH value of about 5.
SH and *BB DOM* were omitted from further analysis

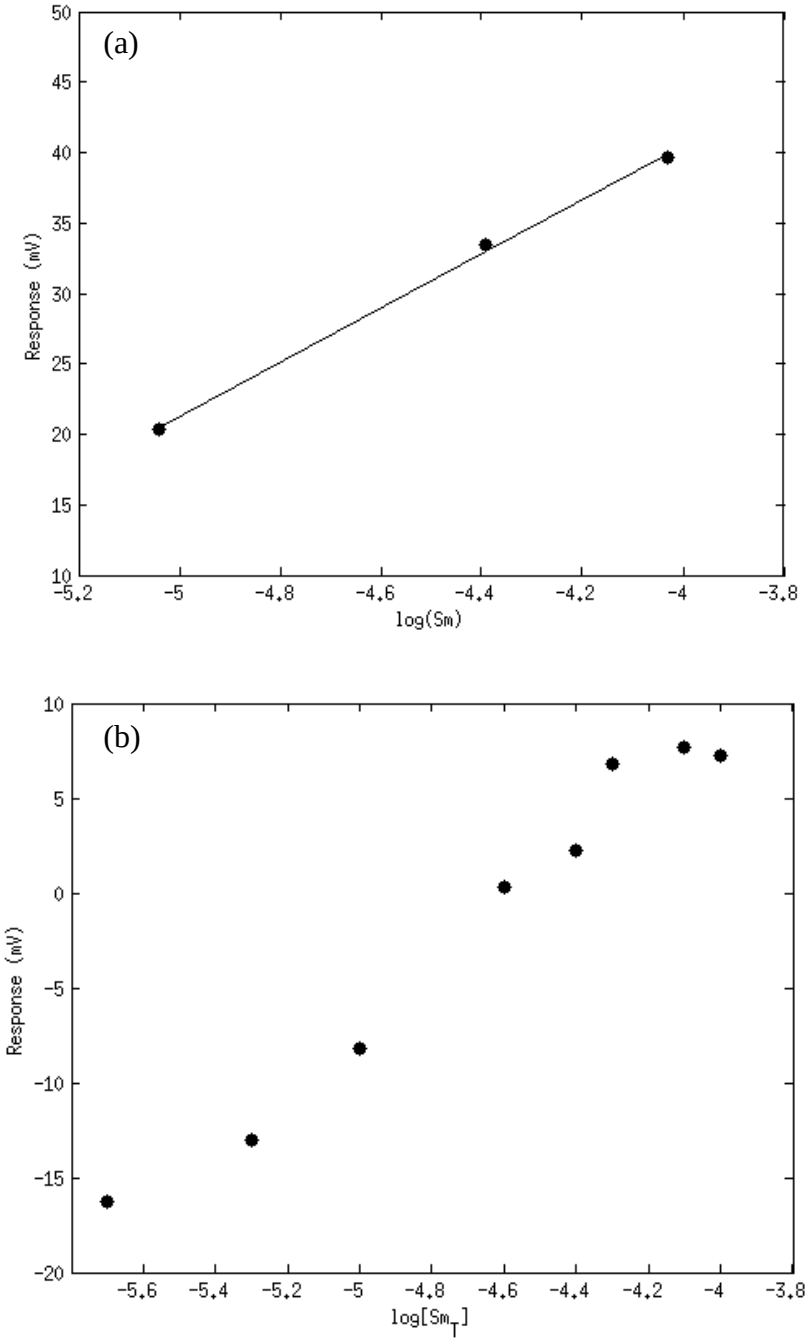

Figure 3-1. (a) An example of Sm-SE calibration curve (line of best fit slope = 19.3, R^2 = 0.998). (b) An example of the DOM titration curve of SW DOM with Sm Trial 1.

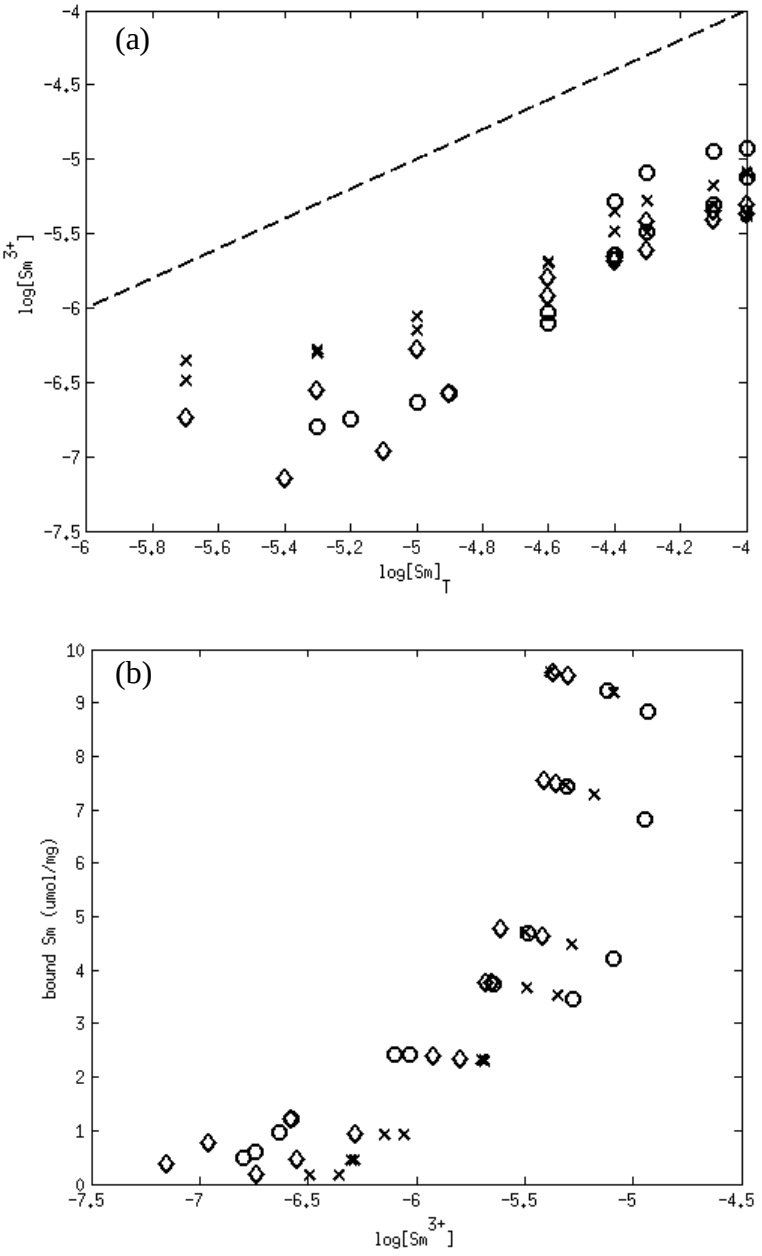

Figure 3-2. (a) Free Sm plotted against total Sm, both in log units. A black dashed line represents a 1:1 line, points are measured values (KB DOM (x), SW DOM (◊) and LM DOM (○)). All of the samples were below the line signifying presence of binding. (b) Binding isotherm (bound Sm (μmol/mg C) vs. log free Sm). Samples showed similar binding. The vertical rise of bound Sm at higher concentrations of free Sm implies precipitate formation.

3.3.2 Ionic Strength Effects

During the ISE development it was discovered that IS had a dramatic effect on the response of the electrode. Stable readings were observed when the electrode was calibrated in the IS matrix standards (Appendix B2). Although it was possible to remove excess ions from the standards by using MilliQ water for dilution, DOM concentrates still had some salinity associated with them. Two samples stood out during the DOM titrations; they were BB DOM and SH DOM. BB DOM IS value (5.8 mM) is two orders of magnitude greater than that of the SW, KB and LM DOM (19 µM – 59 µM). As a result, there are very little changes in the voltage readings of BB DOM upon addition of the metal (Table 3-3), with the reading fluctuating slightly between 31-43 mV. SH DOM IS (0.49 mM) is only order of magnitude greater than that of the other three samples. Therefore, there are some change observed during the titration; however the voltage readings does not cover a wide range of values (e.g. 24.3 mV to 39.8 mV) as seen in other samples (-5 mV to 38 mV (LM DOM), Table 3-3). This results in slightly higher free Sm concentrations than that measured in other DOM samples, ranging from -5.09 to -4.95 for log[Sm^{3+}]; note that the first value is actually greater than the total Sm added (-5.7, Table 3-3). Due to the effect of the IS on these samples, they were omitted from further analysis.

It is well known that the electrode responds to the activity of the ion of interest (Harris 2003). The activity coefficient value decreases with increasing ionic strength of the solution. It is more evident for multivalent ions, as charge plays an important role in activity coefficient calculations. For example, Sm^{3+} activity coefficient decreases from 1 for IS of 0 M to 0.445 for IS of 0.01 M (Harris 2003). Thus, in solutions with high IS that

were found in this study, the response of the electrode may have been dampened due to decreased Sm activities. Another potential reason for the observed stable readings of BB DOM is the formation of $Sm_2(CO_3)_3$ precipitate, since CO_3^{2-} concentration was high in this sample (0.25 mM). As the precipitate is forming upon addition of more metal the amount of the free metal ion in the sample remains the same, thus, giving a stable reading.

A potentially significant explanation, however, for the observed IS effect with the readings is the low selectivity of the ligand. Glipizide was reported to be selective for Sm ion with selectivity coefficients of 10^{-3} (Ganjali et al. 2003); however, when calibration was performed using Dy ion the response detected was the same as with Sm ion. The slope of the calibration line was 18.8, while Sm calibration slope was 16.2. This apparent lack of selectivity would create a problem during a titration if both metal concentrations were changing; however, in the setup of the experiments only one metal was added, thus, the detected response corresponded to only that ion. In case of SH DOM and BB DOM the presence of other cations such as Ca^{2+} and Mg^{2+} in higher concentrations than those in other samples (Table B1) may have saturated the ligand, thus, making the electrode non-responsive. The voltage values recorded for BB DOM and SH DOM titrations were much higher than those for the other DOM samples, with the exception of the KB DOM Trial 1, which is explained by a very low slope recorded during calibration. High voltages of BB and SH DOM overestimate the presence of the free ion. In case of SH DOM, increased response resulted in the calculated concentrations being an order of magnitude higher than those in other samples. In BB DOM sample, where there was no significant response detected. All ISEs have an upper detection limit, where the cation saturates the ligand and

the electrode is no longer able to respond to the cation (Qin and Bakker 2002). What is observed, however, is a decrease of the voltages as a function of the anion concentrations that are being added during the titration from stock solution (Bakker et al. 1994; Bakker et al. 1997; Qin and Bakker 2002; Mathison and Bakker 1998; Peshkova et al. 2015). This happens because the membrane is saturated with the positive anions and it is able to non-selectively interact with the anions being added (Bakker et al. 1994). This is not very evident in the BB DOM sample; however, the lack of voltage changes is likely due to saturation of ligand at the electrode. In summary, reduced Sm activity, possible precipitate formation and interference from the other cations in solution prevented free Sm measurements in SH and BB DOM samples.

3.3.3 Binding Constants, Binding Capacity and Speciation

Binding parameters were calculated by nonlinear regression performed on the titrations of KB, SW and LM DOM samples with Sm. Inorganic complexation was incorporated into the model. One ligand model was selected as it was the simplest model that was able to describe the data (Figure 3-3). The most evident model disagreement is observed at the vertical increase in the isotherms due to formation of the $Sm(OH)_3$ solid. Some values are behind the solid formation line. This may be explained by noise in the readings or a slight variation in the K_{sp} value, which would move the solid formation line along the x-axis, with decrease in pK_{sp} resulting in higher concentration of free Sm at saturation point. The binding constant (log K) and capacities (Lt) are summarized in Table 3-4, with 95% CI calculated using SE. The binding constants are indicative of medium to strong binding (log K: 5.08-6.29). The values are smaller compared to the ones calculated from FQ experiments (6.48-6.78), but they are also close to the ones

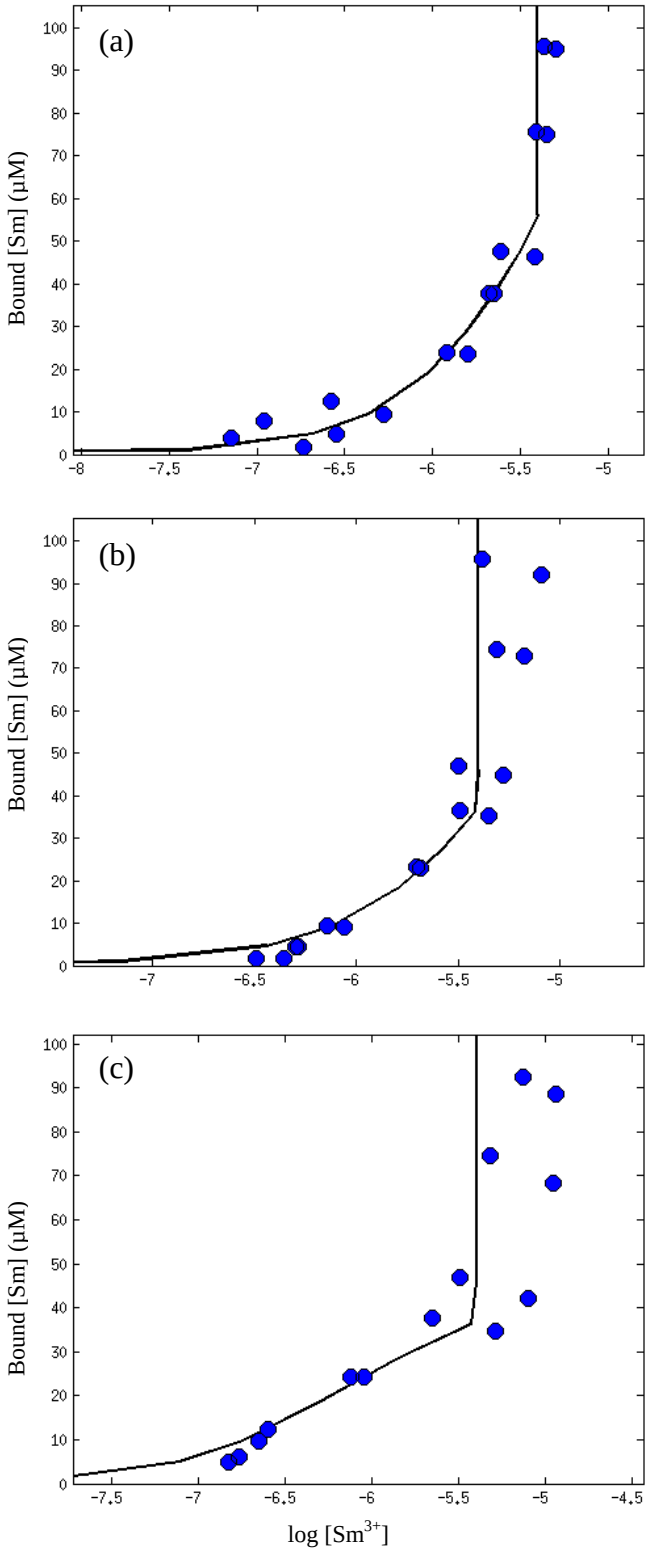

Figure 3-3. Binding isotherms of SW DOM (a), KB DOM (b) and LM DOM (c) titrated with Sm. One ligand model was used to create the model fit (black line, data – blue dots). $Sm(OH)_3$ solid formation was observed at log [Sm^{3+}] of just over -5.5.

reported for fulvic acids (FA) interactions with Eu and Ce, separately (FA: 3.5-5.95 (Eu) and 5.39 (Ce); Shin et al. 1996; El-Akl et al. 2015) and the binding site of the lake sediment humic acid (HA) with La, Ce, Ho and Yb (5.01-5.57; An-Chao et al. 1998). LM DOM binding parameters (log K of 6.29 and Lt of 3.72 μmol/mg C) are the closest to the ones reported during FQ experiments (log K of 6.78 and Lt of 2.72 μmol/mg C) compared to the other DOM sources. Binding capacities of the other DOM samples are much larger than the ones from FQ experiment (12 and 10 μmol/mg C, SW and KB DOM, respectively). A more detailed comparison between ISE and FQ experiments will be discussed in Section 3.3.4.

Comparing binding parameters to the qualitative DOM characteristics (SAC_{340} and FI_{370}, see Section 1.2.2) did not reveal any apparent trends (Table 3-5). There is no statistically significant correlation observed with 95% confidence, with p values ranging 0.094-0.98. It is likely due to the fact that the three DOM samples were very similar in their characteristics' values, with SAC_{340} ranging from 29.56 to 38.88 and FI_{370} from 1.04 to 1.09. A more diverse dataset with larger range of values is required in order to observe any meaningful trends.

Table 3-4. Summary of the binding parameters calculated for DOM binding with Sm.

Binding parameter	**SW DOM**	**KB DOM**	**LM DOM**
log K	5.28	5.08	6.29
95% CI	0.03	0.17	0.003
Lt (μmol/mg C)	12	10	3.7
95% CI	1.6	0.27	0.053

95% CI: 95 % confidence interval calculated using SE, not SD.

Table 3-5. Line of best fit parameters for the comparison between SAC_{340} and FI_{370} and binding parameters in ISE experiments.

Comparison	Slope	Intercept	R^2 value	p value
Log K vs SAC_{340}	0.095	2.28	0.47	0.23
Log K vs FI_{370}	-11.4	17.7	0.22	0.38
Lt vs SAC_{340}	-0.87	38.7	0.85	0.094
Lt vs FI_{370}	11.5	-3.53	0.0047	0.98

Although the binding parameters were different from one another, the speciation plots (Figure 3-6 to Figure 3-6) show similar behaviour in the species distribution. All samples had an observed $Sm(OH)_3$ precipitate formation (green line on the plots). The binding capacities of DOM are never reached during the titration, because of the buffering effect of solid formation. In the absence of high concentrations of anions in the ISE sample solutions DOM is the most dominant ligand before the samples became saturated with 85%, 92% and 97% of Sm bound in the Sm-DOM complex for KB, SW and LM DOM samples, respectively. Carbonate, sulphate and hydroxide aqueous complexes have very little contribution to Sm speciation with highest collective percentage of 6.6% observed in KB DOM sample. Free Sm concentrations are also low during the titration and represented about 5% of total Sm. Midway through the titration Sm starts to precipitate as the hydroxide solid, which becomes the more dominant species in KB and LM DOM (59% each), while in SW DOM sample it comprises 39% with Sm-DOM still dominating. Although the binding capacity of LM DOM is the lowest, stronger binding constant allows LM DOM to bind more Sm in the same relative conditions at the beginning of the titration. Therefore, the protective nature of each of the DOM samples will vary depending on the total Sm added.

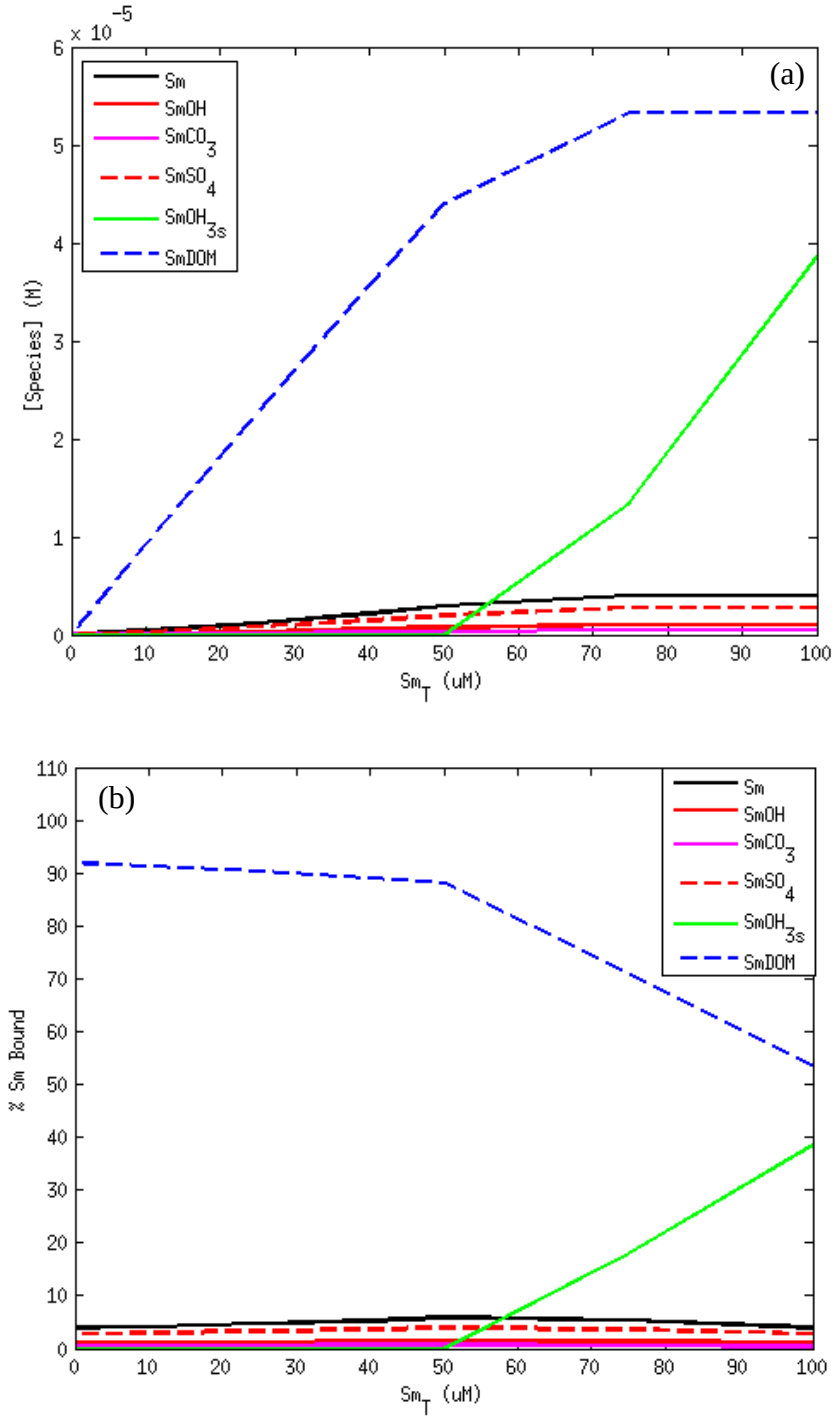

Figure 3-4. Speciation plots for SW DOM titrated with Sm during ISE titrations, plotted as [species] (a) and % Sm bound in species (b). Only dominant species concentrations and percentages are shown. Charge was omitted for clarity.

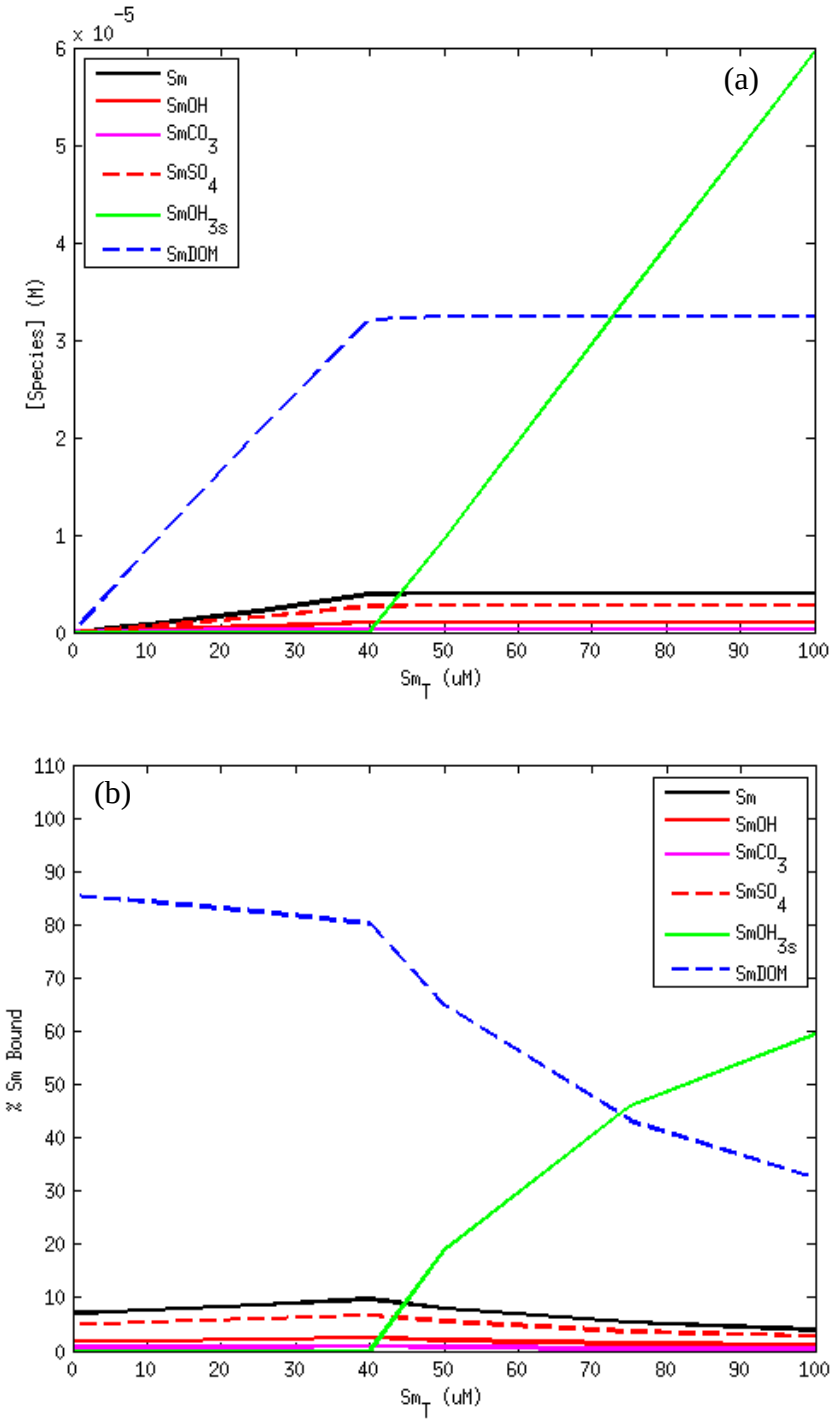

Figure 3-5. Speciation plots for KB DOM titrated with Sm during ISE titrations, plotted as [species] (a) and % Sm bound in species (b). Only dominant species concentrations and percentages are shown. Charge was omitted for clarity.

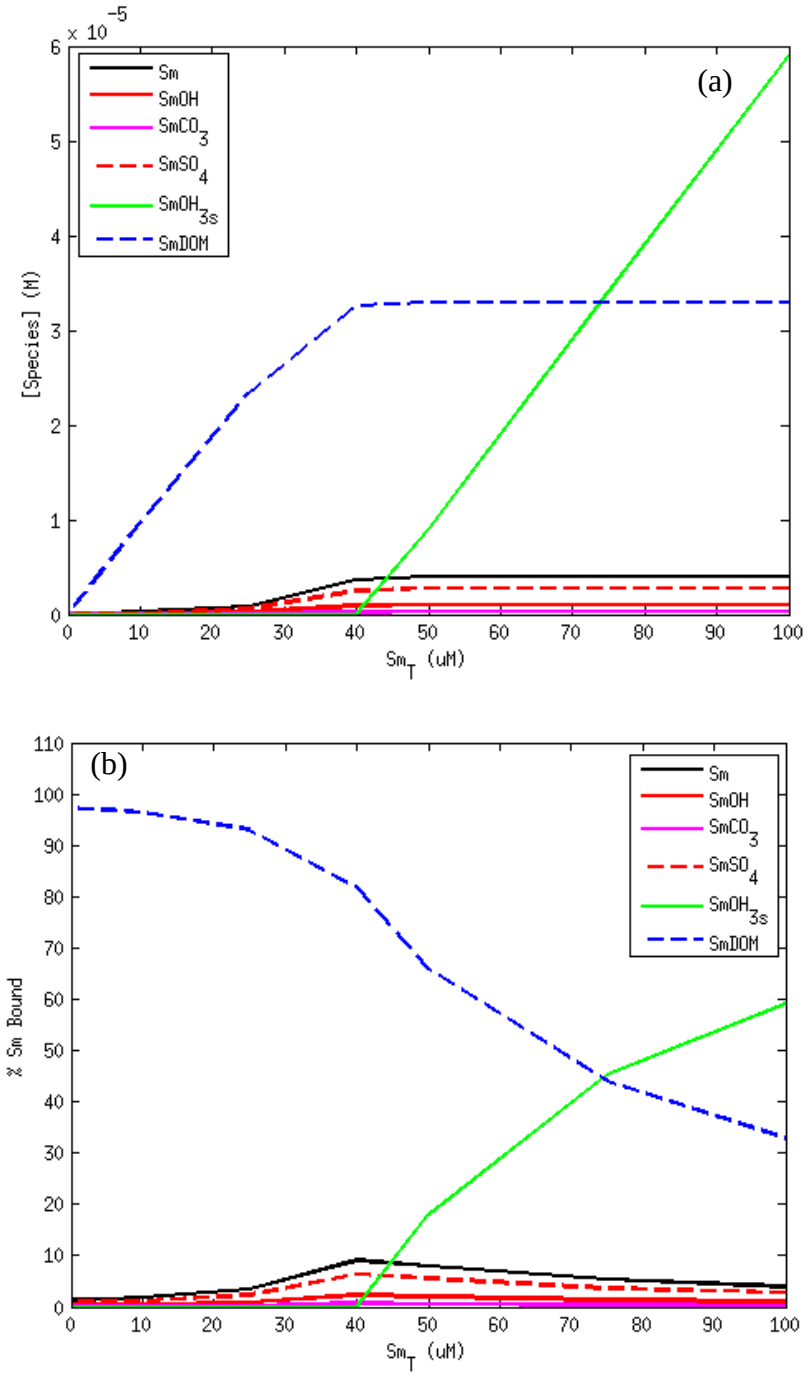

Figure 3-6. Speciation plots for LM DOM titrated with Sm during ISE titrations, plotted as [species] (a) and % Sm bound in species (b). Only dominant species concentrations and percentages are shown. Charge was omitted for clarity.

3.3.4 Comparison to the FQ Results

One of the main objectives of this thesis project is to validate an analytical technique in its ability to measure lanthanides speciation. The two techniques that were chosen measure the speciation in different ways. FQ requires the presence of fluorescent ligands in the DOM and modeling to calculate free metal concentrations in water, whereas ISE measures it directly. However, ISE proved to have a lot of interferences from the presence of other ions in water. In order to provide a more complete understanding of Sm speciation, the results from both experiments were compared.

FQ binding parameters were used to calculate free and bound Sm concentrations under the same conditions that were used for ISE experiments. The binding isotherms were employed for comparisons and are seen in Figure 3-7. There is a general agreement in the amounts of Sm calculated and measured by both techniques. Free Sm concentrations measured by ISE are within a log unit of the ones predicted by FQ (Figure 3-8). As mentioned previously (Section 2.2.4 and 3.2.4) the speciation model for the RW FQ modeling is very sensitive to the selection of the K_{sp} value for the $Sm(OH)_3$ solid formation. The selected value was chosen based on the best agreement between precipitation observed in the ISE samples and the model. The likely reason why the solid was not observed in the FQ experiments is that Sm was kept undersaturated in the sample by the aqueous complexes with carbonate and sulfate.

The best agreement between the two techniques is observed in the LM DOM sample (Figure 3-7c). It is also reflected in the similarity of the binding constants, discussed in Section 3.3.2. There is an over-prediction of bound Sm concentration

compared to ISE by the FQ technique at lower free Sm. Similar effect is observed in the KB DOM sample (Figure 3-7b). What is evident in both KB and SW DOM comparisons (Figure 3-7b and Figure 3-7a, respectively) is that FQ under-predicted bound Sm concentrations just before precipitation occurred. This may explain the higher binding capacities observed for these two samples from ISE than FQ (10-12 μmol/mg C vs 1.20-1.34 μmol/mg C, respectively), as this signifies a presence of other ligands that were able to bind more metal.

The observed lower free Sm concentrations from ISE experiments may be an evidence of the existence of non-fluorescent ligands that are not able to be captured by the FQ experiments. Based on the binding parameters between the two techniques it is possible to infer that additional ligand/s is/are likely to exhibit weaker binding, since the log K values from ISE experiments decreased from those obtained by FQ. This presence of the weak and strong binding sites has been previously reported for Eu binding to fulvic acids (Shin et al. 1996) and La, Ce, Ho and Yb binding to forest and lake sediment humic acids (An-Chao et al. 1998). It is also incorporated into WHAM modeling (Section 1.2.3; Tipping et al. 2011). Since there was so little differences between Sm and Dy binding observed in FQ experiments (Section 2.3.2), it is likely that similar type of binding maybe be also expected with Dy. Overall, since ISE is able to measure binding with all potential ligands it can be considered to be a more promising technique for accurate measurements; however, the limited response of the lanthanide selective electrode may hinder analysis of some samples and requires further improvement.

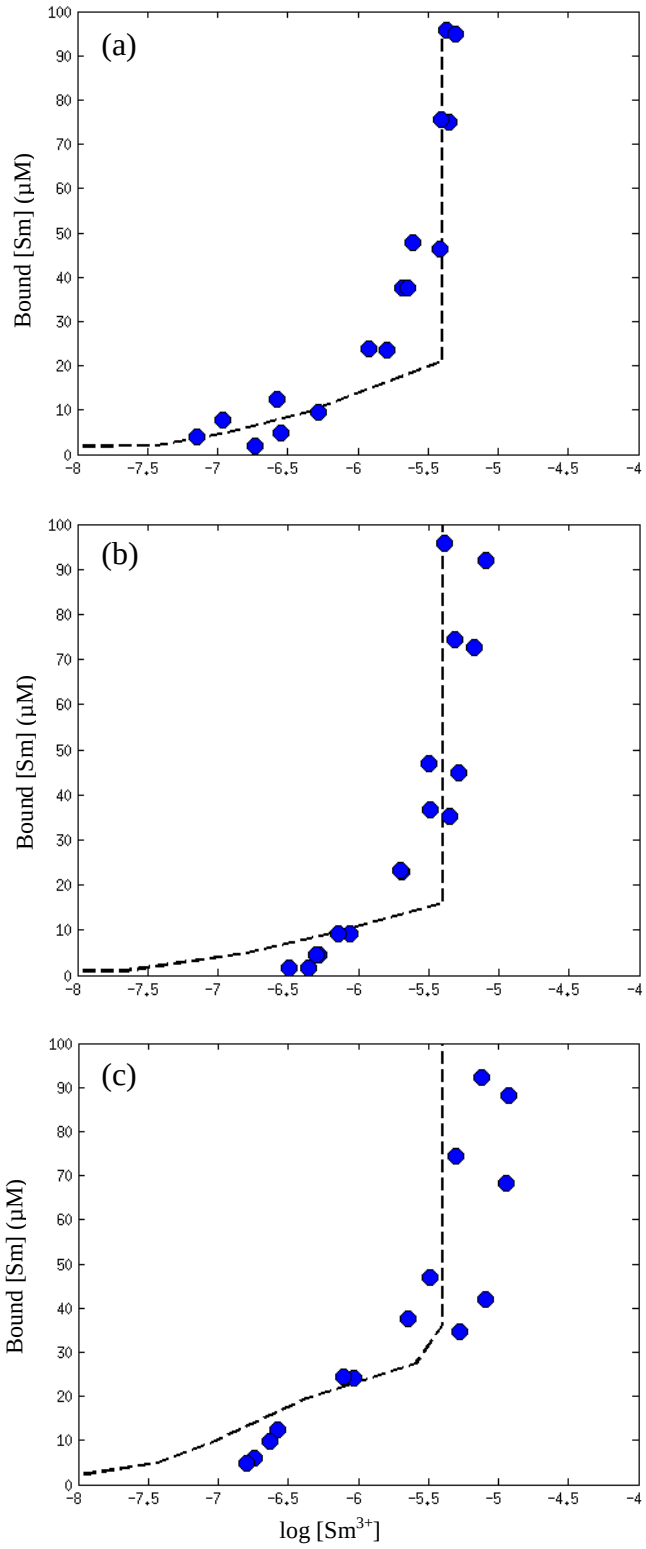

Figure 3-7. Binding isotherm comparisons for SW DOM (a), KB DOM (b) and LM DOM (c) between the data measured by ISE and calculated by FQ for the ISE experimental conditions.

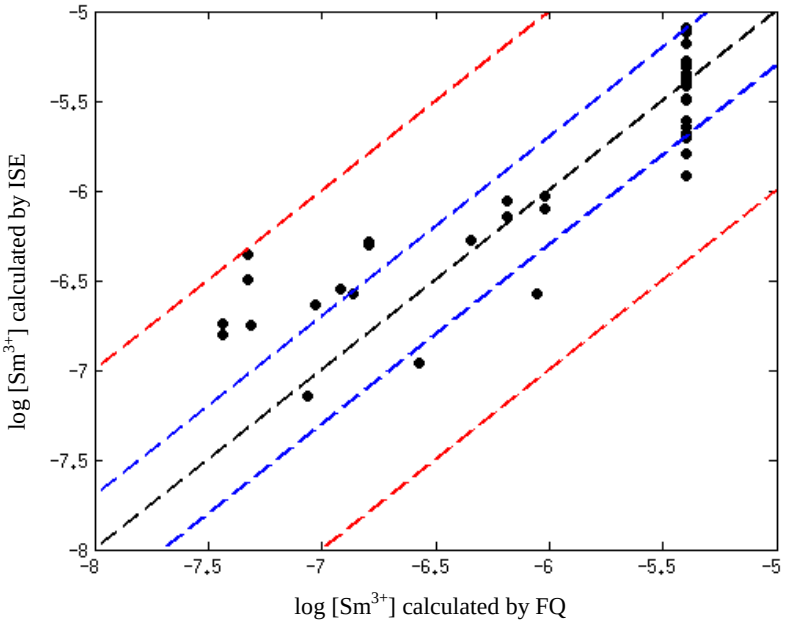

Figure 3-8. Comparison of calculated by FQ free Sm with measured by ISE free Sm. Black dashed lines represents 1:1 line, with two boarders identified 0.3 log units (blue) and 1 log unit (red).

3.4 Summary and Conclusions

Sm-specific ISE was constructed and used to measure free Sm concentrations in five DOM sources. After a period of ISE method development it was determined that IS of the sample has a dramatic effect on the ISE response. Furthermore, titrations of five DOM sources with Sm indicated that two sources (BB and SH DOM) that had the highest IS had issues with free Sm measurements. The interference of IS solution may have a number of explanations, including reduction in the activity of Sm and precipitate formation; however, a more viable explanation may be the interference from other cations in the solution, which can be a result of the lack of selectivity of the ISE ligand. A

development of a ligand that can bind lanthanides selectively, even if it is not selective for the specific lanthanides, may dramatically improve ISE measurements.

The analysis of the binding of the DOM sources with Sm, nevertheless, was possible. A one ligand model was able to describe the data relatively well considering the variation in the response. The calculated binding parameters reveal a moderate to strong binding (5.08-6.29) with binding capacities of 3.7-12 μmol/mg C. Since the sample solutions contained low concentrations of inorganic ligands, most of the Sm is bound to the DOM molecule. This is true until $Sm(OH)_3$ solid started to precipitate and the formation of the Sm-DOM complex is stopped.

Comparisons graph of the ISE data and FQ prediction of the data under the same conditions show that the presence of non-fluorescent ligands that cannot be measured by the FQ technique. These ligands are likely to exhibit a weaker binding. Overall, the two techniques show agreement, and are able to predict free Sm concentrations within a log unit of values. ISE might be a better suited technique for measurements of Sm speciation as it covers a wider range of ligands; however, it needs improvement.

3.5 References

Al-Reasi, H.A., Wood, C.M., Smith, D.S. 2011. Physicochemical and spectroscopic properties of natural organic matter (NOM) from various sources and implications for ameliorative effects on metal toxicity to aquatic biota. Aquatic Toxicology 103: 179-190.

Al-Reasi, H.A., Wood, C.M., Smith, D.S. 2013. Characterization of freshwater natural dissolved organic matter (DOM): Mechanistic explanations for protective effects against metal toxicity and direct effects on organisms. Environment international 59: 201-207.

An-Chao, G., Shen, Z., Høiland, H. 1998. Complex behaviour of trivalent rare earth elements by humic acids. Journal of Environmental Sciences 10: 302-308.

Armstrong, R.D., Horvai, G. 1990. Review Article: properties of PVC based membrane used in ion-selective electrodes. Electrochimica Acta 35: 1-7.

Bakker, E., Buhlmann, P., Pretsch, E. 1997. Carrier-based ion-selective electrodes and bulk optodes. 1. General characteristics. Chemical Reviews 97: 3083-3132.

Bakker, E., Buhlmann, P., Pretsch, E. 1997. Carrier-based ion-selective electrodes and bulk optodes. 1. General characteristics. Chemical Reviews 97: 3083-3132.

Bakker, E., Xu, A., Pretsch, E. 1994. Optimum composition of neutral carrier based pH electrodes. Analytica Chimica Acta 295: 253-262.

ChemInfo Services Inc. 2012. Review of the rare earth elements and lithium mining sectors. Final Report. Prepared for Environment Canada. Accessed http://www.miningwatch.ca/sites/www.miningwatch.ca/files/review_of_the_rare_earth_elements_and_lithium_mining_sectors.pdf January 15, 2016.

Craggs, A., Moody, G.J., Thomas, J.D.R. 1974. PVC matrix membrane ion-selective electrodes. Journal of Chemical Education 51: 541-544.

Di Toro, D.M., Allen, H.E., Bergman, H.L., Meyer, J.S., Paquin, P.R., Santore, R.C. 2001. Biotic Ligand Model of the acute toxicity of metals. 1. Technical basis. Environmental toxicology and Chemistry 20: 2383-2396.

Dong, W., Li, W., Tao, Z. 2002. Use of the ion exchange method for the determination of stability constants of trivalent metal complexes with humic and fulvic acids II. Tb^{3+}, Yb^{3+} and Gd^{3+} complexes in weakly alkaline conditions. Applied Radiation and Isotopes 56: 967-974.

El-Akl, P., Smith, S., Wilkinson, K.J. 2015. Linking the chemical speciation of cerium, to its bioavailability in water for freshwater alga. Environmental Toxicology and Chemistry 34: 1711-1719.

EPA (United States Environmental Protection Agency). 2012. Rare Earth Elements: A Review of Production, Processing, Recycling, and Associated Environmental Issues. Office of Research and Development. EPA/600/R-12/575. Revised December 2012. Accessed http://www.miningwatch.ca/files/epa_ree_report_dec_2012.pdf on January 15, 2016.

Ganjali, M.R., Pourjavid, M.R., Rezapour, M., Haghgoo, S. Novel samarium(III) selective membrane sensor based on glipizid. Sensors and Actuators B 89: 21-26.

Gu, Z., Wang, X., Gu, X., Cheng,J., Wang, L., Dai, L., Cao, M. 2001. Determination of stability constants for rare earth elements and fulvic acids extracted from different soils. Talanta 53: 1163-1170.

Harris, D.C. (ed). 2003. Quantitative Chemical Analysis (6th ed). USA (NY): W.H. Freeman and Company pp. 320-337, 393.

Lead, J.R., Hamilton-Taylor, J., Peters, A., Reiner, S., Tipping, E. 1998. Europium binding by fulvic acids. Analytica Chimica Acta 369: 171-180.

Leenheer, J.A., Croue, J-P. 2003. Characterizing dissolved aquatic organic matter. Environmental Science and Technology 37: 19A-26A.

Mathison, S., Bakker, E. Effect of transmembrane electrolyte diffusion on the detection limit of carrier-based potentiometric ion sensors. Analytical Chemistry 70: 303-309.

Oesch, U., Simon, W. 1980. Lifetime of neutral carrier based ion-selective liquid-membrane electrodes. Analytical Chemistry 52: 692-700.

Paquin, P.R., Gorsuch, J.W., Apte, S., Batley, G. E., Bowles, K.C., Cambell, P.G.C., Delos, C.G., Di Toro, D.M., Dwyer, R.L., Galvez, F., Gensemer, R.W., Goss, G.G., Hogstrand, C., Janssen, C.R., McGeer, J.C., Naddy, R.B., Playle, R.C., Santore, R.C., Scheider, U., Stubblefield, W.A., Wood, C.M., Wu, K.B. 2002. The biotic ligand model: a historic overview. Comparative Biochemistry and Physiology, Part C 133, 3-35.

Peshkova, M.A., Koltashova, E.S., Khripoun, G.A., Mikhelson, K.N. 2015. Improvement of the upper limit of the ISE Nernstian response by tuned galvanostatic polarization. Electrochimica Acta 167: 187-193.

Qin, Y., Bakker, E. 2002. Evaluation of the separate equilibrium processes that dictate the upper detection limit of neutral ionophore-based potentiometric sensors. Analytical Chemistry 74: 3134-3141.

Santore, R.C., Di Toro, D.M., Paquin, P.R., Allen, H.E., Meyer, J.S. 2001. Biotic ligand model of the acute toxicity of metals. 2. Application to acute copper toxicity in freshwater fish and daphnia. Environmental Toxicology and Chemistry 20: 2397-2402.

Shin., H.S., Lee, B.H., Yang, H.B., Yun, S.S., Moon, H. 1996. Bimodal normal distribution model for binding of trivalent europium by soil fulvic acid. Journal of Radioanalytical and Nuclear Chemistry 209: 123-133.

Slaveykova, V.I., Wilkinson, K.J. 2005. Predicting the bioavailability of metals and metal complexes: critical review of the biotic ligand model. Environmental Chemistry 2: 9-24.

Sokalski, T., Ceresa, A., Zwickl, T., Pretsch, E. 1997. Large improvement of the lower detection limit of ion-selective polymer membrane electrodes. Journal of American Chemical Society 119: 11347-11348.

Spahiu, K., Bruno, J. 1995. A selected thermodynamic database for REE to be used in HLNW performance assessment exercises. MBT Technologia Ambiental. Cerdanyola, Spain.

Stark, T.D., Choi, H., Diebel, P.W. 2005. influence of plasticizer molecular weight on plasticizer retention on PVC geomembranes. Geosynthetics international 12: 1-12.

Tipping, E., Lofts, S., Sonke, J. E. 2011. Humic ion-binding model VII: a revised parameterisation of cation-binding by humic substances. Environmental Chemistry 8: 225-235.

Wood, C.M., Al-Reasi, H.A., Smith, D.S. 2011. The two faces of DOC. Aquatic Toxicology 105S: 3-8.

Zhao, C-M., Wilkinson, K.J. 2015. Biotic ligand model does not predict the bioavailability of rare earth elements in the presence of organic ligands. Environmental Science and Technology 49: 2207-2214.

CHAPTER 4: COMPARISONS OF FQ AND ISE SPECIATION MODELS WITH WHAM AND THEIR APPLICATION IN TOXICOLOGICAL STUDIES

Abstract

Protection of the aquatic life from the release of lanthanides into the environment relies on the establishment of a regulatory criterion, which would ensure aquatic species safety. Models such as BLM, incorporate observed toxicity and speciation in order to perform risk assessments that can be used to create the values of the criterion. In this chapter speciation models created by FQ and ISE experiments were applied to the available toxicological data, in order to determine if these models are able to describe lanthanide toxicity. Additionally, they were compared to the predictions of WHAM, which is a speciation model that is often used when working with BLM. It was revealed that there were large disagreements between WHAM and the two models, where the former overestimated the binding of the metals at lower concentrations and underestimated it higher concentrations. This resulted in the inability of WHAM to explain Dy toxicity using free metal ion calculated from measured dissolved values. The LC_{50} values based on the free metal ion predicted by the FQ and ISE models are not able to explain metal toxicity. However, this may be attributed to the fact that lanthanide speciation is very dependent on correct prediction of solid formation and pH values control. Precipitation is observed in all toxicological samples, which tends to buffer the metal complexes and a small change in pH values results in large differences in speciation. A more rigorous control of these parameters during toxicological studies is required to accurate assess lanthanide speciation and toxicity.

4.1 Introduction

The protection of aquatic ecosystems against potential toxicity of metals requires a development of site specific guidelines or criteria that can be referred to for the allowed amounts of metal released in the effluent from industrial activities. An extensive risk assessment study is required for this purpose. The model that is often used to predict metal toxicity in the risk assessment process is called the Biotic Ligand Model (BLM). It assumes that the interaction of the free metal at the biotic ligand is proportional to the observed toxicity (Di Toro et al. 2001; Paquin et al. 2002; Santore et al. 2001; Slaveykova and Wilkinson 2005). Thus, metal speciation models are essential for BLM predictions. It is especially important to understand the interaction with dissolved organic matter (DOM), which is often variable based on the type of DOM (see Section 1.2.2) and poorly studied for some metals, such as the metals of interest to this project, lanthanides. There is little information available on both the speciation and toxicity of lanthanides (RNNR 2014). However, it was shown that the DOM-lanthanide complex itself may have some toxicity associated with it (Zhao and Wilkinson 2015). A better understanding of lanthanide speciation is required before the BLM can be developed for these metals.

The speciation model that is often used when working with BLM is the Windermere Humic Aqueous Model (WHAM, Tipping 1994). The model includes both types of complexation, inorganic and organic. When it comes to lanthanides the information is limited as it incorporates only a small number of datasets for DOM lanthanide interactions, usually no more than one (Tipping et al. 2011). In addition, most of those sets focus on binding of select number of lanthanides (Eu (majority), Tb, Dy and Sm), with only one study available for the rest of lanthanides (Sonke 2006; Sonke and

Salters 2006; Tipping et al. 2011). Nevertheless, the model was able to successfully predict lanthanide binding to fulvic and humic acids, both of which can be a part of larger DOM molecule (Lead et al. 1998; Pourret et al. 2007; Shin et al. 1996).

WHAM is often used to calculate the free metal ion during toxicological studies. As mentioned previously, BLM assumes that the free metal ion is the most bioavailable form of the metal (Di Toro et al. 2001; Paquin et al. 2002; Santore et al. 2001; Slaveykova and Wilkinson 2005). When two tests are compared, where the toxicity of the metal is measured in the presence and the absence of DOM, the resulting lethal concentration at which 50% of the population has died (LC_{50}) will vary between the two tests. Presence of DOM, if it is protective, will increase the LC_{50} value, calculated using measured dissolved metal concentrations. However, if the same results are recalculated for LC_{50} values using free metal concentration, there should be no significant differences between the two tests. This relationship will hold true only in the case where free metal is the only one that causes toxicity, if there are other species that have a lethal effect on the organism, the LC_{50} values will not converge.

In previous chapters the speciation of DOM with Sm ad Dy were measured and discussed. Two models were developed based on the binding parameters obtained from two analytical techniques, ion-selective electrode and fluorescence quenching (ISE and FQ). The results from these techniques were compared, and it was discovered that there are potentially multiple ligands in the DOM macromolecule that can interact with lanthanides. The results from ISE experiments revealed that there is more binding than can be measured by FQ. Thus, FQ overestimated the amount of free metal present in water. In the following section, the speciation models developed during this study were

compared to WHAM predictions matching the experimental conditions used for each technique. Furthermore, the free lanthanide ions were calculated and applied to the dose response curves to calculate LC_{50} values measured during the toxicological studies. The general assumption of BLM is that the toxicity is caused by the free metal ion; therefore, LC_{50} values plotted against free metal should show a collapse of the slope of the line that represents the dependence of lethal concentrations on free metal ion. The validity of the three speciation models (ISE, FQ and WHAM) was assessed based on how well are they able to predict toxicity.

4.2 Methods

ISE and FQ binding parameters (Table 2-4 and Table 3-4) were used to calculate the free metal ion concentrations. The MATLAB code used for this purpose is found in Appendix C5. For comparisons with WHAM the calculated free ion concentrations from FQ experiments and measured by ISE were used. For the comparison with toxicological studies all models were adjusted to experimental conditions of the study and the free ion concentrations were calculated from the dissolved measured concentrations. The conditions are summarized in the next sections.

4.2.1 WHAM Modeling

WHAM (version 7.02., Tipping et al. 2011) was used to calculate the speciation of Sm and Dy. The concentrations of inorganic ligands used as inputs into the model are summarized in Table 4-1. The values for pH was selected as 7.3 and the total metal concentrations were 2 µM, 5 µM, 10 µM, 25 µM, 40 µM, 50 µM, 75 µM and 100 µM. DOM was entered into the model as dissolved organic carbon (DOC) and it was assumed

to be in colloidal phase and at 90% fulvic and 10% humic acid (Santore et al. 2001; Lofts 2012; BLM manual 2007); thus, the 10 ppm DOC was broken down to 9 ppm fulvic and 1 ppm humic acid. Free metal concentrations were reported in the output as aqueous concentration of either [Sm^{3+}] or [Dy^{3+}] depending on the comparison.

Table 4-1. Summary of WHAM inputs of inorganic ligands used in both FQ and ISE experiments. The measurement and calculation of these values were discussed previously (Section 2.2.4 and 3.3.4).

DOM Sources	**FQ experiments**		**ISE experiments**		**Both**
	[CO_3^{2-}] mM	**[SO_4^{2-}] mM**	**[CO_3^{2-}] µM**	**[SO_4^{2-}] mM**	**[Cl^-] µM**
SW DOM	1.003	3.3	2.87	0.15	40.8
KB DOM	1.002	3.3	2.24	0.15	-
LM DOM	1.002	3.3	1.78	0.15	88.5
BB DOM	1.25	3.3	247	0.15	5450
SH DOM	1.003	3.3	2.77	0.15	557

4.2.2 Toxicological Studies (Acute)

All acute toxicity tests data were obtained from toxicological group at Wilfrid Laurier University. The selection of the experimental conditions for FQ and ISE experiments, such as pH, range of metal concentrations, DOM selection and DOC concentration were influenced by the toxicological studies. An effort has been made to replicate the toxicity tests conditions in order to produce speciation models with conditional binding constants that could be applied to the dose response curves. All forms of precipitation were included in the model, as the tests lasted much longer than the titrations, and the precipitation is likely to occur (Section 2.2.4, Johnson and O'Rourke 1954). The toxicological studies involved the acute toxicity (96 hrs) tests performed in accordance with standard test on *Hyalella azteca* (Environment Canada 2013). One set of

Table 4-2. Dose response information for toxicity of Sm with and without the presence of SW DOM to *Hyalella azteca* reported as percent survival. Data measured by Alyssa Verdin (Verdin 2014).

[Sm] µg/L	[Sm] µM	Percent Survival (%)							
		Sm only (0.6 ppm DOC)						8 ppm DOC	
0	0	90	100	100	80	90	70	100	100
400	2.66	80	50	40	60	80	30	80	100
800	5.32	40	60	30	30	20	50	100	100
1,600	10.64	60	30	30	50	40	30	80	90
3,200	21.28	20	10	20	10	10	20	50	40
6,400	42.56	0	0	0	0	0	0	0	10
10,000	66.51	-	-	-	-	-	-	0	0

Table 4-3. Dose response information for toxicity of Dy with and without the presence of SW DOM to *Hyalella azteca* reported as percent survival. Data measured by Oliver Vukov (Vukov 2015).

[Dy] µg/L	[Dy] µM	Dissolved [Dy] µM	Percent Survival (%)				Dissolved [Dy] µM	(%)		Dissolved [Dy] µM	(%)	
			Dy only (0.4 ppm DOC)					9.3 ppm DOC			13 ppm DOC	
0	0	0.021	90	100	100	90	0.021	100	100	0.0059	100	100
200	1.23	0.71	70	90	90	80	-	-	-	-	-	-
800	4.92	1.53	90	100	30	72.7	3.2	90	100	4.04	90	90
1,600	9.85	1.96	40	30	20	45.5	4.04	100	90	7.0	70	70
3,200	19.69	2.62	0	0	0	8.3	5.42	20	40	10.6	50	40
6,400	39.38	2.93	0	0	-	-	6.65	0	0	19.6	0	0
12,800	78.77	0.022	-	-	-	-	5.19	0	0	29.6	0	0

Table 4-4. Dose response information for toxicity of Dy with and without the presence of SW DOM to *Hyalella azteca* reported as percent survival. Data measured by Che Lu (Lu 2015).

[Dy] µg/L	[Dy] µM	Dissolved [Dy] µM	Percent Survival (%)				Dissolved [Dy] µM	(%)		Dissolved [Dy] µM	(%)			
			Dy only (0.4 ppm DOC)					9.6 ppm DOC			12.55 ppm DOC			
0	0	0.037	100	100	100	100	0.037	90	100	0.022	90	90	95	100
200	1.23	0.54	90	100	100	100	3.34	80	100	2.41	90	100	100	90
800	4.92	2.23	70	80	70	60	4.53	60	40	4.85	80	90	100	100
1,600	9.85	2.52	60	50	0	40	7.64	20	0	6.14	10	30	90	90
3,200	19.69	3.66	20	0	20	-	14.73	0	0	8.69	10	0	30	40
6,400	39.38	3.69	0	0	0	0	25.35	0	0	23.34	0	0	0	0

experiments was provided for Sm and two sets for Dy (study 1 and 2). The dose response values from the toxicological studies were provided and summarized in Table 4-2 and Table 4-3. Experimental anion concentrations used for modeling are presented in Table 4-5. The average pH values of 7.65, 7.6 and 7.625 were chosen for two Dy and Sm tests, according to the experimental conditions. The average of dissolved measured concentrations from initial and final readings was used for LC_{50} calculations of Dy; however, nominal values were used for Sm comparisons, as the measured values were not available. The LC_{50} values were obtained from the dose response curves together with 95% confidence intervals using a method described by Meyer and Adams (2010). The code for the modeling is found in Appendix C6.

Table 4-5. Anion concentrations modeling input for FQ and ISE speciation models for toxicological studies comparisons. The water chemistry was selected based on the recipe discussed in Borgmann (1996).

Anion	**[Anion] µM**
Cl^-	1025
HCO_3^{-} [a]	500
SO_4^{2-}	125
Br^- [b]	5

(a) In modeling represents total carbonate.
(b) Br^- was only used in Dy toxicity studies.

4.3 Results and Discussion

The next section describes the results from the comparison of the ISE and FQ speciation models with WHAM. This includes the discussion of the ISE and FQ models validity in the prediction of the toxicity response of Sm and Dy on *Hyalella azteca.*

4.3.1 Comparison with WHAM

WHAM was used to predict free metal ion in water for the experimental conditions of ISE and FQ. The comparisons are plotted on Figure 4-1. The modeling was done for all available DOM samples. The general trend observed in the comparisons between FQ and WHAM is that at lower concentrations of the free ion WHAM tends to underestimate the concentrations measured by FQ model; however, as the free ion increases it starts to overestimate the ion. This means that at high Sm concentrations WHAM predicts less binding by the DOM than is observed during FQ experiments and it is the opposite at the lower end of the free ion. It is important to note here that the LC_{50} values, discussed in the next sections in more details, occur around log of -7 for both Sm and Dy (using nominal values, which were generally more conservative than using measured dissolved concentrations); therefore, under the FQ conditions this value will be underestimated by WHAM according to the Figure 4-1 (more so for Dy than Sm). If WHAM is used for the purpose of speciation prediction for the toxicological studies it will predict a stronger binding, which would signify that the DOM is more protective than according to FQ model predictions.

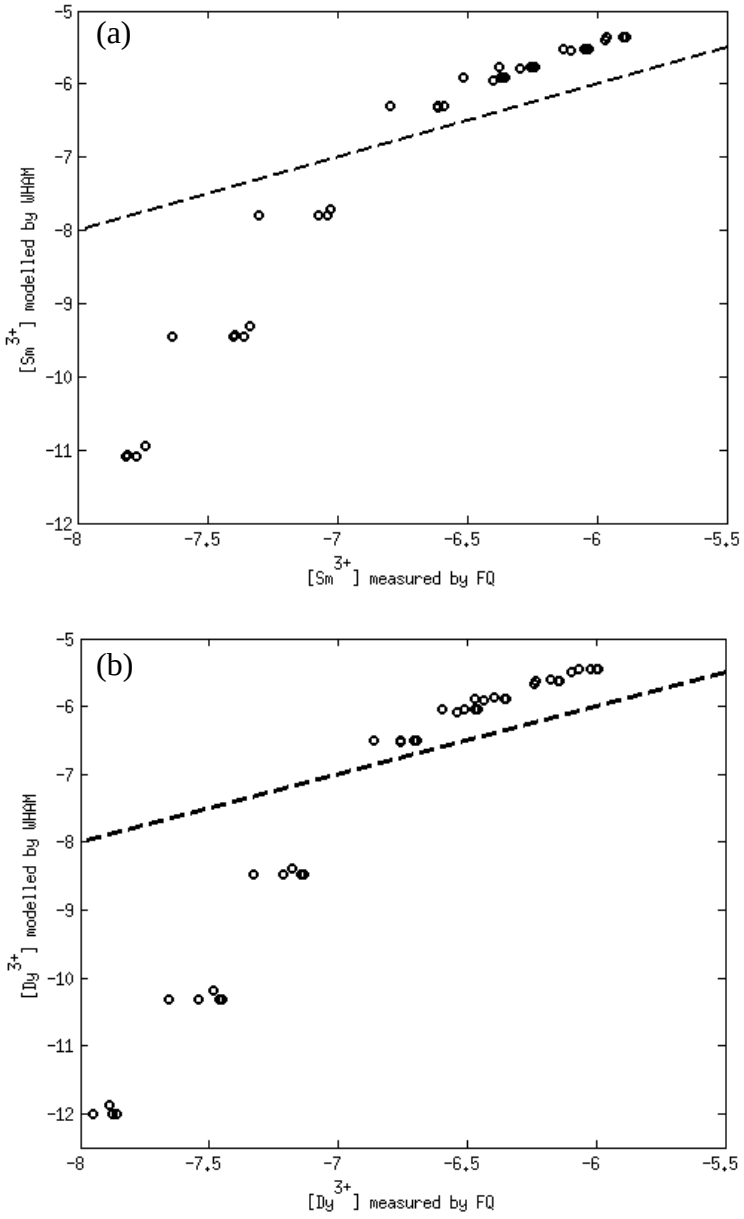

Figure 4-1. WHAM comparisons with FQ speciation model for Sm (a) and Dy (b). Dashed line represents a 1:1 line.

Similarly to FQ comparison, there are two distinct areas where WHAM disagrees with ISE model for the experimental conditions of ISE (Figure 4-2a). At lower concentration of the free Sm WHAM dramatically underestimates the free metal ion concentration measured by the ISE or overestimates the binding. In contrast, at a higher

end of Sm, the free ion is overestimated (Figure 4-2b) or, conversely, the binding is underestimated. The overestimation of the free ion it is actually greater than that observed in the FQ experiments. The possible reason for this is the lack of precipitate formation included in the WHAM modeling. This may not be an issue for metals or conditions that do not produce solids, but in the case of ISE modeling hydroxide solid was observed, as it is evident in the stabilization of the free Sm concentrations seen in the binding isotherms plots (Figure 3-7). Thus, WHAM would overestimate the concentrations of the aqueous ion. Similar to the FQ comparison, WHAM would underestimate the free metal ion in the conditions of the ISE experiment around LC_{50} value of -7 for a log of free Sm. The underestimation however is much greater in this case. A closer look at high total Sm reveals that there is a small area of one point per titration where the two models agree (around log [Sm^{3+}] of -6). This means that for these DOM samples WHAM was only able to predict the binding for a very short range of free ion. It can be concluded that WHAM may not be the best model for the Sm speciation prediction for the samples used in this study. The previous work that has shown a better WHAM agreement (Lead et al. 1998; Pourret et al. 2007) usually used isolated humic and fulvic acid, which may not be representative of the natural organic matter. Additionally, different techniques were used such as equilibrium dialysis and ultrafiltration, which as discussed in Section 1.3 are not the most reliable speciation techniques as they do not measure true speciation.

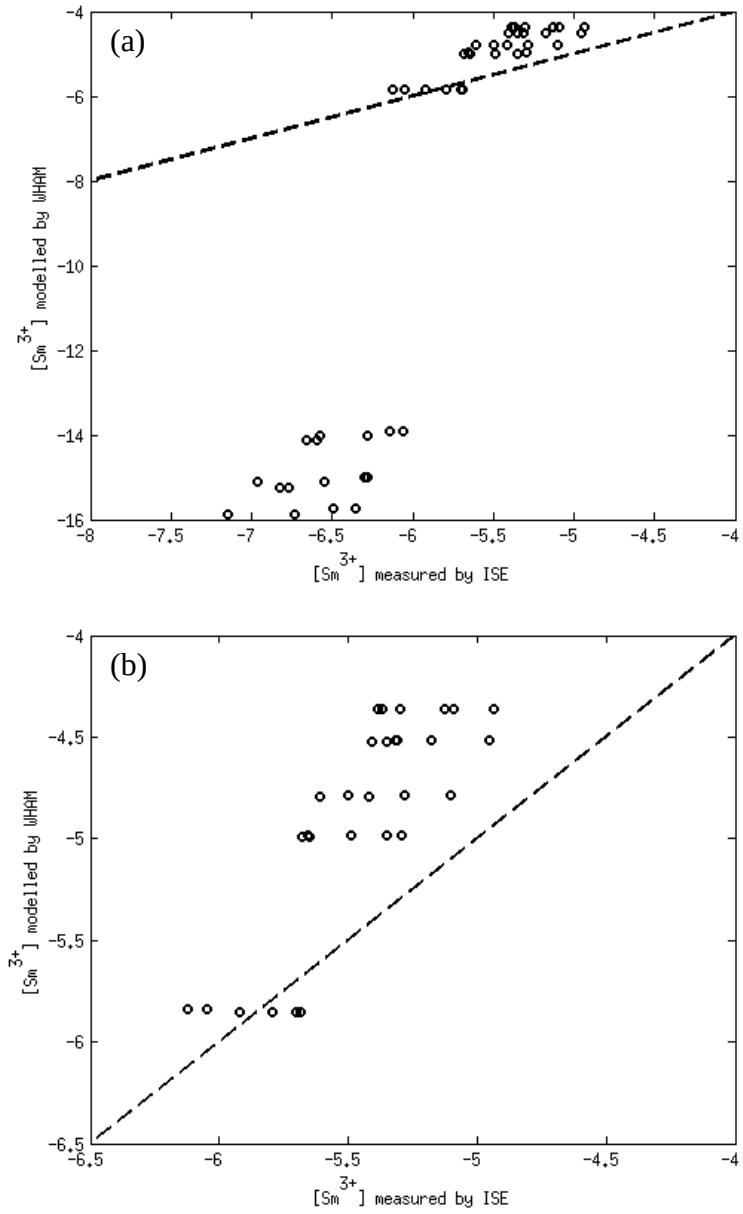

Figure 4-2. WHAM comparisons with ISE speciation model, where graph (a) shows a complete comparison, while (b) shows a close up on the higher free Sm concentrations. A dashed line respresents a 1:1 line.

4.3.2 Speciation Models Applications in Toxicological Studies

The speciation models for Dy and Sm were used to calculate the free metal ion in test solutions of the toxicological studies. As mentioned previously (Section 4.2.2) the

binding parameters obtained from FQ and ISE techniques are conditional to the chemistry of experimental solutions used. As much as possible the conditions selected were representative of the toxicity tests conditions. The same DOM source (SW DOM) and range of metal concentrations were used in both studies. The main differences were noticed in the pH ranges (FQ and ISE: 7.3, toxicology: 7.6) and anion concentrations in the matrix (Table 4-1 and Table 4-5). Although influence of the anions was eliminated by modeling inorganic speciation together with the DOM binding, the binding constants were still conditional to the pH value.

4.3.2.1 Speciation

The speciation was greatly dependent on the pH values of the samples. Large variation in the metal species distribution is observed over a small range of pH values. Figure 4-3 shows the difference in the samples containing 9.3 ppm of DOC and varying concentrations of Dy over the range of pH values recorded during the experiments (7.4-7.8). The change of 0.4 in pH values has an influence on the type of precipitate forming, with higher pH value producing hydroxide solid, while lower pH value being dominated by the carbonate solid. Lower pH value also has a slightly greater concentration of free metal ion with the range of 0.013-0.55 μM, as opposed to 0.0056-0.14 μM at pH of 7.8. These results signify the importance of a rigorous pH monitoring and control during toxicological studies, as it will greatly influence the distribution of the metal.

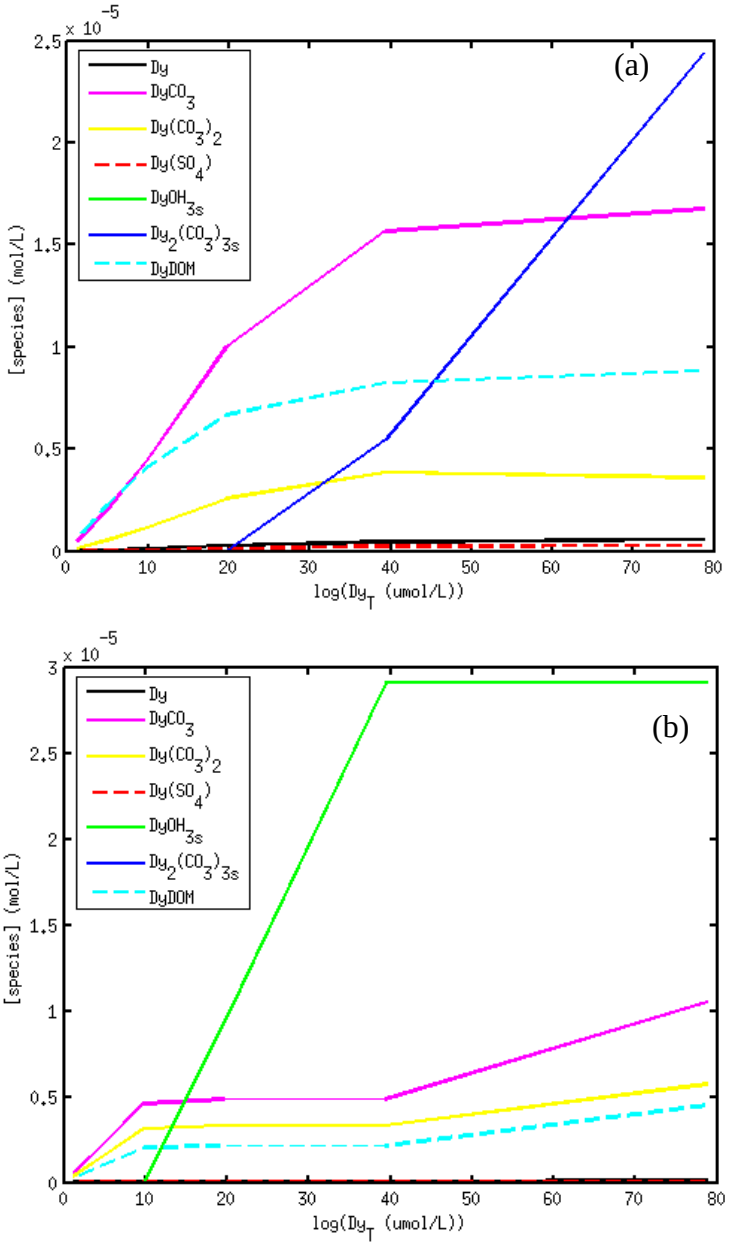

Figure 4-3. Speciation plots for Dy with 9.3 ppm SW DOM at pH 7.4 (a) and 7.8 (b) using experimental conditions of the toxicological studies.

Even though there were no distinguishable differences observed between Sm and Dy in FQ experiments large differences were seen in the speciation of the metals under the toxicological experimental conditions (Figure 4-4), which were very similar for both metals as the tests followed the standard procedure (Environment Canada 2013). Figure 4-4 shows speciation of select studies, 9.3 and 8 ppm DOC tests for Dy and Sm, respectively. In the case of Dy test, aqueous carbonate complex is the most dominant species (Figure 4-4a), with DOM and 1:2 carbonate complexes being the second most dominant. There is also an observed precipitation of the hydroxide solid (green line), which would explain the reduction in the dissolved Dy added into the test solutions observed during the study (Table 4-3 and Table 4-4). Very different speciation trends are observed in Sm tests (Figure 4-4b). A large portion of the metal is found to be a part of carbonate solid (blue line). These dissimilarities were attributed to the slight differences in the pK_{sp} values for hydroxide (25.5 for Sm vs. 25.9 for Dy) and carbonate solids (32.5 for Sm and 31.5 for Dy), and are not a result of the differences in binding to DOM. Regardless of the differences in speciation, DOM was able to bind some portion of the metal in both studies, therefore, it is expected to be protective against toxicity.

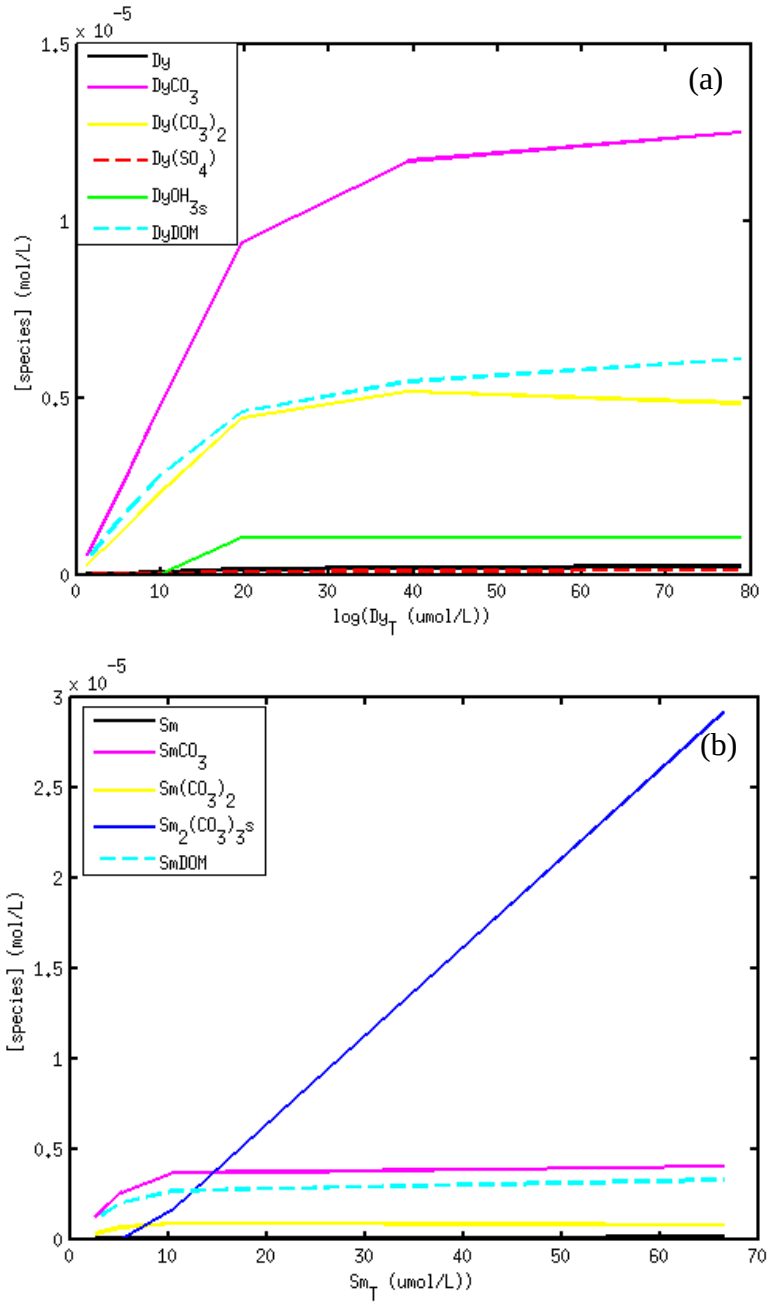

Figure 4-4. Speciation plots for Dy with 9.3 ppm SW DOM (a) and for Sm with 8 ppm SW DOM (b) using experimental conditions of the toxicological studies.

Table 4-6 outlines all the free metal concentrations calculated for all samples using nominal values for model input. Both techniques FQ and ISE were able to predict similar free Sm concentrations. This was expected, as both techniques had generally good

agreement, with FQ only slightly overestimating free Sm (Figure 4-6). As discussed in previous section, however, there are large disagreements between both FQ and ISE models and WHAM at lower end of the total metal. Similar results were observed when WHAM is used to calculate the free metal ion in the tests that had DOM added, the free metal concentrations were predicted to be around 10^{-13} μM (Table 4-6 and Figure 4-5). For the samples that had very little measured DOC, WHAM tends to overestimate the free metal ion concentrations, as it does not incorporate precipitation; however, it is shown to occur in the samples based on the speciation models created using FQ and ISE experiments.

Table 4-6. Free metal concentrations (μM) modeled for the toxicological studies experimental conditions using speciation models from FQ, ISE experiments as well as WHAM.

Samarium						
Total [Sm] μM	**Sm only (0.6 ppm DOC)**			**8 ppm DOC**		
	FQ	**ISE**	**WHAM**	**FQ**	**ISE**	**WHAM**
2.66	0.039	0.040	0.056	0.024	0.031	1.35×10^{-13}
5.32	0.071	0.071	0.17	0.050	0.063	7.09×10^{-13}
10.64	0.073	0.073	0.39	0.072	0.073	5.20×10^{-11}
21.28	0.077	0.077	0.86	0.076	0.076	0.13
42.56	0.085	0.085	1.86	0.084	0.085	1.0
66.51	-	-	-	0.095	0.096	2.12
Dysprosium						
Total [Dy] μM	**Dy only (0.4 ppm DOC)**		**9.3 ppm DOC**		**13 ppm DOC**	
	FQ	**WHAM**	**FQ**	**WHAM**	**FQ**	**WHAM**
1.23	0.0116	0.009	-	-	-	-
4.92	0.047	0.11	0.033	3.03×10^{-13}	0.030	1.34×10^{-13}
9.85	0.096	0.26	0.070	4.55×10^{-12}	0.062	8.47×10^{-13}
19.69	0.14	0.56	0.14	0.0012	0.14	5.66×10^{-10}
39.38	0.19	1.21	0.19	0.452	0.18	0.19
78.77	-	-	0.23	1.74	0.23	1.38

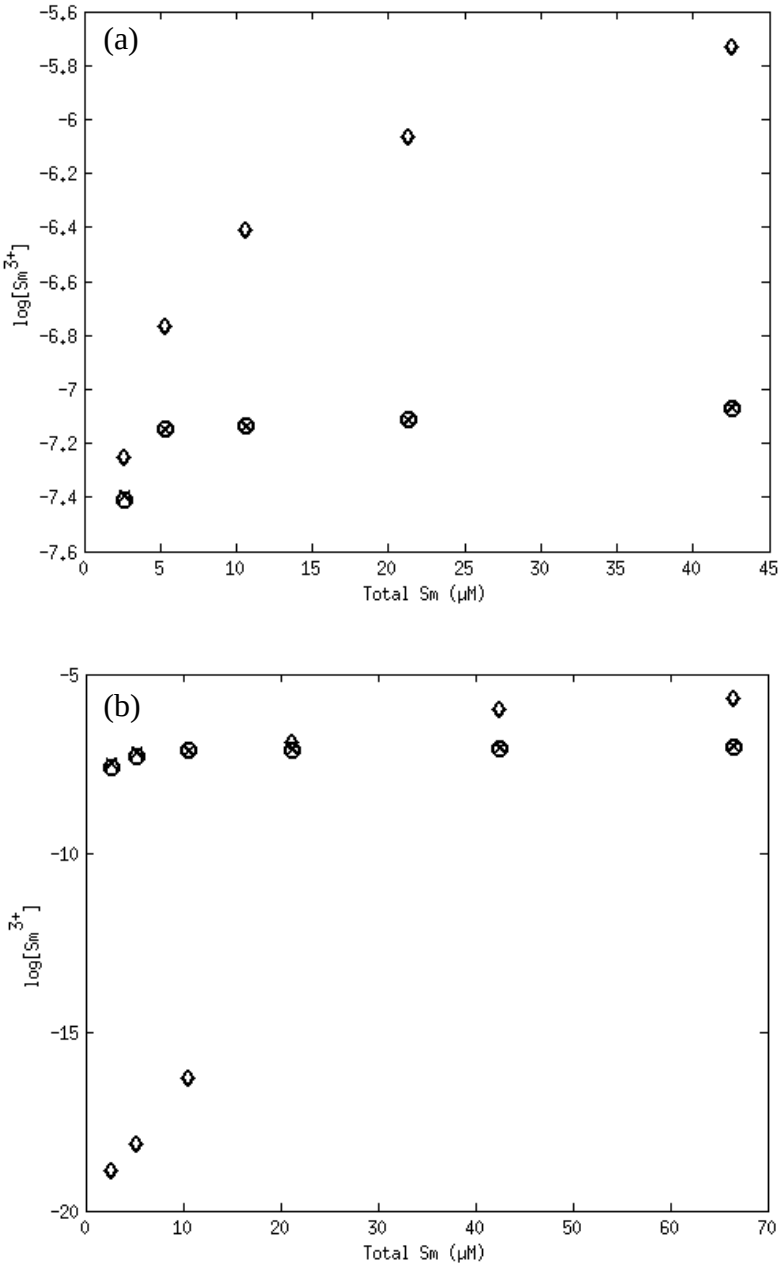

Figure 4-5. Comparison of log [Sm^{3+}] measured by FQ (○), ISE (x) and WHAM (◊) (Table 4-6) for 0.6 ppm DOC (a) and 8 ppm DOC. ISE and FQ are very similar in their magnitude in both cases, whereas WHAM tends to overestimate the concentration of free Sm at low [DOC], and dramatically underestimate it in the presence of DOC at lower concentration of the metal.

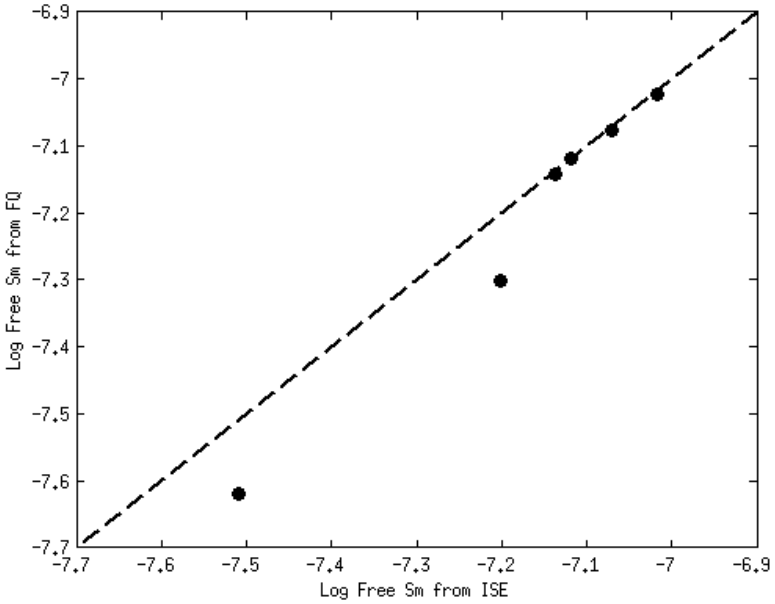

Figure 4-6. Comparison of free [Sm] measured by FQ and ISE. A dashed line represents a 1:1 line. FQ tends to slightly overestimate free Sm at lower end of concentrations.

4.3.2.2 LC_{50} calculations

All three speciation models were applied to the dose response data to calculate LC_{50} values for Sm toxicity studies. Nominal concentrations were used, as measured values were not available. The comparisons are seen in Figure 4-7. DOM was protective against Sm toxicity, as the LC_{50} showed significant increase between the two tests (Figure 4-7a). There are no significant differences in LC_{50} values calculated using free Sm predicted by FQ and ISE models (Figure 4-7b), as both techniques predict very similar free Sm concentrations (Table 4-6 and Figure 4-6). The change of the LC_{50} values over the DOC concentration decreased from 1.99 using nominal [Sm] to 0.0034-0.0035 using free [Sm]. However, there are still significant differences between the two LC_{50} values. According to the speciation graph (Figure 4-7b), a large portion of the metal is bound in the solid, and thus, the free metal ion remains relatively constants (Table 4-7),

regardless of the presence or absence of the DOM; this makes the LC_{50} value difficult to calculate within a confident degree of accuracy, as the gradient of concentrations is so small. Additionally, it is important to note that there is a large variability in the dose response curves for the tests containing Sm only (Table 4-2), with value ranges of 30-80% survival for the solutions with total Sm concentration of 2.66 μM. The large range of survival percentages may add more error to the LC_{50} calculations. Conversely, since WHAM does not include precipitation, there was a much larger range of free metal concentration available for calculations. These LC_{50} values (Figure 4-7b) were greater than the ones predicted by FQ and ISE models; with no significant differences between the two values. In the case of Sm toxicity, WHAM calculated free metal is able to better explain observed toxicity; however, it predicted lower toxicity of free Sm based on the higher LC_{50} values calculated.

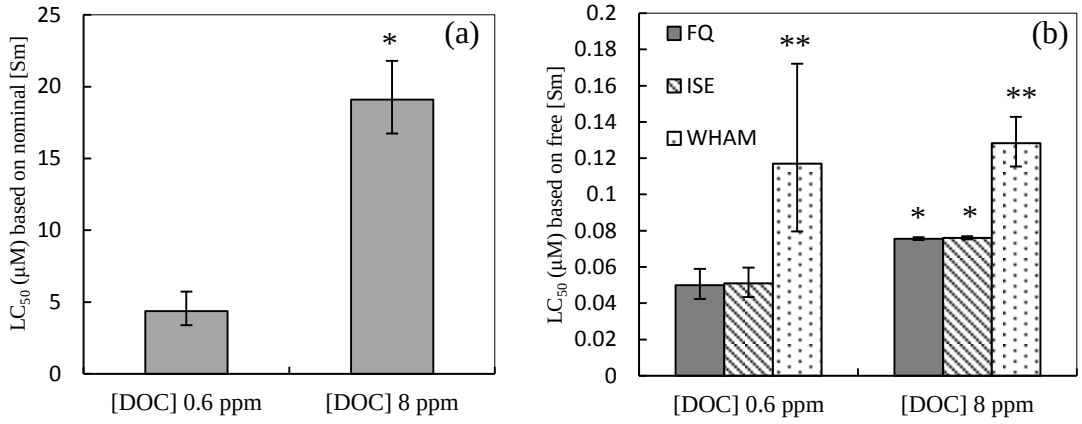

Figure 4-7. LC_{50} comparisons for the SW DOM tests, with values calculated using nominal [Sm] (a) and free [Sm] (b) predicted by the three models (FQ, ISE and WHAM). The error bars represent the 95% CI; (*) shows significant differences between the two [DOC] tests and (**) shows significant differences between the speciation models.

Table 4-7. Summary of the line of best fit parameters for the LC_{50} values comparisons.

Comparison	Slope	Intercept
Dysprosium 1		
LC_{50} and Dissolved [Dy]	0.53	1.14
LC_{50} and Free FQ [Dy]	0.0029	0.0132
LC_{50} and Free WHAM [Dy]	-0.0009	0.01
Dysprosium 2		
LC_{50} and Dissolved [Dy]	0.34	2.11
LC_{50} and Free FQ [Dy]	0.0014	0.025
LC_{50} and Free WHAM [Dy]	-0.007	0.079

FQ model was applied to the dose response data from both Dy studies. The plots summarizing LC_{50} values correlation with DOC concentration are shown in Figure 4-8 and Table 4-7. SW DOM was protective against Dy toxicity as observed by the increase of the LC_{50} values calculated using nominal Dy concentrations (Figure 4-8a). The slope of the line between the LC_{50} calculated using dissolved and free Dy decreased from 0.54 and 0.34 to 0.0029 and 0.0014, for two studies, respectively. Regardless of the decrease however, there were still significant differences between the LC_{50} values calculated using free Dy ion of the first study (Figure 4-8b1). The second Dy study, however, had an observed collapse of the LC_{50} vs DOC slope of the line (Figure 4-8b2), with the 95% CI of the second point (9.6 ppm DOC) overlapping with the other two points. In the case of the second study, the free metal ion produced by the FQ model was able to explain the observed toxicity; however, it was not able to explain the toxicity in the first study. It is important to note that LC_{50} values calculated using WHAM show a dramatic decreased with the increase of DOC concentration (Figure 4-9), which does not provide a meaningful explanation for the observed toxicity. This can be explained by very low measured dissolved concentrations (Table 4-3 and Table 4-4, 0.0059-29.6 μM). WHAM tends to dramatically underestimate free metals ion at such low total metal concentrations

in the presence of DOM ([Dy^{3+}] around 10^{-19} M), which resulted in very low predicted LC_{50} values.

The inability of the FQ and ISE models to explain metal toxicity for Sm and one of the Dy studies as a function on the free metal ion, apart from difficulty in predicting accurate metal distribution, may signify the influence of other complexes and/or solids on the toxicity of the metals. An example of this has been shown by Zhao and Wilkinson (2015), where organic complexes participated in the uptake of lanthanides. Thus, the toxicity of other complexes and solids needs to be assessed by further toxicological experimentation.

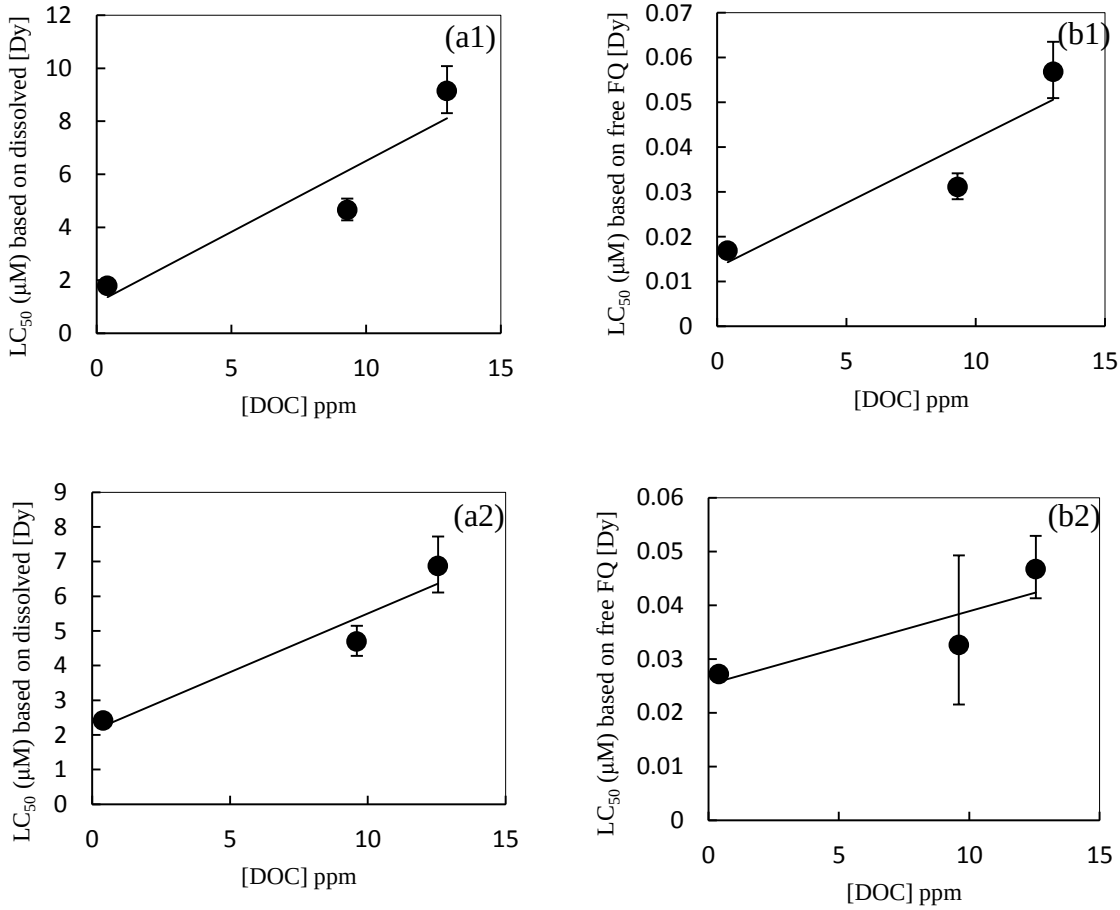

Figure 4-8. LC_{50} values calculated using measured dissolved [Dy] (a1 and a2) from study two studies and free FQ [Dy] (b1 and b2) from two studies plotted against [DOC] of the SW DOM. The error bars represent 95% CI.

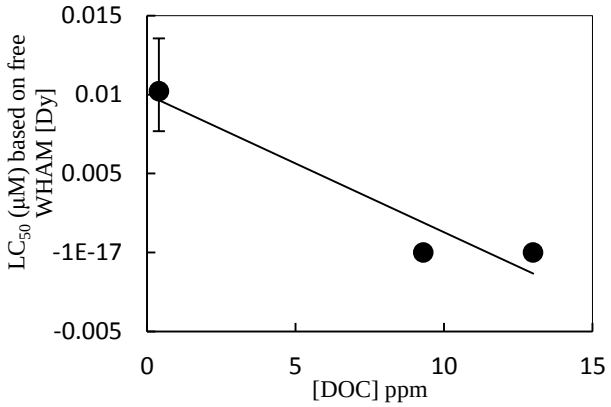

Figure 4-9. LC_{50} values calculated using free [Dy] predicted by WHAM using the average of dissolved [Dy] measured in the first study at the beginning and the end of the experiments.

For the purpose of establishing site specific criteria for the release of lanthanides into the environment it is important to note the toxicity is observed at the concentrations of the metal much higher than what would be found naturally in the environment (0.0003 to 0.8 nM, refer to Table 1-4). The highest concentration of dissolved Sm (also the highest of the two lanthanides) was found in rivers affected by the acid mine drainage in Spain (0.242 μM; Gimeno et al. 2000). This value, however, is still an order of magnitude lower than the lowest LC_{50} value observed in this study for Sm (4.37 μM, using nominal values) and Dy (1.79 μM, using measured dissolved values). The general procedure required for the establishment of the site specific criteria is to apply a safety factor of 10 to the lowest observed effect value (Avalon 2013; CCME 2003). If it is applied to the LC_{50} value reported in this study, the criterion (0.437 μM and 0.179 μM) would be in the same range as the highest observed concentrations in the environment. The LC_{50} values

reported by Borgmann et al. (2005) for Sm toxicity using measured Sm values in soft water produced a criterion that was much lower than the one reported in this study (0.049 μM). This indicates that certain areas that are heavily influenced by the releases of lanthanides may exceed the site specific criterion for the protection of aquatic life. The criterion may also change if a more sensitive organism is discovered in the area of the industrial input. Finally, acute toxicity tests used in this analysis generally provide much higher effects concentration than reported in chronic studies. Therefore, even lower criteria are expected using chronic tests. These cases may require the development of more sensitive analytical techniques, than presented in this study. However, with the current information available on lanthanide toxicity the two techniques cover the range of concentrations where the toxicity is observed, although they may not be relevant to the naturally occurring levels.

4.4 Summary and Conclusions

The speciation models produced by experiments using FQ and ISE analytical techniques were compared to WHAM. WHAM tends to disagree with both models and overestimate the DOM-lanthanide binding at the lower metal concentrations and underestimate it at higher concentrations. This has a significant impact on the ability of WHAM to explain observed Dy toxicity, as it shows a dramatic decrease in the LC_{50} values calculated using free Dy with the increase of the DOC concentration. Conversely, WHAM predicted Sm concentrations produce LC_{50} values that are able to explain DOM protective effects. Both FQ and ISE models were not able to explain Sm toxicity, however the values calculated using the models from these techniques predict lower LC_{50} values than shown by WHAM, which means that the models predict higher toxicity of the

free Sm ion. LC_{50} values calculated using free Dy from the FQ model using measured dissolved concentrations show a general reduction in the slope of the correlation line, with the second study showing no significant changes in LC_{50} values calculated using free Dy. However, LC_{50} values calculated using free Dy of the first study are still significantly difference from one another. Thus, in case of Dy the ability of FQ model to explain toxicity is inconclusive.

There were large differences between the two lanthanides noticed in the speciation plots for the experimental conditions of toxicological studies. The slight variability in the pK_{sp} values of hydroxide and carbonate solids had a dramatic effect on the way the metals distributed in the solutions, with Dy forming a small amount hydroxide solid, but mostly trapped as carbonate and DOM complexes, whereas Sm was mostly found in the carbonate solid. This speciation was observed using the average pH values for three sets of studies (Sm and two Dy); however, pH had also a significant impact on the metal distribution with a change if 0.4 resulting in the formation of either carbonate or hydroxide solids of Dy. The high sensitivity of the model to the solubility products as well as pH values implies that the accuracy in these factors is very important for the realistic speciation results. Understanding the conditions at which lanthanides form precipitates is also vital for the accurate LC_{50} calculations, as solid formation tends to stabilize free metal ion and add variability in the mortality. A more robust understanding of these parameters is required in order to assess the true speciation and toxicity of lanthanides.

4.5 References

Avalon Rare Metals Inc. (Avalon). 2013. Nechalacho rare earth element project effluent quality criteria report. Prepared by TetraTech. Accessed: http://www.mvlwb.ca/Boards/mv/Registry/2010/MV2010L2-0005/MV2010D0017%20-%20MV2010L2-0005%20-%20Avalon%20-%20Attachment%20J_Effluent%20Quality%20Criteria.pdf on January 15, 2016.

The Biotic Ligand Model (BLM) Windows Interface, Version 2.2.1. 2007. User's guide and reference manual. HydroQual Inc, Mahwah, NJ. Accesed http://www.hydroqual.com/blm/BLM_manual.pdf on January 15, 2016.

Borgmann, U. 1996. Systematic analysis of aqueous ion requirements of *Hyalella azteca*: a standard artificial medium including the essential bromide ion. Archives of Environmental Contamination and Toxicology 30: 356-363.

Borgmann, U., Couillard, Y., Doyle, P., Dixon, D.G. 2005. Toxicity of sixty-three metals and metalloids to *Hyalella azteca* at two levels of water hardness. Environmental Toxicology and Chemistry 24: 641-652.

CCME (Canadian Council of Ministers of the Environment). 2003. Canadian Water Quality Guidelines for the Protection of Aquatic Life. Site-specific guidance. CCME, Winnipeg. Accessed www.ccme.ca on January 15, 2016.

Di Toro, D.M., Allen, H.E., Bergman, H.L., Meyer, J.S., Paquin, P.R., Santore, R.C. 2001. Biotic Ligand Model of the acute toxicity of metals. 1. Technical basis. Environmental toxicology and Chemistry 20: 2383-2396.

Environment Canada. 2013. Biological test method: test for survival and growth in sediment and water using the freshwater amphipod *Hyalella azteca* (2nd ed). Environmental Protection Service. Ottawa, ON. Accessed https://ec.gc.ca/Publications/4BA9E8C1-30EA-48AE-B593-F8F763EED8F0%5CRM33---accessible.PDF on January 15, 2016.

Gimeno Serrano, M.J., Auque Sanz, L.F., Nordstrom, D.K. 2000. REE speciation in low-temperature acidic waters and the competitive effects of aluminum. Chemical Geology 165: 167-180.

Johnson, R.A., O'Rourke, J.D. 1954. The kinetics of precipitate formation: barium sulfate. Journal of American Chemical Society 76: 2124-2126.

Lead, J.R., Hamilton-Taylor, J., Peters, A., Reiner, S., Tipping, E. 1998. Europium binding by fulvic acids. Analytica Chimica Acta 369: 171-180.

Lofts, S. 2012. User's guide to WHAM7. Natural Environment Research Council Centre for Ecology and Hydrology.

Lu, C. 2015. The effects of water chemistry and organism source on dysprosium toxicity to *Hyalella azteca*. (Master's Thesis) Thesis and Dissertations. Wilfrid Laurier University.

Meyer, J.S., Adams, W.J. 2010. Relationship between biotic ligand model-based water quality criteria and avoidance and olfactory responses to copper by fish. Environmental Toxicology and Chemistry 29: 2096-2103.

Paquin, P.R., Gorsuch, J.W., Apte, S., Batley, G. E., Bowles, K.C., Cambell, P.G.C., Delos, C.G., Di Toro, D.M., Dwyer, R.L., Galvez, F., Gensemer, R.W., Goss, G.G., Hogstrand, C., Janssen, C.R., McGeer, J.C., Naddy, R.B., Playle, R.C., Santore, R.C., Scheider, U., Stubblefield, W.A., Wood, C.M., Wu, K.B. 2002. The biotic ligand model: a historic overview. Comparative Biochemistry and Physiology, Part C 133, 3-35.

Pourret, O., Davranche, M., Gruau, G., Dia, A. 2007. Competition between humic acid and carbonates for rare-earth elements complexation. Journal of Colloid and Interface Science 305: 25-31.

Standing Committee on Natural Resources (RNNR). 2014. The rare earth elements industry in Canada - summary of evidence. 41st Parliament, 2nd session. Accessed http://www.miningwatch.ca/sites/www.miningwatch.ca/files/rareearthelements-summary-e.pdf on January 15, 2016.

Santore, R.C., Di Toro, D.M., Paquin, P.R., Allen, H.E., Meyer, J.S. 2001. Biotic ligand model of the acute toxicity of metals. 2. Application to acute copper toxicity in freshwater fish and daphnia. Environmental Toxicology and Chemistry 20: 2397-2402.

Shin., H.S., Lee, B.H., Yang, H.B., Yun, S.S., Moon, H. 1996. Bimodal normal distribution model for binding of trivalent europium by soil fulvic acid. Journal of Radioanalytical and Nuclear Chemistry 209: 123-133.

Slaveykova, V.I., Wilkinson, K.J. 2005. Predicting the bioavailability of metals and metal complexes: critical review of the biotic ligand model. Environmental Chemistry 2: 9-24.

Tang, J., Johannesson, K.H. 2003. Speciation of rare earth elements in natural terrestrial waters: Assessing the role of dissolved organic matter from the modeling approach. Geochimica et Cosmochimica Acta 67: 2321-2339.

Tipping, E. 1994. WHAM - a chemical equilibrium model and computer code for waters, sediments, and soils incorporating a discrete site/electrostatic model of ion-binding by humic substances. Computers and Geosciences 20: 973-1023.

Tipping, E., Lofts, S., Sonke, J. E. 2011. Humic ion-binding model VII: a revised parameterisation of cation-binding by humic substances. Environmental Chemistry 8: 225-235.

Verdin, A. 2014. BI499 Thesis Project. Wilfrid Laurier University. Personal communications.

Vukov, O. 2015. Developing a site specific understanding of the toxicity of rare earth elements, cerium and dysprosium, to *Daphnia pulex* and *Hyalella azteca*. (Master's Thesis) Thesis and Dissertations. Wilfrid Laurier University.

Zhao, C-M., Wilkinson, K.J. 2015. Biotic ligand model does not predict the bioavailability of rare earth elements in the presence of organic ligands. Environmental Science and Technology 49: 2207-2214.

CHAPTER 5: CONCLUSIONS AND FUTURE WORK

Understanding and accurately measuring chemical speciation of lanthanides is an integral part of the risk assessment of these metals. With the potential increase of the lanthanide release into the environment, it is important to consider how these metals will interact with the inorganic and organic ligands, such as the DOM. This thesis focuses on the testing and applying of two analytical techniques that were used to study the speciation. The following section will look at the objectives of the project and how they have been met, with an outline of the limitations and gaps that require future analysis.

5.1 Objective 1: Technique Validation through Comparison

The validity of two techniques chosen to measure lanthanide speciation (fluorescence quenching (FQ) and ion-selective electrode (ISE)) was assessed. It involved the prediction of the free metal ion by both techniques, which is the form of metals that is assumed to be the most bioavailable (stated in the BLM framework, Di Toro et al. 2001; Paquin et al. 2002; Santore et al. 2001; Slaveykova and Wilkinson 2005). If both techniques are able to predict similar values of free metal, then it was likely that the values are correct. The comparison was discussed in Section 3.3.4. There is a general agreement observed between the two techniques, when comparing free metal ion predicted by FQ and measured by the ISE; the values are within a log unit of each other. One of the main differences that are seen between the two techniques is that FQ slightly over-predicts free lanthanide concentrations. This implied that DOM has non-fluorescent ligands that are able to bind Sm, but are not detected by the FQ technique. Comparing the binding parameters between the two techniques revealed that the

additional ligands measured by the ISE has a potentially weaker binding (log K: 5.08-6.29 vs 6.60-6.78, ISE and FQ, respectively), as the binding constant values show a general decrease for all ISE samples. The presence of the additional ligands also results in the increased calculated binding capacity of the ISE measured samples (3.7-12 μmol/mg C vs 1.20-2.72 μmol/mg C, ISE and FQ, respectively). Generally, both ISE and FQ are able to provide very similar free metal concentrations when applied to the experimental conditions of the toxicological studies (Figure 4-6), which did not result in any significant difference between the calculated LC_{50} using nominal Sm values (Figure 4-7).

For further analysis into the techniques validation, the speciation models were compared to WHAM. The experimental conditions of each set of experiments from FQ and ISE were replicated in WHAM and the calculated free metal ion concentrations were compared. There is no agreement between the models. WHAM tends to overestimate DOM and lanthanide binding at lower concentrations of the metal, whereas at higher values it tends to underestimate it. Although WHAM was validated by experimental data by other researchers (Lead et al. 1998; Pourret et al. 2007), they used isolate fulvic and humic acids, however natural DOM is much more diverse than these samples. Additionally, according to the comparisons to toxicity tests discussed in Section 4.3.2.2, WHAM dramatically overestimates Dy binding to DOM, which results in very low LC_{50} values in the presence of DOM, presented as free metal ion (accepted as the bioavailable form) calculated using measured dissolved concentrations as model inputs. Further discussion into these comparisons is found in the next section. Generally, FQ and ISE models provide much more reasonable results for the free metal ion than WHAM. Future

studies into lanthanide speciation should be incorporated into WHAM to cover a larger range of diverse DOM samples and, thus, create a better binding prediction. A large improvement of WHAM would also be achieved by integrating the solid complexes of lanthanides, as they showed to be very important in speciation, as discussed below.

According to the comparison of the two techniques, ISE showed the most promise, as it is able to capture and measure binding of all potential ligands. However, there are significant issues with the response of the ISE in solutions with high ionic strength (IS). The interference of IS may have a number of explanations, including reduction in the activity of Sm and precipitate formation; however, a more feasible explanation may be related to the interference from other cations in the solution, which can be a result of the lack of selectivity of the ISE ligand. A development of a ligand that can bind lanthanides selectively, even if it is not selective for the specific lanthanides, may dramatically improve ISE measurements. The dependence of the ISE response on the IS has another indirect influence of the ISE performance. The lack of anions in the matrix resulted in the saturation of the samples with respect to hydroxide solid. It is impossible to measure binding between DOM and Sm during precipitate formation, as it tends to buffer the free ion and, thus, hindering further formation of the aqueous complexes. The development of the ISE that is able to function in the higher IS solution may provide a larger range of measurements for free Sm concentrations, which in turn may uncover more information into the binding of multiple ligands that are potentially present in the DOM molecule.

Another issue that was encountered during the prediction of the binding constants and capacities was related to the modeling of solid formations. The hydroxide and

carbonate solids of lanthanides are very varied in the NIST database (Martell and Smith 2004; Verweij 2013) with some of the values having an error of pK_{sp} of ±9. The variation in the values is attributed to the differences in experimental conditions, i.e. IS, temperature and recording time (kinetics) of solid formation (Diakonov et al. 1998). Due to these issues the selection of constants is dependent on the experimental observations. This is possible to be done for the hydroxide solid of Sm, since it is observed in the ISE experiments; however, it is not possible in Dy experiments, as no precipitate data is available. The speciation models are extremely sensitive to the value of solubility products; therefore, a more accurate determination is essential for the creation of the realistic speciation models. Future investigations into the understanding of the influence of experimental conditions as well as kinetics on various solid formations are required for this purpose.

5.2 Objective 2: Method Application

Both techniques predicted DOM and lanthanide binding and were used to study lanthanide speciation. As mentioned in previous section, the agreement between the two techniques was generally good. The binding is categorized as medium to strong with values for binding constants (log K) ranging for both techniques from 5.08±0.17 to 6.78±0.0170, with binding capacities varying from 0.53±0.00030 μM/mg C to 12.±1.6 μM/mg C. These ranges include both Sm and Dy, as there were no differences observed in the binding of the two metals due to similarities in chemical behaviour of all lanthanides. As a result of the differences in the experimental conditions of both sets of experiments, the importance of the DOM-lanthanide complex varies, as the concentrations of carbonate and sulfate change between the sets of experiments.

Generally, if the concentration of carbonate is high the majority (>50%) of the metal is bound to it, as it is seen in FQ and toxicological studies (Figure 4-4, Figure B14-Figure B25). Sulfate has a less dominant role if found in high concentrations and only becomes important when the binding capacity of the DOM is reached (Figure 2-4).

Another way lanthanide speciation was studied is by looking at the DOM quality characteristics such as SAC_{340} and FI_{370}. Expected significant correlations (p values 0.0065-0.034) between characteristics and binding capacity are observed in FQ samples (Al-Reasi et al. 2011; Wood et al. 2011). However, the relationships were not very strong ($R^2 \sim 0.5$). Binding constants showed correlations with characteristics in Sm samples, however it is unlikely that there are large differences between DOM sources and associated log K values, since it is dependent on the lanthanide binding functional groups, which are often similar between various types of DOM. In the ISE experiments the comparison results of DOM source characteristics and binding paramters are inconclusive, as the range of characteristics is too small to observe any meaningful trends. A larger pool of DOM samples that covers a more diverse set of characteristics would be able to provide more information for the creation of toxicity and binding predictions based on the type of DOM.

The final application of the speciation models involved the analysis of the toxicological data. Mentioned in Section 5.1, FQ-produced models generally are able to provide more reasonable values than WHAM for the free Dy ion. The ability of the model to explain metal toxicity when the LC_{50} values were converted to represent free Dy is inconclusive, as it works on the data of only one of the toxicological studies provided. In the case of Sm toxicity, WHAM predicted free Sm ion LC_{50} are generally the same for

different DOC concentrations, while FQ and ISE models are significantly different. The reason for this difference is attributed to the use of the higher nominal Sm concentrations for calculations, as opposed to, generally accepted in literature, measured dissolved concentrations, which are much lower in the region of the models where WHAM tends to underestimate free metal ion. FQ and ISE models' inability to explain metal toxicity is likely explained by the high sensitivity of the model to the pH and solubility product values. Precipitation is observed in all samples as dissolved values are always much lower than the added metal. Formation of the solid buffers the free metal ion thus causing the reduction in the gradient of concentrations; this makes it impossible to calculate LC_{50} values. Additionally, speciation, which includes precipitate formation, is greatly dependent on pH values. Small changes in the pH results in very different metal distribution, with lower pH value producing carbonate solids with greater amount of free metal, while with higher pH value producing hydroxide solid and less free metal ion. To truly assess the toxicity of lanthanides pH control and monitoring should be rigorously maintained.

Speciation models are an important part of the toxicity prediction necessary for the accurate risk assessment of lanthanides. Models such as WHAM suffer from the lack of the available data for these metals on complexes formation with DOM as well as understanding solid precipitation. Improvements to these models are, thus, necessary. Additionally, when it comes to lanthanides, they tend to co-occur in nature, due to their similarity in chemistry and binding. It is traditional to study metals individually when trying to assess their speciation and toxicity; however, it may not be representative of the environment to do so for lanthanides. Previous research (Tai et al. 2010) has shown that

there might not be any synergistic or inhibitory effect of lanthanides onto each other, and the toxicity remains constants for the same amounts of either one or mixture of metals. However, further research into these mixtures is required and may provide more information in the natural occurrence and toxicity of lanthanides.

5.3 References

Di Toro, D.M., Allen, H.E., Bergman, H.L., Meyer, J.S., Paquin, P.R., Santore, R.C. 2001. Biotic Ligand Model of the acute toxicity of metals. 1. Technical basis. Environmental toxicology and Chemistry 20: 2383-2396.

Diakonov, I.I., Ragnarsdottir, K.V., Tagirov, B.R. 1998. Standard thermodynamic properties and heat capacity equations of rare earth hydroxides: II. Ce III/-, Pr-, Sm-, Eu III/-, Gd-, Tb-, Dy-, Ho-, Er-, Tm-, Yb-, and Y-hydroxides. Comparison of thermochemical and solubility data. Chemical Geology 151: 327-347.

Lead, J.R., Hamilton-Taylor, J., Peters, A., Reiner, S., Tipping, E. 1998. Europium binding by fulvic acids. Analytica Chimica Acta 369: 171-180.

Martell, A.E., Smith, R.M. 2004. NIST Standard Reference Database 46 Version 8.0, Gaithersburg, USA.

Paquin, P.R., Gorsuch, J.W., Apte, S., Batley, G. E., Bowles, K.C., Cambell, P.G.C., Delos, C.G., Di Toro, D.M., Dwyer, R.L., Galvez, F., Gensemer, R.W., Goss, G.G., Hogstrand, C., Janssen, C.R., McGeer, J.C., Naddy, R.B., Playle, R.C., Santore, R.C., Scheider, U., Stubblefield, W.A., Wood, C.M., Wu, K.B. 2002. The biotic ligand model: a historic overview. Comparative Biochemistry and Physiology, Part C 133, 3-35.

Pourret, O., Davranche, M., Gruau, G., Dia, A. 2007. Competition between humic acid and carbonates for rare-earth elements complexation. Journal of Colloid and Interface Science 305: 25-31.

Santore, R.C., Di Toro, D.M., Paquin, P.R., Allen, H.E., Meyer, J.S. 2001. Biotic ligand model of the acute toxicity of metals. 2. Application to acute copper toxicity in freshwater fish and daphnia. Environmental Toxicology and Chemistry 20: 2397-2402.

Shin., H.S., Lee, B.H., Yang, H.B., Yun, S.S., Moon, H. 1996. Bimodal normal distribution model for binding of trivalent europium by soil fulvic acid. Journal of Radioanalytical and Nuclear Chemistry 209: 123-133.

Slaveykova, V.I., Wilkinson, K.J. 2005. Predicting the bioavailability of metals and metal complexes: critical review of the biotic ligand model. Environmental Chemistry 2: 9-24.

Tai, P., Zhao, Q., Su, D., li, P., Stagnitti, F. 2010. Biological toxicity of lanthanides elements on algae. Chemosphere 80: 1031-1035.

Verweij, W. 2013. Equilibria and constants in CHEAQS: selection criteria, sources and assumptions. Model Version 10 (February 2013). Accessed http://home.tiscali.nl/cheaqs/ on March 10, 2013.

APPENDIX A: EXPERIMENTAL WORK

A1 Fluorescence Quenching, Initial Studies

Overall, six FQ titrations were run during the preliminary stage of the project. Five of these experiments were done with Tb and KB DOM, while one was performed with Sm and KB DOM. The volume of the sample was 50 mL and it was increased by a maximum of 1.5 mL upon addition of metal to minimize the dilution effect on DOM fluorescence. The metal stock solution was prepared according to this volume requirement, with the exception of Sm, which was supplied as a stock of 1000 ppm in 5% nitric acid. Nitrate is known to absorb light around 200 nm (Pruitt 2009). A separate titration was run to make sure that there was no interference with DOM fluorescence measurements observed as a result of nitric acid; none was detected. The samples usually contained 10 ppm of DOC, except of one sample with 5 ppm of DOC. Ionic strength and pH were kept constant at 0.01 M and 5.0±0.2, respectively. The single excitation wavelength method used 340 nm to promote fluorescence, which corresponds to peak produces by humic-like substances at emission wavelength of 450 nm. The scans were done using slow or medium scan speeds, and the readings were done in triplicates. Running average calculation was performed in order to minimize noise, and the median wavelength of maximum values was used to obtain the maximum fluorescence intensities used in modeling of binding constant and capacity. The quartz cuvette that was used to run samples was baked daily in the oven for ~30 min in soapy water, before each experiment, to remove any possible DOM adsorbed onto the cuvette walls. MilliQ water blank was run to detect any residual contamination on the cuvette. Calibration of the pH electrode was also performed daily. The reduction of fluorescence intensities (F) was

observed after each addition of metal stock solution. Tb and KB DOM replicates are plotted on Figure A1. The results were normalized to the initial F of each sample as well as mg of C for comparison. There was a lot of variability detected in the preliminary FQ studies most likely due to the error introduced by sample handling; that is why a flow-through cuvette was used for other titrations.

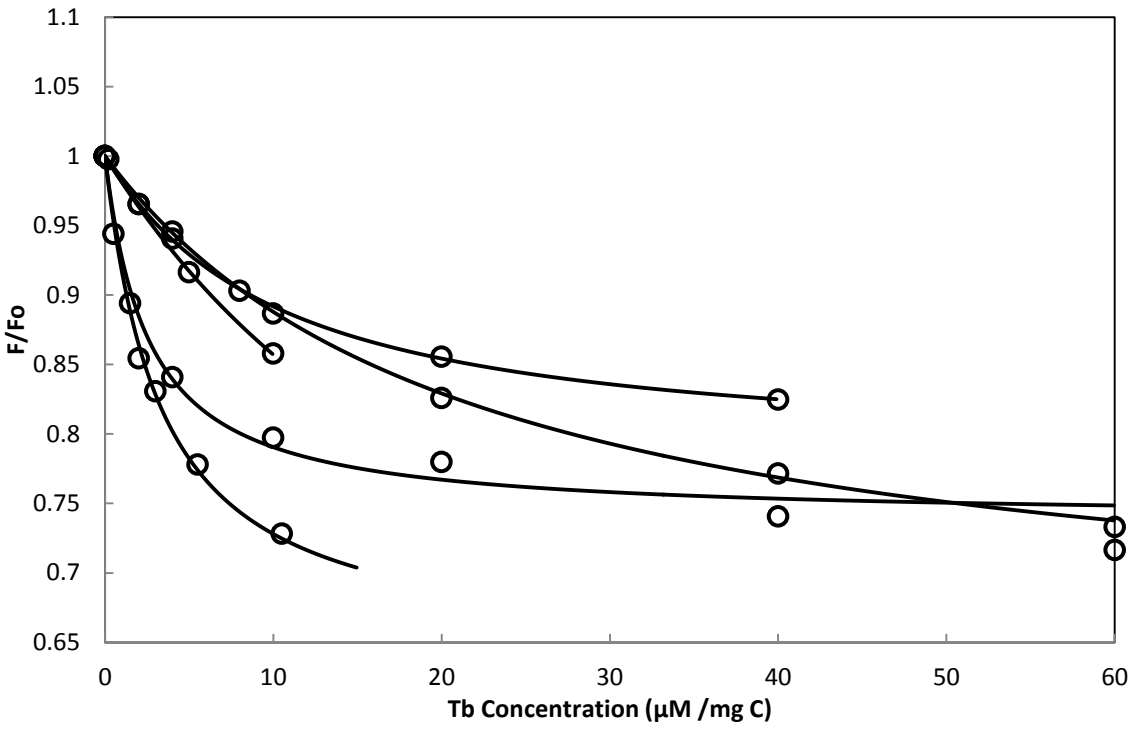

Figure A1. The reductions of fluorescence intensity (F), normalized to the initial intensity (F_0) of each sample, vs. Tb concentrations normalized to mg of C of KB DOM. Circles represent measurements and line represent RW fitting.

As mentioned in Section 1.4.1, FQ can be caused by dynamic collisions with the quencher or by static interactions via complexation. In order to determine which of these mechanisms is responsible for the quenching temperature and absorbance readings were taken as described in Lakowicz (2010). Preliminary results were inconclusive, as there

was no strong evidence against one or the other. Absorbance readings taken during titrations can be seen in Figure A2.

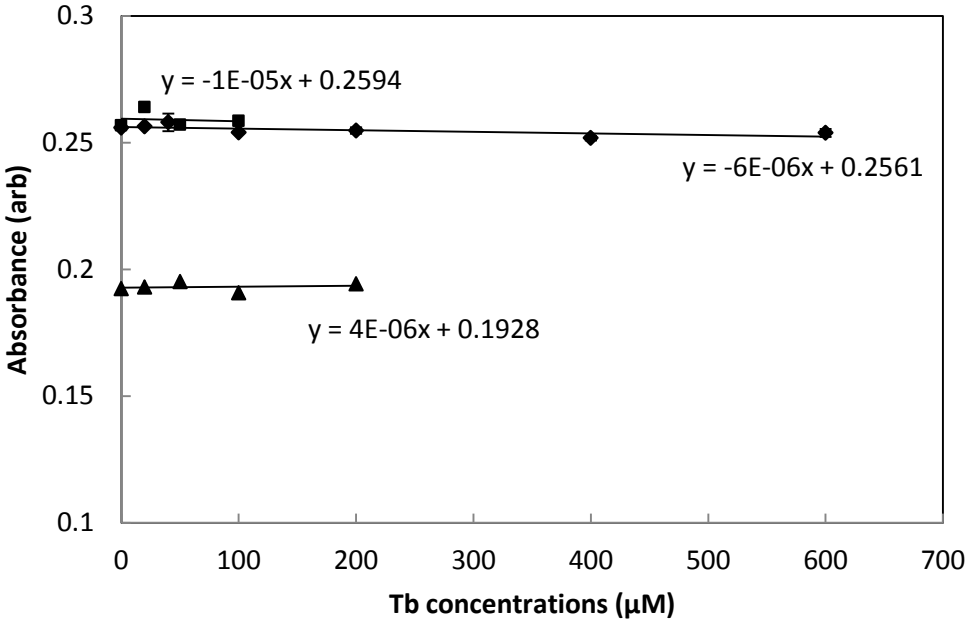

Figure A2. Absorbance readings taken during Tb FQ titration. The top two replicates were done using 10 ppm DOC, while the lower replicate used 5 ppm DOC. There is no observed decrease or increase in the slope of the absorbance line, as shown by the slope of the line of best fit.

Although no reduction of the absorbance during titration is indicative of the collisional quenching, due to complexity of DOM molecular structure it is possible that more than one area of the molecule is responsible for the absorbance, additionally, some of the fluorophores may be inaccessible to the metal binding but might have a strong absorbance spectra. Temperature dependence study was also inconclusive. There was a small increase in the slope (m) of the lines (Figure A3), which again indicates collisional quenching (refer to Figure 1-4); however, the variation was within the uncertainty range of the reading, measured as standard deviations. It is possible that the molecular structure

of DOM is too complex, and these techniques are not appropriate for the determination of the quenching mechanism.

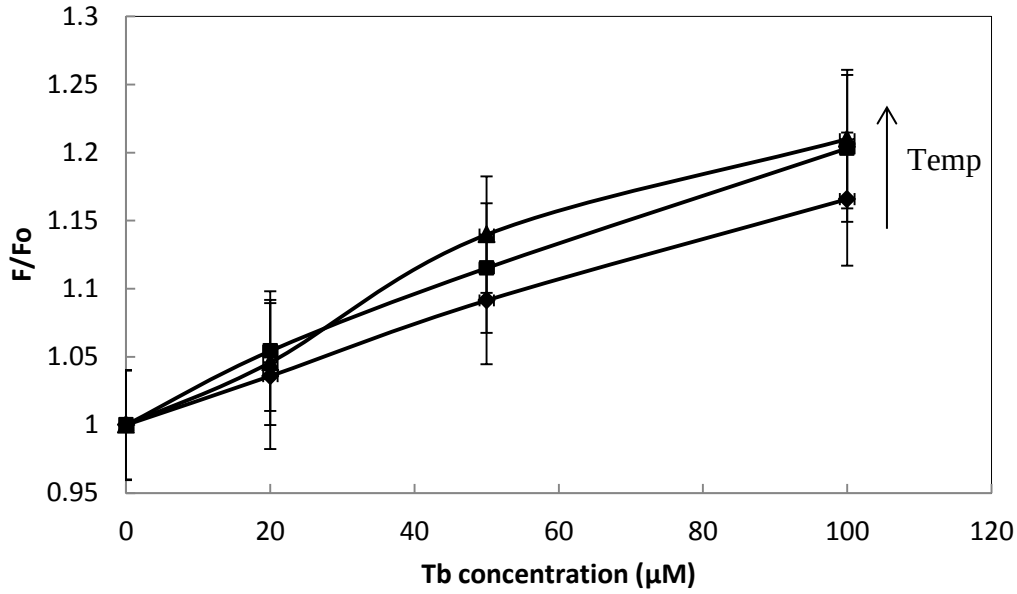

Figure A3. Temperature dependence of FQ over the range of 20 to 40 °C. The increase of slope is observed (m = 0.0017 at 20 °C, m = 0.002 at 30 °C, m = 0.0021 at 40 °C); however, the data has overlapping error bars (standard deviation).

A2 ISE Membrane Preparation and Method Development

There were three stages in the development of ISE. Stage 1 involved the attempt at making an ISE using TMP as a ligand, as proposed by Ganjali et al. (2008). The synthesis of TMP is discussed in Appendix A3. Stage 2 involved a different recipe and ligand (glipizide) proposed by Ganjali et al. (2003). This part of the ISE development involved construction of the ISE following the method described in the paper. Stage 3 used the same recipe and ligand as Stage 2; however, the membrane was prepared separately and was incorporated into commercially available ISE body. These stages and all of the changes are discussed next.

As part of the Stage 2 construction process, a glass tube was dipped into the membrane mixture; and the membrane would form as the liquid deposited in the tube by capillary action dried over time. These membranes were usually very thin and brittle. Most of them would leak and break as they conditioned in the solution. The only two membranes that were stronger than others and managed to contain the inner filling solution showed no response. Few adjustments were made to the membrane composition; however, no improvement in the membrane integrity was observed. The summary of the membrane mixtures are shown in Table A1.

The ISE construction improved dramatically after obtaining commercially available set-up. The main issues that were observed at this point of the ISE development were related to the response of the electrode. Table A1 shows the membrane mixtures used and Table A2 summarizes issues associate with each membrane. There were three main conclusions that were drawn from these experiments:

Table A1. ISE membrane mixture compositions tried during method development Stage 2 and 3.

Preparation as described in paper (Stage 2)											
Chemical	**Units**	**Paper**	**Membranes**								
			1	**2**	**3**	**4**	**5**	**6**	**7**	**8**	**9**	**10**
PVC	mg	30	30.35	34.66	31.63	30.99	63.22	35.89	31.2	32.77	31.03	62.68
NaTPB	mg	6	6.27	6.87	5.17	11.2 [a]	10.01	5.87	6	5.84	4.9	10.41
Glipizide	mg	11	11.11	11.3	11.01	11.3	21.87	14.03	13.05	0	7.94	0
BA	µL	50.3	50.3	50.3	50.3	50.4	101	51	50.4	50.4	50.4	100
Commercially available set-up (Stage 3)												
Chemical	**Units**	**Paper**	**Membranes**									
			11	**12**	**13**	**14**	**15**	**16**	**17**	**18**	**19**	**20**
PVC	mg	30	30.85	123.64	40.54	56.58	30.73	30.41	31.09	30.68	30.93	30.2
NaTPB	mg	6	5.48	19.65	7.81	11.2 [a]	6.7 [a]	6.57	4.94	5.54	5.2	6.6
Glipizide	mg	11	10.94	44.32	11.57	16.76	10.57	11.26	10.44	13.72	14.89	12.2
BA	µL	50.3	50.4	19.65	85.4	112	50.3	50.4	53 [b]	51 [b]	50	51
Membranes (continued)												
Chemical	**Units**	**Paper**	**21**	**22**	**23**	**24**	**25**	**26**	**27**	**28**	-	-
PVC	mg	30	37.3	30.9	35.3	35.5	37.11	30.02	30.38	30.31	-	-
NaTPB	mg	6	6.8	6.2	7.7	7.54	7.08	5.73	5.5 [a]	5.5 [a]	-	-
Glipizide	mg	11	18	14.3	17.1	17.16	17.2	15.68	15.5	14.67	-	-
BA	µL	50.3	63.1	50.2	58.2	58.2	61.5	50	50.2	25.5/25.5 [c]	-	-

(a) Oleic Acid was used instead of NaTPB (µL)
(b) NPOE was used instead of BA
(c) A mixture of BA and NPOE were used (1:1)
Notes:
Membrane #1,2,4-6,8-10 broke, #3 and #7 showed no response
Membrane #12 was used to prepare two membrane, #23, 24 and 25 were prepared in a larger diameter disk
Membranes #22 and #23 were used for all DOM experiments

1. The use of IS in the sample solution was interfering with the ISE response. The mV values showed very small or no increase after addition of Sm. The final DOM samples were, thus, prepared in MilliQ water.
2. Static titrations performed better than flow-through cell titrations. The readings were generally very unstable; additionally, the range of response values for titrations with DOM was much smaller than during static titrations. Static titrations were resumed for all samples.
3. Better response was detected with increased ligand amount. When it came to membrane composition, membranes containing more ligand showed a better response, determined by the slope of the calibration line. The amount of the ligand was increased based on the recipe of the electrode that gave best response.

Table A2. Summary of the issues associated with membranes from Stage 3.

Membrane	**Was IS used?**	**Issues/Comment**
11	No	Connection issues
12	No	Slope not steep enough
13-15	Yes	No response
16	Yes	Response detected with low slope for solution with lowest IS
17, 18	Yes	Used NPOE, no response
19	No	Showed response, trial DOM titrations were performed with some success
20	No	No response, most likely because it expired
21	No	Broke when trying to place it into a flow-through cell
22-23	No	No major issues, ran DOM titrations
24-28	No	No response (unknown reason)

A3 Synthesis of the ISE Ligand

In Stage 1 of the ISE development a membrane recipe from Ganjali et al. (2008) was chosen. The paper describes a construction of an asymmetric potentiometric design, where the membrane containing the ion selective ligand has a direct solid contact with the wire or another conductor; different from the conventional symmetric design, which has the membrane placed between sample and reference solution (Janata 2009; Ganjali et al. 2008). The authors provide calibration curve showing a linear response of electric potential for Sm concentrations ranging from 10^{-9} M to 10^{-4} M. Additionally, the electrode performed well within the wide range of naturally occurring neutral pH values (3-8). The interference from other ions was considered to be negligible with the selectivity coefficients values below 10^{-3} for all major cations and other lanthanide ions. The electrode was reported to have a lifetime of 4 weeks. The paper provides a synthesis of the ligand (TMP, Figure A4). The first step of the synthesis involved salicylaldehyde (Sigma-Aldrich Corp.,St. Louis, MO, USA) and N-aminorhodanine (Sigma-Aldrich Corp., St. Louis, MO, USA), which were used as the initial reagents to produce an imine (N=C in the middle). The double bond was then reduced to produce the final ligand using a strong reducing agent ($Zn(BH_4)_2$, used in paper). However, the second step of the synthesis was not successful; the details of synthesis trials are outlined in Table A3.

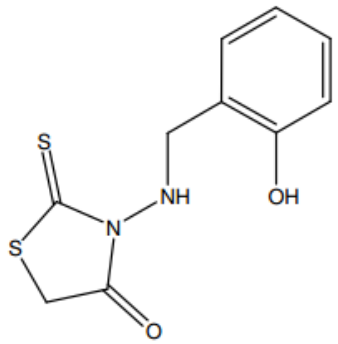

Figure A4. Chemical structure of TMP (2-2-thoxothiazolidin-4-one-methyl-phenol).

Table A3. A summary of the synthesis of TMP (Sm-ISE ligand). Step 2 of the reaction (reduction) did not produce the desired product (reactions 2-8).

#	Reagents	Amount	Solvent and amount	Other additives	Reaction details	Results
1	Salicylaldehyde N-Aminorhodanine	1.24 g (0.01 mol) 1.4856 (0.01 mol)	EtOH (10 mL)	1 drop AcOH	Heated and refluxed for 1 hour, Separated using vacuum filtration	Yellow powder, NMR showed imine product (^{1}H NMR (400MHz, CDCl3) δ 10.919 (1H, s), 9.129 (1H, s), 7.437 (1H, m), 7.369 (1H, m), 7.079-7.058 (1H, m), 6.985 (1H, m), 4.107 (2H, s))
2	Step 1 Product $NaBH_4$	0.5 g (0.002mol) 0.075 g (0.002mol)	EtOH (10 mL)	-	Stirring for 4.5 hours followed by a liquid/liquid extraction and column separation (Hex:EtOAc,1:2)	orange oil, no product detected
3	Step 1 Product $NaBH_4$	0.5 g (0.002mol) 0.075 g (0.002mol)	EtOH (10 mL)	-	Changes from reaction 2: use of ice bath, decreased reaction time (1.5 hrs)	yellow powder (most likely unreacted reagent), no product detected
4	Step 1 Product $NaBH_4$	0.5 g (0.002mol) 0.019 g (0.0005mol)	EtOH (10 mL)	-	Same as reaction 3	Insoluble orange powder, no product detected
5	Step 1 Product $Zn(BH_4)_2$	0.5 g (0.002mol) 0.8 mL	Et_2O (5 mL)	silica powder	reaction under N_2 for 6 hrs	No product detected
5a	continued	-	-	-	overnight reaction	No product detected
5b	continued	-	+Et_2O (5 mL)	-	heated and refluxed for 3.5 hrs then left for 78 hrs to react	Some potential product detected
6	Step 1 Product $Zn(BH_4)_2$	0.5 g (0.002mol) 2.5 mL	Et_2O (5 mL)	-	heated and refluxed for 4 hrs, liquid/liquid extraction	Insoluble powder, possible mixture
7	Step 1 Product $Zn(BH_4)_2$	0.5 g (0.002mol) 2 mL	Et_2O (5 mL)	silica powder	heated and refluxed for 4 hrs, attempted column separation	Insoluble powder, did not separate
8	Step 1 Product $Zn(BH_4)_2$	0.5 g (0.002mol) 2 mL	THF (15 mL)	silica powder	heated and refluxed for 5 hrs, attempted column separation	Insoluble powder, did not separate

A4 ISE Response over Time

During Stage 3 of the ISE development the external calibration was performed before each experiment, due to inconsistent calibration results. Table A4 summarizes the calibration line of best fit parameters for different membranes and Figure A5 shows the slope change over time. It is evident from the figure and from the standard deviation (SD) of the slope that the electrode did not respond reproducibly. Additionally, the response was not always linear as presented by the average R^2 value below 0.99.

Table A4. Summary of the ISE calibration parameters recorded over time.

Date	Slope	Intercept	R^2
Membrane 12			
11-Mar-15	15.7	83	0.835
12-Mar-15	10.0	99	0.897
Membrane 16			
01-Apr-15	5.9	63	0.709
Membrane 19			
24-Apr-15	7.3	53	0.917
28-Apr-15	12.7	95	0.989
05-May-15	14.4	100	0.998
Membrane 21			
01-Jun-15	16.5	100	0.992
03-Jun-15	16.8	106	0.992
04-Jun-15	17.1	109	0.996
Membrane 22			
10-Jun-15	8.9	77	0.981
11-Jun-15	11.8	78	0.997
15-Jun-15	10.3	91	0.907
17-Jun-15	16.2	101	1.000
18-Jun-15	16.0	105	1.000
24-Jun-15	18.8	113	0.989
25-Jun-15	11.5	95	0.989
26-Jun-15	9.6	91	0.996
27-Jun-15	8.9	76	0.994
28-Jun-15	9.1	82	0.994

Date	Slope	Intercept	R^2
29-Jun-15	13.8	91	0.998
30-Jun-15	7.9	82	0.998
07-Jul-15	6.0	78	0.978
08-Jul-15	14.9	107	0.985
AVG	***11.7***	***90***	***0.986***
SD	***3.7***	***12***	***0.024***
Membrane 23			
15-Jul-15	24.3	130	0.993
20-Jul-15	19.3	118	0.998
22-Jul-15	13.5	95	0.968
23-Jul-15	15.8	105	0.988
24-Jul-15	23.4	132	0.973
28-Jul-15	18.3	119	0.994
29-Jul-15	15.0	105	0.993
30-Jul-15	16.2	112	0.995
31-Jul-15	14.5	104	0.999
04-Aug-15	22.8	137	0.993
05-Aug-15	23.7	145	0.985
11-Aug-15	14.2	99	0.972
12-Aug-15	14.9	103	0.990
13-Aug-15	15.9	105	0.986
AVG	***18.0***	***115***	***0.988***
SD	***4.0***	***15***	***0.010***

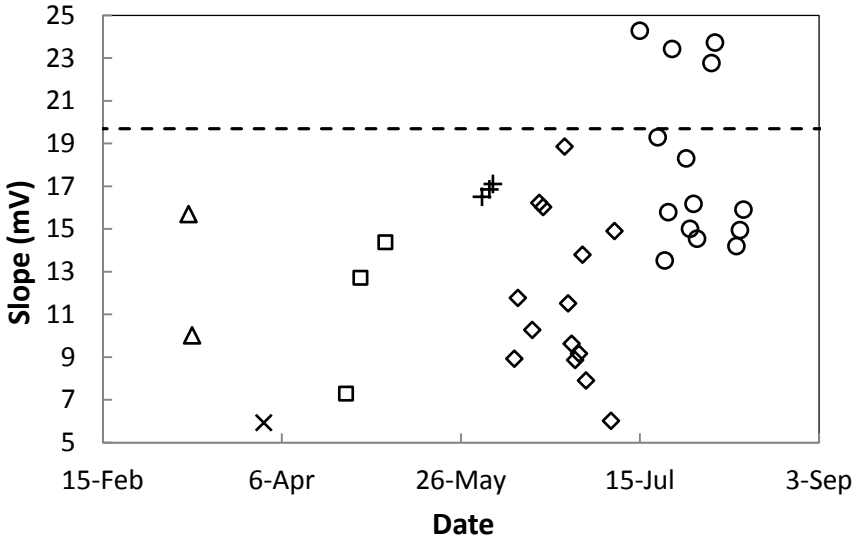

Figure A5. Slope change recorded over time. Different symbols represent different membranes. Dashed line is the Nernstian slope (19.7 mV).

A5 Comparisons of Sm and Dy binding to DOM with Tb and Eu

During the initial studies, Eu and Tb were considered for further lanthanide analysis. The selection of the metals changed after considering the available toxicological information. FQ titrations were still performed for these lanthanides with KB DOM only. The same protocol was followed for these titrations as for Sm and Dy FQ studies (Section 2.2). The quenching observed in the SIMPLISMA-resolved dominant component for these samples was very similar in magnitude, with the final reduction of the initial fluorescence ranging from 0.42 to 0.47 for all four lanthanides. However, the main difference observed in the speciation of both of these metals is in the magnitude of the hydroxide solid pK_{sp} value. The value is greater for Eu and Tb (26.5 and 26.3, respectively) than for Sm and Dy (25.5 and 25.9, respectively), see Section 2.2.4 and Table 1-3 (Martell and Smith 2004; Verweij 2013; Spahiu and Bruno 1995). When running RW model the increased solubility product values results in the production of the hydroxide solid, not observed in the other two samples. Based on the similar shapes of quenching curves, it is likely that there is no solid formed; however, the deviation from the RW model is not dramatic enough to disregard the solid formation (Figure A6). Predicted precipitation resulted in the higher binding parameters. The comparison graphs are shown in Figure A7. Both constant and capacity were significantly greater for Eu and Tb than for Sm and Dy. This means that DOM should be able to bind more of Eu and Tb than the other two lanthanides. However, due to high sensitivity of the model to the hydroxide solid formation constant and the fact that the quenching curves were very similar, it is more likely that all four lanthanides behave the same when it comes to the

binding to DOM. To truly assess the binding more information on the solubility constants are necessary.

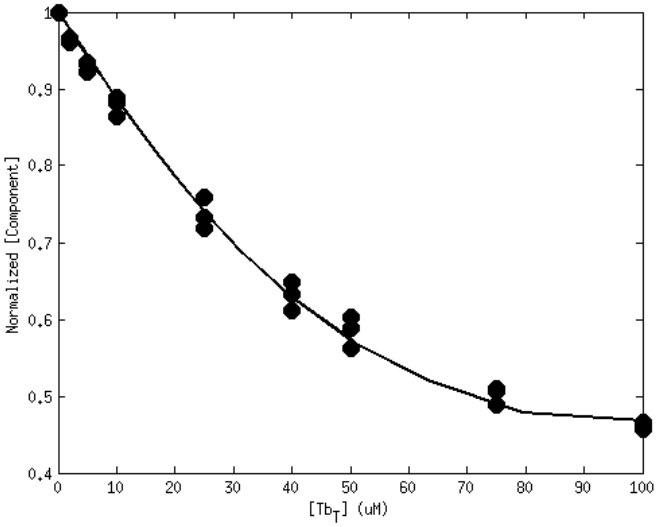

Figure A6. RW model (line) for the measured quenching (circles) of the KB DOM titrated with Tb. A slight flat line of the model at higher Tb concentrations is representative of the hydroxide solid formation.

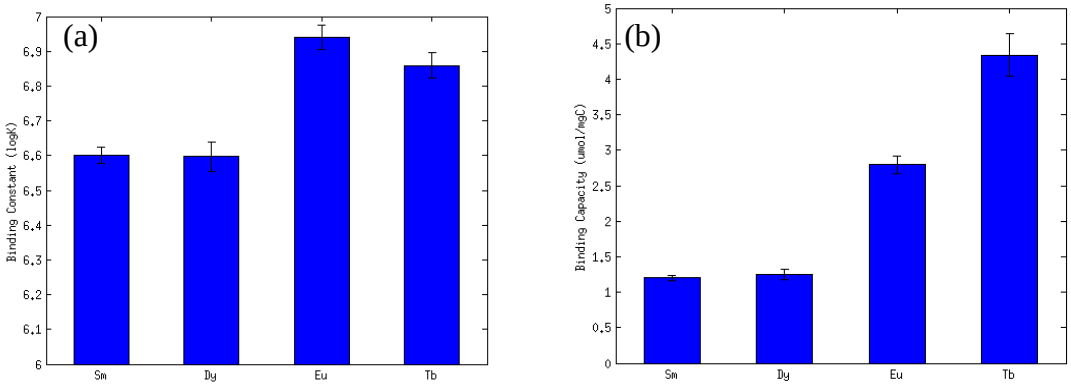

Figure A7. Comparions of binding constants (a) and capacities (b) between four lanthanides (Sm, Dy, Eu and Tb). The error bars represent 95% CI using SD.

References

Ganjali, M.R., Memari,Z., Faridbod, F., Norouzi, P. 2008. Samarium Microsensor: an asymmetric potentiometric membrane sensor. International Journal of Electrochemical Science 3: 1169-1179.

Ganjali, M.R., Pourjavid, M.R., Rezapour, M., Haghgoo, S. Novel samarium(III) selective membrane sensor based on glipizid. Sensors and Actuators B 89: 21-26.

Janata, J. 2009. Principles of Chemical Sensors (2nd ed). USA (NY): Springer pp. 151-153.

Lakowicz, J.R. 2010. Principles of Fluorescence Spectroscopy (3rd ed). USA (NY): Springer p. 277-318.

Martell, A.E., Smith, R.M. 2004. NIST Standard Reference Database 46 Version 8.0, Gaithersburg, USA.

Pruitt, P. 2009. Nitrate measurement in less than 30 seconds. A new UV absorbance technique. Solutions: Covering Analytical Methods and Practices. Water Environment Laboratory 16(1).

Spahiu, K., Bruno, J. 1995. A selected thermodynamic database for REE to be used in HLNW performance assessment exercises. MBT Technologia Ambiental. Cerdanyola, Spain.

Verweij, W. 2013. Equilibria and constants in CHEAQS: selection criteria, sources and assumptions. Model Version 10 (February 2013). Accessed http://home.tiscali.nl/cheaqs/ on March 10, 2013.

APPENDIX B: FIGURES AND TABLES

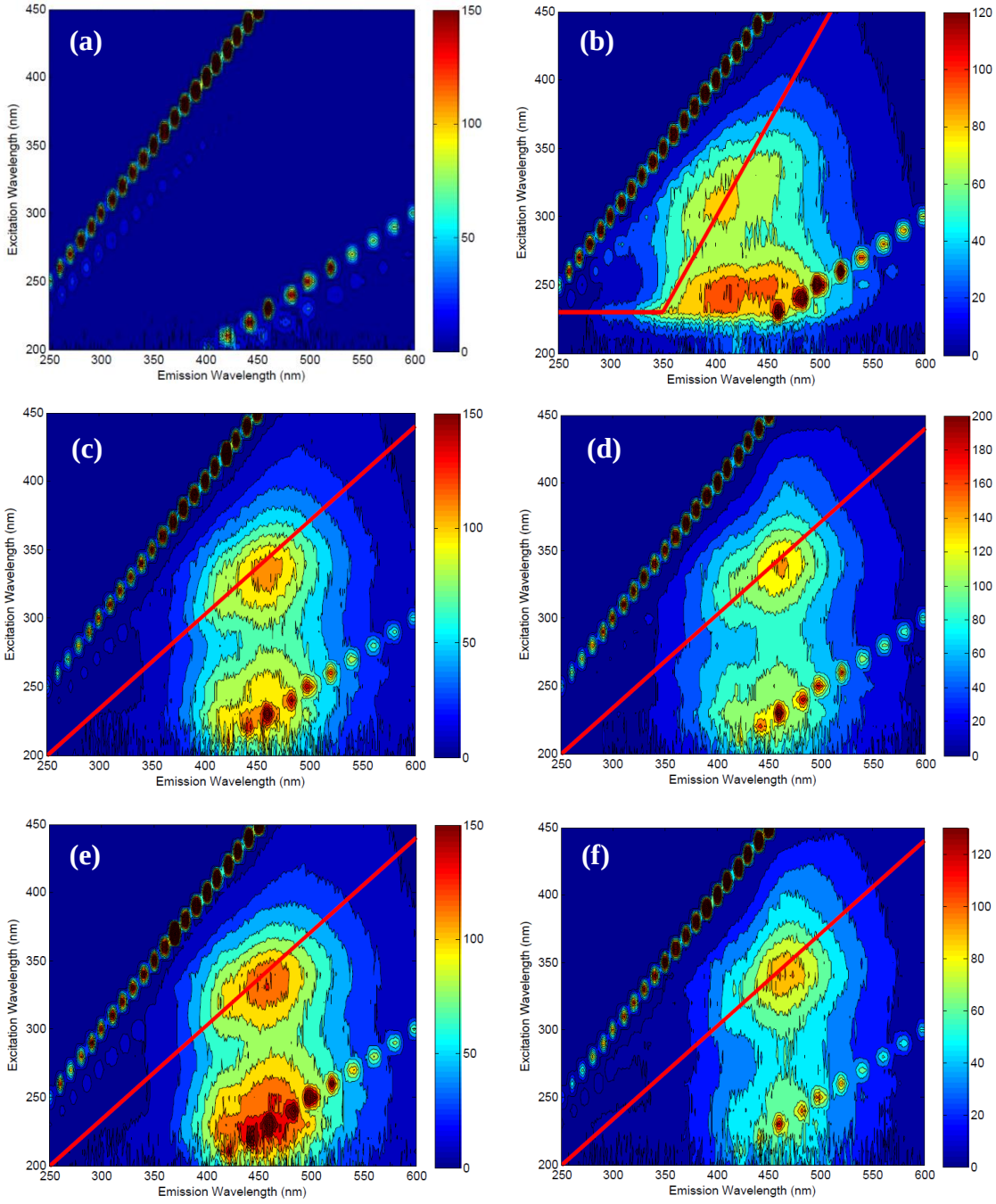

Figure B1. EEMs of a MilliQ blank (a) and five DOM sources: BB DOM (b), KB DOM (c), SH DOM (d), SW DOM (e) and LM DOM (f). The red lines represent a selected slice used for variable angle synchronous scan readings. MilliQ blank shows Rayleigh (larger peaks) and Raman scattering (smaller peaks) of water, which are also present in all DOM plots.

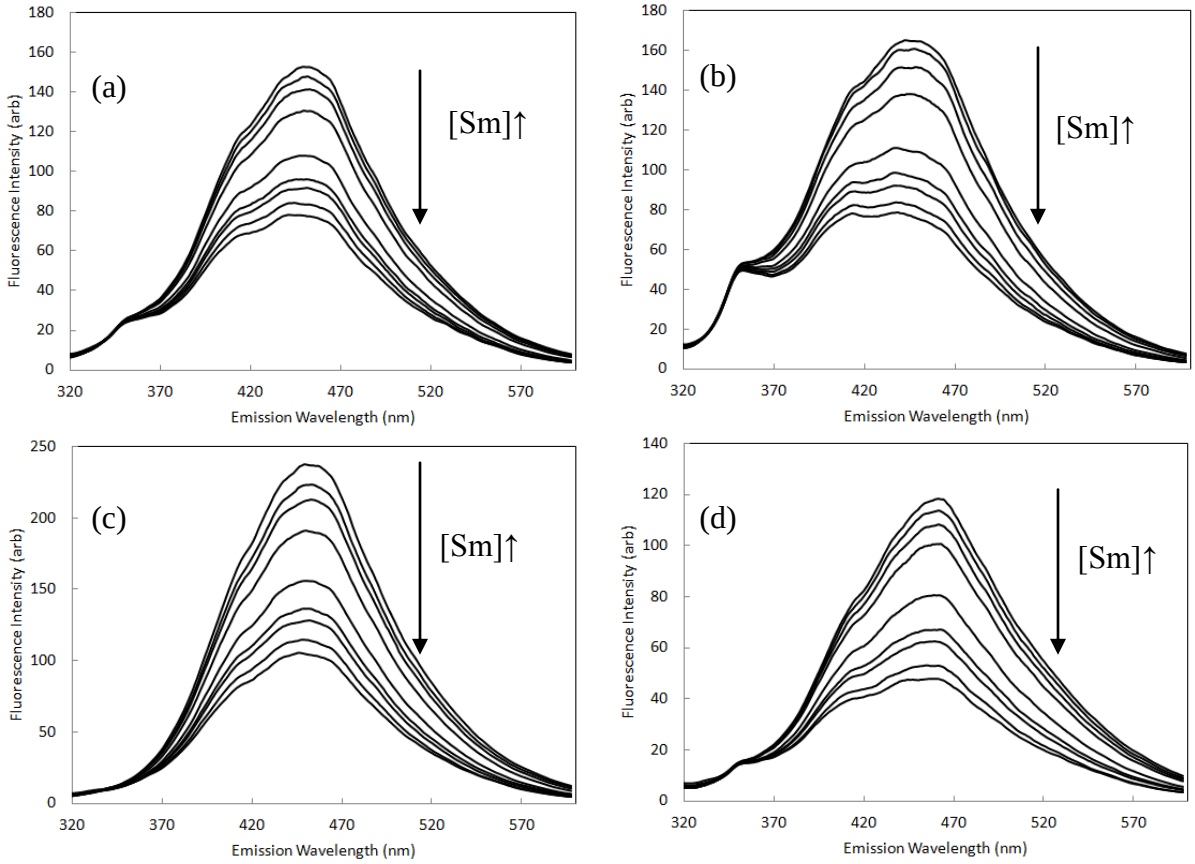

Figure B2. A quenching of fluorescence intensity during titration of Sm and of KB DOM (a), SH DOM (b), SW DOM (c) and LM DOM (d). The values that at plotted are an average of all trials as well as running averages of all the readings. Excitation wavelength range is 250-440 nm.

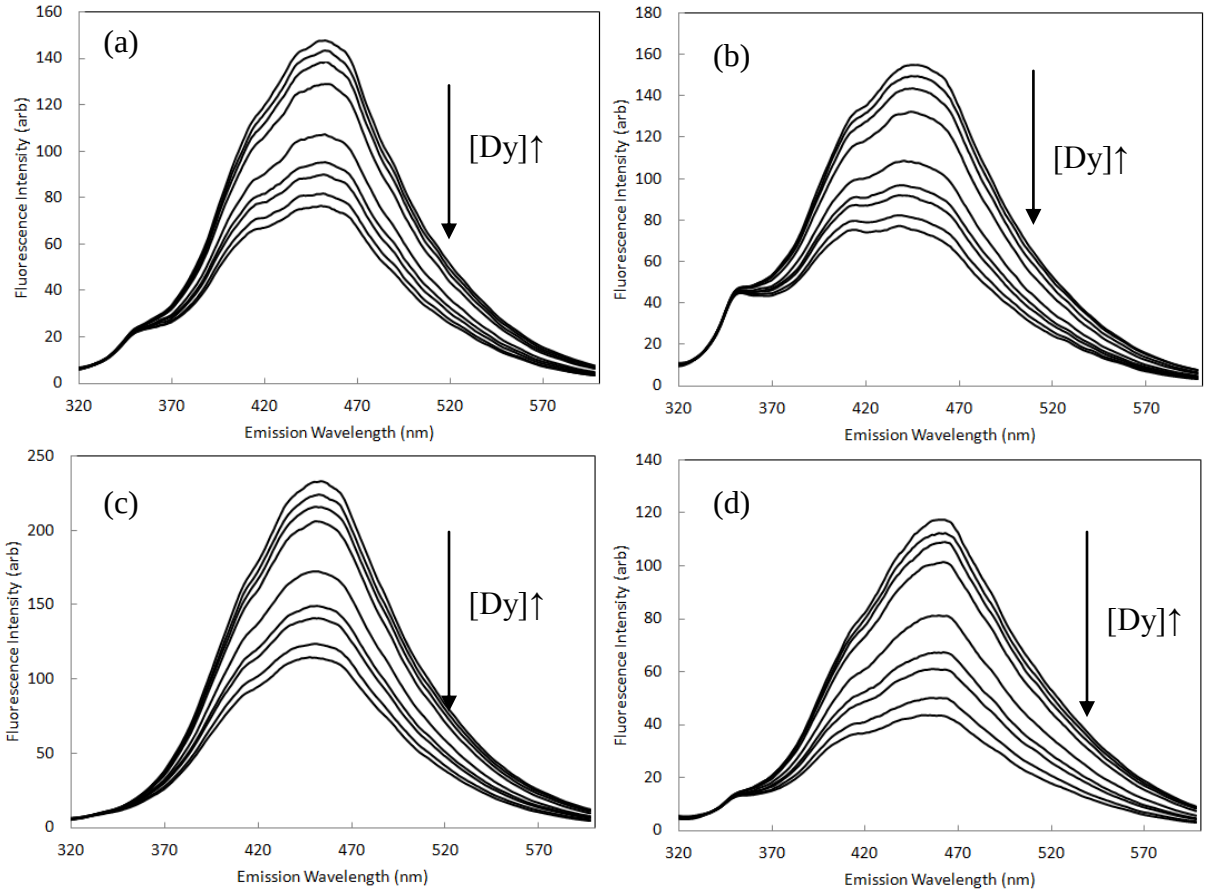

Figure B3. A quenching of fluorescence intensity during titration of Dy and of KB DOM (a), SH DOM (b), SW DOM (c) and LM DOM (d). The values that at plotted are an average of all trials as well as running averages of all the readings. Excitation wavelength range is 250-440 nm.

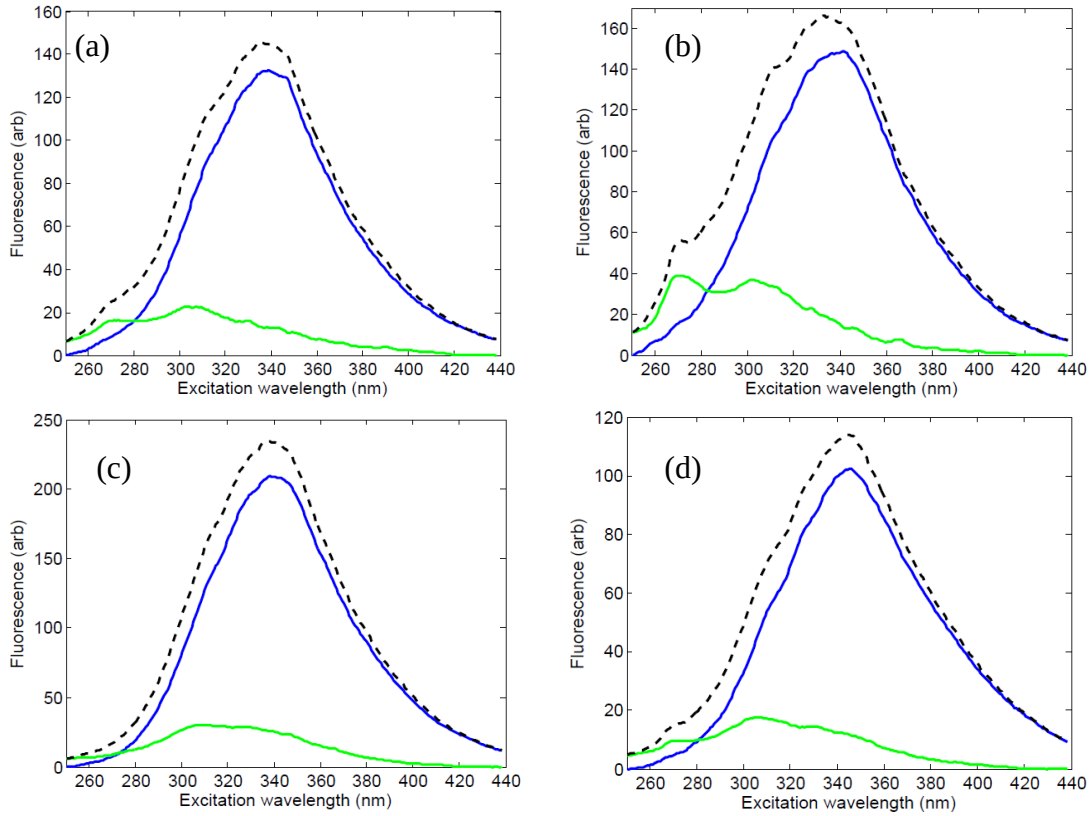

Figure B4. SIMPLISMA-resolved spectra of KB DOM (a), SH DOM (b), SW DOM (c) and LM DOM (d). There were two components identified (blue and green), with the blue one being more dominant. The dashed line represents the data of the DOM fluorescence alone. Emission wavelength range is 320-600 nm.

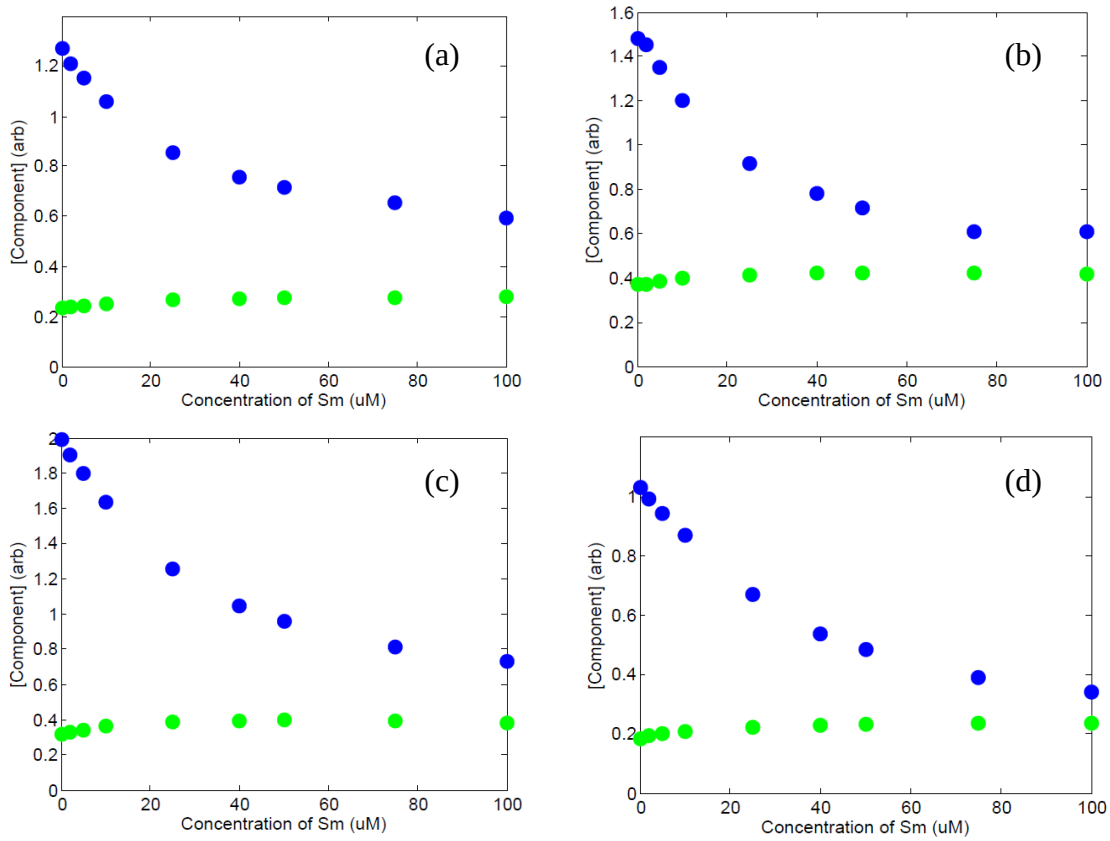

Figure B5. SIMPLISMA-resolved concentrations of two components for KB DOM (a), SH DOM (b), SW DOM (c) and LM DOM (d) at each point in the titration with Sm. The blue component is the most dominant one and it exhibits quenching whereas green component remains constant in concentrations. The RW model analysis was performed on the dominant component.

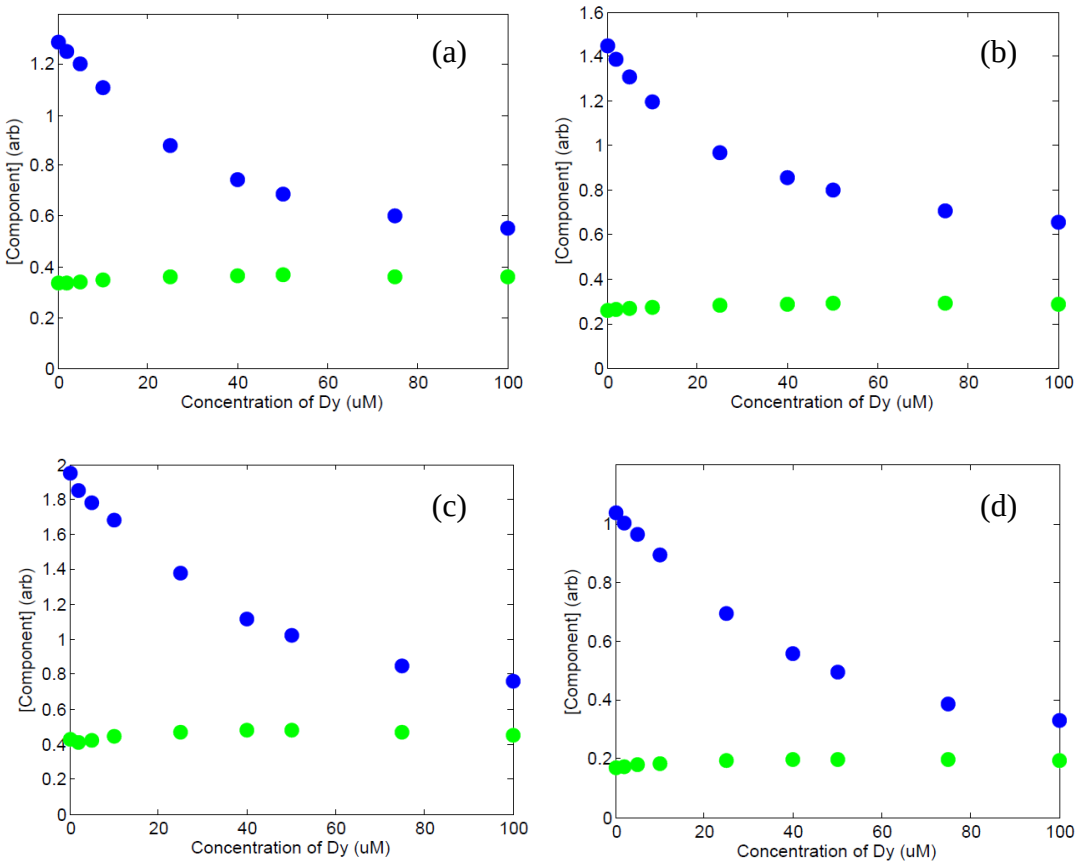

Figure B6. SIMPLISMA-resolved concentrations of two components for KB DOM (a), SH DOM (b), SW DOM (c) and LM DOM (d) at each point in the titration with Dy. The blue component is the most dominant one and it exhibits quenching where as green component remains constant in concentrations. The RW model analysis was performed on the dominant component.

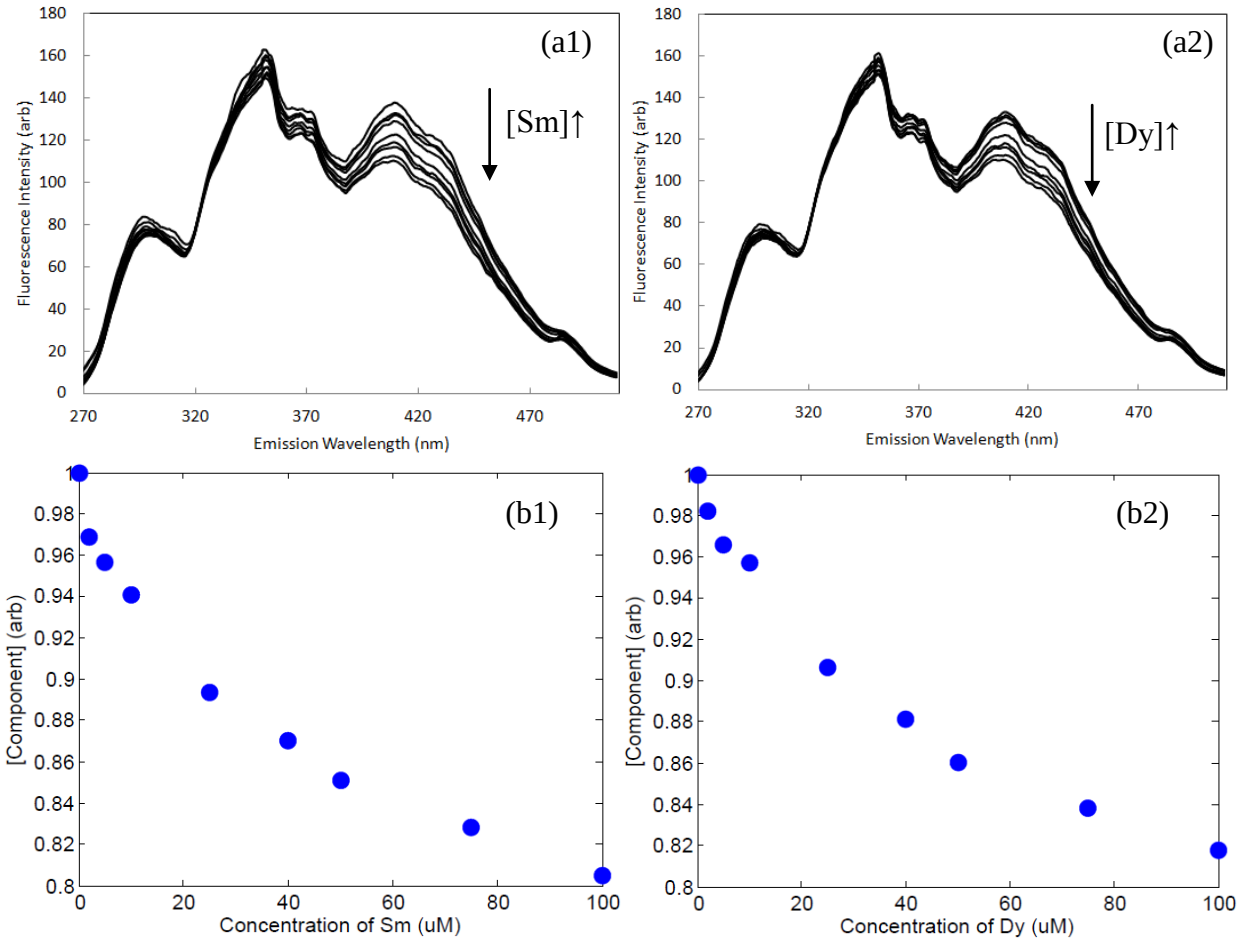

Figure B7. A quenching of fluorescence intensity during titration of Sm (a1) and Dy (a2). The values that at plotted are an average of all trials as well as running averages of all readings. Excitation wavelength is 230 nm for the emission wavelength of 270-350 nm, and 350-450 nm for emission 350-510 nm. Although there are a number of changing peaks only one of them exhibited consistent quenching (around emission wavelength of 410 nm). The entire spectrum was used as an input in SIMPLISMA, as it wasn't resolved, but it was able to produce the quenching curve of the component at each point in the titration for Sm (b1) and Dy (b2). These values were used for the RW modeling.

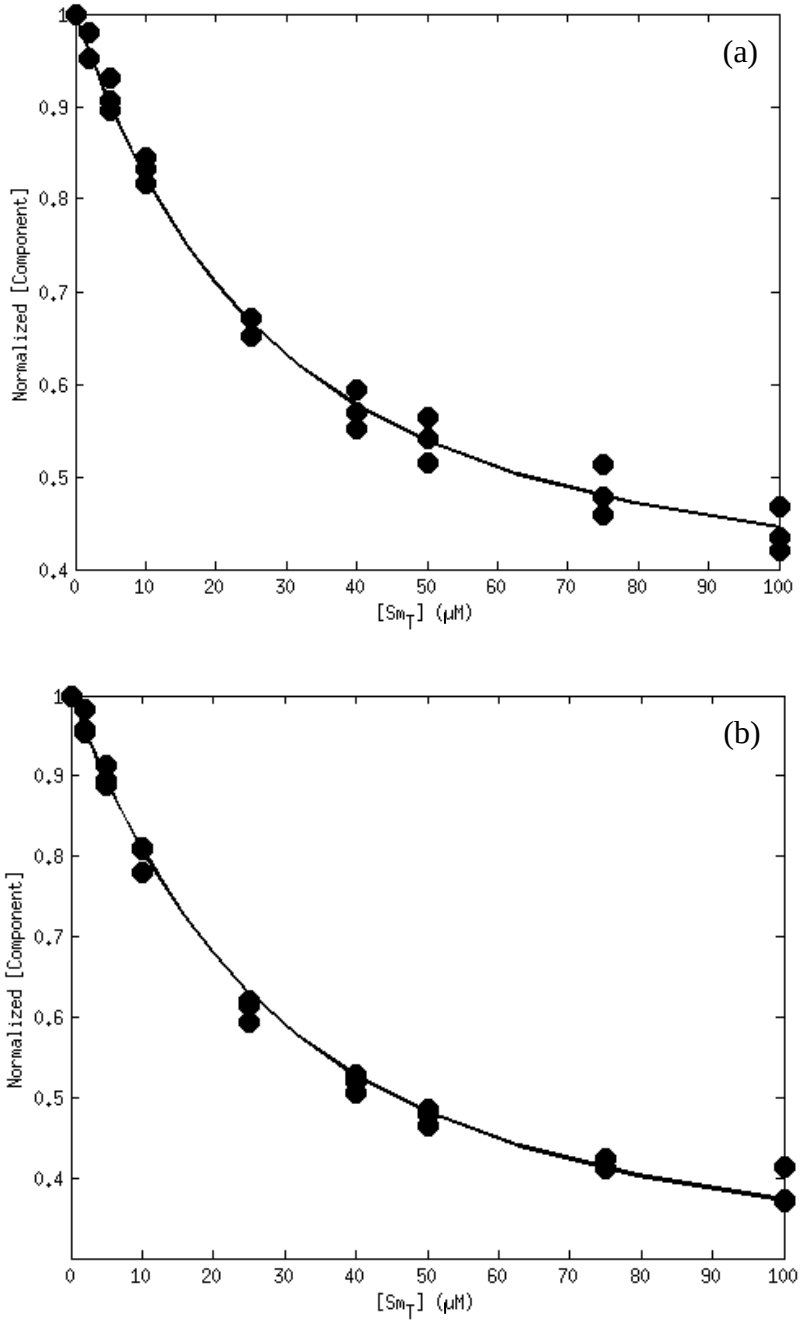

Figure B8. RW model fits for KB DOM (a) and SH DOM (b) titrated with Sm. The quenching curve data was produced from the normalized concentrations of the dominant component resolved by SIMPLISMA.

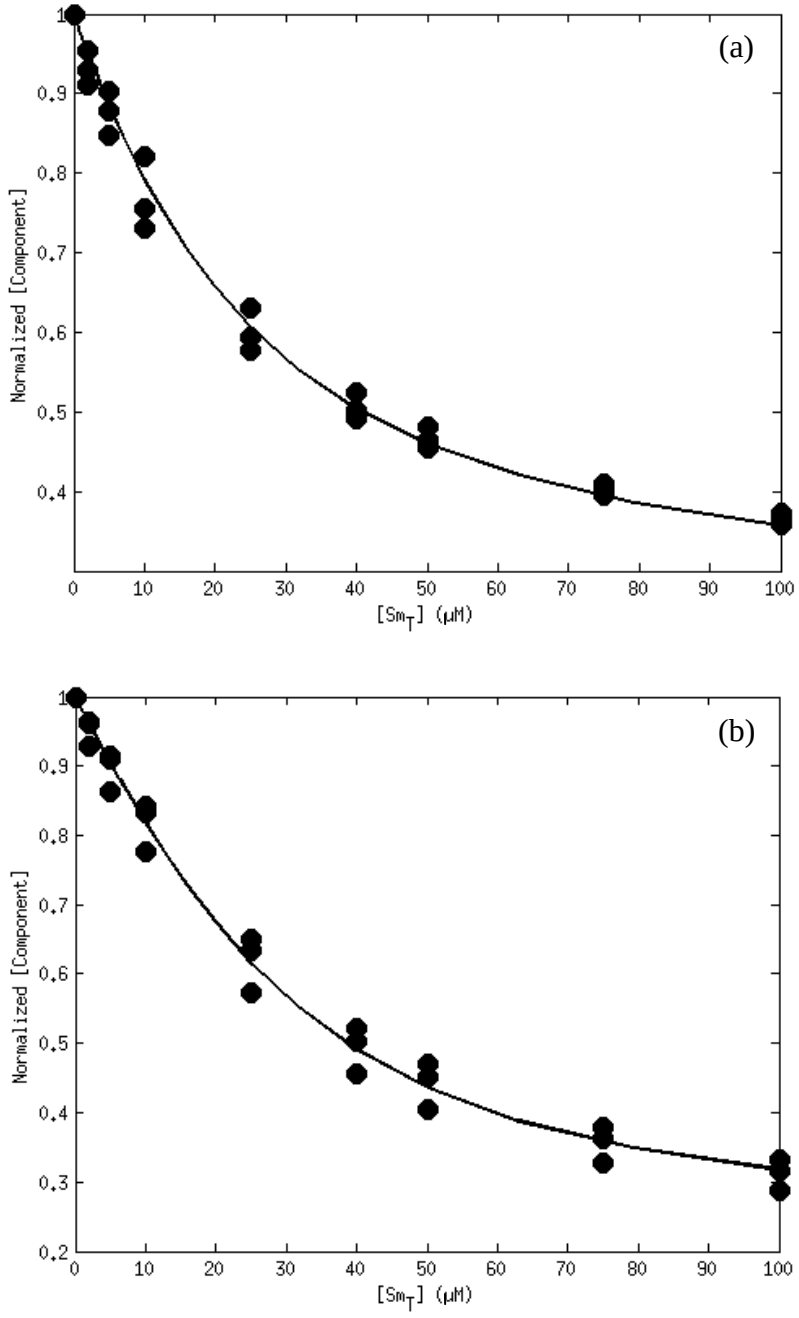

Figure B9. RW model fits for SW DOM (a) and LM DOM (b) titrated with Sm. The quenching curve data was produced from the normalized concentrations of the dominant component resolved by SIMPLISMA.

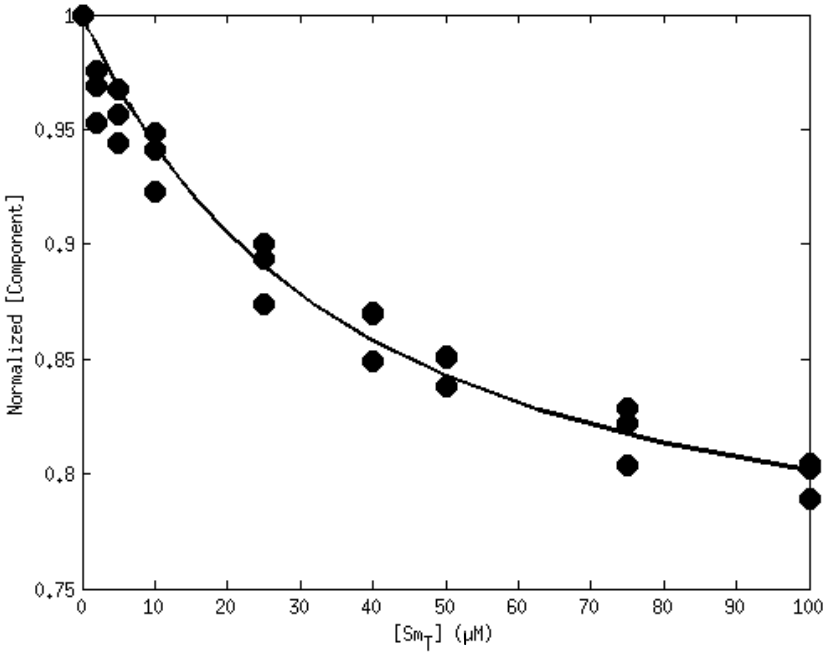

Figure B10. RW model fits for BB DOM titrated with Sm. The quenching curve data was produced from the normalized concentrations of the dominant component resolved by SIMPLISMA.

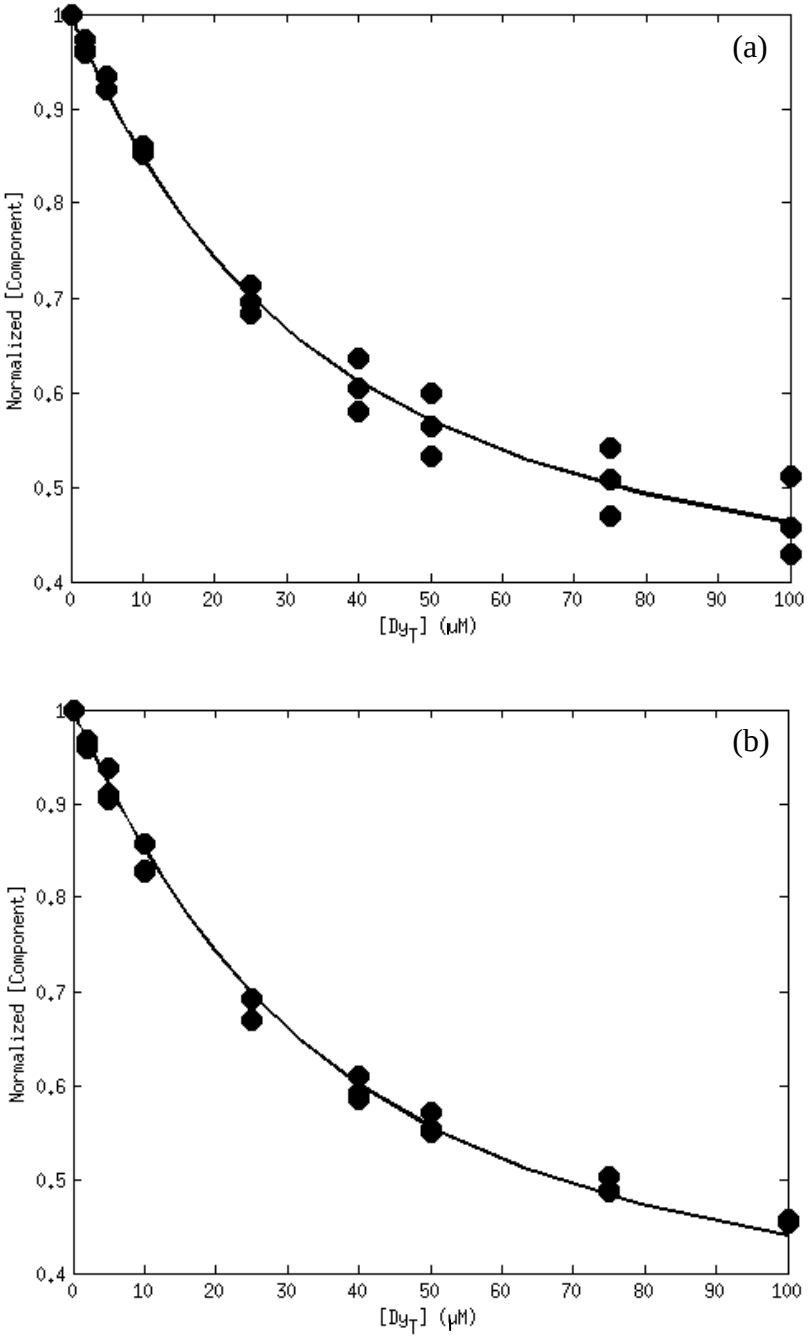

Figure B11. RW model fits for KB DOM (a) and SH DOM (b),titrated with Dy. The quenching curve data was produced from the normalized concentrations of the dominant component resolved by SIMPLISMA.

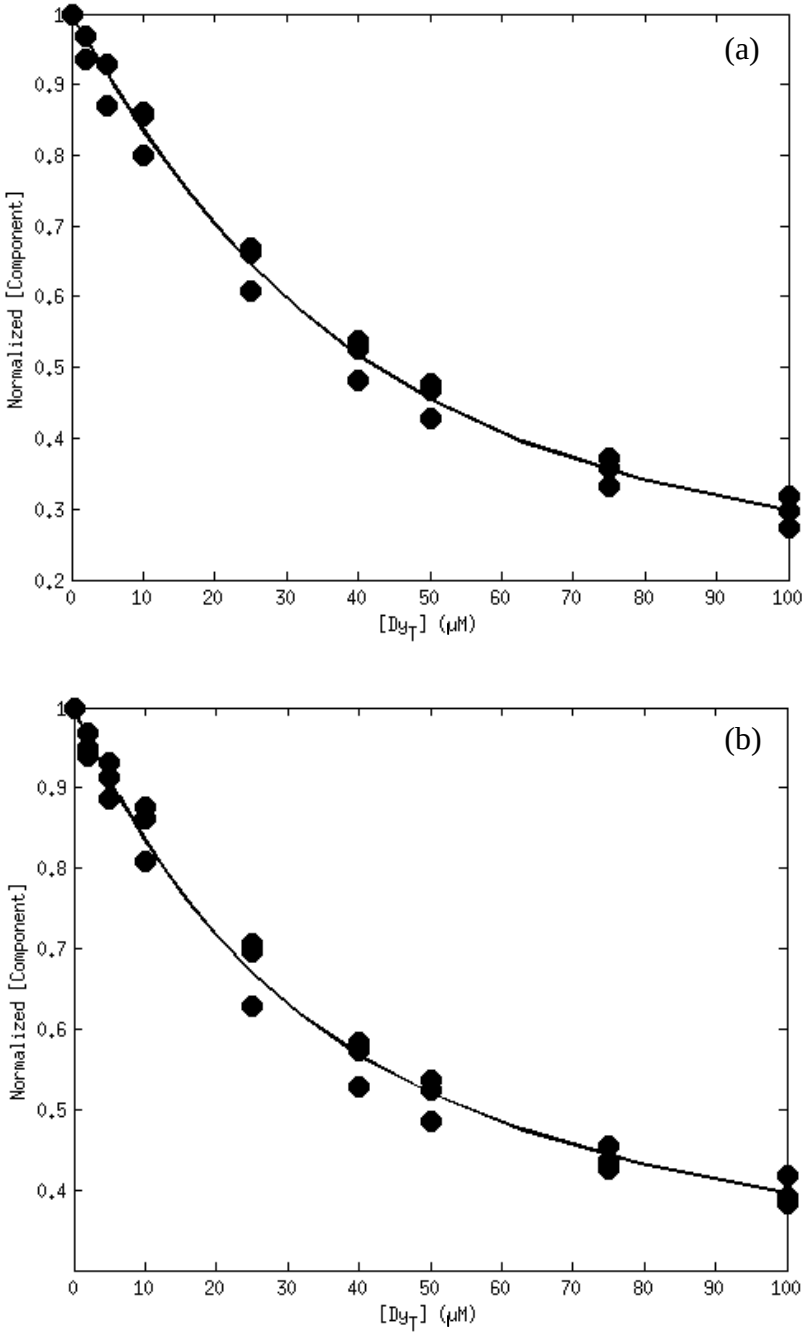

Figure B12. RW model fits for SW DOM (a) and LM DOM (b) titrated with Dy. The quenching curve data was produced from the normalized concentrations of the dominant component resolved by SIMPLISMA.

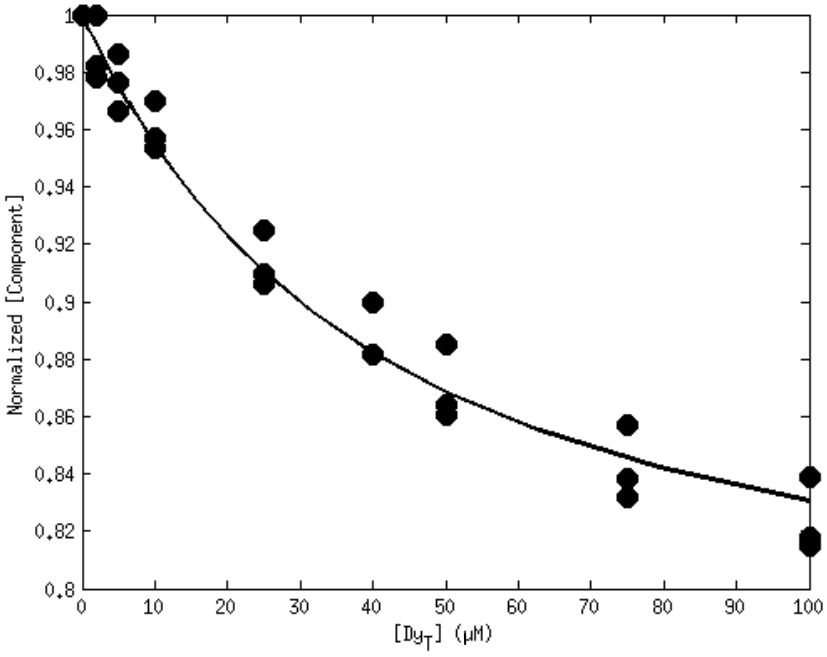

Figure B13. RW model fits for BB DOM titrated with Dy. The quenching curve data was produced from the normalized concentrations of the dominant component resolved by SIMPLISMA.

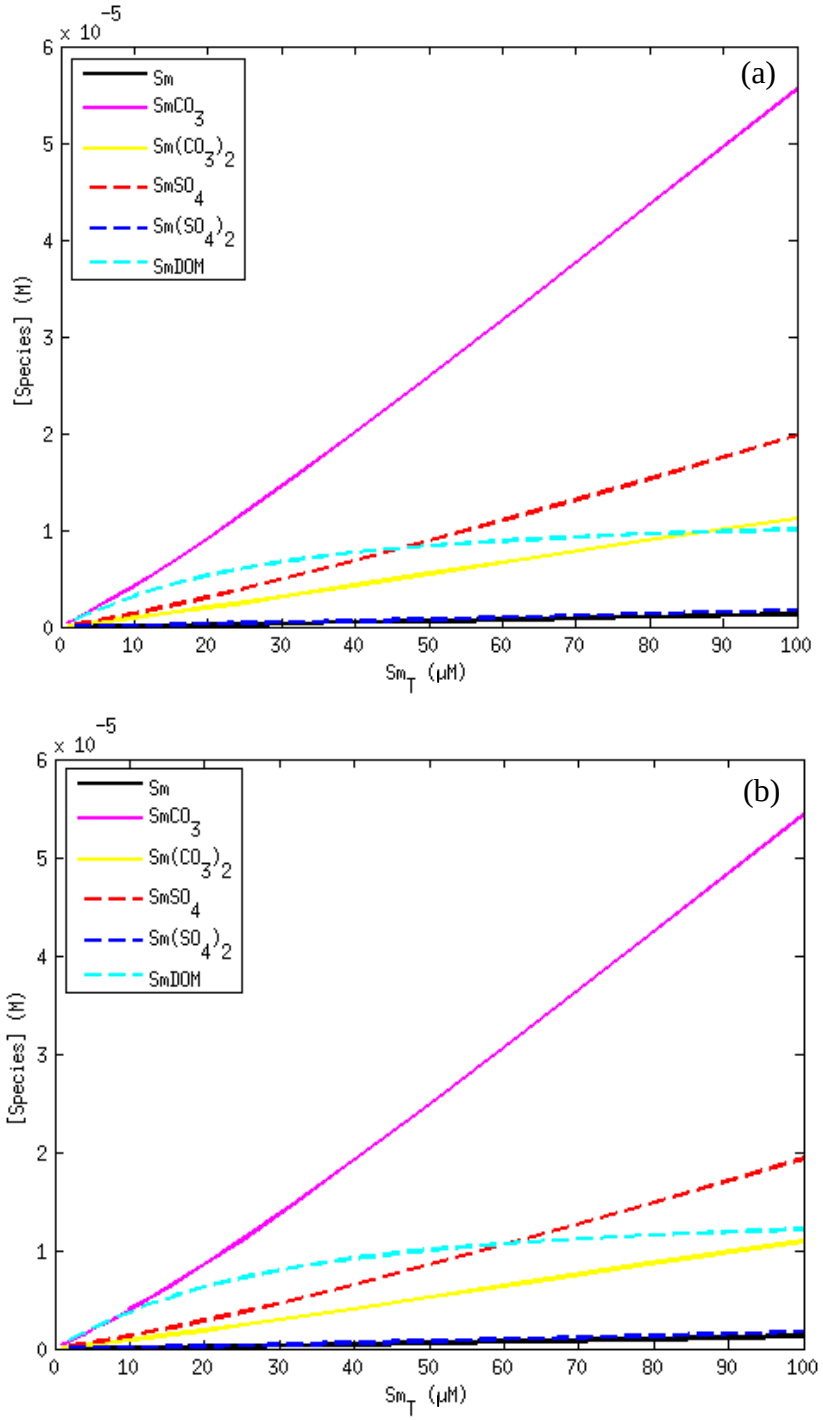

Figure B14. Speciation plots for KB DOM (a) and SH DOM (b) titrated with Sm during FQ titrations. Only dominant species concentrations are shown. Charge was omitted for clarity.

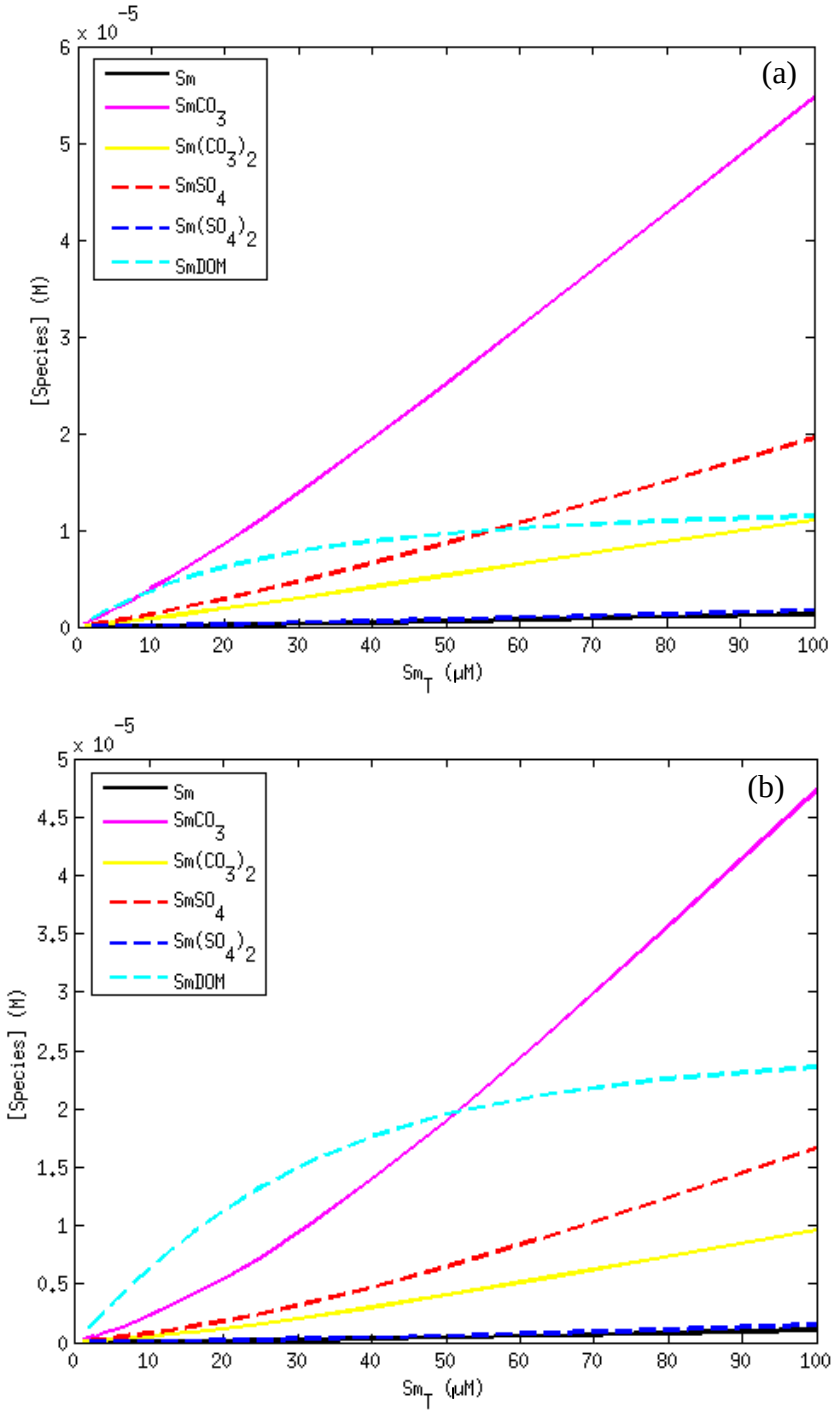

Figure B15. Speciation plots for SW DOM (a) and LM DOM (b) titrated with Sm during FQ titrations. Only dominant species concentrations are shown. Charge was omitted for clarity.

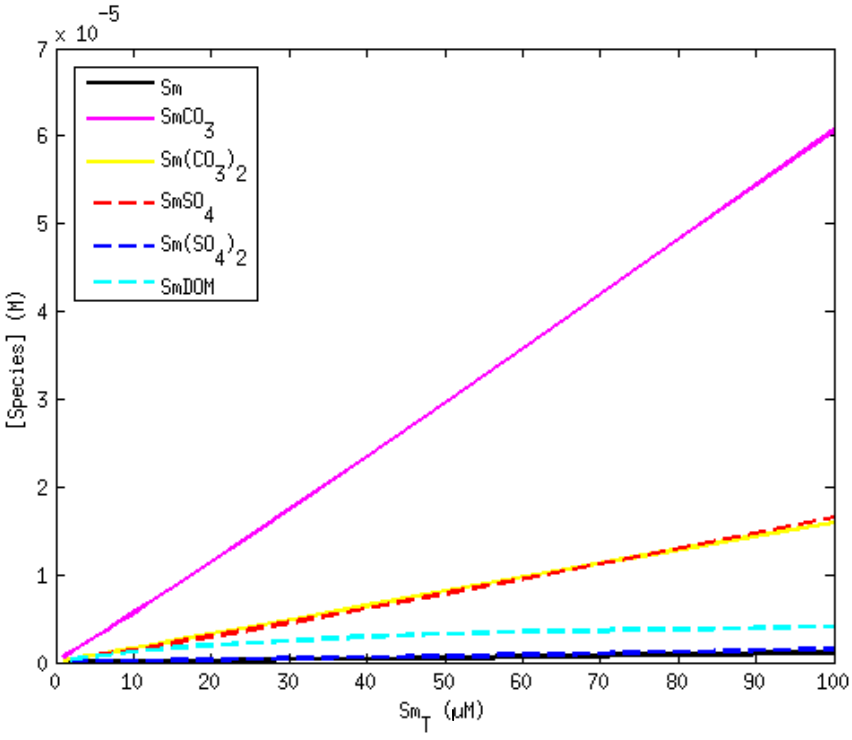

Figure B16. Speciation plots for BB DOM titrated with Sm during FQ titrations. Only dominant species concentrations are shown. Charge was omitted for clarity.

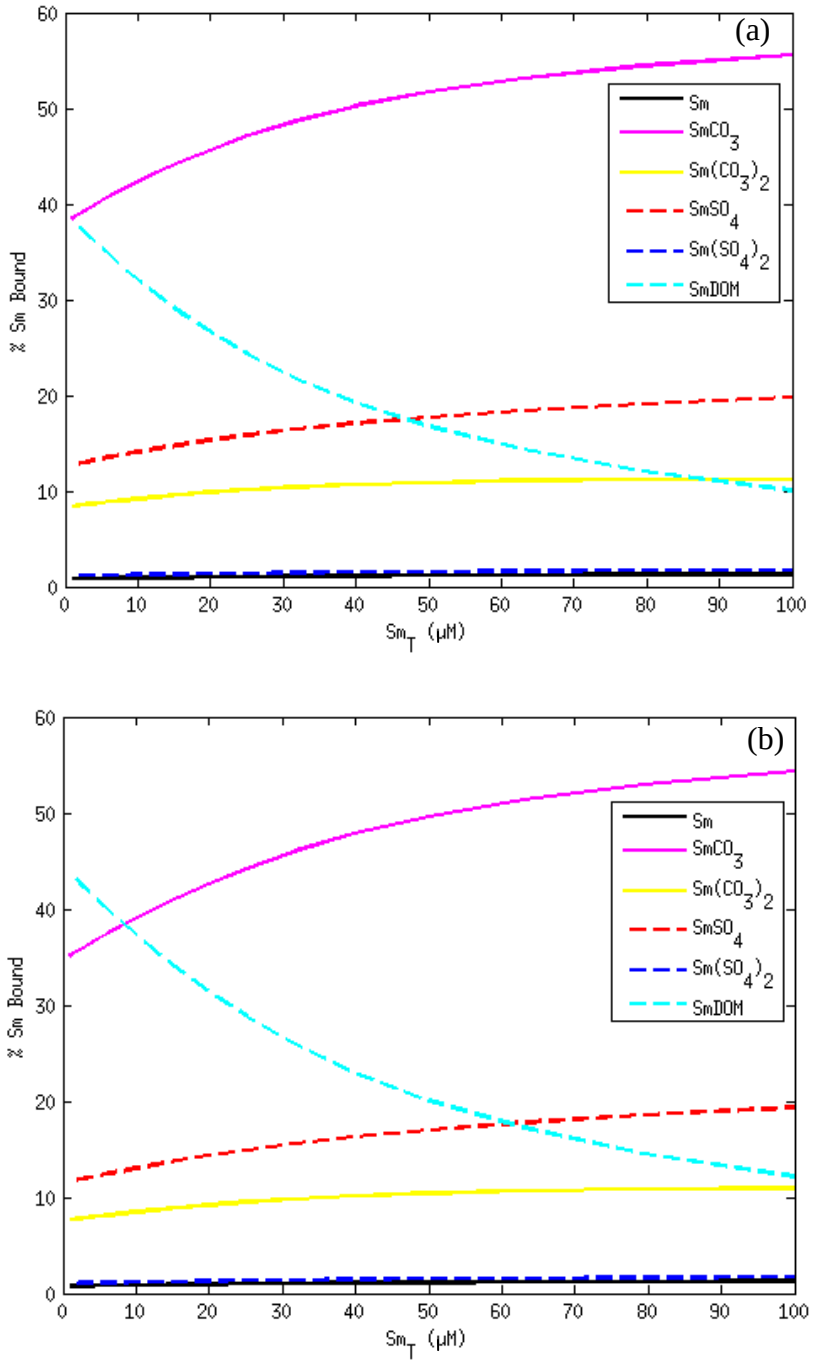

Figure B17. Speciation plots for KB DOM (a) and SH DOM (b) titrated with Sm during FQ experiments. The concentrations were converted to represent percent Sm bound in the specific complex. Charge was omitted for clarity.

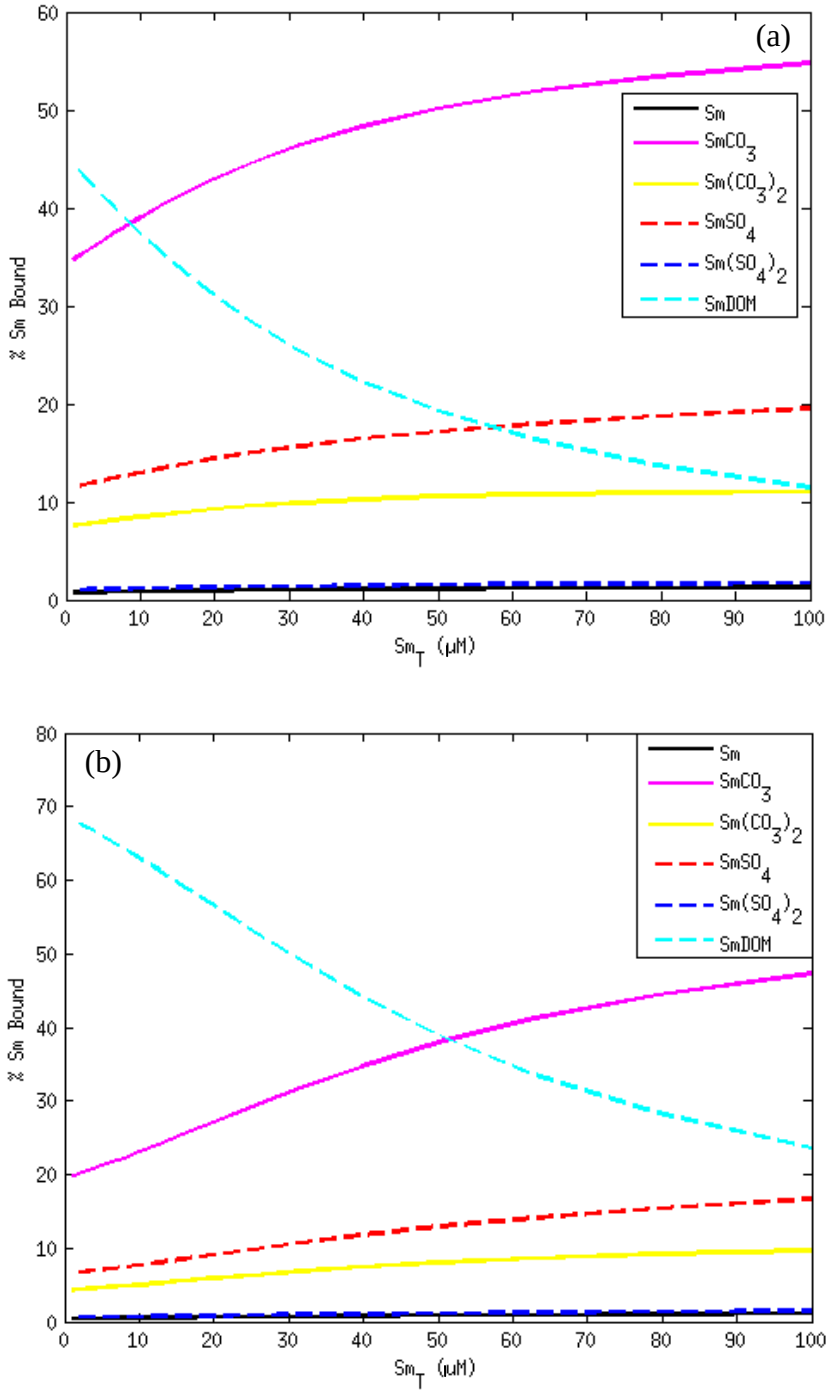

Figure B18. Speciation plots for SW DOM (a) and LM DOM (b) titrated with Sm during FQ experiments. The concentrations were converted to represent percent Sm bound in the specific complex. Charge was omitted for clarity.

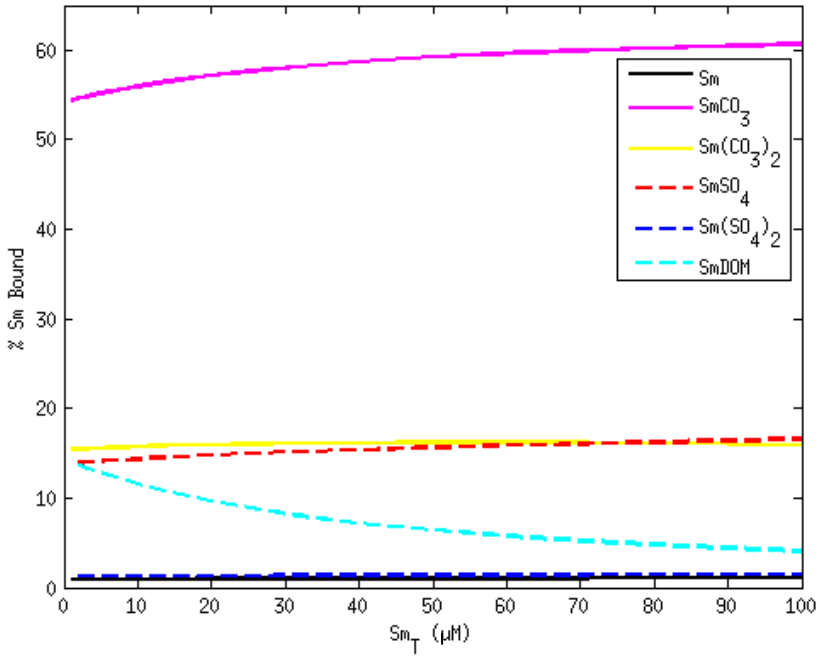

Figure B19. Speciation plots for BB DOM titrated with Sm during FQ experiments. The concentrations were converted to represent percent Sm bound in the specific complex. Charge was omitted for clarity.

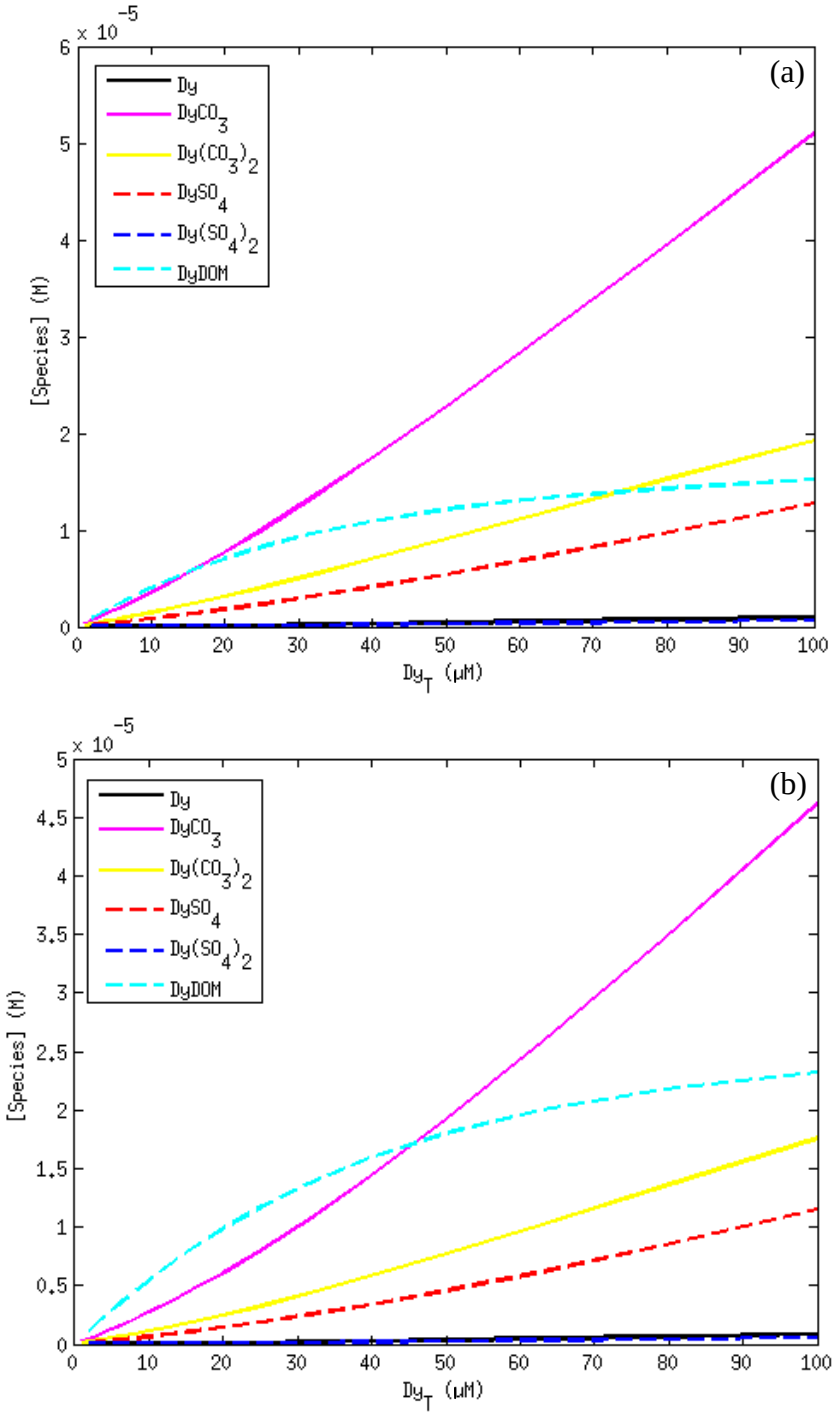

Figure B20. Speciation plots for KB DOM (a) and SH DOM (b) titrated with Dy during FQ titrations. Only dominant species concentrations are shown. Charge was omitted for clarity.

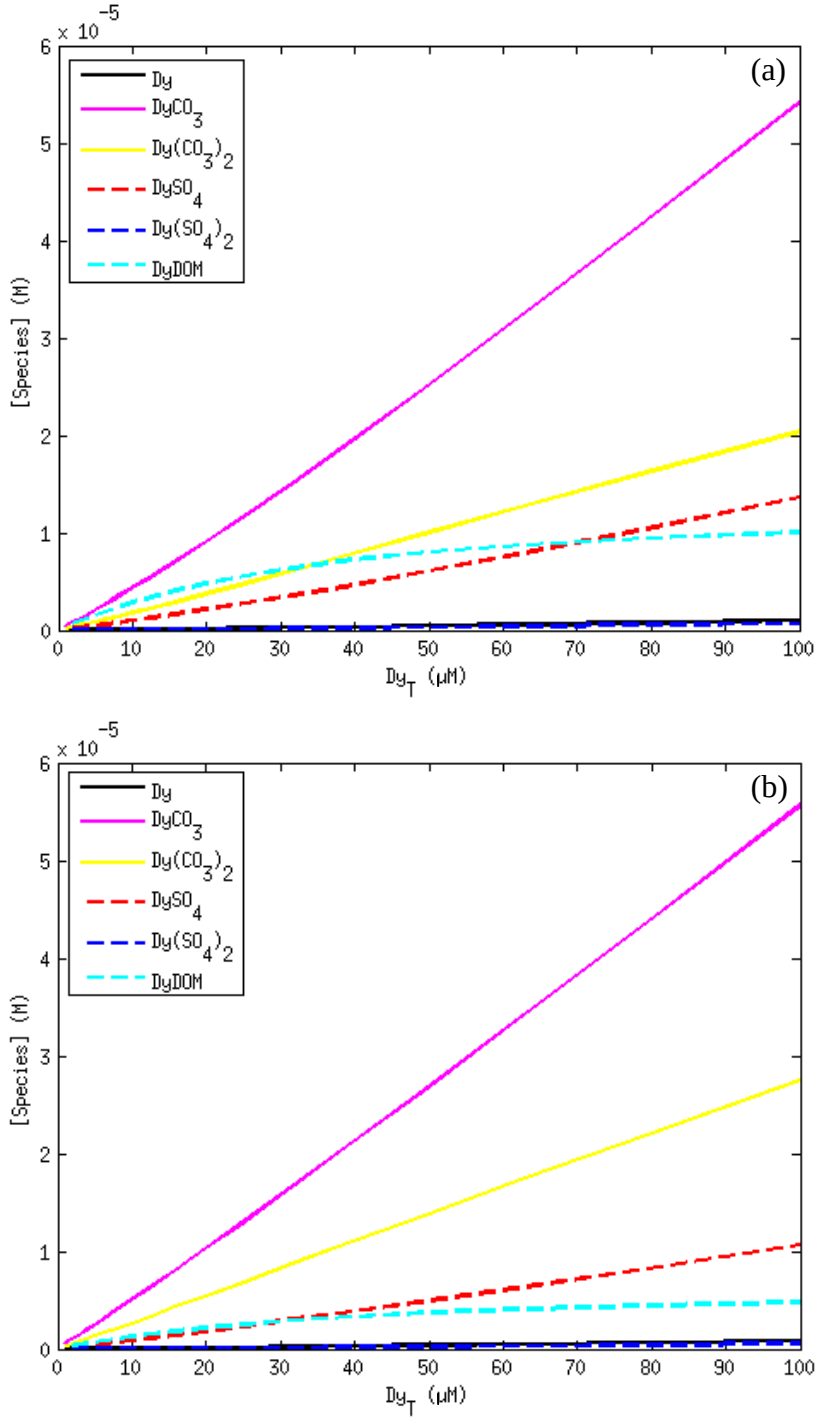

Figure B21. Speciation plots for SW DOM (a) and LM DOM (b) titrated with Dy during FQ titrations. Only dominant species concentrations are shown. Charge was omitted for clarity.

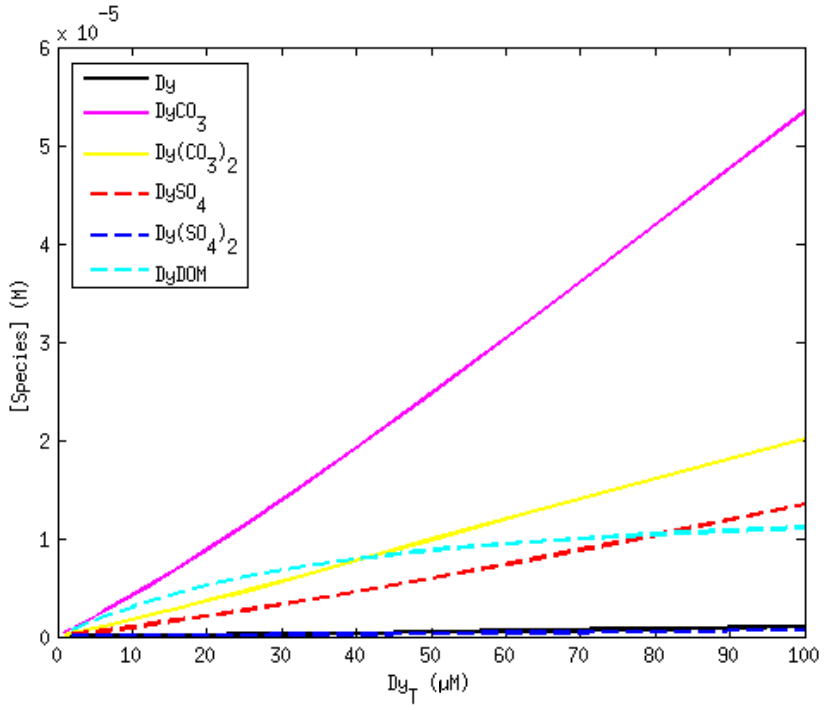

Figure B22. Speciation plots for BB DOM titrated with Dy during FQ titrations. Only dominant species concentrations are shown. Charge was omitted for clarity.

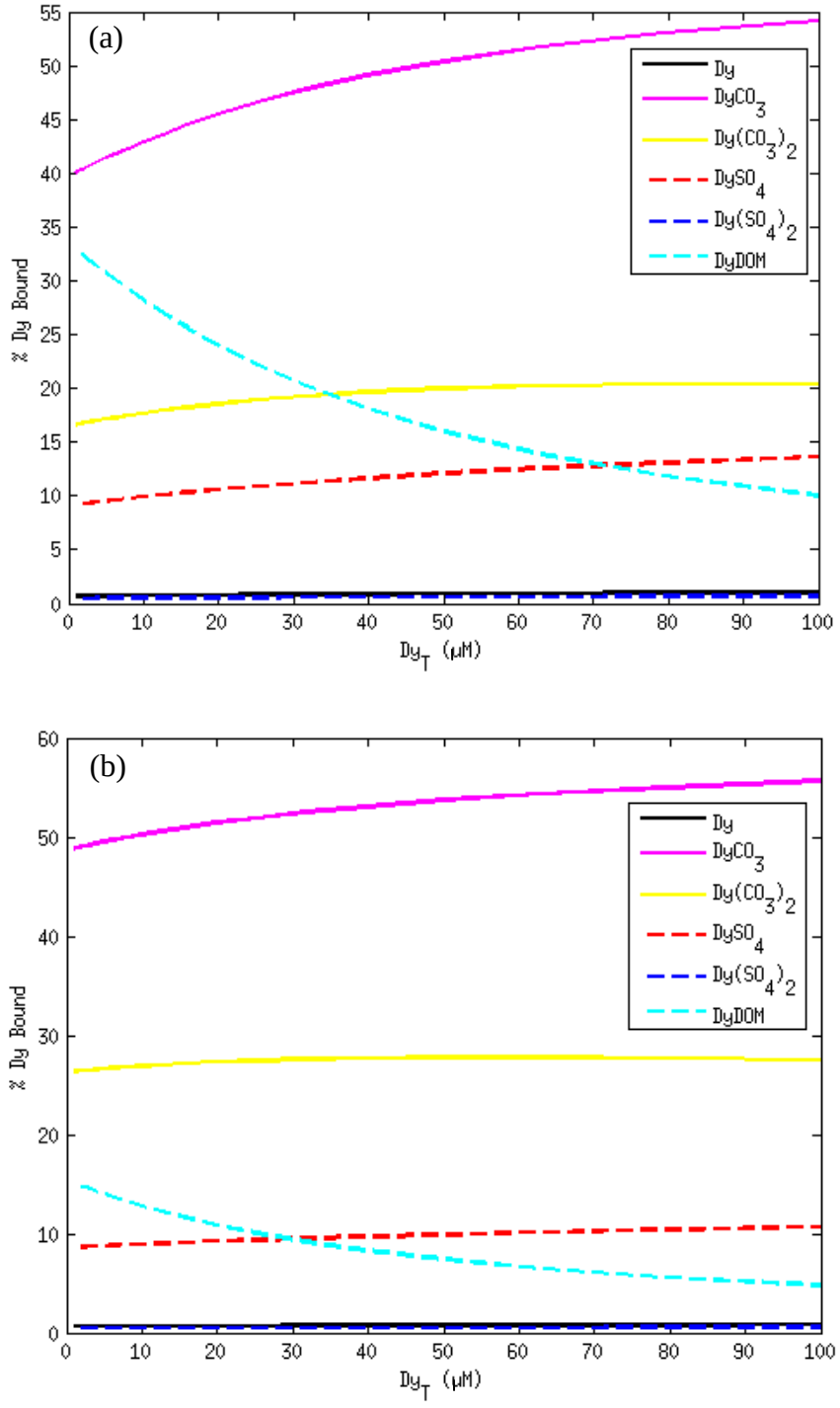

Figure B23. Speciation plots for KB DOM (a) and SH DOM (b) titrated with Dy during FQ experiments. The concentrations were converted to represent percent Dy bound in the specific complex. Charge was omitted for clarity.

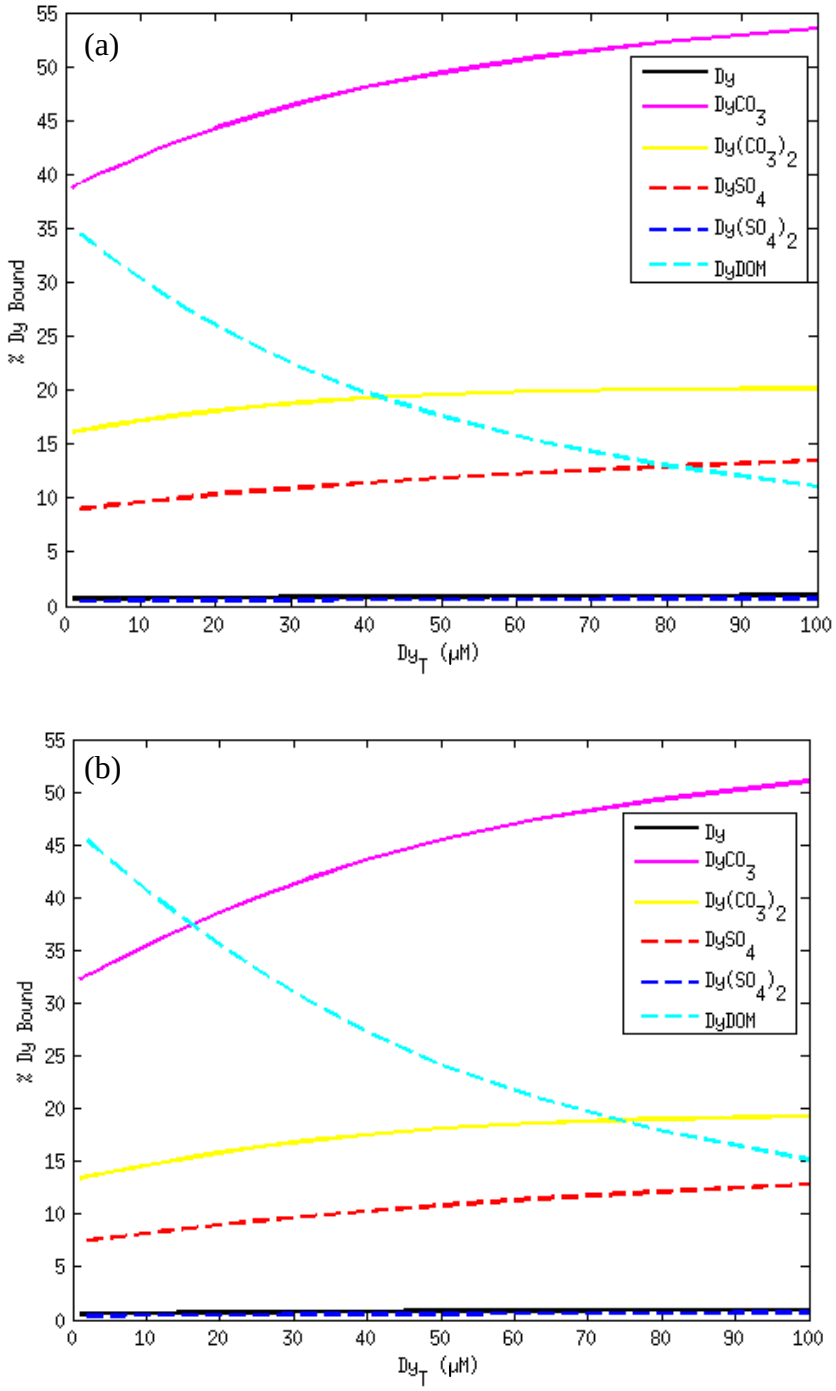

Figure B24. Speciation plots for SW DOM (a) and LM DOM (b) titrated with Dy during FQ experiments. The concentrations were converted to represent percent Dy bound in the specific complex. Charge was omitted for clarity.

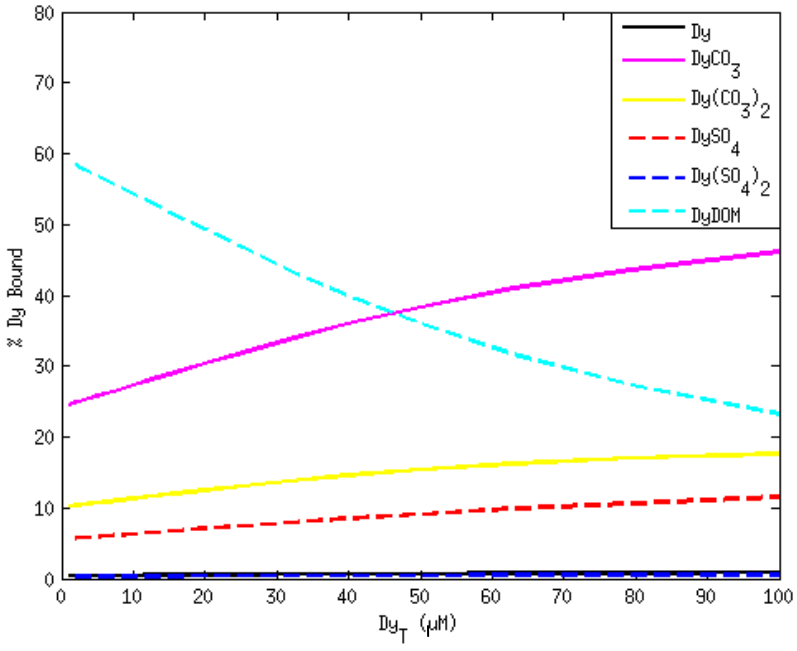

Figure B25. Speciation plots for BB DOM titrated with Dy during FQ experiments. The concentrations were converted to represent percent Dy bound in the specific complex. Charge was omitted for clarity.

Table B1. Concentrations of metals found in five DOM samples used for FQ and ISE titrations measured by ICP-OES. All major cations values are **bolded;** BB DOM and KB DOM major cations are also underlined, as they were contributing to high IS value.

Analyte	Units	LM DOM	BB DOM	SH DOM	SW DOM	KB DOM
Al	mg/L	0.031	BDL	0.017	0.02	0.028
As	mg/L	BDL	BDL	BDL	BDL	BDL
B	mg/L	0.053	0.056	0.024	0.02	0.024
Ba	mg/L	BDL	BDL	0.003	BDL	BDL
Ca	**mg/L**	**0.12**	**19.86**	**2.01**	**0.138**	**0.178**
Cd	mg/L	0.001	BDL	BDL	BDL	BDL
Co	mg/L	0.003	0.001	0.001	0.002	0.002
Cr	mg/L	0.004	0.002	0.003	0.002	0.002
Cu	mg/L	0.004	0.02	0.006	0.002	BDL
Fe	mg/L	0.054	0.009	0.041	0.019	0.094
K	**mg/L**	**0.352**	**14.33**	**0.72**	**0.221**	**0.22**
Mg	**mg/L**	**0.006**	**17.05**	**1.224**	**0.016**	**0.045**
Mn	mg/L	0.005	0.004	0.006	0.002	0.004
Mo	mg/L	0.004	0.011	0.003	0.001	0.001
Ni	mg/L	0.002	0.01	0.001	0.001	0.003
Pb	mg/L	0.004	0.003	BDL	BDL	BDL
Se	mg/L	0.016	0.015	0.014	0.018	0.016
Si	mg/L	0.235	1.339	0.669	0.139	0.654
Sb	mg/L	0.008	0.005	0.003	0.003	0.002
Ti	mg/L	0.003	BDL	BDL	BDL	BDL
Tl	mg/L	0.008	BDL	0.004	BDL	0.004
V	mg/L	0.087	0.026	0.079	0.071	0.086

Na ion was not measured as it saturated the ICP.
Ag, Be and Zn are no reported as they had calibration issues.
Negative response and zeros were reported as BDL (below detection limit).

APPENDIX C: MATLAB AND OTHER CODES

C1: ADL code for synchronous scan reading

```
ex_start = 200
ex_end = 440
em_start = 250
em_end = 600
num_samples = 300
delta_ex = (ex_end - ex_start)/(num_samples-1)
delta_em = (em_end - em_start)/(num_samples -1)
For sample = 0 to (num_samples-1)
   current_ex = ex_start + delta_ex*sample
   current_em = em_start + delta_em*sample
   REM SETVAL("Goto Wavelength", current_ex)
   REM SETUPINST
   LPRINT(current_ex, current_em, READ(current_ex, current_em) )
```

C2: MATLAB code for SIMPLISMA

```
function
[purspec,purint,purity_spec]=simplisma(data,varlist,offset,n,data2);
% function
[purspec,purint,purity_spec]=simplisma(data,varlist,offset,n,data2);
%
% It is a short non interactive version of SIMPLISMA taken from
Windig's
% article Chemometrics and Intelligent Laboratory Systems, 36, 1997, 3-
16.
%
%   INPUT:
%   data contains the data matrix (spectra in rows)
%   data 2 can be ignored or empty.
%       For second derivative applications data contains the
conventional
%       data and data2 contains the inverted 2nd data.
%       to create data2 use function:
%       data2=invder(data);
%   Varlist contains the variable identifiers
%   Offset is a correction factor for low intensity variables (1- no
%   offset, 15 - large offset)
%   n is a number of components
%
%   OUTPUT:
%       purespec contains the pure spectra
%       purint contains the intensities ('concentrations') of the pure
%       spectra in the mixtures
%       purity_spec - spectra containing purity spectra
%
% The program will plot the purity and standard deviation spectra,
where
% the pure variables selected will be marked by a '*'. After each plot,
% any key needs to be pressed to continue.

%INITIALIZE;
if nargin==5;
   temp=data;data=data2;data2=temp;clear temp
end
[nspec,nvar]=size(data); purvarindex=[];
if nargin==4;
   data2=[];
end;

%CACULATE STATISTICS

stddata=std(data)*sqrt(nspec-1)/sqrt(nspec);
meandata=mean(data);
meandataoffset=meandata+((offset/100)*max(meandata));
lengthdata=sqrt((stddata.*stddata+meandataoffset.*meandataoffset)*...
   sqrt(nspec));
lengthmatrix=lengthdata(ones(1,nspec),:);
datalengthscaled=data./lengthmatrix;
puredata=stddata./meandataoffset;
```

```
%DETERMINE PURE VARIABLES
purity_spec=0*[1:nvar];
max_index=0;
for i=1:n+1;
   purvar=datalengthscaled(:,purvarindex);
   for j=1:nvar;
      addcolumn=datalengthscaled(:,j);
      purvartest=[purvar addcolumn];
      matrix=purvartest'*purvartest;
      weight(j)=det(matrix);
   end;
   purityspec=weight.*puredata;
       purity_spec=[purity_spec; purityspec];
   maxindex=find(purityspec==max(purityspec));
   maxindex=maxindex(1);
  figure(2)
  subplot(3,2,1); plot(varlist,purityspec,'g',varlist(maxindex),...
     purityspec(maxindex),'g*');
   max_index=[max_index, maxindex];
  axis([sort([varlist(1) varlist(length(varlist))]) 0
1.1*max(purityspec)]);
  if varlist(1)>varlist(2);
     set(gca,'Xdir','reverse');
  end;
  title(['purity spectrum # ', num2str(i)]);
   stdspec=weight.*stddata;
  subplot(3,2,2);plot(varlist,  stdspec,'g',varlist(maxindex),...
     stdspec(maxindex),'g*');
  axis([sort([varlist(1) varlist(length(varlist))]) 0
1.1*max(stdspec)]) ;
  if varlist(1)>varlist(2);
     set(gca,'Xdir','reverse');
  end;
title(['standard deviation spectrum # ', num2str(i)]);

  pause

   purvarindex=[purvarindex maxindex];
end
close(2)
purvarindex(n+1)=[];

%RESOLVE SPECTRA

purematrix=(data(:,purvarindex));
if isempty(data2)
   purspec=purematrix\data;
else;
   purspec=purematrix\data2;
end;

%RESOLVE INTENSITIES

if isempty(data2);
   purint=data/purspec;
else;
```

```
   purint=data2/purspec;
end;

%SCALE

if isempty(data2);
   tsi=sum(data')';
else;
   tsi=sum(data2')';
end;
a=purint\tsi;
purint=purint*diag(a);
purspec=inv(diag(a))*purspec;
H2.Position=[264 188 339 423];
figure(H2)
subplot(2,1,1),plot(varlist,purspec), set(gca,'Xdir','reverse')
title ('pure spectra')
subplot(2,1,2), plot(purint), title ('pure intensity')
H3.Position=[616 190 339 423];
figure(H3)
for i=1:n+1;
   subplot(n+1,1,i), plot(abs(varlist),purity_spec(i+1,:))
   hold on,
plot(abs(varlist(max_index(i+1))),purity_spec(max_index(i+1)),'g*');
   set(gca,'Xdir','reverse')
   hold off
end
```

C3: MATLAB code for RW and Inorganic Speciation Model, Includes ISE Comparison

```
% fit RW equation but calculate free ion using inorganic speciation

function II=RW_embed_SmKB_speciation

figure(1); clf;

pguess=[7   -4.5  -1]; flagg=1;
%flagg=0;
MC=1;
% put in cons of Sm that match FQ experiments
CT=0.0010022;
SO4T=0.0033;
ClT=1e-30;
pH=7.3;

param7=pH7(pguess,flagg,MC,CT,SO4T,ClT,pH)

% put in cons of Sm that match ISE experiment plus have the organic
% ligand

SmT=[1e-18 2e-6 5e-6 10e-6 25e-6 40e-6 50e-6 75e-6 100e-6];
K=10.^param7(1,2)
LT=10.^param7(1,1)
CT=0.0000022; SO4T=1.5e-04; ClT=1e-30;

[species,names]=determine_species(SmT,pH,K,LT,CT,SO4T,ClT);

for i=1:size(SmT,2)
for j=1:size(species,2)
        txt=[names(j,:),'(i)=species(i,j);'];
        eval(txt)
end
end

figure(2); clf;
plot(SmT*1e6,ML,'k-','linewidth',2); hold on
plot(SmT*1e6,L,'r-','linewidth',2)
plot(SmT*1e6,M,'g-','linewidth',2)
plot(SmT*1e6,MOH3s,'b-','linewidth',2)
xlim ([0 100])
ylim ([0 4E-05])
xlabel('Total Metal (uM)');ylabel('Species (M)');
legend ('SmDOM','Free DOM','Free Sm','SmOH_{3s}');

figure(3); clf;
% plot(log10(M),ML*1e6,'k'); hold on
plot(log10(M),(SmT-M)*1e6,'k--','linewidth',2)
hold on
```

```
Smtot = [-5.7 -5.3 -5 -4.6 -4.4 -4.3 -4.1 -4]; SmT=10.^Smtot;
logSm1 = [-6.3580   -6.2839   -6.0577   -5.6876   -5.4899   -5.4982
-5.3116   -5.3833];
logSm2 = [-6.4929   -6.3013   -6.1463   -5.7024   -5.3499   -5.2815
-5.1777   -5.0916];

plot(logSm1,(SmT-
10.^logSm1)*1e6,'ko','markersize',10,'markerfaSmcolor','b')
plot(logSm2,(SmT-
10.^logSm2)*1e6,'ko','markersize',10,'markerfaSmcolor','b')
%plot(log10Smfree3om,(SmT-
10.^log10Smfree3om)*1e6,'ko','markersize',10,'markerfaSmcolor','c')
xlabel('log [Sm^{3+}]');ylabel('Bound [Sm] (uM)');
axis([-8 -4 0 100])

% inorganic speciation
% plot the speciation without organic and other stuff matching ISE
% experiment

SmT=[1e-18 2e-6 5e-6 10e-6 25e-6 40e-6 50e-6 75e-6 100e-6];
K=4.8305e+06; LT=1e-34;

[species,names]=determine_species(SmT,pH,K,LT,CT,SO4T,ClT);

for i=1:size(SmT,2)
for j=1:size(species,2)
        txt=[names(j,:),'(i)=species(i,j);'];
        eval(txt)
end
end

%plot(log10(M),(SmT-M)*1e6,'b--','linewidth',2)

end

function II=pH7(pguess,flagg,MC,CT,SO4T,ClT,pH)

% get the data
[SmT,Fmeas]=returndata7; %figure(1); plot(SmT,Fmeas,'ko')
% calculate free and bound ligand
%pguess=[6 -4.7 -1];
% if flagg==1; flag=1; colour='k';
tst=returnFerr(pguess,SmT,Fmeas,flag,colour,CT,SO4T,ClT,pH);
% flag=0;
% k=waitforbuttonpress;
% end
flag=0; colour='k';

options = optimset(@fminunc);
options = optimset(options,'Display','none','TolFun',1e-
4,'TolX',0.9e-2,'MaxFunEvals',1000);

f = @(p)returnFerr(p,SmT,Fmeas,flag,colour,CT,SO4T,ClT,pH);
```

```
[p2] = fminunc(f,pguess,options);
pguess=p2; P2=p2;

flag=1; Ffit=returnFerr(p2,SmT,Fmeas,flag,colour,CT,SO4T,ClT,pH);
flag=0;
F1calc=returnFmodel(p2,SmT,Fmeas,CT,SO4T,ClT,pH);
xlabel('[Sm_T] (uM)');ylabel('Normalized [Component]');
for i=1:MC;

     FMEAS=Fmeas;
     n=size(SmT,1);
     index=randperm(n,10);
     % non repeating integers from vector size of number of data
points
     %figure(3); clf; plot(SmT,Fmeas,'ko',SmT,F1calc,'k'); hold on

     for j=1:size(index,2)
         FMEAS(index(j))=F1calc(index(j))+randn*0.02*max(FMEAS);
        % figure(3); hold on;
plot(SmT(index(j)),Fmeas(index(j)),'ro');
     end
     %k=waitforbuttonpress;
%      figure(4); plot(SmT,FMEAS,'ko',SmT,Fmeas,'k.')
%      k=waitforbuttonpress;
     flag=0;
f = @(p)returnFerr(p,SmT,FMEAS,flag,colour,CT,SO4T,ClT,pH);
[p2] = fminunc(f,P2,options);
pguess=p2;

LT(i)=(p2(2)); logK(i)=p2(1); lessefficient(i)=p2(3);

end

II=[LT' logK' lessefficient'];
end


function [MT,F]=returndata7

% data

data=[...
%    [Sm]   F1    F2    F3
1e-18       1       1       1
2E-6    0.9512  0.9519  0.9802
5E-6    0.9055  0.8961  0.9314
10E-6   0.8325  0.8173  0.8439
25E-6   0.6710  0.6511  0.6521
40E-6   0.5943  0.57    0.5521
50E-6   0.5634  0.5413  0.5142
75E-6   0.5136  0.4783  0.4586
100E-6  0.4670  0.4349  0.4204
];
```

```
conc=data(:,1); F1=data(:,2); F2=data(:,3); F3=data(:,4);
 %F1=data(:,2); F2=data(:,3); F3=data(:,4);

 subdata=[...
     conc F1
     conc F2
     conc F3
     ];

sortdata=sortrows(subdata,1);

MT=sortdata(:,1);
F=sortdata(:,2);

%MT=data(:,1); F=data(:,2);

end

function II=returnFmodel(p,SmT,F1meas,CT,SO4T,ClT,pH)

logK=p(1); K=10^logK; LT=10^p(2); lessefficient1=10^p(3);% LT=5.6e-
5;
%K=10^5;

[Sm,SmL,L]=solve_speciation_tableau(K,LT,SmT,CT,SO4T,ClT,pH);

n=size(F1meas,1);
k11=mean(F1meas(1:3))/LT;
k12=lessefficient1*k11;
F1calc=k11*L+k12*SmL;

II=(F1calc);

end

function II=returnFerr(p,SmT,F1meas,flag,colour,CT,SO4T,ClT,pH)

logK=p(1); K=10^logK; LT=10^p(2); lessefficient1=10^p(3);
%LT=5.6e-5;
%K=10^5;

%lessefficient1=0.2617;

[Sm,SmL,L]=solve_speciation_tableau(K,LT,SmT,CT,SO4T,ClT,pH);

n=size(F1meas,1);
k11=mean(F1meas(1:3))/LT;
%lessefficient1=10^(-0.4300);
k12=lessefficient1*k11;
F1calc=k11*L+k12*SmL;
%F1calc=k11*L;
residuals=[F1meas-F1calc'];

II=log10(sum(residuals.^2));
```

```
%II=(sum(residuals.^2));

if flag==1;
    %SmTplot=[0 1e-6:1e-6:10e-6 11e-6:2e-6:45e-6]; SmTplot=SmTplot';
    logSmTplot=-7:0.1:-4; SmTplot=10.^logSmTplot';

[Smfreeplot,SmLplot,Lplot]=solve_speciation_tableau(K,LT,SmTplot,CT,
SO4T,ClT,pH);
    F1calcplot=k11*Lplot+k12*SmLplot;

plot(SmT*1e6,F1meas,'ko','markerfaSmcolor',colour,'markersize',10);
hold on;
    plot(SmTplot*1e6,F1calcplot,colour,'linewidth',2)
    plot(SmTplot*1e6,F1calcplot,'k')
end

end

function [Sm,SmL,L]=solve_speciation(K,LT,SmT)

for i=1:size(SmT,1)

    a=K; b=K*LT+1-K*SmT(i); c=-SmT(i);
    tst=roots([a b c]);

    for j=1:size(tst,1)
        if tst(j)>0; Sm(i)=tst(j);
        end
    end

end
SmL=SmT'-Sm;
L=LT*ones(size(SmT'))-SmL;
end

function
[Sm,SmL,L]=solve_speciation_tableau(K,LT,SmT,CT,SO4T,ClT,pH)

SmT=SmT';

[species,names]=determine_species(SmT,pH,K,LT,CT,SO4T,ClT);

for i=1:size(SmT,2)
for j=1:size(species,2)
        txt=[names(j,:),'(i)=species(i,j);'];
        eval(txt)
end
end

%figure(2); plot(SmT,M,'ko')

Sm=M; SmL=ML; L=L;

end
```

```
function [II,GG]=determine_species(MT,pH,K,LT,CT,SO4T,ClT)

warning('off')

% ligand concetrations
%%%%%%%%%%%%%%%%%%%%%%%%%%%%%%%%%%%%%%%%%%%%%%%%%%%%%%%%%%%%%%%%%%%%%%%%%%%%%%%%
%%%%%%%%5
%CO3T=CT; %SO4T=0.0033e-3; ClT=0.00004e-3;
BrT=0.005E-20;
%%%%%%%%%%%%%%%%%%%%%%%%%%%%%%%%%%%%%%%%%%%%%%%%%%%%%%%%%%%%%%%%%%%%%%%%%%%%%%%%
%%%%%%%%5

[KSOLUTION,KSOLID,ASOLUTION,ASOLID,SOLUTIONNAMES,SOLIDNAMES]=get_equ
ilib_defn(K);

numpts=size(MT,2);
Ncp=size(ASOLID,1);
solid_summary=zeros(numpts,Ncp);

for i=1:size(SOLIDNAMES,1)
    txt=[SOLIDNAMES(i,:),'=zeros(numpts,1);']; eval(txt)
end

for i=1:size(MT,2)

    % adjust for fixed pH


[Ksolution,Ksolid,Asolution,Asolid]=get_equilib_fixed_pH(KSOLUTION,K
SOLID,ASOLUTION,ASOLID,pH);

    Asolid_SI_check=Asolid; Ksolid_SI_check=Ksolid;

    % number of different species
    Nx=size(Asolution,2); Ncp=size(Asolid,1); Nc=size(Asolution,1);

    % initial guess
    iterations=1000; criteria=1e-16;

%%%%%%%%%%%%%%%%%%%%%%%%%%%%%%%%%%%%%%%%%%%%%%%%%%%%%%%%%%%%%%%%%%%%%%%%%%%%%%%%
%%%%%%%%%
    T=[MT(i) CT SO4T ClT BrT LT]; guess=T./10;

%%%%%%%%%%%%%%%%%%%%%%%%%%%%%%%%%%%%%%%%%%%%%%%%%%%%%%%%%%%%%%%%%%%%%%%%%%%%%%%%
%%%%%%%%%%%%

    % calculate species using NR

    solids=zeros(1,Ncp);
```

```
    if i==1;
[species,err,SI]=NR_method_solution(Asolution,Asolid,Ksolid,Ksolutio
n,T',[guess(1:Nx)]',iterations,criteria); end
    if i>1;

[species,err,SI]=NR_method_solution(Asolution,Asolid,Ksolid,Ksolutio
n,T',[species(2:Nx+1)],iterations,criteria);
    end

    for qq=1:Ncp

        [Y,I]=max(SI);

        if Y>1.000000001
            Iindex(qq)=I;
            Asolidtemp(qq,:)=Asolid_SI_check(I,:); %'MOH3s'
            Ksolidtemp(qq,:)=Ksolid_SI_check(I,:);
            solidguess(qq)=T(I)*0.5;
           % solidguess(qq)=min(T)*0.015;
            if i>1;
                %if max(solids)>0
                txt=['solidguess(qq)=',SOLIDNAMES(I,:),'(i-1);'];
eval(txt);
                %end
            end
            guess=[species(2:Nx+1)' solidguess];

[species,err,SItst,solids]=NR_method(Asolution,Asolidtemp',Ksolidtem
p,Ksolution,T',guess',iterations,criteria);
             for q=1:size(solids,1);
                txt=[SOLIDNAMES(Iindex(q),:),'(i)=solids(q);'];
eval(txt)
              end
        end

        Q=Asolid*log10(species(2:Nx+1)); SI=10.^(Q+Ksolid);
Ifirst=I;

    end

    Q=Asolid*log10(species(2:Nx+1)); SI=10.^(Q+Ksolid);
    SI_summary(i,:)=SI;

    species_summary(i,:)=species;
    mass_err_summary(i,:)=(err(1));

    Asolidtemp=[]; Ksolidtemp=[];

end

for i=1:size(species_summary,2)
    txt=[SOLUTIONNAMES(i,:),'=species_summary(:,i);']; eval(txt)
end
%%%%%%%%%%%%%%%%%%%%%%%%%%%%%%%%%%%%%%%%%%%%%%%%%%%%%%%%%%%%%%%%%%%%%%%
```

```
II=[species_summary MOH3s M2CO33s];% UPDATE
%%%%%%%%%%%%%%%%%%%%%%%%%%%%%%%%%%%%%%%%%%%%%%%%%%%%%%%%%%%%%%%%%%%%%%%%%%%%
GG=strvcat(SOLUTIONNAMES,SOLIDNAMES);


end

% -------------------- NR method solids present

function
[species,err,SI,solids]=NR_method(Asolution,Asolid,Ksolid,Ksolution,
T,guess,iterations,criteria)

Nx=size(Asolution,2); Ncp=size(Asolid,2); Nc=size(Asolution,1);
X=guess;

for II=1:iterations

    Xsolution=X(1:Nx); Xsolid=[]; if Ncp>0; Xsolid=X(Nx+1:Nx+Ncp);
end

      logC=(Ksolution)+Asolution*log10(Xsolution); C=10.^(logC); %
calc species

    if Ncp>0;
        Rmass=Asolution'*C+Asolid*Xsolid-T;
    end


    if Ncp==0; Rmass=Asolution'*C-T; end % calc residuals in mass
balanSm

    Q=Asolid'*log10(Xsolution); SI=10.^(Q+Ksolid);
    RSI=ones(size(SI))-SI;

      % calc the jacobian

      z=zeros(Nx+Ncp,Nx+Ncp);

      for j=1:Nx;
            for k=1:Nx;
                        for i=1:Nc;
z(j,k)=z(j,k)+Asolution(i,j)*Asolution(i,k)*C(i)/Xsolution(k); end
            end
    end

    if Ncp>0;
    for j=1:Nx;
            for k=Nx+1:Nx+Ncp;
                 t=Asolid';
                        z(j,k)=t(k-Nx,j);
            end
    end
    end
```

```
    if Ncp>0
    for j=Nx+1:Nx+Ncp;
            for k=1:Nx
                        z(j,k)=-1*Asolid(k,j-Nx)*(SI(j-
Nx)/Xsolution(k));
            end
    end
    end

    if Ncp>0
    for j=Nx+1:Nx+Ncp
        for k=Nx+1:Nx+Ncp
            z(j,k)=0;
        end
    end
    end

    R=[Rmass; RSI]; X=[Xsolution; Xsolid];

    deltaX=z\(-1*R);
    %deltaX=-1*inv(z)*(R);
      one_over_del=max([1, -1*deltaX'./(0.5*X')]);
      del=1/one_over_del;
      X=X+del*deltaX;

    %X=X+deltaX;

      tst=sum(abs(R));
      if tst<=criteria; break; end

end

logC=(Ksolution)+Asolution*log10(Xsolution); C=10.^(logC); % calc
species
RSI=ones(size(SI))-SI;

if Ncp>0; Rmass=Asolution'*C+Asolid*Xsolid-T; end % calc residuals
in mass balanSm
if Ncp==0; Rmass=Asolution'*C-T; end % calc residuals in mass
balanSm

err=[Rmass];

species=[C];
solids=Xsolid;

end

% ----------- NR method just solution species

function
[species,err,SI]=NR_method_solution(Asolution,Asolid,Ksolid,Ksolutio
n,T,guess,iterations,criteria)
```

```
Nx=size(Asolution,2); Ncp=size(Asolid,1); Nc=size(Asolution,1);
X=guess;

for II=1:iterations

    Xsolution=X(1:Nx);

      logC=(Ksolution)+Asolution*log10(Xsolution); C=10.^(logC); %
calc species

    Rmass=Asolution'*C-T;

    Q=Asolid*log10(Xsolution); SI=10.^(Q+Ksolid);
    RSI=ones(size(SI))-SI;

      % calc the jacobian

      z=zeros(Nx,Nx);

      for j=1:Nx;
            for k=1:Nx;
                        for i=1:Nc;
z(j,k)=z(j,k)+Asolution(i,j)*Asolution(i,k)*C(i)/Xsolution(k); end
            end
    end

    R=[Rmass]; X=[Xsolution];

    deltaX=z\(-1*R);
    %deltaX=-1*inv(z)*(R);
      one_over_del=max([1, -1*deltaX'./(0.5*X')]);
      del=1/one_over_del;
      X=X+del*deltaX;

    %X=X+deltaX;

      tst=sum(abs(R));
      if tst<=criteria; break; end

end

logC=(Ksolution)+Asolution*log10(Xsolution); C=10.^(logC); % calc
species
RSI=ones(size(SI))-SI;

Q=Asolid*log10(Xsolution); SI=10.^(Q+Ksolid);
RSI=ones(size(SI))-SI;

Rmass=Asolution'*C-T;

err=[Rmass];

species=[C];
```

```
end


% ----- equilib definition ----------------
Tableau_varymetal_fixedpHSmFQ.m

function
[KSOLUTION,KSOLID,ASOLUTION,ASOLID,SOLUTIONNAMES,SOLIDNAMES]=get_equ
ilib_defn(K);

%%%%%%%%%%%%%%%%%%%%%%%%%%%%%%%%%%%%%%%%%%%%%%%%%%%%%%%%%%%%%%%%%%%
%%%%%%%%%%%%%%%
%H+   M  CO3  SO4 Cl  Br  L logK  species name
Tableau=[...
1   0   0    0   0   0   0  0      {'H'}
0   1   0    0   0   0   0  0      {'M'}
0   0   1    0   0   0   0  0      {'CO3'}
0   0   0    1   0   0   0  0      {'SO4'}
0   0   0    0   1   0   0  0      {'Cl'}
0   0   0    0   0   1   0  0      {'Br'}
0   0   0    0   0   0   1  0      {'L'}
-1  0   0    0   0   0   0  -14    {'OH'}
1   0   1    0   0   0   0  10.3  {'HCO3'}
2   0   1    0   0   0   0  16.6  {'H2CO3'}
1   0   0    0   0   0   0  1.99  {'HSO4'}
-1  1   0    0   0   0   0  -7.9  {'MOH'}
-2  2   0    0   0   0   0  -14.5 {'M2OH2'}
0   1   1    0   0   0   0   7.71 {'MCO3'}
0   1   2    0   0   0   0   13.09 {'MCO32'}
0   1   0    1   0   0   0   3.67  {'MSO4'}
0   1   0    2   0   0   0   5.1   {'MSO42'}
0   1   0    0   1   0   0   -0.39 {'MCl'}
0   1   0    0   0   1   0   -0.2  {'MBr'}
0   1   0    0   0   0   1   log10(K) {'ML'}
];
%
%%%%%%%%%%%%%%%%%%%%%%%%%%%%%%%%%%%%%%%%%%%%%%%%%%%%%%%%%%%%%%%%%%%
%%%%%%%%%%%
n=size(Tableau,2);
ASOLUTION=Smll2mat(Tableau(:,1:n-2));
KSOLUTION=Smll2mat(Tableau(:,n-1));
SOLUTIONNAMES=strvcat(Tableau(:,n));

% -------------- solid values
%H+   M  CO3  SO4 Cl  Br   logK  species name
%%%%%%%%%%%%%%%%%%%%%%%%%%%%%%%%%%%%%%%%%%%%55
STableau=[...
-3  1 0    0    0    0    0 -16.5 {'MOH3s'}%18.1
0   2   3   0    0    0    0 -32.3  {'M2CO33s'}%turns off precipitation
];
%%%%%%%%%%%%%%%%%%%%%%%%%%%%%%%%%%%%%%%%%%%%%%%%%%%%%%%%%
```

```
ASOLID=Smll2mat(STableau(:,1:n-2));
KSOLID=Smll2mat(STableau(:,n-1));
SOLIDNAMES=strvcat(STableau(:,n));

end

% ----------- for fixed pH ----------------

function
[Ksolution,Ksolid,Asolution,Asolid]=get_equilib_fixed_pH(KSOLUTION,K
SOLID,ASOLUTION,ASOLID,pH)

    [N,M]=size(ASOLUTION);
    Ksolution=KSOLUTION-ASOLUTION(:,1)*pH;
    Asolution=[ASOLUTION(:,2:M)];
    [N,M]=size(ASOLID);
    Ksolid=KSOLID-ASOLID(:,1)*pH;
    Asolid=[ASOLID(:,2:M)];

end
```

C4: MATLAB code for ISE and Inorganic Speciation model

```
% fit ISE data for Sm

function II=ISE_SmLM_speciation

figure(1); clf

% input the data ------------------------------------------------

logSmtot1=[-5.2 -4.9 -4.6 -4.4 -4.3 -4.1 -4]; SmT1 = 10.^logSmtot1;
logSmtot2=[-5.3 -5 -4.6 -4.4 -4.3 -4.1 -4]; SmT2=10.^logSmtot2;
logSm1=[-6.7698 -6.5971 -6.0477  -5.2914 -5.1008  -4.9558 -4.9383];
logSm2=[-6.8256 -6.6563 -6.1217  -5.6553 -5.4984  -5.3176 -5.1277];

% pool the data
data=[logSmtot1' logSm1'
logSmtot2' logSm2'];

[Y,I]=sort(data(1,:));
datasort=data(:,I); %use the column indices from sort() to sort all
columns of A.

% input concentrations-----------------------------------------
CT=0.0000018; SO4T=1.5e-04; ClT=8.85e-5; DOC=10; pH=7.3;

% initial guess on parameters [logK1 logK2 logLT1 logLT2]
pguess=[7 -4.5];
% find the best fit parameters

flag=0; colour='k'; options = optimset(@fminunc);
options = optimset(options,'Display','none','TolFun',1e-4,'TolX',1e-
3,'MaxFunEvals',1000);
SmT=10.^datasort(:,2); ISEmeas=datasort(:,1);

% %test the error function
% flag=1;
ISEerr=returnISEerr(pguess,SmT,ISEmeas,flag,colour,CT,SO4T,ClT,pH);
flag=0;
% k=waitforbuttonpress;

% optimize
f = @(p)returnISEerr(p,SmT,ISEmeas,flag,colour,CT,SO4T,ClT,pH);
[p2] = fminunc(f,pguess,options);
pguess=p2; P2=p2;

% test fit
flag=1; colour='k';
ISEerr=returnISEerr(p2,SmT,ISEmeas,flag,colour,CT,SO4T,ClT,pH);
flag=0;
xlabel('log [Sm^{3+}]'); ylabel('Bound [Sm] (uM)');
% determine best fit free ion
```

```
logK1=p2(1); K1=10^logK1;

logLT1=p2(2); LT1=10^logLT1;

[species,names]=determine_speciesv2(SmT',pH,K1,LT1,CT,SO4T,ClT);
for i=1:size(SmT,1)
    for j=1:size(species,2)
        txt=[names(j,:),'(i)=species(i,j);'];
        eval(txt)
    end
end

ISEbestfit=log10(M); MC=100;

% figure(2); clf
% plot(ISEbestfit,1e6*(SmT-10.^ISEbestfit'),'k-','linewidth',2);
hold on

for i=1:MC;
      ISEMEAS=ISEmeas;
      n=size(SmT,1);
      index=randperm(n,5); % non repeating integers from vector size
of number of data points
      for j=1:size(index,2)
          ISEMEAS(index(j))=ISEbestfit(index(j))+0.2*randn;
      end
%        figure(2)
%        plot(ISEMEAS,(SmT-
10.^ISEMEAS)*1e6,'ko','linewidth',2,'markerfacecolor','b')
%        k=waitforbuttonpress
      flag=0;
      f =
@(p)returnISEerr(p,SmT,ISEMEAS,flag,colour,CT,SO4T,ClT,pH);
      [p2] = fminunc(f,pguess,options);
      pguess=P2; % back to original best guess

      logK1(i)=(p2(1));

      logLT1(i)=p2(2);


end
forexport=[logK1' logLT1']

II=-1;
end

function
[KSOLUTION,KSOLID,ASOLUTION,ASOLID,SOLUTIONNAMES,SOLIDNAMES]=get_equ
ilib_defn2(K1);

%%%%%%%%%%%%%%%%%%%%%%%%%%%%%%%%%%%%%%%%%%%%%%%%%%%%%%%%%%%%%%%%%%%%%%%%
%%%%%%%%%%%%%%
%H+   M  CO3  SO4 Cl  Br  L1 L2 logK  species name
```

```
Tableau=[...
1   0   0    0   0   0   0   0     {'H'}
0   1   0    0   0   0   0   0     {'M'}
0   0   1    0   0   0   0   0     {'CO3'}
0   0   0    1   0   0   0   0     {'SO4'}
0   0   0    0   1   0   0   0     {'Cl'}
0   0   0    0   0   1   0   0     {'Br'}
0   0   0    0   0   0   1   0     {'L1'}
-1  0   0    0   0   0   0   -14   {'OH'}
1   0   1    0   0   0   0   10.3  {'HCO3'}
2   0   1    0   0   0   0   16.6  {'H2CO3'}
1   0   0    0   0   0   0   1.99  {'HSO4'}
-1  1   0    0   0   0   0   -7.9  {'MOH'}
-2  2   0    0   0   0   0   -14.5 {'M2OH2'}
0   1   1    0   0   0   0    7.71 {'MCO3'}
0   1   2    0   0   0   0   13.09 {'MCO32'}
0   1   0    1   0   0   0    3.67  {'MSO4'}
0   1   0    2   0   0   0    5.1   {'MSO42'}
0   1   0    0   1   0   0    -0.39 {'MCl'}
0   1   0    0   0   1   0    -0.2  {'MBr'}
0   1   0    0   0   0   1   log10(K1) {'ML1'}
];
%
%%%%%%%%%%%%%%%%%%%%%%%%%%%%%%%%%%%%%%%%%%%%%%%%%%%%%%%%%%%%%%%%%%%
%%%%%%%%%%%%
%low IS log Ks
%%%%%%%%%%%%%%%%%%%%%%%%%%%%%%%%%%%%%%%%%%%%%%%%%%%%%%%%%%%%%%%%%%%
%%%%%%%%%%%%%%%
%H+   M  CO3  SO4 Cl  Br  L logK  species name
% Tableau=[...
% 1   0   0    0   0   0   0  0     {'H'}
% 0   1   0    0   0   0   0  0     {'M'}
% 0   0   1    0   0   0   0  0     {'CO3'}
% 0   0   0    1   0   0   0  0     {'SO4'}
% 0   0   0    0   1   0   0  0     {'Cl'}
% 0   0   0    0   0   1   0  0     {'Br'}
% 0   0   0    0   0   0   1  0     {'L'}
% -1  0   0    0   0   0   0  -14   {'OH'}
% 1   0   1    0   0   0   0  10.3  {'HCO3'}
% 2   0   1    0   0   0   0  16.6  {'H2CO3'}
% 1   0   0    0   0   0   0  1.99  {'HSO4'}
% -1  1   0    0   0   0   0  -7.9  {'MOH'}
% -2  2   0    0   0   0   0  -14.53 {'M2OH2'}
% 0   1   1    0   0   0   0   7.71 {'MCO3'}
% 0   1   2    0   0   0   0   13.09 {'MCO32'}
% 0   1   0    1   0   0   0   3.67  {'MSO4'}
% 0   1   0    2   0   0   0   5.1   {'MSO42'}
% 0   1   0    0   1   0   0   -1.2 {'MCl'}
% 0   1   0    0   0   1   0   -0.2  {'MBr'}
% 0   1   0    0   0   0   1   log10(K) {'ML'}
% ];
%%%%%%%%%%%%%%%%%%%%%%%%%%%%%%%%%%%%%%%%%%%%%%%%%%%%%%%%%%%%%%%%%%%
%%%%%%%%%%%%
n=size(Tableau,2);
```

```
ASOLUTION=cell2mat(Tableau(:,1:n-2));
KSOLUTION=cell2mat(Tableau(:,n-1));
SOLUTIONNAMES=strvcat(Tableau(:,n));

% -------------- solid values
%H+   M  CO3  SO4 Cl  Br   logK  species name
%%%%%%%%%%%%%%%%%%%%%%%%%%%%%%%%%%%%%%%%%%%%%%%55
STableau=[...
-3  1 0   0   0   0   0  -16.5 {'MOH3s'}
0   2   3   0   0   0   0  32.3  {'M2CO33s'}
];
%%%%%%%%%%%%%%%%%%%%%%%%%%%%%%%%%%%%%%%%%%%%%%%%%%%%%%%%%%%%

ASOLID=cell2mat(STableau(:,1:n-2));
KSOLID=cell2mat(STableau(:,n-1));
SOLIDNAMES=strvcat(STableau(:,n));

end

function [II,GG]=determine_speciesv2(MT,pH,K1,LT1,CT,SO4T,ClT)

warning('off')

% ligand concentrations
%%%%%%%%%%%%%%%%%%%%%%%%%%%%%%%%%%%%%%%%%%%%%%%%%%%%%%%%%%%%%%%%%%%%%%
%%%%%%%%%5
BrT=0.005E-20;
%%%%%%%%%%%%%%%%%%%%%%%%%%%%%%%%%%%%%%%%%%%%%%%%%%%%%%%%%%%%%%%%%%%%%%
%%%%%%%%5

[KSOLUTION,KSOLID,ASOLUTION,ASOLID,SOLUTIONNAMES,SOLIDNAMES]=get_equ
ilib_defn2(K1);

numpts=size(MT,2);
Ncp=size(ASOLID,1);
solid_summary=zeros(numpts,Ncp);

for i=1:size(SOLIDNAMES,1)
    txt=[SOLIDNAMES(i,:),'=zeros(numpts,1);']; eval(txt)
end

for i=1:size(MT,2)

    % adjust for fixed pH


[Ksolution,Ksolid,Asolution,Asolid]=get_equilib_fixed_pH(KSOLUTION,K
SOLID,ASOLUTION,ASOLID,pH);

    Asolid_SI_check=Asolid; Ksolid_SI_check=Ksolid;

    % number of different species
    Nx=size(Asolution,2); Ncp=size(Asolid,1); Nc=size(Asolution,1);
```

```
    % initial guess
    iterations=1000; criteria=1e-16;

%%%%%%%%%%%%%%%%%%%%%%%%%%%%%%%%%%%%%%%%%%%%%%%%%%%%%%%%%%%%%%%%%%%%%%%%%%%%%%%
%%%%%%%%%
    T=[MT(i) CT SO4T ClT BrT LT1 ]; guess=T./10;

%%%%%%%%%%%%%%%%%%%%%%%%%%%%%%%%%%%%%%%%%%%%%%%%%%%%%%%%%%%%%%%%%%%%%%%%%%%%%%%
%%%%%%%%%%%

    % calculate species using NR

    solids=zeros(1,Ncp);

    if i==1;
[species,err,SI]=NR_method_solution(Asolution,Asolid,Ksolid,Ksolutio
n,T',[guess(1:Nx)]',iterations,criteria); end
    if i>1;

[species,err,SI]=NR_method_solution(Asolution,Asolid,Ksolid,Ksolutio
n,T',[species(2:Nx+1)],iterations,criteria);
    end

    for qq=1:Ncp

        [Y,I]=max(SI);

        if Y>1.000000001
            Iindex(qq)=I;
            Asolidtemp(qq,:)=Asolid_SI_check(I,:); %'MOH3s'
            Ksolidtemp(qq,:)=Ksolid_SI_check(I,:);
            solidguess(qq)=T(I)*0.5;
           % solidguess(qq)=min(T)*0.015;
            if i>1;
                %if max(solids)>0
                txt=['solidguess(qq)=',SOLIDNAMES(I,:),'(i-1);'];
eval(txt);
                %end
            end
            guess=[species(2:Nx+1)' solidguess];

[species,err,SItst,solids]=NR_method(Asolution,Asolidtemp',Ksolidtem
p,Ksolution,T',guess',iterations,criteria);
             for q=1:size(solids,1);
                txt=[SOLIDNAMES(Iindex(q),:),'(i)=solids(q);'];
eval(txt)
              end
        end

        Q=Asolid*log10(species(2:Nx+1)); SI=10.^(Q+Ksolid);
Ifirst=I;

    end
```

```
    Q=Asolid*log10(species(2:Nx+1)); SI=10.^(Q+Ksolid);
    SI_summary(i,:)=SI;

    species_summary(i,:)=species;
    mass_err_summary(i,:)=(err(1));

    Asolidtemp=[]; Ksolidtemp=[];

end

for i=1:size(species_summary,2)
    txt=[SOLUTIONNAMES(i,:),'=species_summary(:,i);']; eval(txt)
end
%%%%%%%%%%%%%%%%%%%%%%%%%%%%%%%%%%%%%%%%%%%%%%%%%%%%%%%%%%%%%%%%%%%%%%%%
II=[species_summary MOH3s M2CO33s];% UPDATE
%%%%%%%%%%%%%%%%%%%%%%%%%%%%%%%%%%%%%%%%%%%%%%%%%%%%%%%%%%%%%%%%%%%%%%%%
GG=strvcat(SOLUTIONNAMES,SOLIDNAMES);


end

function
[Ksolution,Ksolid,Asolution,Asolid]=get_equilib_fixed_pH(KSOLUTION,K
SOLID,ASOLUTION,ASOLID,pH)

    [N,M]=size(ASOLUTION);
    Ksolution=KSOLUTION-ASOLUTION(:,1)*pH;
    Asolution=[ASOLUTION(:,2:M)];
    [N,M]=size(ASOLID);
    Ksolid=KSOLID-ASOLID(:,1)*pH;
    Asolid=[ASOLID(:,2:M)];

end

function
[species,err,SI]=NR_method_solution(Asolution,Asolid,Ksolid,Ksolutio
n,T,guess,iterations,criteria)

Nx=size(Asolution,2); Ncp=size(Asolid,1); Nc=size(Asolution,1);
X=guess;

for II=1:iterations

    Xsolution=X(1:Nx);

      logC=(Ksolution)+Asolution*log10(Xsolution); C=10.^(logC); %
calc species

    Rmass=Asolution'*C-T;

    Q=Asolid*log10(Xsolution); SI=10.^(Q+Ksolid);
    RSI=ones(size(SI))-SI;

      % calc the jacobian
```

```
      z=zeros(Nx,Nx);

      for j=1:Nx;
            for k=1:Nx;
                        for i=1:Nc;
z(j,k)=z(j,k)+Asolution(i,j)*Asolution(i,k)*C(i)/Xsolution(k); end
            end
    end

    R=[Rmass]; X=[Xsolution];

    deltaX=z\(-1*R);
    %deltaX=-1*inv(z)*(R);
      one_over_del=max([1, -1*deltaX'./(0.5*X')]);
      del=1/one_over_del;
      X=X+del*deltaX;

    %X=X+deltaX;

      tst=sum(abs(R));
      if tst<=criteria; break; end

end

logC=(Ksolution)+Asolution*log10(Xsolution); C=10.^(logC); % calc
species
RSI=ones(size(SI))-SI;

Q=Asolid*log10(Xsolution); SI=10.^(Q+Ksolid);
RSI=ones(size(SI))-SI;

Rmass=Asolution'*C-T;

err=[Rmass];

species=[C];

end

function
[species,err,SI,solids]=NR_method(Asolution,Asolid,Ksolid,Ksolution,
T,guess,iterations,criteria)

Nx=size(Asolution,2); Ncp=size(Asolid,2); Nc=size(Asolution,1);
X=guess;

for II=1:iterations

    Xsolution=X(1:Nx); Xsolid=[]; if Ncp>0; Xsolid=X(Nx+1:Nx+Ncp);
end

      logC=(Ksolution)+Asolution*log10(Xsolution); C=10.^(logC); %
calc species
```

```
    if Ncp>0;
        Rmass=Asolution'*C+Asolid*Xsolid-T;
    end


    if Ncp==0; Rmass=Asolution'*C-T; end % calc residuals in mass
balance

    Q=Asolid'*log10(Xsolution); SI=10.^(Q+Ksolid);
    RSI=ones(size(SI))-SI;

      % calc the jacobian

      z=zeros(Nx+Ncp,Nx+Ncp);

      for j=1:Nx;
            for k=1:Nx;
                        for i=1:Nc;
z(j,k)=z(j,k)+Asolution(i,j)*Asolution(i,k)*C(i)/Xsolution(k); end
            end
    end

    if Ncp>0;
    for j=1:Nx;
            for k=Nx+1:Nx+Ncp;
                 t=Asolid';
                        z(j,k)=t(k-Nx,j);
            end
    end
    end

    if Ncp>0
    for j=Nx+1:Nx+Ncp;
            for k=1:Nx
                        z(j,k)=-1*Asolid(k,j-Nx)*(SI(j-
Nx)/Xsolution(k));
            end
    end
    end

    if Ncp>0
    for j=Nx+1:Nx+Ncp
        for k=Nx+1:Nx+Ncp
            z(j,k)=0;
        end
    end
    end

    R=[Rmass; RSI]; X=[Xsolution; Xsolid];

    deltaX=z\(-1*R);
    %deltaX=-1*inv(z)*(R);
      one_over_del=max([1, -1*deltaX'./(0.5*X')]);
```

```
      del=1/one_over_del;
      X=X+del*deltaX;

    %X=X+deltaX;

      tst=sum(abs(R));
      if tst<=criteria; break; end

end

logC=(Ksolution)+Asolution*log10(Xsolution); C=10.^(logC); % calc
species
RSI=ones(size(SI))-SI;

if Ncp>0; Rmass=Asolution'*C+Asolid*Xsolid-T; end % calc residuals
in mass balance
if Ncp==0; Rmass=Asolution'*C-T; end % calc residuals in mass
balance

err=[Rmass];

species=[C];
solids=Xsolid;

end

function II=returnISEerr(p,SmT,ISEmeas,flag,colour,CT,SO4T,ClT,pH)

logK1=p(1); K1=10^logK1;
logLT1=p(2); LT1=10^logLT1;
SmT=SmT';

[species,names]=determine_speciesv2(SmT,pH,K1,LT1,CT,SO4T,ClT);

for i=1:size(SmT,2)
for j=1:size(species,2)
        txt=[names(j,:),'(i)=species(i,j);'];
        eval(txt)
end
end

ISEcalc=log10(M);

boundmeas=SmT-10.^ISEmeas'; boundcalc=SmT-10.^ISEcalc;

%residuals=[ISEmeas-ISEcalc'];
residuals=[boundmeas-boundcalc];

II=log10(sum(residuals.^2));
%II=(sum(residuals.^2));

if flag==1;
    SmT=[1e-18 1e-6 5e-6 10e-6:10e-6:100e-6 110e-6:50e-6 1000e-6];
    species=[]; names=[]; M=[];
```

```
    [species,names]=determine_speciesv2(SmT,pH,K1,LT1,CT,SO4T,ClT);
    for i=1:size(SmT,2)
    for j=1:size(species,2)
        txt=[names(j,:),'(i)=species(i,j);'];
        eval(txt)
    end
    end

    figure(1); %clf
    plot(log10(M),(SmT-M)*1e6,colour,'linewidth',2); hold on
    plot(ISEmeas,(SmT-
10.^ISEmeas')*1e6,'ko','markersize',10,'markerfacecolor','b')
    t=[min(ISEmeas)-0.9 max(ISEmeas)+0.5 0 1e6*1.1*max(SmT-
10.^ISEmeas')];
    axis(t)
end

end
```

C5: MATLAB code for fixed pH Speciation Modeling

```
function PP=Species_fixedpH

figure(1); clf

%%%%%%%%%%%%%%%%%%%%%%%%%%%%%%%%%%%%%%%%%%%%%%%%%%%%%%%%%%%%%%%%%%%%%55
uMT=[2.66 5.32 10.64 21.28 42.56 66.51]; MT=uMT./1000000;
logMT=log10(MT); pH=7.5;
%%%%%%%%%%%%%%%%%%%%%%%%%%%%%%%%%%%%%%%%%%%%%%%%%%%%%%%%%%%%%%%%%%%%%%
%%

[species,names]=determine_species(MT,pH);

for i=1:size(MT,2)
for j=1:size(species,2)
        txt=[names(j,:),'(i)=species(i,j);'];
        eval(txt)
end
end

%%%%%%%%%%%%%%%%%%%%%%%%%%%%%%%%%%%%%%%%%%%%%%%%%%%%%%%%%%%%%%%%%%%%%%
%%%%
figure(1); plot(logMT,log10(M),'k','linewidth',2)
hold on
plot(logMT,logMT,'k--','linewidth',2)
plot(logMT,log10(MOH),'r','linewidth',2)
plot(logMT,log10(M2OH2),'c','linewidth',2)
plot(logMT,log10(MCO3),'m','linewidth',2)
plot(logMT,log10(MCO32),'y','linewidth',2)
plot(logMT,log10(MSO4),'r--','linewidth',2)
plot(logMT,log10(MSO42),'b--','linewidth',2)
plot(logMT,log10(MCl),'m--','linewidth',2)
plot(logMT,log10(MBr),'g--','linewidth',2)
plot(logMT,log10(MOH3s),'g','linewidth',2)
plot(logMT,log10(M2CO33s),'b','linewidth',2)
plot(logMT,log10(ML),'c--','linewidth',2)
set(gca,'fontsize',14,'linewidth',2)
xlabel('log(M_T (mol/L))','fontsize',14)
ylabel('log([species] (mol/L))','fontsize',14)
legend('Sm','1:1
line','SmOH','Sm_2OH_2','SmCO_3','Sm(CO_3)_2','SmSO_4','Sm(SO_4)_2',
'SmCl','SmBr','SmOH_3_s','Sm_2(CO_3)_3s','SmDOM','location',
'EastOutside','orientation','vertical')

figure(2); plot(logMT,M,'k','linewidth',2)
hold on
plot(logMT,MOH,'r','linewidth',2)
plot(logMT,M2OH2,'c','linewidth',2)
plot(logMT,MCO3,'m','linewidth',2)
plot(logMT,MCO32,'y','linewidth',2)
plot(logMT,MSO4,'r--','linewidth',2)
plot(logMT,MSO42,'b--','linewidth',2)
```

```
plot(logMT,MCl,'m--','linewidth',2)
plot(logMT,MBr,'g--','linewidth',2)
plot(logMT,MOH3s,'g','linewidth',2)
plot(logMT,M2CO33s,'b','linewidth',2)
plot(logMT,ML,'c--','linewidth',2)
set(gca,'fontsize',14,'linewidth',2)
xlabel('log(M_T (mol/L))','fontsize',14)
ylabel('log([species] (mol/L))','fontsize',14)
legend('Sm','SmOH','Sm_2OH_2','SmCO_3','Sm(CO_3)_2','SmSO_4','Sm(SO_
4)_2','SmCl','SmBr','SmOH_3_s','Sm_2(CO_3)_3s','SmDOM','location',
'EastOutside','orientation','vertical')

%%%%%%%%%%%%%%%%%%%%%%%%%%%%%%%%%%%%%%%%%%%%%%%%%%%%%%%%%%%%%%%%%%%%%%%
%%%%5

save species.txt species -ascii

end

function [II,GG]=determine_species(MT,pH)

warning('off')

% ligand concentrations
%%%%%%%%%%%%%%%%%%%%%%%%%%%%%%%%%%%%%%%%%%%%%%%%%%%%%%%%%%%%%%%%%%%%%%%
%%%%%%%%%5
CO3T=500/10^6; SO4T=125/10^6; ClT=1025/10^6; BrT=5/10^20; LT=
12.29e-06*8;
%%%%%%%%%%%%%%%%%%%%%%%%%%%%%%%%%%%%%%%%%%%%%%%%%%%%%%%%%%%%%%%%%%%%%%%
%%%%%%%%5

[KSOLUTION,KSOLID,ASOLUTION,ASOLID,SOLUTIONNAMES,SOLIDNAMES]=get_equ
ilib_defn;

numpts=size(MT,2);
Ncp=size(ASOLID,1);
solid_summary=zeros(numpts,Ncp);

for i=1:size(SOLIDNAMES,1)
    txt=[SOLIDNAMES(i,:),'=zeros(numpts,1);']; eval(txt)
end

for i=1:size(MT,2)

    % adjust for fixed pH


[Ksolution,Ksolid,Asolution,Asolid]=get_equilib_fixed_pH(KSOLUTION,K
SOLID,ASOLUTION,ASOLID,pH);

    Asolid_SI_check=Asolid; Ksolid_SI_check=Ksolid;

    % number of different species
    Nx=size(Asolution,2); Ncp=size(Asolid,1); Nc=size(Asolution,1);
```

```
    % initial guess
    iterations=1000; criteria=1e-16;

%%%%%%%%%%%%%%%%%%%%%%%%%%%%%%%%%%%%%%%%%%%%%%%%%%%%%%%%%%%%%%%%%%%%%%%%%%%%%%%%
%%%%%%%%%
    T=[MT(i) CO3T SO4T ClT BrT LT]; guess=T./10;

%%%%%%%%%%%%%%%%%%%%%%%%%%%%%%%%%%%%%%%%%%%%%%%%%%%%%%%%%%%%%%%%%%%%%%%%%%%%%%%%
%%%%%%%%%%%

    % calculate species using NR

    solids=zeros(1,Ncp);

    if i==1;
[species,err,SI]=NR_method_solution(Asolution,Asolid,Ksolid,Ksolutio
n,T',[guess(1:Nx)]',iterations,criteria); end
    if i>1;

[species,err,SI]=NR_method_solution(Asolution,Asolid,Ksolid,Ksolutio
n,T',[species(2:Nx+1)],iterations,criteria);
    end

    for qq=1:Ncp

        [Y,I]=max(SI);

        if Y>1.000000001
            Iindex(qq)=I;
            Asolidtemp(qq,:)=Asolid_SI_check(I,:); %'MOH3s'
            Ksolidtemp(qq,:)=Ksolid_SI_check(I,:);
            solidguess(qq)=T(I)*0.5;
           % solidguess(qq)=min(T)*0.015;
            if i>1;
                %if max(solids)>0
                txt=['solidguess(qq)=',SOLIDNAMES(I,:),'(i-1);'];
eval(txt);
                %end
            end
            guess=[species(2:Nx+1)' solidguess];

[species,err,SItst,solids]=NR_method(Asolution,Asolidtemp',Ksolidtem
p,Ksolution,T',guess',iterations,criteria);
             for q=1:size(solids,1);
                txt=[SOLIDNAMES(Iindex(q),:),'(i)=solids(q);'];
eval(txt)
              end
        end

        Q=Asolid*log10(species(2:Nx+1)); SI=10.^(Q+Ksolid);
Ifirst=I;

    end
```

```
    Q=Asolid*log10(species(2:Nx+1)); SI=10.^(Q+Ksolid);
    SI_summary(i,:)=SI;

    species_summary(i,:)=species;
    mass_err_summary(i,:)=(err(1));

    Asolidtemp=[]; Ksolidtemp=[];

end

for i=1:size(species_summary,2)
    txt=[SOLUTIONNAMES(i,:),'=species_summary(:,i);']; eval(txt)
end
%%%%%%%%%%%%%%%%%%%%%%%%%%%%%%%%%%%%%%%%%%%%%%%%%%%%%%%%%%%%%%%%%%%%%%%%%%%
II=[species_summary MOH3s M2CO33s];
%%%%%%%%%%%%%%%%%%%%%%%%%%%%%%%%%%%%%%%%%%%%%%%%%%%%%%%%%%%%%%%%%%%%%%%%%%%
GG=strvcat(SOLUTIONNAMES,SOLIDNAMES);


end

% -------------------- NR method solids present

function
[species,err,SI,solids]=NR_method(Asolution,Asolid,Ksolid,Ksolution,
T,guess,iterations,criteria)

Nx=size(Asolution,2); Ncp=size(Asolid,2); Nc=size(Asolution,1);
X=guess;

for II=1:iterations

    Xsolution=X(1:Nx); Xsolid=[]; if Ncp>0; Xsolid=X(Nx+1:Nx+Ncp);
end

      logC=(Ksolution)+Asolution*log10(Xsolution); C=10.^(logC); %
calc species

    if Ncp>0;
        Rmass=Asolution'*C+Asolid*Xsolid-T;
    end


    if Ncp==0; Rmass=Asolution'*C-T; end % calc residuals in mass
balance

    Q=Asolid'*log10(Xsolution); SI=10.^(Q+Ksolid);
    RSI=ones(size(SI))-SI;

      % calc the jacobian

      z=zeros(Nx+Ncp,Nx+Ncp);
```

```
      for j=1:Nx;
            for k=1:Nx;
                        for i=1:Nc;
z(j,k)=z(j,k)+Asolution(i,j)*Asolution(i,k)*C(i)/Xsolution(k); end
            end
    end

    if Ncp>0;
    for j=1:Nx;
            for k=Nx+1:Nx+Ncp;
                 t=Asolid';
                        z(j,k)=t(k-Nx,j);
            end
    end
    end

    if Ncp>0
    for j=Nx+1:Nx+Ncp;
            for k=1:Nx
                        z(j,k)=-1*Asolid(k,j-Nx)*(SI(j-
Nx)/Xsolution(k));
            end
    end
    end

    if Ncp>0
    for j=Nx+1:Nx+Ncp
        for k=Nx+1:Nx+Ncp
            z(j,k)=0;
        end
    end
    end

    R=[Rmass; RSI]; X=[Xsolution; Xsolid];

    deltaX=z\(-1*R);
    %deltaX=-1*inv(z)*(R);
      one_over_del=max([1, -1*deltaX'./(0.5*X')]);
      del=1/one_over_del;
      X=X+del*deltaX;

    %X=X+deltaX;

      tst=sum(abs(R));
      if tst<=criteria; break; end

end

logC=(Ksolution)+Asolution*log10(Xsolution); C=10.^(logC); % calc
species
RSI=ones(size(SI))-SI;

if Ncp>0; Rmass=Asolution'*C+Asolid*Xsolid-T; end % calc residuals
in mass balance
```

```
if Ncp==0; Rmass=Asolution'*C-T; end % calc residuals in mass
balance

err=[Rmass];

species=[C];
solids=Xsolid;

end

% ----------- NR method just solution species

function
[species,err,SI]=NR_method_solution(Asolution,Asolid,Ksolid,Ksolutio
n,T,guess,iterations,criteria)

Nx=size(Asolution,2); Ncp=size(Asolid,1); Nc=size(Asolution,1);
X=guess;

for II=1:iterations

    Xsolution=X(1:Nx);

      logC=(Ksolution)+Asolution*log10(Xsolution); C=10.^(logC); %
calc species

    Rmass=Asolution'*C-T;

    Q=Asolid*log10(Xsolution); SI=10.^(Q+Ksolid);
    RSI=ones(size(SI))-SI;

      % calc the jacobian

      z=zeros(Nx,Nx);

      for j=1:Nx;
            for k=1:Nx;
                        for i=1:Nc;
z(j,k)=z(j,k)+Asolution(i,j)*Asolution(i,k)*C(i)/Xsolution(k); end
            end
    end

    R=[Rmass]; X=[Xsolution];

    deltaX=z\(-1*R);
    %deltaX=-1*inv(z)*(R);
      one_over_del=max([1, -1*deltaX'./(0.5*X')]);
      del=1/one_over_del;
      X=X+del*deltaX;

    %X=X+deltaX;

      tst=sum(abs(R));
      if tst<=criteria; break; end
```

```
end

logC=(Ksolution)+Asolution*log10(Xsolution); C=10.^(logC); % calc
species
RSI=ones(size(SI))-SI;

Q=Asolid*log10(Xsolution); SI=10.^(Q+Ksolid);
RSI=ones(size(SI))-SI;

Rmass=Asolution'*C-T;

err=[Rmass];

species=[C];

end



% ----- equilib definition ----------------
Tableau_varymetal_fixedpHSmFQ.m

function
[KSOLUTION,KSOLID,ASOLUTION,ASOLID,SOLUTIONNAMES,SOLIDNAMES]=get_equ
ilib_defn;

%%%%%%%%%%%%%%%%%%%%%%%%%%%%%%%%%%%%%%%%%%%%%%%%%%%%%%%%%%%%%%%%%%%%%%%%
%%%%%%%%%%%%%%%
%H+   M  CO3  SO4 Cl  Br L logK  species name
Tableau=[...
1   0   0    0   0   0  0   0     {'H'}
0   1   0    0   0   0  0   0     {'M'}
0   0   1    0   0   0  0   0     {'CO3'}
0   0   0    1   0   0  0   0     {'SO4'}
0   0   0    0   1   0  0   0     {'Cl'}
0   0   0    0   0   1  0   0     {'Br'}
-1  0   0    0   0   0  0  -14   {'OH'}
0   0   0    0   0   0  1   0     {'L'}
1   0   1    0   0   0  0   10.3  {'HCO3'}
2   0   1    0   0   0  0   16.6  {'H2CO3'}
1   0   0    0   0   0  0   1.99  {'HSO4'}
-1  1   0    0   0   0  0   -7.9  {'MOH'}
-2  2   0    0   0   0  0   -14.5 {'M2OH2'}
0   1   1    0   0   0  0    7.71 {'MCO3'}
0   1   2    0   0   0  0    13.09 {'MCO32'}
0   1   0    1   0   0  0    3.67  {'MSO4'}
0   1   0    2   0   0  0    5.1   {'MSO42'}
0   1   0    0   1   0  0    -0.39 {'MCl'}
0   1   0    0   0   1  0    -0.2  {'MBr'}
0   1   0    0   0   0  1   5.28   {'ML'}
];
%%%%%%%%%%%%%%%%%%%%%%%%%%%%%%%%%%%%%%%%%%%%%%%%%%%%%%%%%%%%%%%%%%%%%%%%
%%%%%%%%%%%
```

```
n=size(Tableau,2);
ASOLUTION=cell2mat(Tableau(:,1:n-2));
KSOLUTION=cell2mat(Tableau(:,n-1));
SOLUTIONNAMES=strvcat(Tableau(:,n));

% -------------- solid values
%H+   M  CO3  SO4 Cl  Br   logK  species name
%%%%%%%%%%%%%%%%%%%%%%%%%%%%%%%%%%%%%%%%%%%%%%%%%%%%%55
STableau=[...
-3  1 0   0   0   0  0  -16.5 {'MOH3s'}
0   2   3   0   0   0  0  32.3  {'M2CO33s'}
];
%%%%%%%%%%%%%%%%%%%%%%%%%%%%%%%%%%%%%%%%%%%%%%%%%%%%%%%%%%%%%%%%%%%%%%%

ASOLID=cell2mat(STableau(:,1:n-2));
KSOLID=cell2mat(STableau(:,n-1));
SOLIDNAMES=strvcat(STableau(:,n));

end

% ----------- for fixed pH ----------------

function
[Ksolution,Ksolid,Asolution,Asolid]=get_equilib_fixed_pH(KSOLUTION,K
SOLID,ASOLUTION,ASOLID,pH)

    [N,M]=size(ASOLUTION);
    Ksolution=KSOLUTION-ASOLUTION(:,1)*pH;
    Asolution=[ASOLUTION(:,2:M)];
    [N,M]=size(ASOLID);
    Ksolid=KSOLID-ASOLID(:,1)*pH;
    Asolid=[ASOLID(:,2:M)];

end
```

C6: MATLAB code for EC_{50} Calculation

```
data=[...
1           88    95    90 %had to set to 1 to get convergence.
22.78       86    90    86
42.12       80    84    78
84.633      73    75    70
161.3067    58    55    50
388.3       30    30    31
667.5333    4     7     9
1487.333    0     0     0
];

bg=0; % can't have zero in log

conc=data(:,1)+bg; r1=data(:,2); r2=data(:,3); r3=data(:,4);

control=mean(data(1,2:4))
r1=100*(1-(control-r1)./control);
r2=100*(1-(control-r2)./control);
r3=100*(1-(control-r3)./control);

dose=[conc' conc' conc'];
response=[r1' r2' r3'];


%manytoxendpointsdownnotlog(dose,response)
toxendpointsdownlog(dose,response)


function II=toxendpointsdownlog(dose,response)
log10dose=log10(dose);

figure(1); clf;

logmeanresponse=log10(response);

%figure(2);
plot(log10dose,response,'ko','markersize',8,'markerfacecolor','b');
k=waitforbuttonpress;

tst=size(response,1);  if tst>1; meanresponse=mean(response); end

delta=(max(log10dose)-min(log10dose))/10
log10doseplot=[0:delta:max(log10dose)+max(log10dose)];

EC50=mean(dose); logEC50=log10(EC50); nguess=1;

beta0=[logEC50 nguess];

[beta,resid,J,Sigma,mse] =
nlinfit(log10dose,response,@doseresponseLC50,beta0);
```

```
[ypred, delta] =
nlpredci(@doseresponseLC50,log10dose,beta,resid,'Covar',Sigma);
[ypred, delta] =
nlpredci(@doseresponseLC50,log10dose,beta,resid,'jacobian',J)

%nlintool(log10dose,meanresponse,@doseresponseLC50,beta0)

ci = nlparci(beta,resid,'covar',Sigma);

[ypred, delta] =
nlpredci(@doseresponseLC50,log10doseplot,beta,resid,'Covar',Sigma);


logEC50=beta(1); EC50full=10^logEC50; n=beta(2)

figure(1); subplot(221); plot(log10dose,(response),'ko',...
    log10doseplot,ypred,'k',log10doseplot,ypred+delta,'b--
',log10doseplot,ypred-delta,...
    'b--','linewidth',2,'markersize',8,'markerfacecolor','b');
set(gca,'linewidth',2,'fontsize',14)

delta=(max(log10dose)-min(log10dose))/10

axis([0 max(log10dose)+5*delta 0 1.1*max(response)])
xlabel('log[dose]','fontsize',14)
ylabel('response (%)','fontsize',14)


% fit to EC50 expression from Meyer et all appendix --------------

EC50guess=EC50full; nguess=1;

betaguess=[log10(EC50guess) (nguess)];

[beta,resid,J,Sigma,mse] =
nlinfit(log10dose,response,@doseresponseLC50,betaguess);
[ypred, delta] =
nlpredci(@doseresponseLC50,log10dose,beta,resid,'Covar',Sigma);
rsquared50=rsquare((response),ypred)
ci = nlparci(beta,resid,'covar',Sigma);
[ypred, delta] =
nlpredci(@doseresponseLC50,log10doseplot,beta,resid,'Covar',Sigma);

logEC50=beta(1); loglowEC50=ci(1,1); loghighEC50=ci(1,2);
nfit50=beta(2); %hfit50=beta(3);


log50endpoint=[logEC50 loglowEC50 loghighEC50];
endpoint50=10.^log50endpoint

figure(1); subplot(222); plot(log10dose,(response),'ko',...
    log10doseplot,ypred,'k',log10doseplot,ypred+delta,'b--
',log10doseplot,ypred-delta,...
    'b--','linewidth',2,'markersize',8,'markerfacecolor','b');
```

```
set(gca,'linewidth',2,'fontsize',14)

hold on; plot(log10([endpoint50(2) endpoint50(3)]),([50
50]),'k','linewidth',2)
plot(log10([endpoint50(1) endpoint50(1)]),([0
50]),'k','linewidth',2)
plot(log10([endpoint50(2) endpoint50(2)]),([0 50]),'k--
','linewidth',2)
plot(log10([endpoint50(3) endpoint50(3)]),([0 50]),'k--
','linewidth',2)

%delta=(log10(endpoint50(3))-log10(endpoint50(2)))/10

xlabel('log[dose]','fontsize',14)
ylabel('response (%)','fontsize',14)
title('EC50','fontsize',14)

% fit to EC20 expression from Meyer et all appendix --------------

EC20guess=0.5*endpoint50(1);  nguess=1;

betaguess=[log10(EC20guess) nguess];

[beta,resid,J,Sigma,mse] =
nlinfit(log10dose,response,@doseresponseLC20,betaguess);
[ypred, delta] =
nlpredci(@doseresponseLC20,log10dose,beta,resid,'Covar',Sigma);
rsquared20=rsquare((response),ypred')
ci = nlparci(beta,resid,'covar',Sigma);
[ypred, delta] =
nlpredci(@doseresponseLC20,log10doseplot,beta,resid,'Covar',Sigma);

logEC20=beta(1); loglowEC20=ci(1,1); loghighEC20=ci(1,2);
nfit20=beta(2); %hfit20=beta(3);

log20endpoint=[logEC20 loglowEC20 loghighEC20];
endpoint20=10.^log20endpoint

figure(1); subplot(223); plot(log10dose,(response),'ko',...
    log10doseplot,ypred,'k',log10doseplot,ypred+delta,'b--
',log10doseplot,ypred-delta,...
    'b--','linewidth',2,'markersize',8,'markerfacecolor','b');
set(gca,'linewidth',2,'fontsize',14)

hold on; plot(log10([(endpoint20(2)) endpoint20(3)]),([80
80]),'k','linewidth',2)
plot(log10([endpoint20(1) endpoint20(1)]),([0
80]),'k','linewidth',2)
plot(log10([endpoint20(1) endpoint20(1)]),([0
80]),'k','linewidth',2)
plot(log10([endpoint20(2) endpoint20(2)]),([0 80]),'k--
','linewidth',2)
plot(log10([endpoint20(3) endpoint20(3)]),([0 80]),'k--
','linewidth',2)
```

```
%delta=(log10(endpoint20(3))-log10(endpoint20(2)))/10
%axis([log10(endpoint20(2))-delta log10(endpoint20(3))+delta 0 85])
delta=(max(log10dose)-min(log10dose))/10
axis([0 max(log10dose)+5*delta ([0 1.1*max(response)])])

xlabel('log[dose]','fontsize',14)
ylabel('response (%)','fontsize',14)
title('EC20','fontsize',14)

% fit to EC10 expression from Meyer et all appendix --------------

EC10guess=0.5*endpoint20(1); nguess=1;

betaguess=[log10(EC10guess) nguess];

[beta,resid,J,Sigma,mse] =
nlinfit(log10dose,response,@doseresponseLC10,betaguess);
[ypred, delta] =
nlpredci(@doseresponseLC10,log10dose,beta,resid,'Covar',Sigma);
rsquared10=rsquare((response),ypred)
ci = nlparci(beta,resid,'covar',Sigma);
[ypred, delta] =
nlpredci(@doseresponseLC10,log10doseplot,beta,resid,'Covar',Sigma);

logEC10=beta(1); loglowEC10=ci(1,1); loghighEC10=ci(1,2);
nfit10=beta(2); % hfit10=beta(3);

log10endpoint=[logEC10 loglowEC10 loghighEC10];
endpoint10=10.^log10endpoint

figure(1); subplot(224); plot(log10dose,(response),'ko',...
    log10doseplot,ypred,'k',log10doseplot,ypred+delta,'b--
',log10doseplot,ypred-delta,...
    'b--','linewidth',2,'markersize',8,'markerfacecolor','b');
set(gca,'linewidth',2,'fontsize',14)

hold on; plot(log10([endpoint10(2) endpoint10(3)]),([90
90]),'k','linewidth',2)
plot(log10([endpoint10(1) endpoint10(1)]),([0
90]),'k','linewidth',2)
plot(log10([endpoint10(2) endpoint10(2)]),([0 90]),'k--
','linewidth',2)
plot(log10([endpoint10(3) endpoint10(3)]),([0 90]),'k--
','linewidth',2)

%delta=(log10(endpoint10(3))-log10(endpoint10(2)))/10
%axis([log10(endpoint10(2))-delta log10(endpoint10(3))+delta 0 120])
delta=(max(log10dose)-min(log10dose))/10
axis([0 max(log10dose)+5*delta ([0 1.1*max(response)])])

xlabel('log[dose]','fontsize',14)
ylabel('response (%)','fontsize',14)
title('EC10','fontsize',14)
```

```
print manydoseresponse.eps -depsc2

% export to latex
  matrix = [dose' logmeanresponse'];
  %rowLabels = {'row 1', 'row 2'};
  columnLabels = {'dose', 'response'};
  %matrix2latex(matrix, 'out.tex', 'rowLabels', rowLabels,
'columnLabels', columnLabels, 'alignment', 'c', 'format', '%-6.2f',
'size', 'tiny');
%  matrix2latex(matrix, 'out.tex', 'columnLabels', columnLabels,
'alignment', 'c', 'format', '%-6.2f', 'size', 'normalsize');
% The resulting latex file can be included into any latex document
by:
% /input{out.tex}
%

% export to latex
  matrix = [endpoint50 nfit50 rsquared50
      endpoint20 nfit20 rsquared20
      endpoint10 nfit10 rsquared10];
  rowLabels = {'EC50', 'EC20','EC10'};
  columnLabels = {'EC','low','high','slope','r$^2$'};
  %matrix2latex(matrix, 'out.tex', 'rowLabels', rowLabels,
'columnLabels', columnLabels, 'alignment', 'c', 'format', '%-6.2f',
'size', 'tiny');
%  matrix2latex(matrix, 'ECout.tex', 'rowLabels', rowLabels,
'columnLabels', columnLabels, 'alignment', 'c', 'format', '%-6.2f',
'size', 'normalsize');
% The resulting latex file can be included into any latex document
by:
% /input{out.tex}
%



end

function II=doseresponseLC50(beta,dose)

EC50=beta(1); n=(beta(2));

term=(((EC50)*ones(size(dose))./dose).^(-1*n);

response = (100*ones(size(dose))./(ones(size(dose))+term));

II=response;

end

function II=doseresponseLC20(beta,dose)

EC20=beta(1); n=beta(2);
```

```
term=(((EC20)*ones(size(dose)))./dose).^(-1*n);

response = (100*ones(size(dose))./(ones(size(dose))+0.25*term));

II=response;

end


function II=doseresponseLC10(beta,dose)

EC10=beta(1); n=beta(2);

term=(((EC10)*ones(size(dose)))./dose).^(-1*n);

response = (100*ones(size(dose))./(ones(size(dose))+0.111*term));

II=response;

end


function R2=rsquare(y,yhat)
% PURPOSE:  calculate r square using data y and estimates yhat
% ------------------------------------------------------------------
-
% USAGE: R2 = rsquare(y,yhat)
% where:
%        y are the original values as vector or 2D matrix and
%        yhat are the estimates calculated from y using a
regression, given in
%        the same form (vector or raster) as y
% ------------------------------------------------------------------
-------
% OUTPUTS:
%        R2 is the r square value calculated using 1-SS_E/SS_T
% ------------------------------------------------------------------
-
% Note: NaNs in either y or yhat are deleted from both sets.
%
% Felix Hebeler, Geography Dept., University Zurich, Feb 2007

if nargin ~= 2
    error('This function needs some exactly 2 input arguments!');
end

% reshape if 2d matrix
yhat=reshape(yhat,1,size(yhat,1)*size(yhat,2));
y=reshape(y,1,size(y,1)*size(y,2));

% delete NaNs
while sum(isnan(y))~=0 || sum(isnan(yhat))~=0
    if sum(isnan(y)) >= sum(isnan(yhat))
        yhat(isnan(y))=[];
```

```
        y(isnan(y))=[];
    else
        y(isnan(yhat))=[];
        yhat(isnan(yhat))=[];
    end
end

% 1 - SSe/SSt
R2 = 1 - ( sum( (y-yhat).^2 ) / sum( (y-mean(y)).^2 ) );

% SSr/SSt
% R2 = sum((yhat-mean(y)).^2) / sum( (y-mean(y)).^2 ) ;

if R2<0 || R2>1
    error(['R^2 of ',num2str(R2),' : yhat does not appear to be the
estimate of y from a regression.'])
end
end
```